Essays on Real-Financial Interactions and on the Application of Network and Random Matrix Theories to Economic Data

Boyan Yanovski

Department of Economics

Christian-Albrechts University of Kiel

A thesis submitted for the degree of

Dr. Sc. Pol.

Essays on Real-Financial Interactions and on the Application of Network and Random Matrix Theories to Economic Data

Inaugural-Dissertation

zur Erlangung des akademischen Grades eines Doktors

der Wirtschafts- und Sozialwissenschaften

der Wirtschafts- und Sozialwissenschaftlichen Fakultät
der Christian-Albrechts-Universität zu Kiel

vorgelegt von

M.Sc., **Boyan Yanovski**

aus Sofia, Bulgarien

Gedruckt mit Genehmigung der
Wirtschafts- und Sozialwissenschaften
Fakultät der Christian-Albrechts-Universität
zu Kiel

Dekan:
Prof. Dr. Till Requate

Erstberichterstattender:
Prof. Dr. Thomas Lux

Zweitberichterstattender:
Prof. Dr. H.-W. Wohltmann

Tag der mündlichen Prüfung: 17. April 2019

Supervisors

Prof. Dr. Thomas Lux
Institute for Economics, University of Kiel
Chair of Monetary Economics and
International Financial Markets
Olshausenstrasse 40, 24118 Kiel, Germany,
Tel: +49 431 880 3661
E-mail: thomas.lux@bwl.uni-kiel.de

Prof. Dr. H.-W. Wohltmann
Institute for Economics, University of Kiel
Chair of Macroeconomics
Olshausenstrasse 40, 24118 Kiel, Germany,
Tel: +49 431 880-1446
E-mail: wohltmann@economics.uni-kiel.de

Contents

List of Tables

List of Figures

Notation and Abbreviations for Chapter 2

Equations	
APR	actual profit rate
AQ	Tobin's Q adjustment
FQ	fundamental value of Tobin's Q
IC	inflation climate
IF'	investment function in the model with only a real sector
IF	investment function in the model with both sectors
NPR	normal rate of profit
OG	output gap
PC	Phillips curve
PS	profit share
R1	restriction on the parameters ensuring economically meaningful dynamics
R2	restriction on the parameters ensuring a limit cycle behavior of the system
RP	risk premium
SE	sentiment evolution
TR	Taylor rule
Variables	
Y	real output

Y^o	potential real output
C	real consumption
K	amount of fixed capital
I	real investment
I_n	real investment net of depreciation
g	real investment rate
g^o	long-run real investment rate and growth rate of the economy
p	price of real sector good and fixed capital
h	profit share in output
h^o	long-run profit share in output
l	labor share in output
δ	fixed capital depreciation rate
u	output-capital ratio
u^o	normal rate of capital utilization
y	output gap
σ	savings rate out of disposable income
σ_f	profit retention rate
r	actual profit rate
r^n	zero output gap profit rate
r^o	profit rate at the long-run profit share and at a zero output gap
x	sentiment index
Υ^f	markup factor on expected unit labor cost
w^e	expected nominal wage
z	labor productivity
π	real sector inflation rate
π^c	inflation climate in the real sector

π^*	central bank inflation target
L	amount of labor employed to produce Y
L^o	amount of labor needed to produce Y^o
e	employment gap
ω	real wage
q	Tobin's Q – the ratio of liabilities to assets
q^f	equilibrium value of Tobin's Q
p_e	share price
E	number of shares outstanding
M	loans outstanding
m	ratio of loans to replacement cost of fixed capital
q_e	ratio of equity to replacement cost of fixed capital
g_e	growth rate of the number of shares outstanding
$\hat{p_e^*}$	$\hat{p_e}$ such that the the value of the firms (Tobin's Q) does not change
r^{net}	profit rate net of interest payments
r_e	return on equity
r_e^f	fundamental r_e that leaves the value of the firm (Tobin's Q) unchanged
i	base rate set by the central bank
Div	dividends as a share of equity
ξ	uniform risk premium relative to i
ξ_e	equity risk premium relative to i
ξ_m	risk premium on loans relative to riskless rate
N	number of firms

Notation and Abbreviations for Chapter 3

---

q	Tobin's Q – the ratio of liabilities to assets
q^o	long-run equilibrium value of Tobin's Q
p_e	share price
E	number of shares outstanding
p	price of fixed capital
K	amount of fixed capital
L	loans outstanding
λ	ratio of loans to replacement cost of fixed capital
λ^o	a conventional fixed value of the debt to asset ratio
e	ratio of equity to replacement cost of fixed capital
g	fixed capital investment rate
g_L	growth rate of loans outstanding
g_E	growth rate of the number of shares outstanding
g	fixed capital investment rate
π	real sector inflation rate
π_e	stock price inflation rate
π_e^o	π_e such that the the value of the firm (Tobin's Q) does not change

r	firm profit rate net of fixed capital depreciation
r_e	return on equity
r_e^o	fundamental r_e that leaves the value of the firm (Tobin's Q) unchanged
i	loan interest rate
τ_c	corporate income tax rate
τ_v	production tax rate
d	ratio of dividends to capital stock
d_e	ratio of dividends to stock market value
s_f	after-tax profit retention rate
s_f	after-tax profit retention rate
ξ_e	equity risk premium relative to the loan rate
ξ_f^A	a premium chosen for convenience in the specification of model A
ξ_f^B	a premium chosen for convenience in the specification of model B
β	the fraction of loans in the portfolios of rentiers
β^*	a desired fraction of loans in the portfolios of rentiers
ε	the fraction of equity in the portfolios of rentiers
ε^*	a desired fraction of equity in the portfolios of rentiers
Y	real output
h	profit share in output
δ	fixed capital depreciation rate
u	output-capital ratio

Notation and Abbreviations for Chapters 4 and 5

General Symbols	
$\approx$	is approximated as
$\sim$	is similar to
$\overset{iid}{\sim}$	is identically and independently distributed according to
$\equiv$	is identical to
$>>$	is much greater/larger than
$\Rightarrow$	that leads to
$\langle X \rangle$	the expectation of X
$\langle X \rangle_{\text{null model}}$	the expectation under the referenced null model
$\sigma[X]$	the standard deviation of X
$\sigma[X]_{\text{null model}}$	the standard deviation of X under the referenced null model
$\mu[X]_{\text{null model}}$	the rescaled quantity of X under the referenced null model
Abbreviations	
ANND	Average degree of the nearest neighbors
ANNS	Average strength of the nearest neighbors
APR	Equation for the actual profit rate
AQ	Equation for the adjustment of the actual value of Tobin's Q
BiBCM	Bipartite Binary Configuration Model

BiCM	Bipartite Configuration Models
BiECM	Bipartite Enhanced Configuration Model
BiWCM	Bipartite Weighted Configuration Model
(U)BCM	(Undirected) Binary Configuration Model
(U)BRG	(Undirected) Binary Random Graph Model
CM	Configuration Models
DBCM	Directed Binary Configuration Model
DECM	Directed Enhanced Configuration Model
DWCM	Directed Weighted Configuration Model
ERG	Exponential Random Graph
(U)ECM	(Undirected) Enhanced Configuration Model
e-MID	Italian Market for Interbank Deposits
FQ	Equation for the fundamental value of Tobin's Q
IC	Equation for the dynamics of the inflation climate
IF'	Investment function with exogenous profitability benchmark
IF	Investment function with borrowing conditions
NPR	Equation for the normal rate of profit
OG	Equation for the output gap
PC	Phillips curve
PS	Equation for the profit share
R1	Parameter restriction excluding corner solutions
R2	Parameter restriction producing limit cycles
RGM	Random Graph Model
RMT	Random Matrix Theory
Sec.	Section
RP	Equation for the dynamics of the risk premium

SE	Equation for the dynamics of the overall economic sentiment
TR	Equation for the Taylor rule
(U)WCM	(Undirected) Weighted Configuration Model
(U)WRG	(Undirected) Weighted Random Graph Model

Acknowledgements

First of all, I would like to thank my supervisor Professor Dr. Thomas Lux for his guidance and tremendous support during my doctoral studies. I am also grateful to Prof. Dr. Hans-Werner Wohltmann for his willingness to be my second supervisor. In addition, I wish to thank the doctoral Programme "*Quantitative Economics*" at Kiel University and the state of Luxembourg for its financial support during the first two years of my doctoral studies. Special thanks goes also to my two other collaborators Dr. Luu Duc Thi and Dr. Reiner Franke for their great contributions in our joint projects. I also would also like to mention here my family and my girlfriend. This thesis would not have been possible without their love, encouragement, and financial support.

Preface

This thesis comprises four essays. The first two essays develop macroeconomic models of the financial and real sectors, while the second two essays employ novel methods for describing and interpreting existing data on business sentiment and interbank credit relations. The thesis is organized in a book format with the following chapters:

- Chapter 1: Introduction

- Chapter 2: A Pro-cyclical Stock Market under a Counter-cyclical Monetary Policy in a Model of Endogenous Business Cycles.

- Chapter 3: On the Long-Run Equilibrium Value of Tobin's Average Q (*with Dr. Reiner Franke*).

- Chapter 4: Structural Correlations in the Italian Overnight Money Market: An Analysis Based on Network Configuration Models (*with Dr. Luu Duc Thi and Prof. Dr. Thomas Lux*).

- Chapter 5: An Analysis of Systemic Risk in Worldwide Economic Sentiment Indices (*with Dr. Luu Duc Thi and Prof. Dr. Thomas Lux*).

- Chapter 6: Summary and Outlook.

Chapter 1

Research Questions, Approaches and Methodology

This thesis is based on four essays which can be organized in two parts. The first two essays (chapters 2 and 3) develop a particular approach to the relationship between the real and the financial sectors based on Tobin's average Q (see Tobin (1969) and Tobin and Brainard (1976)). Chapter one explores the interactions of the two sectors with monetary policy in a model of endogenous business cycles rooted in the real sector. Chapter two is concerned with different determinants and specifications of the long-run value of Tobin's average Q in the context of economic growth. This work also contributes to the existing literature on the empirical applications of network theory (chapter 4) and random matrix theory (chapter 5) to economic and financial complex systems. I will now provide an overview of the research questions, approaches and methodology in the four essays comprising the thesis, while the main findings are summarized in the last chapter together with an outlook.

First Essay: A Pro-cyclical Stock Market under a Counter-cyclical Monetary Policy in a Model of Endogenous Business Cycles

The real sector of the economy is not independent from the financial sector. On the one hand, the financial sector sets the borrowing conditions in the economy depending on the performance of the real sector and, on the other, the performance of the real sector depends on the borrowing conditions. In order to be able to better understand the evolution of the financial sector over the business cycle, it can be useful to have a dynamic model which incorporates the above-mentioned interdependence and which can reflect the inherent cyclical

nature of macroeconomic data (see Beaudry et al. (2016), for example). For this purpose, in the first essay, an endogenous business cycle model that deals with the real sector is combined with a model of the financial sector based on Tobin's Q (see Tobin (1969) and Tobin and Brainard (1976)). We calibrate the model to fit key properties of the data from the last 25 years. One distinct goal of this essay is to provide potential explanations for the co-movement (often observed in the data) of macro-variables like the output gap, the real base interest rate and stock market indices over the business cycle.

The market value of a firm depends on the profits it is able to generate, but is also affected by the currently prevailing opportunity cost of capital as a benchmark of profitability. Since monetary policy strives to affect this opportunity cost and, more generally, the borrowing conditions in the economy, it plays a role in the determination of the value of the firms in the real sector. Therefore, the evolution of the stock market over the business cycle depends on the behavior and success of monetary policy. Our model explores this potential link between a particular observed behavior of the stock market and monetary policy over the business cycle and the effectiveness of the central bank's attempts to affect the borrowing conditions in the economy.

The recent contributions on business sentiment and expectations dynamics, like the ones by Akerlof and Shiller (2009), Lux (2009) or De Grauwe (2012b), clearly demonstrate the importance of the explicit modelling of the formation of expectations for the understanding of real world macroeconomic business cycle dynamics. In light of these revelations, we formulate an endogenous business cycle model of the real sector in which the sentiment dynamics of the firm expectations about future demand take center stage (similar to Franke (2008 and 2012)). The firms mimic each other's demand expectations (based on their current accuracy) as a means to deal with uncertainty and because the performance of the individual firms depends on the expectations of the rest of the firms in the model. The extent of heterogeneity (or the structure) of the demand expectations thus becomes dynamic, meaning that it varies over of the business cycle, as the firms coordinate towards a particular type of expectation. This gives rise to a strong non-linearity in the model, allowing for the emergence of limit cycles over a wide range of parameter values.

In terms of the modeling of expectations, we refrain from using model consistent "rational expectations" for the following reasons. Firstly, for the agents to be forward looking in the "rational expectations" sense, they need to be operating within a simple well defined dynamic environment with easily quantifiable outcomes and probabilities. In reality, the

agents are interacting within a complex dynamic socio-economic system characterized by fundamental uncertainty (cf. Lavoie (2014, Section 2.2), for example). From an empirical point of view, "rational expectations" are generally rejected by the data (see Lovell (1986)) and dynamic models in which forward looking components are given a significant weight have a hard time replicating the strong persistence observed in macroeconomic data (see Franke et al. (2015), for example). Finally, studies show that firms actually employ simple adaptive rules when making their investment, production and pricing decisions (see Artinger et al. (2015), for example). We are therefore opting for expectation formation approaches with a tighter correspondence to the requirements of the environment and to the behaviour observed in real world economic systems.

The model of the real sector is investment-driven. This is motivated by the observation that in modern economies the availability of finance in excess of earnings (and without reference to savings) allows investment to be largely an autonomous variable (Kregel (1973, pp. 159-160)). The dynamics of the model are characterized by positive feedback dominating the economy locally. On the one hand, investment is affected by sentiment and, on the other, as a component of aggregate demand, investment plays a key role in the formation of future sentiment. An endogenous evolution of profitability - driven by the cost of factor labor over the business cycle - plays the role of a globally stabilizing force. The dynamics of the profit share are extracted from the interaction of a wage and a price Phillips curves. This modeling decision is inspired by the observed regularities, i.e. a distinct phase shift, concerning the evolution of the profit share over the business cycle. In this sense the model resembles the Goodwin (1982) model. This setting allows for complex realistic macroeconomic dynamics without the presence of shocks. The model of the real sector can also be viewed in the context of the recent contributions by Paul Beaudry et al. providing evidence of a deterministic cycle in the US (see Beaudry et al. (2016) and Beaudry et al. (2015)). The dynamic heterogeneity of the expectation structure can be viewed as an alternative theoretical approach to the "strategic complementarities" used in Beaudry et al. (2015).

The model of the financial sector has three components. A central bank attempts to control the borrowing conditions (or the opportunity cost of capital) in the economy via a Taylor (1993) rule. A no-arbitrage condition, equalizing the return on equity (within a given period of time) to the risk-adjusted opportunity cost of capital, yields a fundamental value of the firms in the real sector. In each period the financial markets drive equity prices towards the respective fundamental value at a certain speed. The measure of the value of a firm

used in the model is Tobin's average Q (see Tobin (1969) and Tobin and Brainard (1976)). Finally, the risk premium in the economy is made endogenous by allowing it to depend on the performance of the real sector. This is inspired by the idea that "success breeds a disregard of the possibilities of failure" (Minsky (1986, p. 237)) in the sense that good firm performance over time can lead to laxer borrowing conditions (low risk premium) which might bring about overinvestment. An endogenous risk premium of a similar kind has already been implemented in a macro-model by Scheffknecht and Geiger (2011), for example. In their model, however, the risk premium depends on additional factors like the past variability of different macro-variables.

In our model, the real sector affects the financial sector in two ways. Both channels affect the value of the non-financial firms in the same direction. Firstly, the value of the firms in the real sector represented by Tobin's Q is affected by the profits they generate, as this allows for higher dividends and/or investment in fixed capital. Secondly, the risk premium on loans is inversely related to the profitability of the firms in the real sector, which leads to the second positive effect of profitability on the value of the firms, since a fall (rise) of the risk premium decreases (increases) the opportunity cost of capital. Similar relationships between the opportunity cost of capital or the real interest rate and the value of a firm have previously been used in other macro models (see, for example, Kontonikas and Montagnoli (2006)).

On the other hand, the real sector is linked to the financial one via the investment decision of the firms. They consider the cost of borrowing relative to current profits. Thus, in our model, there exists a positive feedback loop between firm performance and the borrowing conditions in the economy which operates via the risk premium on loans. This channel is similar to the "cost effect" discussed in Lengnick and Wohltmann (2016, 2013), however, here the changes in the cost of capital go into the investment decision of the firms, while in Lengnick and Wohltmann (2016, 2013) they go into their pricing decisions in the goods market. In our work, the interaction between the two sectors involves the cost of borrowing rather than the amount of credit extended. An alternative approach is to use the variations in the value of the firms directly to introduce a wealth effect on the household level (see Kontonikas and Montagnoli (2006), Bask (2011), Westerhoff (2012), Naimzada and Pireddu (2013)) or an effect pertaining to the amount of collateral and thus external finance available to the firms (see Scheffknecht and Geiger (2011) or Ryoo (2010)). We do not model an independent consumption vs saving decision on the household level, because this would lead to issues

related to potential differences in desired saving and investment that would also have to be addressed in the model. Our starting point is an investment driven model, because in terms of the impact on the overall economy, the financial sector appears much more relevant for firm investment decisions than for household consumption vs saving ones. For example, since in reality the richest households hold most of the stocks and at the same time have the lowest propensity to consume, any changes in stock prices or interest rates would hardly affect the overall consumption behaviour in the economy. Conversely, consumption would be affected most by changes in the disposable income of the poorest households, which are not able to save anything.

Boyan Yanovski is the sole author of this essay.

Second Essay: On the Long-Run Equilibrium Value of Tobin's Average Q

A central variable in macroeconomic growth models where firms finance their investment by debt and equities is the ratio of outside finance to the capital stock. This concept was first put forward by Kaldor (1966), who simply referred to it as the "valuation ratio", and then brought to prominence by Tobin (1969) and a number of subsequent writings, from when on it became known as Tobin's (average) Q.

In this essay a long-run equilibrium value of Tobin's Q is derived in the context of economic growth. At the heart of the derivation lies a no-arbitrage condition involving a comparison of the fundamental return on equity with the riskless base interest rate set by the central bank. We take into account that equity is not riskless by adjusting the base interest rate by a risk premium associated with equity risk. This approach involves the concept of a benchmark stock price inflation. It can be understood as the stock price inflation implied by the financing decisions of the firms and by the inflation in the real sector. The financing decision refers to the financing of desired investments in fixed capital and considers retained profits and the issuance of equity and debt. The final solution for the long-run equilibrium value of Tobin's Q involves many variables of macroeconomic significance like the investment rate, the profit rate, inflation, corporate taxes, the base interest rate, an equity risk premium and the debt to asset and equity to asset ratios. A simplified version of this framework is used in Chapter 2 when modelling the links between the financial and the real sectors.

Since Tobin's Q and the debt to asset and equity to asset ratios are not independent, we consider two specifications of the long-run fundamental value. In the first specification it depends on a fixed debt to asset ratio, while in the second a balanced portfolio argument is invoked which leads to a representation involving the desired fractions of equity and loans in the portfolios of rentiers.

We calibrate the model by using US macroeconomic data and investigate the sensitivity of the long-run equilibrium value of Tobin's Q under the two specifications to different values of the equity risk premium.

The essay has been written by myself together with Dr. Reiner Franke. The two authors contributed equally to the essay.

Third essay: Structural Correlations in the Italian Overnight Money Market: An Analysis Based on Network Configuration Models

Understanding the topological structure of complex systems is crucial in many areas, e.g. in ecology, physics, neuroscience, epidemiology, economics, and finance. In this essay we analyze the structural correlations in a particular financial system, i.e. the Italian electronic market for interbank deposits (e-MID). While some of the network properties of the e-MID market have been previously studied (see, for example, De Masi et al., 2006; Fricke, 2012; Fricke et al., 2013; Finger et al., 2013; Fricke and Lux, 2015a; Fricke and Lux, 2015b; Squartini et al., 2015; Cimini et al., 2015a), what is novel in our essay is that: (i) we provide a more comprehensive analysis of the structural correlations in all versions of the network, and employ both local as well as global measures for analyzing such patterns; (ii) we employ configuration models to investigate whether the intrinsic node heterogeneity represented by the degree sequence (in the binary network) and/or strength sequence (in the weighted network) can explain higher order structural correlations observed in the system; (iii) we utilize the so called Directed Enhanced Configuration Model as a null model for the directed weighted version of the network, which makes use of the available information about the direction of the edges in the network.

In the field of network theory, statistics pertaining to properties related to single nodes, linked node pairs and linked node triplets are often referred to as structural correlations of

the first, second and third order respectively. The study of these structural correlations is one of the most common approaches for examining the properties of a network. The degrees and strengths of the nodes in a network are examples of first order structural correlations. The degree of a node is the sum of the connections it has to other nodes, while the strength of a node is the sum of the connections weighted by their intensities. Statistics pertaining to properties related to linked node pairs reveal information about the type of mixing (assortative vs disassortative) that takes place in the network, while those related to linked node triplets are indicative of the clustering behavior.

In terms of second order correlations, a network would exhibit assortative mixing if its nodes are predominantly connected to other nodes having similar degrees or strengths. In contrast, disassortative mixing occurs when the connected nodes are dissimilar (see, for example, Newman, 2002; Newman, 2003a). This concept can be extended to directed networks yielding four mixing categories, i.e. in-in, in-out, out-in, and in-in mixing (see, for example, Foster et al., 2010; Piraveenan et al., 2012; van der Hoorn and Litvak, 2015). It should be emphasized that, in many real world networks, the mixing behavior of the directed version can differ a lot from the one observed in the undirected version. Furthermore, the same directed network can have assortative and disassortative aspects related to the mixing categories mentioned above (see, for example, Foster et al., 2010).

At the level of a single node, in the binary case, second order structural correlations can be expressed in terms of a relationship describing the average degree of the nearest neighbors (ANND) of a node as a function of that node's own degree. If the ANND is an increasing function of degree, this can be considered evidence in favor of assortative mixing. In contrast, a decreasing function would signal disassortativity.

For the whole network, the Pearson correlation coefficient between the degrees of pairs of linked nodes is often used to assess whether a network displays disassortative or assortative mixing (Newman, 2002; Newman, 2003a). This indicator is nothing else but a function of node degree and can also be expressed in terms of the measures ANND collected for the whole network.

In addition, we can decompose the overall assortativity coefficient into the contributions of each node, i.e. we can measure the local assortativity associated with each node. Such a decomposition can reveal which nodes contribute to the overall observed mixing nature of the network and which are associated with the opposite type of mixing (see, for exam-

ple, Piraveenan at al., 2012). For instance, a globally assortative network may be locally disassortative and vice versa. It is worth noting that two networks with the same degree distribution and the same global level of assortativity may display different patterns of local assortativity.

The analysis of the second order structural correlations in the binary case can be straightforwardly extended to weighted networks by employing a measure that takes the average strength of the nearest neighbours (ANNS) of a node or by computing the Pearson correlation coefficient between the strengths of pairs of linked nodes.

As is common in the literature, we use clustering coefficients as measures of the third order structural correlations in the network. A clustering coefficient measures the tendency of two neighbours of a particular node to also be connected to each other (e.g. Newman, 2003b). If we define a node triplet as three nodes connected by at least 2 edges, then, considering a network as a whole, the transitivity ratio is equal to the number of triplets in which all three nodes are directly connected (forming a triangle) as a fraction of all node triplets (e.g. Newman, 2003b). An alternative measure is proposed by Watts and Strogatz (1998), which can capture the observed local clustering. The average of these local clustering coefficients can be used as an alternative measure of clustering for the whole network. The difference between the transitivity ratio and the average clustering coefficient is that, while in the former we calculate the ratio of the means, in the latter we take the mean of the ratios. In addition, for the directed version of a network, it is useful to differentiate between different relationship types depending on the direction of the edges in a triangle, i.e. inward, outward, cyclic, and middleman relationships, since the different relationships have different implications in terms of the risk exposure the individual banks are facing and in terms of systemic risk (see, for example, Fagio, 2007; Tabak et al., 2014). In weighted networks, the weighted clustering coefficients can be formulated in several ways, depending on how we take into account the roles of the strengths and weights of the nodes in each triangle (see, for example, Barrat et al., 2004; Onnela et al., 2005; Zhang and Horvath, 2005; Holme et al., 2007). During our analysis of the evolution of the third order correlations among banks over time, we detected dramatic changes in the network structure surrounding the recent financial crisis in 2007.

To assess whether the observed higher order structural correlations in a network are typical of a network with the observed lower order structural correlations, we employ a randomization procedure based on the observed lower order patterns in the attempt to arrive at a suitable null model to test against for non-random patterns. Such null models create a whole ensem-

ble of networks out of a subset of the information necessary to completely define the observed network. This is why this technique can also be used for filling in unavailable information. The most basic null models are the random graph models (RGM), which specify only global constraints such as the node degree average in the binary case or the node strength average in the weighted case. Since in these models, all nodes are treated homogeneously, there is no difference between the expected topological properties across nodes, which does not happen often in real world networks. In order to capture the intrinsic heterogeneity in the capacity of the individual nodes, a popular approach is to generate the microcanonical ensemble of networks having exactly the same degree sequence (or the same strength sequence in weighted networks) as the one in the observed network (see, for example, Maslov and Sneppen, 2002; Maslov et al., 2004; Zlatic et al., 2011). However, this "hard" approach suffers from various limitations [1]. Based on the maximum-entropy and maximum-likelihood methods, recent advances in the specification of configuration models propose a "soft" approach that enforces the constraints on average over an ensemble of randomized networks (e.g. Garleschelli and Loffredo, 2008; Squartini and Garlaschelli, 2011; Squartini et al., 2011a; Squartini et al., 2011b; Mastrandrea et al., 2014; Squartini et al., 2015). This approach allows us to sample network ensembles more efficiently and in an unbiased manner (Squartini et al., 2015). Our analysis shows that, in the binary case, the degree sequence is informative in terms of explaining the main features of the structural correlations in the e-MID network. In the weighted case, the randomized ensembles produced by the Enhanced Configuration Models, which constrains both the degree as well as the strength sequences, have a much greater predictive power than the randomized ensembles produced by the Weighted Configuration Models, which constrains only the strength sequences.

This essay contributes to the existing literature on structural correlations in financial networks by assessing the role of various local constraints in all versions of the Italian e-MID network.

The essay has been written by myself together with Dr. Luu Duc Thi and Prof. Dr. Thomas Lux. The three authors contributed equally to the essay.

[1] See Squartini and Garlaschelli (2011) or Squartini et al. (2015) for a discussion of this "hard" approach and its limitations.

Fourth Essay: An Analysis of Systemic Risk in Worldwide Economic Sentiment Indices

The analysis of business cycles in different countries is one of the fundamental issues in international economics. So far, much of the analysis is often directed at investigating the synchronization and convergence of "tangible" macroeconomic variables like GDP growth rates, unemployment rates, and so forth (e.g. Bordo and Hebling, 2003; Bordo and Hebling, 2011; Artis et al., 2011; Kose at al., 2012; Ferroni and Klaus, 2015). However, up until now, issues related to the correlations between the expectation structures across different countries have been receiving less attention.

Expectations are a key driver of fluctuations in economic activity since most economically relevant decisions have a strong inter-temporal component (e.g. investment, consumption or saving decisions). This was emphasized, in particular, by Keynes (1936), and later by Minsky (1977) and Akerlof and Shiller (2009). Empirically, such claims are supported by studies by authors like Santero and Westerlund (1996), Howrey (2001), Taylor and McNabb (2007), Carriero and Marcellino (2011), Milani (2011), van Aarle and Kappler (2012), or Milani (2014) in which the structure of the expectations is measured by sentiment or confidence indices. The expectations themselves are formed on the basis of past experience or on currently incoming information signals from the economy. We argue that "global" information signals, like the collapse of the US housing market in 2007, can lead to a homogenization of the expectation structure around the world, as such information can provide a coordination signal for a global phase of pessimistic expectations. Here, we confine ourselves to the phenomenological analysis of coordination of expectations.

This study contributes to the understanding of cross- correlations between economic and business sentiment indices worldwide. We aim to answer three main research questions: (i) how many statistically significant common factors can we extract from the joint dynamics of the sentiment indices worldwide; (ii) how well do these common factors account for the dynamics of the individual indices; and (iii) how does the weight of these factors change over time?

We analyze two data sets, i.e. the Business Confidence Index (BCI) and the Economic Sentiment Indices (ESI). In terms of methods, instead of using traditional approaches based on econometric models, we employ Random Matrix Theory (see, for example, Laloux et al., 1999; Bouchaud and Potters, 2009) and Principal Component Analysis (see, for example,

Jolliffe, 1986; Billio et al., 2012; Wang et al., 2011) to investigate the dynamics of the correlation matrix of country-specific sentiment/confidence indices. We extract the hidden factors encoded in the empirical correlations across countries by analyzing the group of eigenvalues (and their corresponding eigenvectors) deviating from the random bulk. In this way, we can capture the evolution of the statistically significant factors underlying the dynamics of the correlation matrix. The extent to which different countries are affected by these factors can be thought of as the risk of sentiment contagion that the individual countries are facing during a particular period.

In our analysis we observe that the dynamics of the sentiment indices across countries can be explained well by the evolution of a common component. However, during normal times, the sentiment in some countries can "resist" the common factor or can even, on rare occasions, "swim against the tide", meaning that we could detect a significant second factor driving the comovement of the indices.

The essay has been written by myself together with Dr. Luu Duc Thi and Prof. Dr. Thomas Lux. The three authors contributed equally to the essay.

Chapter 2

A Pro-cyclical Stock Market under a Counter-cyclical Monetary Policy in a Model of Endogenous Business Cycles

Author: Boyan Yanovski

Keywords: pro-cyclical stock market; Tobin's average Q; endogenous cycles; heterogeneous expectations; monetary policy

2.1 Introduction

The real sector of the economy is not independent from the financial sector. On the one hand, the financial sector sets the borrowing conditions in the economy depending on the performance of the real sector and, on the other, the performance of the real sector depends on the borrowing conditions. In order to be able to better understand the evolution of the financial sector over the business cycle, it can be useful to have a dynamic model which incorporates the above-mentioned interdependence and which can reflect the inherent cyclical nature of macroeconomic data (see Beaudry et al. (2016), for example). For this purpose, an endogenous business cycle model that deals with the real sector is combined with a model of the financial sector based on Tobin's Q (see Tobin (1969) and Tobin and Brainard (1976)). One distinct goal of this chapter is to provide potential explanations for the co-movement (often observed in the data) of macro-variables like the output gap, the real base interest rate and stock market indices over the business cycle. In Figure 2.1 filtered quarterly real output, stock market and real interest rate data have been suitably

re-scaled as to allow the reader to recognize potential patterns more easily.[1] Thus, Figure 2.1 does not reflect the actual *magnitude* of the fluctuations of the respective series.[2] For more information on the sources of the data and on the way the cyclical component was extracted see the appendix of this chapter (i.e. Section 2.9.4).[3]

The market value of a firm depends on the profits it is able to generate, but is also affected by the currently prevailing opportunity cost of capital as a benchmark of profitability. Since monetary policy strives to affect this opportunity cost and, more generally, the borrowing conditions in the economy, it plays a role in the determination of the value of the firms in the real sector. Therefore, the evolution of the stock market over the business cycle depends on the behavior and success of monetary policy. Our model explores this potential link between a particular observed behavior of the stock market and monetary policy over the business cycle and the effectiveness of the central bank's attempts to affect the borrowing conditions in the economy. Within the context of the model developed in this chapter, we

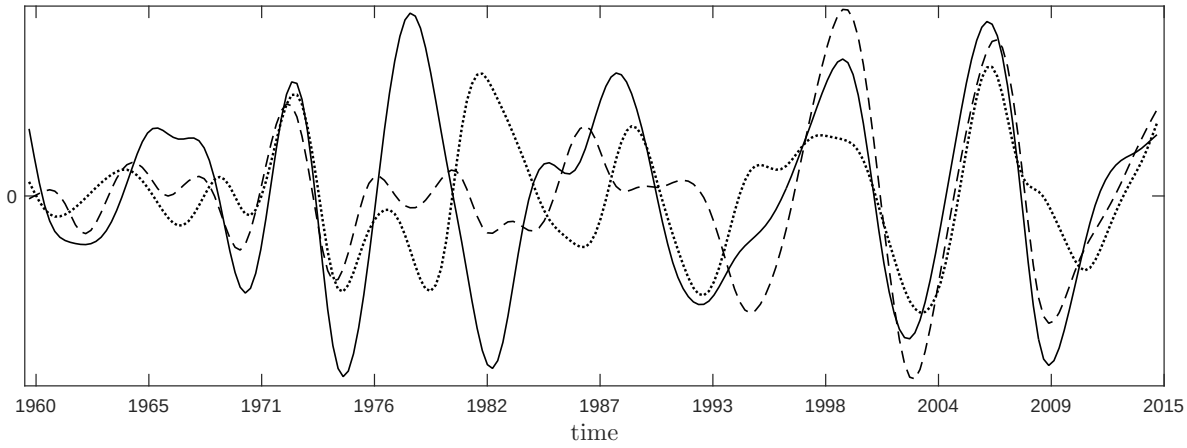

Figure 2.1: The filtered fluctuations of real gross value added of the non-financial sector (solid line), real base interest rate (dotted line) and stock price index S&P 500 (dashed line) around their respective long run trends for the US over the period (1960-2014). The fluctuations have been re-scaled to make them comparable by means of visual inspection.

[1] The real base interest rate, as well as stock market indices seem to be pro-cyclical over most of the sample period. Around the time of the two oil price shocks in the 1970s, however, this regularity breaks down. Maybe this is due to the extreme interventions of the Fed during this period.

[2] The amplitude of the fluctuations of stock market indices is generally much higher than that of the fluctuations of output.

[3] In this chapter we are mainly concerned with the relative positions of the respective variables over the business cycle and with the magnitude of their fluctuations. All the series have been manipulated using the same procedure. Because of this, these manipulation cannot bias the relative positions of the variables under consideration or the relative magnitude of their fluctuations. See the end of the appendix for plots of the raw data.

can identify three factors that contribute to the emergence of a pro-cyclical stock market in the presence of a counter-cyclical monetary policy. We interpret the comovement of the real base interest rate and the output gap in the US during the last 25 years as an indication of a counter-cyclical monetary policy.[4] The first factor is related to the potential inability of the central bank to control the borrowing conditions in the economy.[5] If we adopt the idea that the borrowing conditions are endogenous (as suggested by Minsky (1986)) and assume that the risk premium in the model changes depending on how successful the firms are, then this interdependence can potentially offset monetary policy in a way as to allow for the stock market to be strongly pro-cyclical. This explanation is also supported by data on the risk premium in the US, which is counter-cyclical (see Figure 2.5 at the end of the chapter). The second factor concerns the strength of the reaction of the central bank to inflation and output gaps. Even in the absence of an endogenous risk premium, if the real base interest rate does not change much over the business cycle, the stock market would be dominated by the fluctuations in the performance of the firms.[6] Finally, the speed at which the financial markets react to changes in the fundamentals of the economy can also impact the way the stock market behaves over the business cycle.

The idea that "success breeds a disregard of the possibilities of failure" (Minsky (1986, p. 237)) can also be modelled by using the evolution of debt in the economy rather than the evolution of the risk premium (see, for example, Ryoo (2010)). In the model developed in this chapter, the evolution of debt is not modelled explicitly, and as a result, the second key element of Minsky's financial instability hypothesis is not present in the model. That is to say, unlike Ryoo (2010) or Scheffknecht and Geiger (2011), the model developed in this chapter does not capture the fragility of economic systems with capital structures dominated by debt.

The recent contributions on business sentiment and expectations dynamics, like the ones by Akerlof and Shiller (2009), Lux (2009) or De Grauwe (2012b), clearly demonstrate the importance of the explicit modeling of the formation of expectations for the understanding of real world macroeconomic business cycle dynamics. In light of these revelations, we formulate an endogenous business cycle model in which the sentiment dynamics of the firm

[4] In the context of this paper the real base interest rate refers to the nominal base rate set by the central bank less the rate of inflation.

[5] The central bank is in control of the nominal base interest rate in the economy, while the actual borrowing conditions also depend on other factors, like, for instance, the currently prevailing risk premium.

[6] In the context of this chapter the real base interest rate refers to the nominal base rate set by the central bank less the rate of inflation.

expectations about future demand take center stage (similar to Franke (2008 and 2012)). The firms mimic each other's demand expectations (based on their current accuracy) as a means to deal with uncertainty and because the performance of the individual firms depends on the expectations of the rest of the firms in the model. The extent of heterogeneity (or the structure) of the demand expectations thus becomes dynamic, meaning that it varies over of the business cycle, as the firms coordinate towards a particular type of expectation. This gives rise to a strong non-linearity in the model, allowing for the emergence of limit cycles over a wide range of parameter values.

The model of the real sector is investment-driven. This is motivated by the observation that in modern economies the availability of finance in excess of earnings (and without reference to savings) allows investment to be largely an autonomous variable (Kregel (1973, pp. 159-160)). The dynamics of the model are characterized by positive feedback dominating the economy locally. On the one hand, investment is affected by sentiment and, on the other, as a component of aggregate demand, investment plays a key role in the formation of future sentiment. An endogenous evolution of profitability - driven by the cost of factor labor over the business cycle - plays the role of a globally stabilizing force. The dynamics of the profit share are extracted from the interaction of a wage and a price Phillips curves. This modeling decision is inspired by the observed regularities concerning the evolution of the profit share over the business cycle (see Figure 2.2 (a)). In this sense the model resembles the Goodwin (1982) model. This setting allows for complex realistic macroeconomic dynamics without the presence of shocks. The model of the real sector can also be viewed in the context of the recent contributions by Paul Beaudry et al. providing evidence of a deterministic cycle in the US (see Beaudry et al. (2016) and Beaudry et al. (2015)). The dynamic heterogeneity of the expectation structure can be viewed as an alternative theoretical approach to the "strategic complementarities" used in Beaudry et al. (2015).

The model of the financial sector has three components. A central bank attempts to control the borrowing conditions (or the opportunity cost of capital) in the economy via a Taylor rule. A no-arbitrage condition, equalizing the return on equity (within a given period of time) to the risk-adjusted opportunity cost of capital, yields a fundamental value of the firms in the real sector. In each period the financial markets drive equity prices towards the respective fundamental value at a certain speed. The measure of the value of a firm used in the model is Tobin's average Q (see Tobin (1969) and Tobin and Brainard (1976)). Finally, the risk premium in the economy is made endogenous by allowing it to depend on

the performance of the real sector.

In terms of the modeling of expectations, we refrain from using model consistent "rational expectations" for the following reasons. Firstly, for the agents to be forward looking in the "rational expectations" sense, they need to be operating within a simple well defined dynamic environment with easily quantifiable outcomes and probabilities. In reality, the agents are interacting within a complex dynamic socio-economic system characterized by fundamental uncertainty (cf. Lavoie (2014, Section 2.2), for example). From an empirical point of view, "rational expectations" are generally rejected by the data (see Lovell (1986)) and dynamic models in which forward looking components are given a significant weight have a hard time replicating the strong persistence observed in macroeconomic data (see Franke et al. (2015), for example). Finally, studies show that firms actually employ simple adaptive rules when making their investment, production and pricing decisions (see Artinger et al. (2015), for example). We are therefore opting for expectation formation approaches with a tighter correspondence to the requirements of the environment and to the behaviour observed in real world economic systems.

The remainder of the chapter is organized as follows. Sections 2.2 and 2.3 describe the model of the real sector and the financial sector, respectively. In section 2.4 we combine the two sectors. Section 2.5 discusses the factors contributing to a pro-cyclical stock market in the context of the integrated model. Section 2.6 presents a calibration of the model that fits many properties of data from the last 25 years (1989–2014). Section 2.7 concludes. The appendix consists of 5 section. Some finer details and derivations are presented in the appendix under Sections 2.9.1, 2.9.2 and 2.9.3. Issues concerning the processing of the data and its sources, as well as the parameter values used in simulations are also found in the appendix under Sections 2.9.4 and 2.9.5.

2.2 The model of the real sector

The endogenous business cycle model described in this section was inspired by a particular regularity observed in the US concerning the evolution of the profit share over the business cycle. In particular, the output gap (the cyclical component of output) seems to systematically lag behind the cyclical component of the profit share of output (see Figure 2.2 (a)).[7] We now introduce the various elements of the model of the real sector.

[7] To a smaller extent the same is true for the profit rate. Its cyclical component is still lagging behind the output gap, but only marginally so.

2.2.1 The output gap

In the following, the model is derived in continuous time. A dot ($\dot{}$) over a variable will denote its time derivative.

The output gap in the model is determined by investment via an IS-relationship. Investment is thus predetermined in the very short run. We model a one good closed economy without a government sector. In real terms current gross investment (I) has to equal savings. Real gross domestic income is given by $Y = I_n + \delta K + C$, where C stands for real consumption, I_n stands for net investment and δ and K stand for a constant capital depreciation rate and the fixed capital stock, respectively. We adopt a conventional specification of a consumption function (see, for example, Ando and Modigliani (1963)). Real aggregate consumption depends on wealth and on actual income (Y). We proxy wealth by the real capital stock (K) of the economy. We can also think about this approach in terms of Milton Friedman's permanent income hypothesis (see Friedman (1957)), since the capital stock can be considered an indicator of potential output and thus of permanent income:

$$C(K,Y) = c_1 K + c_2 Y \tag{2.1}$$

The parameters $c_1 > 0$ and $c_2 > 0$ govern the extent to which consumption depends on wealth and on actual income, respectively. One can also interpret eq. (2.1) in terms of a preference for consumption smoothing, since wealth is generally much less volatile than income.[8] Plugging aggregate consumption into the identity $Y = I + C$, yields:

$$Y = I + c_1 K + c_2 Y \tag{2.2}$$

After dividing both sides by K and solving for the output capital ratio $u = Y/K$ we get:

$$u = \frac{g + \delta}{1 - c_2} + \frac{c_1}{1 - c_2} \tag{2.3}$$

Where g is the net investment rate under the assumption of a constant capital depreciation rate (δ). In other words, the capital stock grows at the rate $g = \dot{K}/K$, where $\dot{K} = I_n$ stands for the change in capital stock. At this point we have to impose the restriction $0 < c_2 < 1$.

[8] By making aggregate consumption depend on the capital stock in the economy we can easily account for the stylized fact that consumption is less volatile than output. In the context of a business cycle model with capital, this is a very simple device for achieving that effect. The author believes that this assumption is reasonable at this level of abstraction and for the focus of this paper. In particular, because the capital stock can be considered an indicator of potential income.

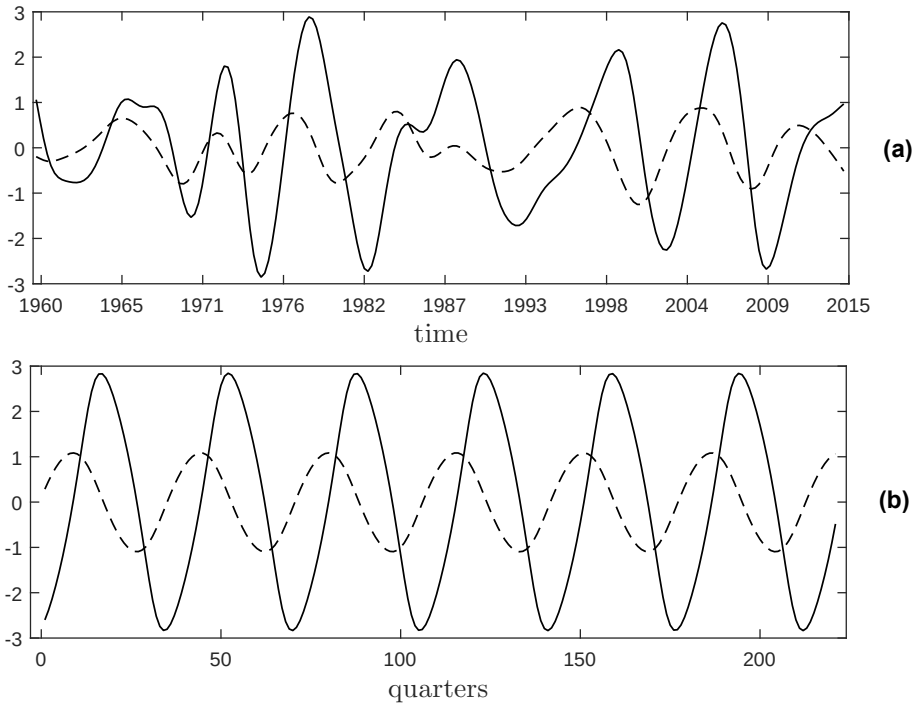

Figure 2.2: **(a)** – The fluctuations of the profit share (dashed line) and of real gross value added of the non-financial sector (solid line) around their respective long-run trends for the US; **(b)** – The fluctuations of the profit share (dashed line) and of real output (solid line) generated by a simulation of the model of the real sector. The dashed line corresponds to the evolution of $h-h^o$, because of this it fluctuates around 0.

If we assume that on average in the long-run the capital stock in the economy exogenously grows at the rate g^o, then the "normal" rate of utilization is given by $u^o = (g^o+\delta)/(1-c_2)+c_1/(1-c_2)$. For simplicity, we assume here that since the firms grow on average by g^o, they also observe on average a utilization rate associated with g^o (via eq. (2.3)) and perceive it as "normal". Additionally, we assume that $c_1 = u^o(1-c_2)-g^o-\delta$ to ensure that consumption out of wealth would be such that, on average, the normal utilization rate u^o is realized, i.e. we impose in eq. (2.3) that $\frac{g^o+\delta}{1-c_2}+\frac{c_1}{1-c_2}=u^o$. Generally, in the context of the current research question we are interested in the business cycle dynamics produced by the model (i.e. the fluctuations of u around u^o) and we do not focus on the long-run relationships implied by the model. However, in 2.9.3 we sketch the long-run adjustment process implied by the model for the case when $c_1 \neq u^o(1-c_2)-g^o-\delta$. There we make the long-run growth rate of the economy (g^o) endogenous and discuss why in the model the firms always observe the utilization rate u^o on average in the long-run even for $c_1 \neq u^o(1-c_2)-g^o-\delta$.

Define potential output as $Y^o := u^o K$ and the output gap as $y := (Y-Y^o)/Y^o$, so that $y =$

$(u-u^o)/u^o$. We can then solve eq. (2.3) for the investment driven output gap (**OG**):

$$y = \frac{g-g^o}{(1-c_2)\,u^o} \tag{OG}$$

It is assumed that due to the presence of excess capacity (not explicitly modeled here) output is able to immediately adjust to aggregate demand. In other words, the "normal" output-capital ratio u^o represents a situation in which not all of the capital is being used to produce the respective amount of output. We assume, for simplicity, that there is an upper limit of utilization $\bar{u}$ after which the output cannot be accommodated by the existing capital stock and that the model economy never reaches this limit. We also assume that labor is perfectly flexible. Labor demand has an effect on the real wage in the economy, but the necessary amount of labor is always supplied to accommodate the aggregate demand for the real sector good Y (see Section 2.2.3).

It is worth noting, at this point, that the overall savings rate in the economy ($\sigma = I/Y$) is endogenous in this setting. We can solve eq. (2.2) for σ. After some algebra we arrive at:

$$\sigma = 1 - c_2 - \frac{c_1}{(1+y)\,u^o} \tag{2.4}$$

We see that the savings rate is pro-cyclical ($\partial\sigma/\partial y > 0$), which is in line with the idea of consumption smoothing.[9]

2.2.2 The investment function

We employ a slightly modified Bhaduri and Marglin (1990) investment function. The aggregate net investment rate (g) depends, on the one hand, on the current expectation structure (x) across firms (regarding future demand) and, on the other, on the currently prevailing normal rate of profit (r^n):

$$g = f(x, r^n) \tag{2.5}$$

Where $\partial g/\partial x > 0$ and $\partial g/\partial r^n > 0$.

Next, we look at the two components determining investment in more detail.

[9] The endogenous savings rate is able to mitigate the unrealistically strong multiplier effect of a constant savings rate in IS-relationships. For a discussion on the strength of the multiplier under a constant savings rate see, for example, Franke (2015a).

The normal rate of profit

Define Π and Π_a as gross profit in real terms and gross profit adjusted for depreciation in real terms ($\Pi_a := \Pi - \delta K$), respectively. The actual gross profit rate in the economy is defined as $r := \Pi_a / K$. We can express the real gross profit adjusted for depreciation as $\Pi_a = Y - \delta K - (1-h)Y$, where $h := \Pi / Y$ is the profit share and $(1-h)$ is the labor share. After dividing by K and recalling that $(u = Y/K = (1+y)u^o)$ we arrive at:

$$r = h(1+y)u^o - \delta \tag{APR}$$

The normal rate of profit is the profit rate associated with normal utilization (u^o) or, in other words, with a zero output gap ($y = 0$):

$$r^n = h u^o - \delta \tag{NPR}$$

This profit rate concept is often associated with the Bhaduri-Marglin investment function (see Bhaduri and Marglin (1990)). In the investment function (see eq. (2.5)), the firms first consider how much to invest in order to avoid over/under-utilization given their expectations about future demand (captured by the expectation structure (x)). In the second step, they consider the profitability of that investment provided they were able to avoid over/under-utilization. The corresponding measure of profitability is thus r^n.

Finally, aggregate demand (Y) is assumed to be accommodated by the firms according to their capital stock, such that the output capital ratio (u) and the output gap (y) are the same across all firms. This implies that the actual rate of profit (r) also does not vary across firms.[10]

The structure of the expectations

The firms in the model are heterogeneous with respect to their expectations about the future demand (and the associated future utilization). There are two types of expectations in the model. The individual firms can either expect a positive output gap or a negative one (meaning under- or over-utilization).[11] The key point in this framework is that the

[10] Even though the profit rate is assumed to be identical across firms, the firms still have an incentive to correctly guess future demand, since the profit of each firm in absolute terms depends on this (see section 2.2.2). The same profit rate is applied to capital stocks that can differ across firms.

[11] Introducing fixed magnitudes as demand expectations or a continuous distribution of expectations (as opposed to the current specification in which there are two types of expectations that represent intervals:

firms influence each other when forming their expectations. The currently observed output gap (y) is seen as evidence in favor of the expectation of the firms that predicted demand correctly (these are the firms with an expectation matching the sign of y). Accordingly, the firms that got it wrong adjust their expectations towards the expectation of the firms that got it right. In other words, the key assumption here is that information (in this case the observed output gap) is not independent of the agents in the economy. Information rather flows through the firms as they influence each other when forming their expectations. This assumption is in the spirit of the idea of ecological rationality (see, for example, Simon (1955) or Lavoie (2014, Section 2.2)). In the model as a whole we also have the case that the performance of the individual firms is influenced by the expectations and investment of the rest of the firms in the economy, because (as discussed in the next paragraphs) positive expectations translate into high aggregate investment which results in high aggregate demand for all firms. It is thus rational for the firms to mimic each other's expectations. The above approach was first introduced in the field of economics by Lux (1995) in the context of speculative trading in financial markets. It has then later been used for modeling sentiment dynamics in the real sector of the economy by Franke (2012). An empirical validation of the approach using business survey data can be found in Lux (2009). This modeling decision is also similar to the one implemented in De Grauwe (2012a), for instance, where agents employing a fundamentalist rule interact with agents employing a backward-looking rule of thumb. Both approaches make use of the non-linearities naturally emerging from the fact that the extent of heterogeneity in a population is limited. The modeling method used in this chapter is able to capture these kind of non-linearities and is, at the same time, simple enough to be mathematically tractable under certain conditions (see Section 2.9.1 of the appendix). Interacting agents are also often used to model exchange rate and stock market dynamics (see, for example, Lux (1998) or De Grauwe and Kaltwasser (2012)).

A natural consequence of this framework is that the heterogeneity of the population of firms with respect to their expectations becomes dynamic. For an intuitive understanding of the non-linearities involved consider the following two extremes. In the first extreme all the firms have the right expectation (e.g. the observed output gap is positive ($y > 0$) and all the firms expect it to be positive). In this case further confirmations of the dominant expectations would have no impact on the *structure* of the expectations (x). In the other extreme half the firms expect a positive output gap, while the other half expects a negative one. In this

$y > 0$ or $y < 0$) would not change the setting conceptually. Because of this, we stick to the simplest possible specification.

case the observed output gap (y) would have a very strong impact on the *structure* of the expectations (x) because there is a large pool of firms that can switch to the expectation that matches the sign of y.

Figure 2.3 is a stylized representation of the resulting relationship between the structure of the expectations (x) and the observed output gap (y). The variable x is standardized in such a way as to take on values between -1 and 1, where the former value is associated with all firms expecting a negative output gap and the latter with all firms expecting a positive output gap (for more details see Section 2.9.1 of the appendix). Figure 2.3 combined with the investment function (eq. (2.5)) and the IS-relationship (eq. (**OG**)) shows us that in this model the relationship between the observed output gap (y) and the ensuing investment is strongly non-linear. A particular observed output gap impacts the structure (x) of the expectations about the future output gap (see next paragraph for the mathematical specification). This expectation structure is associated with a particular investment (via eq. (2.5)), which is in turn associated with a realization of the next output gap (via eq. (**OG**)).

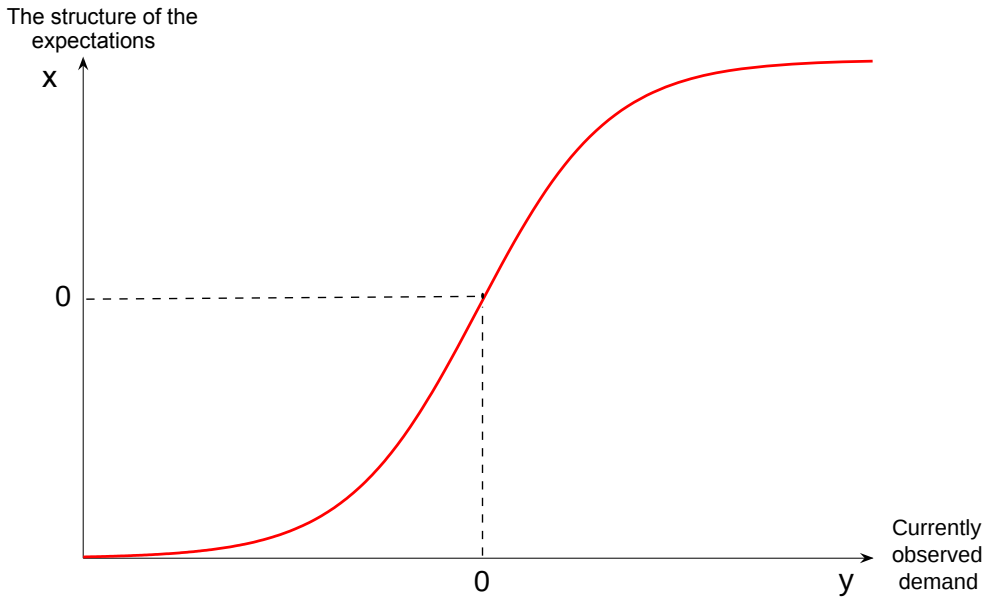

Figure 2.3: A stylized representation of the relationship (resulting from eq. (**SE**)) between the structure of the demand expectations in the economy and the observed demand.

A mathematical translation of these ideas can be made by using a framework developed by Weidlich and Haag (1983). Formally, the relationship between the structure of the expectations (x) and the observed output gap (y) can be represented by the following differential

equation:[12]

$$\dot{x} = \nu \left[(1-x) \exp(\vartheta_y y) - (1+x) \exp(-\vartheta_y y) \right], \quad -1 \leq x \leq 1 \tag{SE}$$

This equation is derived in the appendix in Section 2.9.1. The positive parameter ϑ_y governs the strength with which the signal (y), as opposed to the idiosyncratic characteristics of the firms, affects their decisions to switch from one expectation to another. The positive parameter ν, on the other hand, determines how quickly the switching takes place.

Next, let us aggregate investment so as to arrive at the aggregate net investment rate g (see eq. (2.5)). $E^j(y)$ denotes firm j's expectation about future demand.[13] On average, each firm invests at a positive rate g^o due to labor augmenting technical progress. Firm j's net investment rate (g_j) depends on the normal profit rate (r^n). Whenever profitability (r^n) exceeds a certain threshold r^o, this results in additional investment. We keep r^o constant for now.[14] We define this threshold as $r^o = h^o u^o - \delta$, where h^o stands for a "normal" profit rate around which the economy fluctuates ($0 < h^o < 1$).[15] In addition, an expectation about a positive (negative) output gap is associated with a higher (lower) investment rate. The parameters g^o, ϕ_x and ϕ_r are all positive and uniform across firms. The investment function of firm j is specified as:

$$g_j = g^o + \phi_r (r^n - r^o) + \begin{cases} \phi_x & \text{if } E^j(y) > 0 \\ -\phi_x & \text{if } E^j(y) < 0 \end{cases}$$

For a given profitability r^n (and later for given borrowing constraints) the investments under the two expectations ($E^j(y) < 0$ and $E^j(y) > 0$) should be viewed as the minimum and maximum feasible investment, respectively. Ultimately, investment in fixed capital is constrained by factors like technology, available internal finance and borrowing conditions from above and new technology integration and long-term survival from below. These constraints are not explicitly modelled here.

[12] Figure 2.3 shows the relationship between the structure of the expectations (x) and the observed output gap (according to eq. (**SE**)) after the adjustments of x have finished. In other words, Figure 2.3 shows the relationship between x and y if we impose $\dot{x} = 0$ and solve eq. (**SE**) for x.

[13] When the expectation $E^j(y)$ is formed, y is not yet observable. The realized output gap y is the result of investment made on the basis of $E^j(y)$ among other things.

[14] This threshold will later be made endogenous (in the presence of a financial sector) and will reflect the currently prevailing borrowing conditions in the economy.

[15] Since it enters r^o, the parameter h^o can also be understood as a benchmark profit share which governs the profitability requirement of the firms for expanding their business (investing).

Across the N firms the aggregate net investment rate is approximately $g = (\sum_{j=1}^{N} g_j)/N$. The approximation is good if the inequality in the distribution of the capital stock across firms is not too extreme. We use this approximation in order to avoid having to track the capital stock of all firms over time[16]. The same aggregation approach is used in Franke (2012). Define the fraction of firms expecting a positive output gap as n^+. Then the aggregate net investment rate becomes:

$$g = g^o + \phi_r (r^n - r^o) + n^+ \phi_x - (1 - n^+) \phi_x \tag{2.6}$$

The variable describing the structure of the demand expectations is defined as $x := n^+ - n^-$, where n^- stands for the fraction of firms expecting a negative output gap ($n^- = 1 - n^+$). The aggregate investment function can thus be written as:

$$g = g^o + \phi_r (r^n - r^o) + \phi_x x \tag{IF$'$}$$

2.2.3 The evolution of profitability

As discussed in the previous section the normal rate of profit (r^n) is one of the two driving forces of investment in the model. In section 2.2.2 we saw that profitability itself depends on the profit share (see eq. (**NPR**)). Next, we derive the equation governing the evolution of the profit share from the dynamics of the real wage. The price and wage setting in the economy are modeled independently and later combined to arrive at the dynamics of the real wage. A similar approach has been taken, for example, in Chiarella et al. (2005, pp. 27f).

The price Phillips curve

We start by looking at the price (p) setting for the real sector good. The firms follow a mark-up pricing rule of the type $p = \Upsilon^f w^e / z$, where Υ^f strands for the mark-up factor that the firms apply, while w^e and z are the expected nominal wage and labor productivity, respectively. Labor is homogeneous, all firms pay the same nominal wage (w), apply the same mark-up factor (Υ^f) and form the same expectation about the nominal wage (w^e). In addition, assume that the observed output gap y (as a measure of aggregate demand) triggers a reaction on the part of the firms with respect to the mark-up factor Υ^f. The mark-up factor

[16] The firms are heterogeneous in terms of their current expectations, but we do not follow the path of each firm over time.

increases (decreases) if the observed output gap is positive (negative). Finally, we assume that the level of the mark-up factor also depends on the duration of the observed output gap. Hence we use a dynamic specification:

$$\hat{\Upsilon}^f = \kappa y \tag{2.7}$$

Where κ is a non-negative parameter and $\hat{\Upsilon}^f$ is the growth rate of Υ^f. Note that for $\kappa = 0$ the firms use a constant mark-up rule. The mark-up factor Υ^f is an ex ante mark-up factor that the firms use to set p. Ex post, the actual mark-up factor would also depend on the actual evolution of the nominal wage (w). When setting p the firms need to form an expectation about the evolution of the nominal wage. All firms form the same expectation about its evolution: $\hat{w}^e = \pi^c + \hat{z}$, where π^c stand for the current inflation climate in the economy, while $\hat{z}$ denotes the growth rate of labor productivity. In other words, the firms expect the nominal wage to grow by expected inflation (π^c) plus the growth rate of labor productivity ($\hat{z}$). After inserting eq. (2.7) and the nominal wage expectations ($\hat{w}^e = \pi^c + \hat{z}$) into the price setting rule expressed in terms of growth rates ($\pi = \hat{\Upsilon}^f + \hat{w}^e - \hat{z}$) we get:

$$\pi = \pi^c + \kappa y \tag{PC}$$

This is a standard representation of a Phillips curve (see, for example, Blanchard and Illing (2009)).

Next, we turn to the specification of the inflation expectations, which are assumed to be uniform across firms. The New-Keynesian Phillips curve and its hybrid form, both based on the "rational expectations" paradigm (see Roberts (1995)), are unsatisfactory from a theoretical point of view due to issue related to the coordination required to arrive at a "rational expectations" equilibrium.[17] In particular, the derivation of aggregate behavior from individual one is highly problematic (see, for example, Hildenbrandt and Kirman (1988)), which does not allow, even in theory, for a convincing motivation of the inclusion of future variables (or a certainty equivalence thereof) into macroeconomic models. Also, monetary policy interventions and long-term commitments do not really warrant the usage of the "ra-

[17] Including forward looking (in a mathematical sense) components into a model (i.e. assuming "rational expectations") even with a very small weight actually imposes an equilibrium onto the model economy in which perfect coordination takes place. Without a sound understanding of whether and how an economy characterized by great complexity could approach such an equilibrium, any results achieved by using the "rational expectations" framework are likely to be irrelevant to the economic process the researcher is trying to model.

tional expectations" approach since such news can be integrated into the specification of a model in terms of current period variables or parameters (see next paragraph). From an empirical point of view, as noted by Rudd and Whelan (2007), for example, this approach fails "to provide a useful empirical description of the inflation process."

In light of the above discussion we take the expectation formation process implemented in Franke (2012, p. 12) originally suggested by Franke (2007). The inflation climate (π^c) constitutes adaptive expectations that adjust to the observed inflation and are influenced by the central bank's long-run target inflation rate π^*. The specification allows for a very flexible inflation process:

$$\dot{\pi^c} = \alpha \left[\gamma \pi^* + (1-\gamma)\, \pi - \pi^c\right] \tag{IC}$$

The parameter α governs how quickly the climate adjustment to the observed inflation (π), while the parameter γ can be interpreted as the central bank's credibility with respect to its target inflation rate (π^*) and governs the general variability of the inflation climate. Both parameter take on values between 0 and 1. For γ close to 1 the climate is dominated by the constant target rate π^* and thus barely fluctuates, while for $\gamma = 0$ we have standard adaptive expectations.

The nominal wage Phillips curve

Define the employment gap as $e = (L - L^o)/L^o$, where L stands for the amount of labor employed to produce Y, while L^o is the amount of labor needed to produce the potential output Y^o. If we assume that labor productivity (z) is independent of output, we can rewrite the output gap as $y = (Lz - L^o z)/(L^o z)$. We see that in this case $y = e$ and thus the output gap can be considered a proxy of the labor market conditions.[18]

Next, we assume that the presence of an employment gap represents a difference in bargaining power between the workers and the firms in the economy. Whenever the workers have more bargaining power ($e > 0$) they are able to drive up the nominal wage. Accordingly, for $e < 0$ there would be downward pressure on the nominal wage. In addition, we assume that in the absence of bargaining power (i.e. $e = y = 0$) factor labor is able to negotiate nominal wage

[18] The author is aware of the empirical regularity known as Okun's law. It states that in reality employment does not move one-to-one with output. This effect can be achieved in the model by relaxing the assumption that productivity is independent of output. However, since this adds complexity to the model and since (for the purposes of this chapter) we are rather interested in the sign of the relationship (between employment and output), we simply take the output gap as a proxy of the labor market conditions.

growth reflecting the current inflation climate and the growth in labor productivity. As in eq. (8) we assume that the effect of bargaining power depends on its duration. A standard nominal wage Phillis curve satisfies these assumptions:

$$\hat{w} = \pi^c + \kappa_{nw}\, y + \hat{z} \tag{2.8}$$

Where κ_{nw} is a non-negative parameter.

The real wage Phillips curve and profitability

We can arrive at the real wage Phillips curve by combining the nominal wage with the price Phillips curve (eq. (**PC**) with eq. (2.8)). The growth rate of the real wage ($\hat{\omega} = \hat{w} - \pi$) is thus given by:

$$\hat{\omega} = (\kappa_{nw} - \kappa)\, y + \hat{z} \tag{2.9}$$

Next, we assume that the nominal wage (see eq. (2.8)) reacts more strongly to an output gap than the price of the real sector good does (see eq. (**PC**)), i.e. we assume $\kappa_{nw} > \kappa$. We can justify this assumption by arguing that the existence of bargaining power (i.e. $y \neq 0$) naturally implies that one side is likely to gains an advantage in the process of negotiations. For the firms this advantage is expressed in terms of the ability to employ labor at a lower real wage, while if factor labor has bargaining power, it can enjoy a higher real wage. Hence, for $y > 0$ ($y < 0$) the real wage increases (decreases).[19] A different way to look at this assumption is that during booms increases in the degree of competition are limiting the opportunities for price increases, while during recessions prices do not fall as quickly as nominal wages because of decreases in the level of competition.[20] However, it should be noted that such argumentation usually evolves firm entry and exit, which are not modeled here. Also, note that under a more strict assumption – that the firms use a constant mark-up factor Υ^f when setting the price of the real sector good (i.e. $\kappa = 0$) – the inequality $\kappa_{nw} > \kappa$ holds automatically. After inserting the composite parameter $\kappa_{rw} := (\kappa_{nw} - \kappa) > 0$ the real wage Phillips curve becomes:

$$\hat{\omega} = \kappa_{rw}\, y + \hat{z} \tag{2.10}$$

[19] This assumption also plays a role in other models like the one in Chiarella et al. (2005, p. 228).

[20] There is a slew of literature documenting and modeling the pro-cyclical firm entry and exit dynamics. See, for example, Jaimovich and Floetotto (2008).

The evolution of the real wage has direct implications for the evolution of the profit share (h) and thus (via eq. (**NPR**)) for the normal rate of profit (r^n). To see this we can start from the definition of the labor share: $l := (wL)/(pY) = w/(zp)$, where w, p and z stand for the nominal wage, the goods market price level and labor productivity, respectively. In terms of growth rates the labor share can be expressed as:

$$\hat{l} = \hat{w} - \pi - \hat{z} \tag{2.11}$$

After inserting eq. (2.10) in the above equation we get:

$$\hat{l} = \hat{w} - \pi - \hat{z} = \hat{\omega} - \hat{z} = \kappa_{rw}\, y \tag{2.12}$$

Finally, by recalling that the profit share can be expressed as $h = 1 - l$ and after applying some algebra we arrive at the equation governing the evolution of the profit share:

$$\dot{h} = -(1-h)\,\kappa_{rw}\, y, \qquad 0 < h < 1 \tag{**PS**}$$

Note that since p, w and Υ^f are not firm-specific, h is not firm-specific and thus the normal rate of profit (r^n) also does not differ across firms.

Equation (**PS**) describes the result of a conflict between factor labor and the firms in an economy. In this sense, it can be considered in the Post-Keynesian tradition. Stockhammer (2004, ch. 2), for example, also considers a relationship between the profit share and the conditions on the labor market. It might also be useful to draw a parallel here between the "decreasing returns to capital" that Beaudry et al. (2015) refer to as a potentially globally stabilizing force in the economy and the profitability dynamics derived in this section. The derivations of the profitability dynamics in this chapter can be consider an example of how one could theorize about the underlying mechanics. The central assumption that allows the model to function, however, is simply that such forces exist and that it takes time for them to unfold. There seems to be a consensus in the economic literature about the existence of such a stabilizing force. It is the view of the author that the particular theory used to motivate it is of secondary importance.

Equation (**PS**) also implies certain dynamics for the actual ex post mark-up factor (Υ^a). The ex post mark-up factor is simply a residual of the actual price, wage and productivity dynamics. The price of the real sector good can be expressed as: $p = \Upsilon^a\, w/z$. In terms of

growth rates this reads: $\pi = \hat{\Upsilon}^a + \hat{w} - \hat{z}$. By combining this expression with eq. (2.10) and after rearranging we arrive at the implied dynamics of the actual ex post mark-up factor:

$$\hat{\Upsilon}^a = -\kappa_{rw}\, y \tag{2.13}$$

Franke (2015b, p. 22) proposes a similar relationship for the mark-up dynamics in a different context.

Equation (**PS**) together with equation (**NPR**) determine how the normal rate of profit (r^n) evolves in the model.

2.2.4 Key features of the model of the real sector

The model of the real sector is driven by the dynamic equations (**SE**) and (**PS**) together with the contemporaneous equations (**IF′**), (**OG**) and (**NPR**):

$$\dot{x} = \nu\left[(1-x)\exp(\vartheta_y y) - (1+x)\exp(-\vartheta_y y)\right], \quad -1 \le x \le 1 \tag{SE}$$

$$\dot{h} = -(1-h)\,\kappa_{rw}\, y\,, \qquad 0 < h < 1 \tag{PS}$$

$$g = g^o + \phi_r\,(r^n - r^o) + \phi_x x \tag{IF′}$$

$$y = \frac{g - g^o}{(1-c_2)\,u^o} \tag{OG}$$

$$r^n = h\,u^o - \delta \tag{NPR}$$

$$r^o = h^o\,u^o - \delta$$

The above system greatly resembles the model developed in a similar context by Franke (2008). Since this system of differential equations is two dimensional, we can analytically explore many of its properties. This is done in the appendix (Section 2.9.2). Here we present the results of the analysis, simulate the system and provide intuition.

First, note that the system has a point of rest at $(x,h) = (0,h^o)$. The system can also have points of rest associated with corner solution involving $h = 1$ and $h = 0$. However, since such points of rest are hardly economically meaningful, we exclude the potentially attractive ones

by applying a restriction on the parameters:

$$\phi_x/\phi_r < (0.5 - |h^o - 0.5|)\, u^o \tag{R1}$$

The intuition behind this restriction is that the stabilizing forces coming from the changes in profitability via the parameter ϕ_r must be sufficiently stronger than the destabilizing forces coming from the changes in the structure of the expectations via the parameter ϕ_x. If this is the case, there are no attractive points of rest associated with the corner solutions $h = 1$ and $h = 0$. For a discussion of this issue in the context of the standard Goodwin model see Desai et al. (2006).

In the following, we only consider the parameter space satisfying (**R1**). In this case, since the system is globally stable, sustained cyclical behavior occurs if the point of rest $(x,h) = (0,h^o)$ is repelling (see Section 2.9.2 of the appendix). The condition for this being the case is:

$$2\,\nu\,\frac{\phi_x\,\vartheta_y - (1-c_2)\,u^o}{\phi_r\,\vartheta_y} > (1-h^o)\,u^o\,\kappa_{rw} \tag{R2}$$

We can identify the parameters contributing to the satisfaction of the above restriction by examining how the parameters affect the difference (D) between the two sides of the inequality (**R2**):

$$D = 2\,\nu\,\frac{\phi_x\,\vartheta_y - (1-c_2)\,u^o}{\phi_r\,\vartheta_y} - (1-h^o)\,u^o\,\kappa_{rw}$$

The derivatives $\partial D/\partial\vartheta_y$, $\partial D/\partial\nu$ and $\partial D/\partial\phi_x$ are all positive. These parameters measure the strength with which the past expectation structure affects the future expectation structure via investment (see equations (**OG**), (**IF′**) and (**SE**)). This phenomenon can be understood as a version of Harrodian instability since it describes a feedback loop between expectations and investment (see Harrod (1939)). For example, if most firms expect a positive output gap ($x > 0$), this can trigger investment (via eq. (**IF′**)), which as a component of aggregate demand drives up the output gap (via eq. **OG**), which, in turn, can make even more firms optimistic (via eq. (**SE**)). Conversely, expectations about a negative output gap can feed on themselves and can drive the output gap down. If the Harrodian instability is strong enough, endogenous business cycles occur in the model. The inequality (**R2**) is the analytic translation of this statement in the context of the current model.

The intuition behind the cyclical behavior of the model of the real sector runs as follows. During recessions, in the presence of a negative output gap, profitability increases since factor

labor is willing to accept an increasingly lower real wage in order to become employed. These increases in profitability are corrected by an increasing output gap that puts factor labor in a better bargaining position. High profitability pushes the economy out of a recession by causing more investment. Conversely, low profitability causes the economy to go into a recession by bringing about less investment. The system is locally unstable because around the zero output gap the structure of the expectations is very heterogeneous and evidence in favor of a particular type of expectation makes the structure more homogeneous, which strongly affects aggregate investment. During expansions and contractions the system is dominated by self-reinforcing expectations. The system is globally stable since the degree of homogeneity of the structure of expectations is finite. Near the boundaries characterized by perfect homogeneity (all firms having the same expectation) profitability becomes the major driving force in the economy.

In Figure 2.2 (b) the model of the real sector has been simulated under a parametrization that allows it to roughly match properties of the filtered real world data presented in Figure 2.2 (a). In particular, we see that, in the model, the output gap is lagging behind the profit share gap (which is defined as: $h - h^o$). We observe the same regularity in the filtered data (see Figure 2.2 (a)). The simulated series also roughly match the average amplitude and period of the fluctuations of the filtered real world data. See the appendix (Section 2.9.5) for the parameter values used in the simulation.

2.3 The financial sector

The financial sector we are going to introduce now comprises three components. First, we introduce the Taylor rule, with which the central bank attempts to control the borrowing conditions in the economy. We then derive a value of Tobin's Q based on the fundamentals from the real sector. The financial markets adjust towards this fundamental value of Tobin's Q. Finally, we introduce the endogenous risk premium and make it dependent on the performance of the firms in the real sector.

2.3.1 The Taylor rule

The central bank's behavior is specified in terms of a difference equation as:

$$\frac{di}{dt} = \mu_i \left[i^o + \mu_\pi \left(\pi - \pi^* \right) + \mu_y \, y - i \right] \qquad \textbf{(TR)}$$

Equation (**TR**) constitutes a standard Taylor (1993) rule with interest rate smoothing. Monetary policy reacts to inflation (diverging from its target) and to output gaps by changing the base interest rate (i). The interest rate smoothing (captured here by the positive parameter μ_i) reflects the idea that the central bank faces uncertainty that might prompt it to change the base interest rate slowly. The lower μ_i is, the slower the central bank's reaction is. The parameter i^o is the nominal base interest rate set by the central bank (in the limit, as time goes to infinity) in the absence of an output gap or a deviation of inflation from its target. We denote the time derivative of the base interest rate as di/dt to avoid placing an additional dot over the letter i.

2.3.2 Tobin's Q

It is intuitive that the stock market can be affected, on the one hand, by the performance of the real sector and, on the other, by the interest rate environment, which constitutes the opportunity cost of capital in the economy. What follows is a translation of this intuition in terms of a mathematical specification.

We now derive a value of Tobib's Q that reflects the fundamentals in the model economy. The approach used in this section was introduced in the working paper by Franke and Ghonghadze (2014). Here we derive a more general case in which the firms can finance investment by issuing equity or debt (see Franke and Yanovski (2016)). The financing decisions are assumed not to be firm-specific. In the following derivation, we consider variables on the aggregate level.

The derivation involves a concept of a benchmark stock price inflation. It can be understood as the stock price inflation implied by the financing decisions of the firms and by the inflation in the real sector.[21] To derive this benchmark value of stock price inflation we can start from the definition of Tobin's Q:

$$q := \frac{p_e E + M}{pK}$$

Where p_e is the stock price index, p is the price level on the goods market, K is the stock of fixed capital, E is the number of shares outstanding and M is the firms' stock of debt. Tobin's Q is a measure of the value of a firm since it considers the value of a firm's equity

[21] Since we have a one-good economy, the replacement value of a firm's capital stock is determined by the inflation rate in the real sector. Via this channel stock price inflation is affected by the inflation rate in the real sector.

relative to the replacement cost of the firm's capital stock and relative to the stock of debt. If we write this definition in terms of growth rates, we get:

$$\begin{aligned}\hat{q} &= \frac{q_e}{q}\hat{q}_e + \frac{m}{q}\hat{m}\,, \text{or} \\ \hat{q} &= \frac{q_e}{q}(\hat{p}_e + g_e - \pi - g) + \frac{m}{q}\hat{m}\end{aligned} \tag{2.14}$$

Where $m := M/pK$, $q_e := p_e E/pK$, $\hat{p}_e$ is the stock price inflation, g_e is the growth rate of the shares issued, g is the growth rate of the real capital stock and π is goods market inflation. By setting $\hat{q} = 0$ we can solve for $\hat{p}_e$ and get the benchmark stock price inflation:

$$\hat{p}_e^* := \hat{p}_e|_{\hat{q}=0} = \pi + g - g_e - \frac{m}{q_e}\hat{m} = \pi + g - g_e - \frac{m}{q_e}(\hat{M} - g - \pi) \tag{2.15}$$

Intuitively, setting $\hat{q} = 0$ (and solving for $\hat{p}_e$) amounts to enforcing that the equity price increases if retained profits (instead of equity or debt) are being used for financing investment. If $(\pi + g - g_e - \frac{m}{q_e}\hat{m}) > 0$, each share is now backed by more capital stock and thus the price of equity must go up.

Next, let us look at the definition of the net profit rate:

$$r^{net} = \frac{pY - W - \delta pK - (i + \xi_m)M}{pK} \tag{2.16}$$

Where i is the base interest rate set by the central bank, while $i + \xi_m$ is rate at which the firms can actually borrow. The premium ξ_m is associated with risk related to the servicing of debt. W is the nominal wage bill, pY is total nominal output and δ is the rate of capital depreciation. Next, consider the financing identity:

$$\begin{aligned}pI_n &= \sigma_f r^{net} pK + p_e \dot{E} + \dot{M}\,, \text{which can be rewritten as} \\ pI_n &= \sigma_f r^{net} pK + p_e E g_e + M\hat{M}\end{aligned}$$

Where $I_n p$ denotes net nominal investment in fixed capital and σ_f and g_e are the retention rate and the growth rate of shares outstanding, respectively. The financing identity states that investment can be financed via retained profits (the first term) or via issuing equity or

debt (the second and third terms, respectively). Solving for σ_f gives us:[22]

$$\sigma_f = \frac{g - q_e g_e - m(\hat{M})}{r^{net}} = \frac{g - q_e g_e - m(\hat{m} + g + \pi)}{r^{net}} \tag{2.17}$$

This is the retention rate needed to finance investment given the finance policy of the real sector (issuing equity, debt or retaining profits). The return on equity is given by:

$$r_e = Div + \hat{p}_e = \frac{(1 - \sigma_f) r^{net} p K}{p_e E} + \hat{p}_e$$

Where Div stands for dividends as a share of equity. The fundamental return on equity (r_e^f) is the return on equity associated with the benchmark value of stock price inflation ($\hat{p}_e = p_e^*$, see eq. (2.15)), i.e.:

$$r_e^f = \frac{(1 - \sigma_f) r^{net} p K}{p_e E} + \pi + g - g_e - \frac{m}{q_e} \hat{m} \tag{2.18}$$

Inserting eq. (2.17) in (2.18) gives us:

$$r_e^f = \frac{r^{net} - g + m g + m \pi}{q - m} + \pi + g \tag{2.19}$$

Next, we can set up a no-arbitrage condition involving a comparison of the fundamental return on equity with the riskless base interest rate set by the central bank. When doing this, however, we should take into account that equity is not riskless. We can do this by adjusting the base interest rate by a risk premium (ξ_e) associated with equity risk. The no-arbitrage condition equates the base rate (adjusted for equity risk) to the fundamental return on equity:

$$\frac{r^{net} - g + m g + m \pi}{q - m} + \pi + g = i + \xi_e \tag{2.20}$$

The fundamental value of Tobin's Q can be obtained by solving the no-arbitrage condition for q. We insert eq. (2.16) in (2.20) and solve for q to arrive at:

$$q^f = \frac{r - g + m(\xi_e - \xi_m)}{i + \xi_e - g - \pi} \tag{2.21}$$

[22] We can also derive the fundamental value of Tobin's Q by solving the financing identity for other firm decision variable (e.g. g_e). In this sense, in the context of this model, it does not matter which decision variable is chosen to be residually determined.

Where r is the gross rate of profit as defined in eq. (**APR**). Of course, this specification of the fundamental value of Tobin's Q only makes sense if $(i+\xi_e-g-\pi)>0$. We assume that this is always the case. The fundamental value of Tobin's Q is an expression of the value of the firm that satisfies the no-arbitrage condition (eq. (2.20)).

Recall that ξ_m is the premium associated with risk related to the servicing of debt. It can be argued that generally $\xi_e > \xi_m$ because debt is a senior claim as compared to equity. In the absence of a hierarchy of claims we have $\xi_m = \xi_e$. Since $m \geq 0$ and since ξ_e would fall in case there is no hierarchy of claims, the case in which $\xi_m = \xi_e$ can be considered a lower bound of the fundamental value of Tobin's Q. For simplicity, we now assume that $\xi_m = \xi_e$ in order to avoid having to model the dynamics of credit money. The uniform risk premium ($\xi = \xi_m = \xi_e$) will be modeled instead to reflect the endogenous borrowing constraints suggested by Minsky (1986) (see next subsection). The final specification of the fundamental value of Tobin's Q thus becomes:[23]

$$q^f = \frac{r-g}{i+\xi-\pi-g} \tag{FQ}$$

The interpretation of eq. (**FQ**) is straightforward. Given a particular investment rate (g), the gross profit rate (r) generated by the real sector over a particular period of time relative to the actualized real opportunity cost of capital over the same period ($i+\xi-\pi$) determines the fundamental value of the real sector for that period. If the two rates are equal, i.e. $r=(i+\xi-\pi)$, the fundamental value of Tobin's Q would take on a value of one.

If we look at the fundamental value of Tobin's Q at the level of the individual firms, we see that the q^f that we have derived on the aggregate level is only approximately the average fundamental value of Tobin's Q across all firms:[24]

$$q^f = \frac{r-1/N\sum_1^N g_j}{i+\xi-\pi-1/N\sum_1^N g_j} \approx \frac{1}{N}\sum_1^N q_j^f := \frac{1}{N}\sum_1^N \frac{r-g_j}{i+\xi-\pi-g_j}$$

In the following we treat q^f as the average fundamental value of Tobin's Q across all firms.

The no-arbitrage condition captured by eq. (2.20) is the driving force of the stock market in the model. The fundamental value of Tobin's Q that stems from it is a concept that allows

[23] For a discussion on the fundamental value of Tobin's Q for $\xi_m \neq \xi_e$ see Franke and Yanovski (2016).

[24] Recall that only the capital stocks of the firms are varying across firms (g_j). In the determination of q^f the capital stock growth rate generally plays a very small role because it is present with the same sign both in the denominator and in the numerator of q^f.

us to have a stock market valuation tool that depends only on the interest rates, profits and capital stock growth realized within a single period. Other approaches, like, for example, the discounted present value, require knowledge about the future distribution of the above variables. The valuation concept used in this chapter has the weakness that it does not consider potential valuation effects coming from a changing interest rate term structure. However, since the average holding period for the last 25 years in the US has been around 1 year, such valuation effects should be very limited because of the short investment horizon (see, for example, Della Croce et al. (2011, p. 7)).[25]

We assume that the financial markets drive the equity price (which is in the numerator of q) in a direction that restores the no-arbitrage condition. If $r_e^f > i + \xi$, there will be excess demand for equity driving the stock price index up and if $r_e^f < i + \xi$, excess supply of equity would bring the stock price index down. The intuition is that the agents observe the current firm profits relative to the current value of equity and compare these to the risk adjusted interest rate in the economy. If, for instance, profits are relatively high, the demand for stocks pushes the value of equity up, which decreases the return on equity until it becomes equal to the risk-adjusted interest rate. This is the case because for given profits the equity return is decreasing for an increasing value of equity. The actual value of Tobin's Q (q) on the aggregate level is assumed to move towards the fundamental value (q^f) because of arbitrage according to the adjustment equation:

$$\dot{q} = \rho_q (q^f - q) \qquad (\mathbf{AQ})$$

Where the parameter ρ can take on values between 0 and 1. We assume that the adjustment process is not firm-specific. The dynamics of the stock market described above can be considered in the tradition of the modeling approach of Taylor and O'Connell. "Wealthholders try to look through Wall Street to "fundamentals" on the production side" (see Semmler (1991, p. 7)).

Introducing momentum traders in the model of the stock market (like in Franke and Ghonghadze (2014), for example) does not change the behavior of the model in a qualitative way in terms of the dynamics of the stock market over the business cycle as long as the stock

[25] In general, the existence of valuation effects coming from changes in the term structure of interest rates should make the stock market less pro-cyclical, if we assume that the term structure reacts positively to expectations about future economic performance. Because of this, including such effects in the model would not help us better understand the pro-cyclical stock market observed during the last 25 years.

market remains ultimately driven by q^f.[26]

Finally, we assume that debt (M) expands and contracts together with equity ($p_e E$). In other words, we assume that the fraction $p_e E/M$ is a constant. This assumption ensures that the equity part of Tobin's Q (q_e) is always proportional to q, which allows us to talk about the evolution of the stock market when referring to q in our model. In the data, stock price indices and measures of the value of a firm (like Tobin's average Q) behave very similarly at business cycle frequencies (see Figure 2.8 at the end of the chapter). We take this as a motivation to talk about the situation on the financial markets when referring to q as simulated by the model.

2.3.3 The endogenous risk premium

The nominal interest rate environment in this model is specified as $(i+\xi)$. The central bank can attempt to alter the borrowing conditions in the economy by changing the base interest rate (i), however, an endogenous risk premium (ξ) might render these attempts futile.[27] The interest rate at which borrowing takes place depends on the perception of the lender about the related risk. This perception is obviously affected by the current or past performance of the borrower. As Minsky puts it, "success breeds a disregard of the possibilities of failure" (Minsky (1986, p. 237)). We take up this idea and specify an adjustment equation for the risk premium as a function of the observed performance of the firms in the real sector. In our model, we can proxy the observed performance by the term $(r-i+\pi-\xi^c)$. The parameter ξ^c stands for some constant benchmark premium that lenders use to assess performance, such that $(r-i+\pi-\xi^c)<0$ indicates bad performance, while $(r-i+\pi-\xi^c)>0$ indicates good performance. The evolution of the risk premium is thus determined by the extent to which the actual profit rate (r) is in excess of the real base interest rate $(i-\pi)$. The adjustment equation reads:

$$\dot{\xi} = -\rho_\xi (r-i+\pi-\xi^c) \qquad \textbf{(RP)}$$

[26] In particular, such extensions can help us to deterministically model fluctuations in macroeconomic data that take place at a much higher frequency than the average business cycle frequency. However, such high frequency fluctuations do not exhibit a strong regularity in the data. It thus might be more useful to model high frequency fluctuations as shocks.

[27] An alternative approach to model endogenous borrowing constraints would be to endogenize the amount of credit that lenders in the economy would be willing to extend to the firms (see, for example, Ryoo (2010)). However, since we model the behavior of the central bank in terms of an interest rate rule, we endogenize the risk premium as opposed to the stock of firm debt for reasons of consistency.

Note that the adjustment equation for the risk premium does not depend on the capital structure in the economy. This is the case since the risk premium was assumed to be uniform across equity and debt ($\xi = \xi_e$).[28] The evolution of the risk premium has a dynamic specification to reflect the idea that the *level* of the risk premium depends on the *duration* of a particular excess performance. The intuition being that the lenders in the economy relax (tighten) the borrowing constraints as they observe good (bad) performance over a long time period.

2.4 The integrated model of the real and financial sectors

We now put all the components of the real sector and the financial sector together. To integrate the two sectors we need to extend the investment function from the model of the real sector. The new investment function has the following specification:

$$g = g^o + \phi_r (r^n - i - \xi + \pi^c) + \phi_x x \qquad \textbf{(IF)}$$

Instead of the constant parameter r^o, the firms now compare their normal profit rate (r^n) with the perceived borrowing conditions in the economy ($i + \xi - \pi^c$). The firms use their inflation expectations (π^c) in order to assess the borrowing conditions, since actual inflation (π) is not yet observed. The terms $i + \xi - \pi^c$ and r^n are comparable because we assumed a one good economy (consumption and capital goods have the same price). The integrated model

[28] The idea that "success breeds a disregard of the possibilities of failure" (Minsky (1986, p. 237)) can also be modeled by using the evolution of debt in the economy rather than the evolution of the risk premium (see, for example, Ryoo (2010)). The second key element of Minsky's financial instability hypothesis is not present in this model. That is to say, unlike Ryoo (2010), the model developed in this chapter does not capture the fragility of economic systems with capital structures dominated by debt.

of the two sectors can thus be expressed as the following system of differential equations:

$$\dot{x} = \nu\left[(1-x)\exp(\vartheta_y y) - (1+x)\exp(-\vartheta_y y)\right], \quad -1 \leq x \leq 1 \tag{SE}$$

$$\dot{h} = -(1-h)\,\kappa_{rw}\, y\,, \qquad 0 < h < 1 \tag{PS}$$

$$\dot{\pi}^c = \alpha\left[\gamma\pi^* + (1-\gamma)\,\pi - \pi^c\right] \tag{IC}$$

$$\frac{di}{dt} = \mu_i\left[i^o + \mu_\pi\left(\pi - \pi^*\right) + \mu_y\, y - i\right] \tag{TR}$$

$$\dot{q} = \rho_q\left(q^f - q\right) \tag{AQ}$$

$$\dot{\xi} = -\rho_\xi\left(r - i + \pi - \xi^c\right) \tag{RP}$$

$$g = g^o + \phi_r\left(r^n - i - \xi + \pi^c\right) + \phi_x x \tag{IF}$$

$$y = \frac{g - g^o}{(1-c_2)\,u^o} \tag{OG}$$

$$\pi = \pi^c + \kappa y \tag{PC}$$

$$r^n = h\,u^o - \delta \tag{NPR}$$

$$r = h\,u^o\,(1+y) - \delta \tag{APR}$$

$$q^f = \frac{r-g}{i+\xi-\pi-g} \tag{FQ}$$

$$i^o = h^o\,u^o - \delta + \pi^* - \xi^c$$

We assume that in the absence of an output gap or deviations of inflation from its target, the central bank sets a nominal base rate i^o that allows the risk premium to come to rest ($\dot{\xi} = 0$). The above system is no longer two dimensional and we explore its properties by means of simulations. The model is calibrated for measurements at a quarterly frequency.[29] In the simulations to come we are going to examine the endogenous fluctuations of the model economy around the point of rest characterized by: $x = 0$, $h = h^o$, $\pi^c = \pi^*$, $i = i^o$, $q = 1$ and $\xi = \xi^c$.

The stabilizing and destabilizing forces (profitability and Harrodian instability) from the real sector are still present alongside two additional destabilizing forces and one additional stabilizing force. The inflation expectations (π^c) are destabilizing since ceteris paribus deviations from π^* loosen (tighten) the borrowing conditions in real terms, which leads to a higher (lower) output gap, higher (lower) inflation and ultimately to expectations about even higher (lower) inflation (see equations (IF), (OG), (PC) and (IC)). The risk premium (ξ) is

[29] This means that parameters like u^o, g^o or π^* are set to reflect their empirical counterparts at a quarterly frequency.

also destabilizing since deviations from ξ^c loosen (tighten) the borrowing conditions for the firms, which ceteris paribus increases (decreases) the actual gross rate of profit (r) leading to an even lower (higher) risk premium (see equations (**IF**), (**OG**), (**APR**) and (**RP**)). The central bank's reaction function (see eq. (**TR**)) constitutes the new stabilizing force. The central bank increases (decreases) the base nominal interest rate (i) in reaction to a positive (negative) output gap or high (low) inflation, which ceteris paribus decreases (increases) investment, the output gap and consequently inflation (see equations (**TR**), (**IF**), (**OG**) and (**PC**)).

Recall that the Harrodian instability is local in our model, while all other stabilizing and destabilizing forces are global. If all the destabilizing forces, excluding Harrodian instability, are weaker than all the stabilizing ones, and if we make Harrodian instability (which is a local force) strong enough, we can expect to get a sustained cyclical behavior of the system.[30] We are going to use parametrizations of the model producing such endogenous cycles to study the behavior of Tobin's Q over the business cycle while holding some of the properties of the system fixed. In all the explorations we try to keep the amplitudes, cycle period and relative positions of some of the variables fixed.[31] In particular, as with the calibration of the model of the real sector, the output gap and the profit share fluctuate with an amplitude of around $\pm 3\%$ and $\pm 1\%$, respectively. Inflation fluctuates around the target of the central bank with an amplitude of around $\pm 0.5\%$ and lags slightly behind the output gap.[32] We observe that the real base interest rate is also mostly pro-cyclical in the data, which implies that the central bank reacts strongly enough to compensate for inflation (see Figure 2.1). We thus set the reaction parameters μ_{pi} and μ_y in eq. (**TR**) high enough, to make the real base interest rate pro-cyclical. We keep the cycle period around 25 quarters by suitably adjusting parameters that have an effect on the cycle period (e.g. the parameter ν in eq. (**SE**)).

2.5 The determinants of a pro-cyclical stock market

Equation (**FQ**) summarizes the driving forces of the stock market in the model since Tobin's Q (q) adjusts towards q^f (see eq. (**AQ**)). The key determinants of q^f are the real

[30] We can make Harrodian instability strong enough by increasing one of the parameters involved in it (for example, ϑ_y, see condition (**R2**)).

[31] Explorations with respect to the parametrization of the model indicate that the model seems to produce mostly *regular* cyclical behavior.

[32] The amplitude refers to inflation over a quarter. This implies an amplitude of the yearly inflation rate of $\pm 2\%$. Inflation is mostly pro-cyclical in the data with a slight lag behind the output gap.

base interest rate, the risk premium and the gross actual profit rate (see eq. (**FQ**)). Next, we explore how these determinants affect the behavior of the stock market over the business cycle.

2.5.1 The gross actual profit rate

If we look at eq. (**APR**), we see that r is determined by the output gap (y) and by the profit share (h). We already know that the output gap is lagging behind the profit share (see Figure 2.2 (b)), which implies that r is lagging behind h but leading y. Thus we can conclude that r is strongly pro-cyclical in the model. If we look at eq. (**FQ**) again, we see that this allows the stock market to be pro-cyclical depending on the dynamics of the denominator of q^f.

2.5.2 Monetary policy

Generally, if the central bank is very aggressive in its reaction to high inflation and output gaps, it could prevent the stock market (q) from being pro-cyclical. Intuitively, if we look at equation **FQ** we see that if, for example, i increases whenever r is high, this does not allow the stock market to be pro-cyclical. The strength of the reaction of i to r (via equations (**TR**) and (**APR**)) is one of the major determinants of the behavior of the financial markets in this model. A situation in which the model is calibrated such that the central bank reacts very strongly to y and π is shown in Figure 2.4, where the real base interest rate exhibits an amplitude of around $\pm 0.9\%$.[33] This involves setting high values for the parameters μ_y and μ_π in eq. (**TR**). In reality, however, the central banks does not seem to be reacting very aggressively since the average amplitude of the fluctuations of the real base interest rate in the filtered data is around $\pm 0.25\%$. See the appendix (Section 2.9.5) for the parameter values used in the simulation.

If the central bank reacts very slowly to y and π, this induces the real base interest rate to lag behind y (and thus behind r) a lot, which allows the stock market to be more pro-cyclical (a higher correlation of q with the output gap is achieved).[34] However, this is something that we do not observe in the filtered data, where the real base interest rate usually does not lag a lot behind the output gap (see Figure 2.2).

[33] As in Figure 2.1 the fluctuations have been re-scaled, so that the patterns can be recognized more easily.

[34] We can allow for the central bank to react very slowly by setting a value for the parameter μ_i in the Taylor rule close to 0.

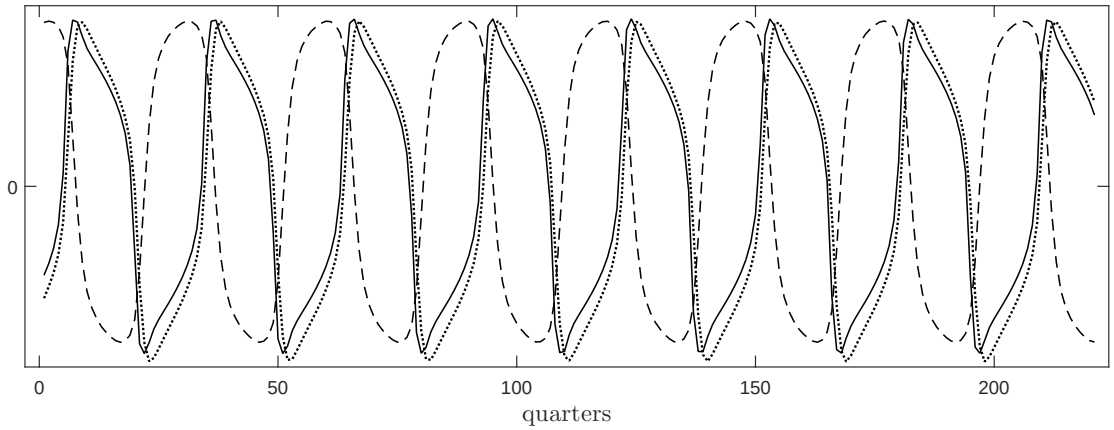

Figure 2.4: The fluctuations of the real base interest rate (dotted line), of real output (solid line) and of Tobin's Q (dashed line) generated by a simulation of the integrated model in which a very aggressive monetary policy is preventing the stock market from being pro-cyclical. The fluctuations have been re-scaled to make them comparable by means of visual inspection.

Note that, generally, even if the central bank reacts immediately to observed output gaps, its base interest rate will always be at least slightly lagging behind the output gap (see Figure 2.4). This is so by definition since the central bank can only *react* to the observed macro-variables, because real time data from the macro-economy does not exist. Because of this the numerator and the denominator of q^f do not move simultaneously as the central bank reacts, but rather the numerator moves first and the denominator follows. This allows for a continuous shift of the cyclical nature of q^f from a pro-cyclical one to a counter-cyclical one depending on the degree of aggression of the central bank's reactions. If the denominator and the numerator of q^f were moving simultaneously, then changes in the aggression of monetary policy would only change the amplitude of the fluctuations of q^f and not its position relative to the business cycle.

2.5.3 The endogenous risk premium

The endogenous risk premium can offset monetary policy, since it loosens (tightens) the borrowing conditions, whenever the model economy is in a boom (recession). We can say this since y and r move very closely together and since we know from eq. (**APR**) that the risk premium depends on r.[35] The endogenous risk premium can thus contribute to a pro-

[35]For the endogenous risk premium to be able to offset monetary policy, the difference $(r-i+\pi-\xi^c)$ must be positive during a boom and negative during recessions (see eq. (**APR**)). We impose this to be the case by parametrizing the model such that the central bank is not being too aggressive in its reaction to y and π.

cyclical stock market. For instance, if an increase in the base interest rate due to a positive output gap takes place together with a fall in the risk premium due to a high actual gross profit rate, the denominator of q^f can remain roughly unchanged, so that the numerator is left as the key determinant of the behavior of q^f, and we already know that the numerator (r) follows y very closely.

2.5.4 The adjustment of the financial markets

Finally, the speed of adjustment of the stock market to changes in q^f also plays a role in determining the behavior of the stock market over the business cycle (see eq. (**AQ**)). Even if q^f is not strongly pro-cyclical, for example, because of the behavior of the central bank, a slow adjustment process (of q towards q^f) can render the financial markets strongly pro-cyclical or even lagging behind the output gap.

2.6 A final calibration of the integrated model

In this section, we are going to calibrate the integrated model such that it can fit some of the properties of the filtered data. In particular, we are going to be aiming for a pro-cyclical stock market given a pro-cyclical real base interest rate. Naturally, we are also going to attempt to match the average amplitude of the fluctuations of the respective variable observed in the filtered data.

Recall that we have already committed to reproducing certain regularities of inflation, the output gap and the profit share at the end of Section 2.4. Given the amplitude and relative positions of inflation and the output gap we now set the parameter of the reaction function of the central bank such that the resulting real base interest rate is pro-cyclical, fluctuating with an amplitude of around $\pm 0.25\%$. The dynamic of the output gap and profit share to which we have committed determine the behavior of the gross actual profit rate (r), which is the crucial component of the numerator of q^f. Finally, q^f is also affected by the risk premium (ξ). The strength of the reaction of ξ (see eq. (**RP**)) to the performance of the real sector determines to what extent monetary policy is offset and thus has an effect on the behavior of q^f over the business cycle. We use this parameter (ρ_ξ) together with the adjustment speed (ρ_q) of the actual Tobin's Q (see eq. (**AQ**)) to allow the integrated model to yield a pro-cyclical stock market. In particular, we set the adjustment speed to $\rho_q = 0.3$, which implies that per time step 30% of the distance between q and q^f is made good. The

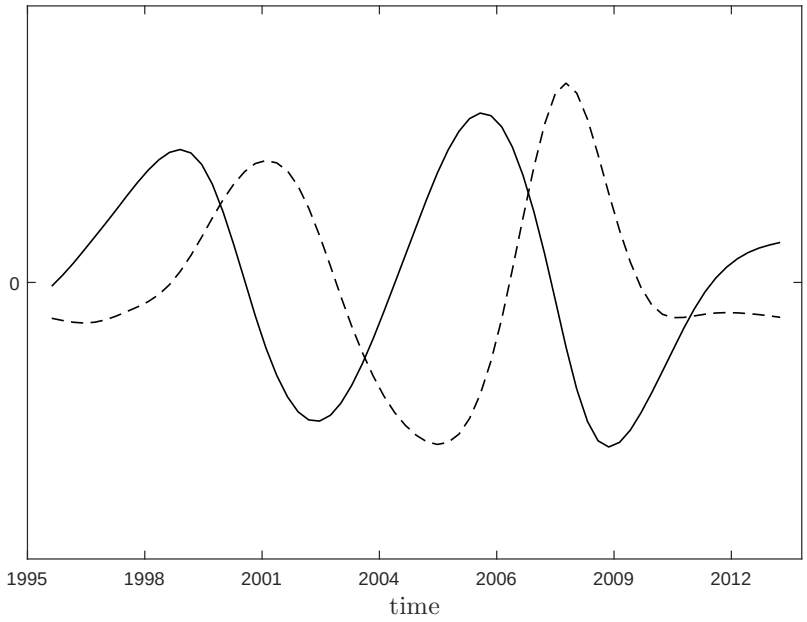

Figure 2.5: The filtered fluctuations of real gross value added of the non-financial sector (solid line) and of the BofA Merrill Lynch US High Yield Master II Option-Adjusted Spread (dashed line) around their respective long run trends for the US over the period (1983-2014). The fluctuations have been re-scaled to make them comparable by means of visual inspection.

resulting amplitude of the q is roughly twice as large as the amplitude of the output gap (y), i.e. roughly $\pm 6\%$. Filtered empirical measures of Tobin's Q yield a similar average amplitude.

The above calibration implies certain dynamics of the risk premium. In particular, under the above calibration the risk premium is counter-cyclical in the model. If we take the BofA Merrill Lynch US High Yield Master II Option-Adjusted Spread as a proxy for the risk premium in the US, we see that the risk premium seems to be counter-cyclical (see Figure 2.5)[36].

Figure 2.6 shows the re-scaled dynamics of the real base interest rate, the output gap and Tobin's Q resulting from a simulation of the model using the final parametrization just discussed. The fluctuations are re-scaled in order to make the patterns easier to recognize and to make Figure 2.6 comparable to Figure 2.1.

[36]This measure captures the spreads on bonds issued by firms rated BB or below. The spreads on bonds with higher ratings exhibit very low volatility and are thus considered by the author to be a poor proxy of the overall risk premium in the economy.

Lag number at which maximum correlation with the output gap occurs:

	filtered smoothed data	model
profit share (h)	-7 (0.91)	-7 (0.98)
base interest rate (i)	1 (0.91)	1 (1)
inflation (π)	0 (0.63)	0 (0.99)
real base interest rate ($i-\pi$)	1 (0.84)	1 (0.99)
Tobin's Q (q)	-1 (0.7)	-1 (0.98)
the negative of the risk premium ($-\xi$)	5 (0.92)	1 (0.99)

Table 2.1: The lag number at which maximum correlation between the output gap (y) and the respective variables occurs in the data and in the model. We take the negative of the risk premium since it is counter-cyclical. In brackets we see the correlation itself at the respective lag. All the data is quarterly, so the lags are in terms of quarters.

Empirical standard deviation of the respective variables:

	filtered smoothed data	model
output gap (y)	1.5	1.87
profit share (h)	0.95	0.61
base interest rate (i)	0.2	0.2
inflation (π)	0.088	0.085
real base interest rate ($i-\pi$)	0.15	0.11
Tobin's Q (q)	5.6	9.8
risk premium (ξ)	0.30	0.45

Table 2.2: The empirical standard deviation of the respective variables (in terms of the number of percentage points) observed in the data and in the model. The standard deviation of the smoothed filtered data is generally smaller than that of just the filtered data.

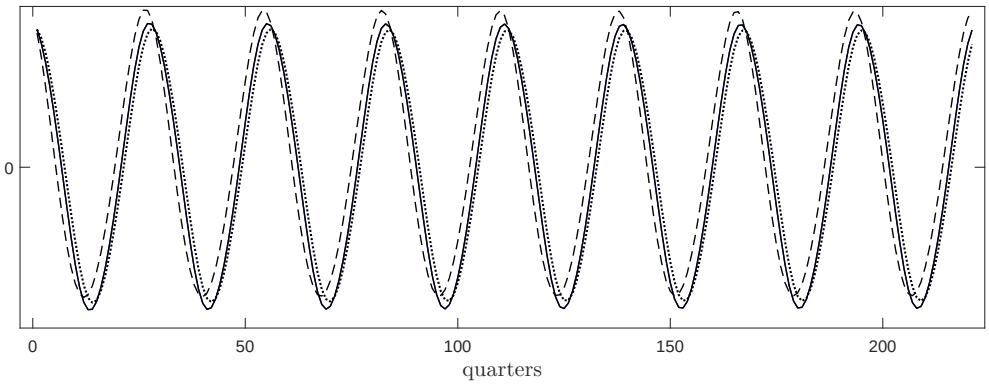

Figure 2.6: The fluctuations of the real base interest rate (dotted line), of real output (solid line) and of Tobin's Q (dashed line) generated by a simulation of the integrated model in which both the real base interest rate and Tobin's Q are pro-cyclical. The fluctuations have been re-scaled to make them comparable by means of visual inspection.

Table 2.1 and 2.2 show the performance of the final calibration of the model in terms of some of the empirical moments exhibited by the filtered smoothed data during the last 25 years (1989–2014).

2.7 Conclusion

This chapter develops a particular approach to the relationship between the real and the financial sectors based on Tobin's average Q derived in the context of economic growth. We explored the interactions between the two sectors with monetary policy in the context of a model of endogenous business cycles rooted in the real sector. Using this model we examined the link between a particular observed behavior of the stock market and monetary policy over the business cycle and the effectiveness of the central bank's attempts to affect the opportunity cost of capital in the economy. This allows us to provide potential explanations for the pro-cyclical stock market observed in particular during the last 25 years in the US.

Within this framework, we identify several factors that contribute to a pro-cyclical stock market. Firstly, the value of the firms in the real sector (Tobin's average Q) is affected by the profits generated in it. Therefore, a timid or ineffective monetary policy can allow for the stock market to be dominated by the fluctuations of the profits in the real sector. We modelled the potential ineffectiveness of monetary policy in terms of an endogenous risk premium. Finally, the adjustment speed of the financial markets to changes in the fundamentals of the model economy is also an important factor affecting the behavior of the

stock market over the business cycle.

Using the above mentioned factors, we calibrate the model to fit key properties of the data from the last 25 years (1989–2014). In particular, the model can generate a pro-cyclical stock market in the presence of a counter-cyclical monetary policy.

The insights from this study can be used to assess the effectiveness of monetary policy. In the context of the model a strongly procyclical stock market can be interpreted as a signal that monetary policy is not able to significantly affect the borrowing conditions in the economy.

2.8 References

Akerlof, G. A., Shiller, R. J., 2009. *Animal Spirits: How Human Psychology Drives the Economy, and Why It Matters for Global Capitalism.* Princeton University Press Princeton.

Ando, A., Modigliani, F., 1963. *The "life cycle" hypothesis of saving: Aggregate implications and tests.* The American economic review 53 (1), 55-84.

Artinger, F., Petersen, M., Gigerenzer, G., Weibler, J., 2015. Heuristics as adaptive decision strategies in management. *Journal of Organizational Behavior 36 (S1).*

Bask, M., 2011. Asset Price Misalignments and Monetary Policy. *International Journal of Finance & Economics 540.*

Beaudry, P., Galizia, D., Portier, F., 2015. Reviving the Limit Cycle View of Macroeconomic Fluctuations. *National Bureau of Economic Research.*

Beaudry, P., Galizia, D., Portier, F., 2016. Is the Macroeconomy Locally Unstable and Why Should We Care? *C.E.P.R. Discussion Papers (11305).*

Bhaduri, A., Marglin, S., 1990. Unemployment and the Real Wage: The Economic Basis for Contesting Political Ideologies. *Cambridge Journal of Economics 14 (4), 375–393.*

Blanchard, O., Illing, G., 2009. *Makrooekonomie.* Pearson Deutschland GmbH.

Chiarella, C., Flaschel, P., Franke, R., 2005. *Foundations for a Disequilibrium Theory of the Business Cycle: Qualitative Analysis and Quantitative Assessment.* Cambridge University Press, Cambridge.

De Grauwe, P., 2012a. Booms and busts in economic activity: A behavioral explanation. *Journal of Economic Behavior & Organization 83 (3), 484–501.*

De Grauwe, P., 2012b. *Lectures on behavioral macroeconomics.* Princeton University Press.

De Grauwe, P., Kaltwasser, P. R., 2012. Animal spirits in the foreign exchange market. *Journal of Economic Dynamics and Control 36 (8), 1176–1192.*

Della Croce, R., Stewart, F., Yermo, J., 2011. Promoting Longer-Term Investment by Institutional Investors. *OECD Journal: Financial Market Trends 2011 (1), 145–164.*

Desai, M., Henry, B., Mosley, A., Pemberton, M., 2006. A clarification of the Goodwin model of the growth cycle. *Journal of Economic Dynamics and Control 30 (12), 2661–2670.*

Franke, R., 2007. A sophisticatedly simple alternative to the New-Keynesian Phillips curve. *Time and Space in Economics. Springer, pp. 3–28.*

Franke, R., 2008. Microfounded Animal Spirits and Goodwinian Income Distribution Dynamics. Effective Demand, Income Distribution and Growth. *Research In Memory of the Work of Richard M. Goodwin, London: Routledge 2008, 372–398.*

Franke, R., 2012. Microfounded Animal Spirits in the New Macroeconomic Consensus. *Studies in Nonlinear Dynamics & Econometrics 16 (4), 1–41.*

Franke, R., 2015a. A Simple Approach to Overcome the Problems From the Keynesian Stability Condition. *Working Paper. University of Kiel.*

Franke, R., 2015b. Can Monetary Policy Tame Harrodian Instability? *Working Paper. University of Kiel.*

Franke, R., Ghonghadze, J., 2014. Integrating Real Sector Growth and Inflation Into An Agent-Based Stock Market Dynamics. *FinMaP-Working Papers. University of Kiel.*

Franke, R., Jang, T.-S., Sacht, S., 2015. Moment matching versus Bayesian estimation: Backward-looking behaviour in a New-Keynesian baseline model. *The North American Journal of Economics and Finance 31, 126–154.*

Franke, R., Yanovski, B., 2016. On the long-run equilibrium value of Tobin's average Q. *European Journal of Economics and Economic Policies (1), 103–113.*

Friedman, M., 1957. A Theory of the Consumption Function. *National Bureau of Economic Research General Series.*

Goodwin, R. M., 1982. A growth cycle. *Essays in Economic Dynamics, 165-170.*

Harrod, R. F., 1939. An Essay in Dynamic Theory. *The Economic Journal, 14–33.*

Hildenbrandt, W., Kirman, A. P., 1988. *Equilibrium analysis: variations on themes by Edgeworth and Walras.* North-Holland, Amsterdam et al.

Hodrick, R. J., Prescott, E. C., 1997. Postwar US Business Cycles: an Empirical Investigation. *Journal of Money, credit and Banking, 1–16.*

Jaimovich, N., Floetotto, M., 2008. Firm dynamics, markup variations, and the business cycle. *Journal of Monetary Economics 55 (7), 1238–1252.*

Kontonikas, A. and Montagnoli, A., 2006. Optimal Monetary Policy and Asset Price Misalignments. *Scottish Journal of Political Economy 53: 636–654.*

Kregel, J. A., 1973. *Reconstruction of Political Economy: An Introduction to Post-Keynesian Economics.* Springer.

Lavoie, M., 2014. *Post-Keynesian Economics: New Foundations.* Edward Elgar Publishing, Cheltenham.

Lengnick, M. and Wohltmann, H.-W., 2013. Agent-Based Financial Markets and New Keynesian Macroeconomics: A Synthesis. *Journal of Economic Interaction and Coordination 8(1): 1–32.*

Lengnick, M. and Wohltmann, H.-W., 2016. Optimal monetary policy in a new Keynesian model with animal spirits and financial markets. *Journal of Economic Dynamics and Control 64: 148–165.*

Lovell, M. C., 1986. Tests of the rational expectations hypothesis. *The American Economic Review 76 (1), 110-124.*

Lux, T., 1995. Herd behaviour, bubbles and crashes. *The economic journal, 881–896.*

Lux, T., 1998. The socio-economic dynamics of speculative markets: interacting agents, chaos, and the fat tails of return distributions. *Journal of Economic Behavior & Organization 33 (2), 143–165.*

Lux, T., 2009. Rational forecasts or social opinion dynamics? Identification of interaction effects in a business climate survey. *Journal of Economic Behavior & Organization 72 (2), 638–655.*

Minsky, H. P., 1986. *Stabilizing an Unstable Economy.* New Haven, CT: Yale University Press.

Naimzada, A. K. and Pireddu, M., 2013. Dynamic Behavior of Real and Stock Markets with Varying Degree of Interaction. *DEMS Working Paper 245*

Roberts, J. M., 1995. New Keynesian economics and the Phillips curve. *Journal of money, credit and banking 27 (4), 975–984.*

Rudd, J., Whelan, K., 2007. Modeling inflation dynamics: A critical review of recent research. *Journal of Money, Credit and Banking 39 (s1), 155–170.*

Ryoo, S., 2010: Long waves and short cycles in a model of endogenous financial fragility. *Journal of Economic Behavior and Organization, 74, 163–186.*

Scheffknecht, L. and Geiger, F., 2011. A Behavioral Macroeconomic Model with Endogenous Boom-Bust Cycles and Leverage Dynamics. *Discussion Paper, University of Hohenheim.*

Semmler, W., 1991. *Financial Dynamics and Business Cycles: New Perspectives.* ME Sharpe, Armonk.

Simon, H. A., 1955. A Behavioral Model of Rational Choice. *The Quarterly Journal of Economics, 99–118.*

Stockhammer, E., 2004. *The Rise of Unemployment in Europe: A Keynesian Approach. New directions in modern economics.* Edward Elgar Publishing, Cheltenham.

Taylor, J. B., 1993. Discretion versus policy rules in practice. *Carnegie-Rochester conference series on public policy 39, 195–214.*

Tobin, J., 1969. A General Equilibrium Approach to Monetary Theory. *Journal of Money, Credit and Banking 1 (1), 15–29.*

Tobin, J., Brainard, W. C., 1976. Asset Markets and the Cost of Capital. Cowles Foundation for Research in Economics, Yale University, *Cowles Foundation Discussion Papers (427).*

Weidlich, W., Haag, G., 1983. *Concepts and Models of a Quantitative Sociology. The Dynamics of Interacting Populations.* Vol. 14 of Springer Series in Synergetics. Springer, Berlin.

Westerhoff, F., 2012. Interactions between the Real Economy and the Stock Market: A Simple Agent-Based Approach. *Discrete Dynamics in Nature and Society 504840.*

Zipperer, B., Skott, P., 2011. Cyclical Patterns of Employment, Utilization and Profitability. *Journal of Post Keynesian Economics 34 (1), 25–58.*

2.9 Appendix

2.9.1 The structure of demand expectations

Let N, n^- and n^+ be the total number of firms, the fraction of firms expecting a negative output gap and the fraction of firms expecting a positive output gap, respectively. Next, we define a measure of the structure of the expectations in the economy as $x = n^+ - n^-$. The index can only take on values between -1 and 1 ($-1 \leq x \leq 1$). A value of x close to 1 would indicate that most of the firms expect a positive output gap, while a value close to -1 would mean that the majority expects a negative output gap. Let us consider next an arbitrary period Δt and assume that each firm can switch its attitude only once within this period. In addition, let p^{-+} be the probability *per unit of time* (uniform across all firms) that a firm expecting a negative output gap will switch to expecting a positive one, and p^{+-} be the probability of the opposite change happening. Thus, $\Delta t\, p^{-+}$ and $\Delta t\, p^{+-}$ constitute the probabilities that these switches occur within the time interval $[t, t + \Delta t)$.

The population shares of the positive output gap expectation and of the negative output gap

expectation can be expressed in terms of x as $n^+ = (1+x)/2$ and $n^- = (1-x)/2$, respectively.[37] A specification of the evolution of these shares over time can be obtained by using the aforementioned transition probabilities (p^{+-} and p^{-+}). Over the period of time Δt the population share of the positive output gap expectation decreases exactly by $\Delta t\, p^{+-}\,(1+x)/2$ and increases exactly by $\Delta t\, p^{-+}\,(1-x)/2$ if we assume that the number of firms (N) tends to infinity. This is assumed here. With signs reversed, the same holds true for the evolution of the population share of the negative output gap expectation over Δt. The net effect of these share dynamics on x can be summarized in the following differential equation in continuous time (if we let Δt approach zero)

$$\dot{x} = (1-x)\, p^{-+} - (1+x)\, p^{+-} \tag{2.22}$$

This probabilistic approach allows for the individual agents (the firms) to form distinct expectations due to some firm idiosyncrasy. New information affects the probability of switches across the different expectations. In our case, the switching probabilities are a function of the observed output gap (y). The following specification of the transition probabilities was taken from Weidlich and Haag (1983, p. 41):

$$p^{-+} = \nu \exp(\vartheta_y y), \qquad p^{+-} = \nu \exp(-\vartheta_y y) \tag{2.23}$$

The specification assumes that the percentage change in the respective transition probability is linear in the absolute change of y.[38] The observed output gap affects both transition probabilities (p^{-+} and p^{+-}) in a symmetric fashion.

Inserting (2.23) into (2.22) yields the complete specification of the dynamics of the structure of the demand expectations:

$$\dot{x} = \nu\,[(1-x)\exp(\vartheta_y y) - (1+x)\exp(-\vartheta_y y)] \tag{SE}$$

2.9.2 Stability analysis of the model of the real sector

There is a technicality concerning the boundaries of eq. (**PS**). We have to define what happens as the system approaches the boundaries $h = 1$ or $h = 0$. We assume that as the system approaches $h = 1$ or $h = 0$ at some very small distance ε from the boundaries $\dot{h}$

[37] Consider the following algebraic manipulations: $n^+ = n^+/2 + n^+/2 = (1-n^-)/2 + n^+/2 = (1+n^+-n^-)/2 = (1+x)/2$. The second relationship follows analogously.

[38] Formally, the assumption reads $dp^{-+}/p^{-+} = \alpha\, dy$ for some constant α.

becomes 0. In the following, when we refer to points of rest involving $h=1$ or $h=0$ we will actually be referring to points of rest involving $h=1-\varepsilon$ or $h=0+\varepsilon$. We skip the ε to make the notation less cumbersome. The model of the real sector has 4 isoclines. IS_{h1}, IS_{h2} and IS_{h3} stand for the isoclines that give rise to $\dot{h}=0$, while IS_x is the isocline associated with $\dot{x}=0$:[39]

$$h=1 \tag{IS_{h1}}$$

$$h=0 \tag{IS_{h2}}$$

$$h=h^o-\frac{\phi_x}{\phi_r u^o}x \tag{IS_{h3}}$$

$$h=h^o+\frac{\ln[(1+x)/(1-x)]}{2u^o B}-\frac{\phi_x}{\phi_r u^o}x \tag{IS_x}$$

Define the composite parameters $A=\frac{\phi_x \vartheta_y}{(1-c_2)u^o}>0$ and $B=\frac{\phi_r \vartheta_y}{(1-c_2)u^o}>0$. First, note that the isocline IS_x lies always above the isocline IS_{h3} for $x>0$ and is below it for $x<0$. This is because the isoclines are identical but for $\frac{\ln[(1+x)/(1-x)]}{2u^o B}$, which is negative for $x<0$ and positive for $x>0$. This implies that IS_x and IS_{h3} can cross each other only once, i.e. at $(0,h^o)$. Next, we exclude potentially attractive points of rest involving the corner solutions $h=1$ and $h=0$.

Excluding the potentially attractive points of rest involving $h=1$

The isoclines IS_x and IS_{h1} can potentially cross three times resulting in points of rest involving $h=1$. The two such points of rest located below the IS_{h3} isocline can be potentially attractive because below the IS_{h3} isocline the profit share is increasing (see Figure 2.7 (c)). Obviously, by definition, $h=1$ can only be approached from below. We exclude any potentially attractive points of rest involving $h=1$ by making sure that at the lowest possible value of x (i.e. $x=-1$) the isoclines IS_{h3} takes on a value below 1. In other words, we do not allow IS_{h3} and IS_{h1} to intersect. In this way, we can guarantee that IS_x and IS_{h1} never intersect below the IS_{h3} isocline, since IS_x lies below IS_{h3} for $x<0$. In IS_{h3} we thus impose $h^o-\frac{\phi_x}{\phi_r u^o}(-1)<1$ which leads to the restriction:

$$\phi_x/\phi_r<(1-h^o)u^o \tag{2.24}$$

[39] The eq. (**SE**) can be rewritten as $\dot{x}=2\nu[\tanh(\vartheta_y y)-x]\cosh(\vartheta_y y)$. When solving for h to obtain the isocline IS_x, the identity $\operatorname{arctanh}(x)=0.5\ln[(1+x)/(1-x)]$ was used.

The point of rest involving $h = 1$ that is located above the IS_{h3} isocline and results from a potential intersection of IS_x with IS_{h1} is always repelling and is thus not seen as a concern (see Figure 2.7 (b)).[40]

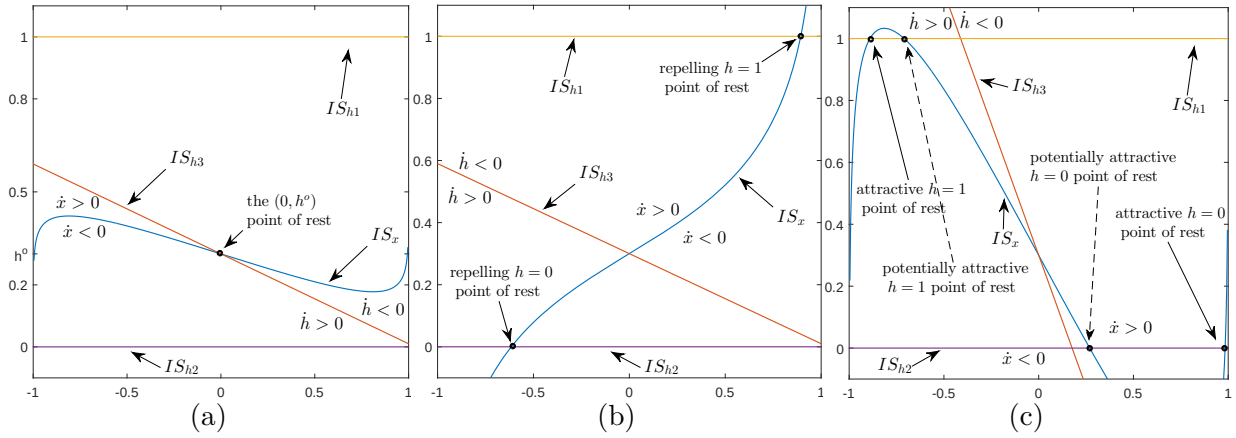

Figure 2.7: **(a)** – The position of the isoclines in the standard case in which there is only one point of rest $(0, h^o)$; **(b)** – The position of the isoclines in the case in which there is only one *attractive* point of rest $(0, h^o)$; **(c)** – The position of the isoclines in the case in which there exist *attractive* points of rest associated with the corner solutions $h = 1$ and $h = 0$.

Excluding the potentially attractive points of rest involving $h = 0$

Symmetrically, isoclines IS_x and IS_{h2} can also potentially cross three times resulting in points of rest involving $h = 0$. The two such points of rest located above the IS_{h3} isocline can be potentially attractive because above the IS_{h3} isocline the profit share is decreasing (see Figure 2.7 (c)). Obviously, by definition, $h = 0$ can only be approached from above. We exclude any potentially attractive points of rest involving $h = 0$ by making sure that at the highest possible value of x (i.e. $x = 1$) the isocline IS_{h3} takes on a value above 0. In other words, we do not allow IS_{h3} and IS_{h2} to intersect. In this way, we can guarantee that IS_x and IS_{h2} never intersect above the IS_{h3} isocline, since IS_x lies above IS_{h3} for $x > 0$. In IS_{h3} we thus impose $h^o - \frac{\phi_x}{\phi_r u^o}(1) > 0$ which leads to the restriction:

$$\phi_x/\phi_r < h^o u^o \tag{2.25}$$

The point of rest involving $h = 0$ that is located below the IS_{h3} isocline and results from a potential intersection of IS_x with IS_{h2} is always repelling and is thus not seen as a concern (see Figure 2.7 (b)).[41]

[40] This point of rest is repelling since h is decreasing above the IS_{h3} isocline.
[41] This point of rest is repelling since h is increasing below the IS_{h3} isocline.

Combing the inequalities (2.24) and (2.25) result in the restriction:

$$\phi_x/\phi_r < (0.5 - |h^o - 0.5|)\, u^o \qquad \textbf{(R1)}$$

This restriction excludes the existence of potentially attractive points of rest involving the corner solutions $h = 1$ and $h = 0$.[42] In Figure 2.7 (a) we see the standard constellation of the isoclines under parametrizations presented in this chapter.

Sustained cyclical behavior

The system is obviously globally stable since it is only defined for $-1 \leq x \leq 1$ and $0 < h < 1$. In addition, under the restriction **R1**, we can say that all trajectories starting from within these boundaries must eventually enter, and then cannot leave, the rectangle given by the 4 points: $(-1, IS_{h3}(-1))$, $(1, IS_{h3}(-1))$, $(-1, IS_{h3}(1))$ and $(1, IS_{h3}(1))$.[43] This is the case because above the IS_{h3} isocline h is falling, while below it h is increasing. The conditions of the Poincaré-Bendixson Theorem are thus satisfied. Under the restriction **R1** sustained cyclical behavior is thus given if the point of rest $(0, h^o)$ is repelling (see Figure 2.7 (a)).

To derive the condition for that we can look at the Jacobian matrix around $(0, h^o)$. We can rewrite the system comprised of equations (**SE**) and (**PS**) as:

$$\dot{x} = F_x(x,h) \quad \text{and} \quad \dot{h} = F_h(x,h)$$

We use the following type of notation for the partial derivatives: $F_{xx} = \partial F_x / \partial x$. The Jacobian matrix then becomes:

$$J = \begin{bmatrix} F_{xx} & F_{xh} \\ F_{hx} & F_{hh} \end{bmatrix} = \begin{bmatrix} \dfrac{2\nu\,[A - \cosh^2(\vartheta_y y)]}{\cosh^2(\vartheta_y y)} & \dfrac{2\nu B u^o}{\cosh^2(\vartheta_y y)} \\ -(1-h)\,\kappa_{rw} A & \kappa_{rw} A x + \kappa_{rw} B (2h u^o - \delta - r^o - u^o) \end{bmatrix}$$

[42] We can actually have a laxer restriction on the parameters by deriving a restriction preventing the intersections IS_x with IS_{h1} and IS_x with IS_{h2}, but still allowing for intersections IS_{h3} with IS_{h1} and IS_{h3} with IS_{h2}. However, this restriction turns out to be very cumbersome and uninformative. Because of this, we use a stronger restriction than what is sufficient.

[43] Of course, this only makes sense if this rectangle is smaller than than the one given by the space over which the system is defined, i.e. $(-1,1)$, $(1,1)$, $(-1,0)$ and $(1,0)$. The restriction described by the inequality **R1** guarantees that.

Around the point of rest $(0, h^o)$ it reads:

$$J = \begin{bmatrix} 2\nu(A-1) & 2\nu B u^o \\ -(1-h^o)\kappa_{rw} A & -(1-h^o)u^o \kappa_{rw} B \end{bmatrix} = \begin{bmatrix} ? & + \\ - & - \end{bmatrix}$$

Only the upper-diagonal entry of the matrix can change its sign depending on the magnitude of the composite parameter A. The point of rest $(0, h^o)$ is repelling for $\text{trace}(J) > 0$ and $\det(J) > 0$. The determinant of J is bigger than 0 for any A. The trace of J is bigger than 0 if:

$$2\nu(A-1) > (1-h^o)u^o \kappa_{rw} B$$

After inserting the identities of A and B we get:

$$2\nu \frac{\phi_x \vartheta_y - (1-c_2)u^o}{\phi_r \vartheta_y} > (1-h^o)u^o \kappa_{rw} \qquad (\mathbf{R2})$$

Thus the model of the real sector exhibits sustained cyclical behavior under the conditions **R1** and **R2**.

2.9.3 Relaxing the restriction on the parameter c_1 and the implications for long-run growth

In the following I will discuss why, in the long-run, u^o is always realized in the model economy, such that the firms use u^o as their measure for "normal" utilization. We are also going to relax the restriction for the parameter c_1 and look at what happens in case $c_1 \neq u^o(1-c_2) - g^o - \delta$. We are going to consider these issues in the context of the model of the real sector to limit the scope of the discussion. If we drop the parameter restriction the resulting model of the real sector is:

$$\dot{x} = \nu\left[(1-x)\exp(\vartheta_y y) - (1+x)\exp(-\vartheta_y y)\right], \quad -1 \leq x \leq 1 \qquad (\mathbf{SE})$$

$$\dot{h} = -(1-h)\kappa_{rw} y, \qquad 0 < h < 1 \qquad (\mathbf{PS})$$

$$g = g^o + \phi_r(r^n - r^o) + \phi_x x \qquad (\mathbf{IF}')$$

$$y = \frac{g + \delta + c_1 - (1-c_2)u^o}{(1-c_2)u^o} \qquad (\mathbf{OG}')$$

$$r^n = h u^o - \delta \qquad (\mathbf{NPR})$$

The expression for the output gap (y) has changed now and we now treat r^o as a stand alone parameter reflecting the cost of capital. Recall that when discussing profitability in Section 2.2.3 we linked the "normal" rate of utilization to a situation in which the wage share does not change since the labor market is neither overheated, nor is there slack. Thus, whenever utilization is higher (lower) than u^o, profitability would decrease (increase) leading to decreases (increases) of investment, such that the rate of utilization decreases (increases) until it returns to u^o. Also, note that even if the firms use a different utilization rate (say $u_f^o \neq u^o$) to determine the normal profit rate in eq. (**NPR**), the long-run utilization rate would still be u^o, which is the utilization rate associated with a constant wage share. Again, this is because profitability (and thus via eq. (**OG′**)) investment and actual utilization) would continue changing until there is no slack or overheating on the labor market, which happens at u^o. This happens for any given fixed profitability benchmark r^o used by the firms. We now know (see eq. (2.3)) that $\frac{g+\delta}{1-c_2} + \frac{c_1}{1-c_2} = u^o$ will hold in the long run, which guarantees that the output gap (y) would be zero in the long run.

In the expression $\frac{g+\delta}{1-c_2} + \frac{c_1}{1-c_2} = u^o$ there is only one endogenous variable, namely the net investment rate (g). This allows us to see how the model economy would react to different consumption behaviors, in particular for different values of the parameter c_1, which stands for consumption out of wealth. A higher (lower) consumption out of wealth (or also out of current income (c_2), for that matter) is associated with a lower (higher) long-run net investment rate in the economy and thus with a lower (higher) overall growth rate. In particular, the long-run growth rate is given by: $g^{long} = u^o\,(1-c_2) - \delta - c_1$. In the context of this model the intuition for this result is that changes in the consumption behavior lead to long periods characterized by non-zero output gaps (see eq. (**OG′**)) during which factor labor is either scarce (for higher consumption) or abundant (for lower consumption). This leads to a permanent shift in the long-run level of profitability, because of the shift in the wage share in the economy (see eq. (**PS**)). At the resulting higher or lower long-run profitability, the long-run investment rate is now also different (see eq. (**IF′**)).

We can now drop the parameter g^o, i.e. set $g^o = 0$, since the long-run investment rate is now endogenously determined by the expression $g^{long} = u^o\,(1-c_2) - \delta - c_1$. In this way we can get a clear interpretation of the determinants of long-run growth in the model. Since $y = 0$ in the long run, $x = 0$ and we can rewrite eq. (**IF′**)) as $g^{long} = \phi_r\,(r^n - r^o)$. If we re-interpret the parameter r^o as the cost of capital, then the long-run growth rate (g^{long}) of the model economy is a function of the difference between the long-run profit rate ($r^{long} = h^{long}\,u^o - \delta$)

and the cost of capital (r^o). We can now think of this modified model of the real sector in terms of a model of endogenous growth.

By plugging (**NPR**) and g^{long} into (**IF′**) and solving for h we get the only potentially economically meaningful globally attractive point of rest (recall that the other two points of rest are associated with the corner solutions $h = 0$ and $h = 1$). The point of rest is $(x^*, h^*) = (0, \frac{u^o\,(1-c_2)+(\phi_r-1)\,\delta-c_1+\phi_r\,r^o}{\phi_r\,u^o})$. Obviously, $0 < \frac{u^o\,(1-c_2)+(\phi_r-1)\,\delta-c_1+\phi_r\,r^o}{\phi_r\,u^o} < 1$ has to be satisfied. If that is the case, then the stability analysis is analogous to the one presented in the appendix (Section 2.9.2), if not, for parameter combinations that do not satisfy these inequalities, there is no economically meaningful point of rest.

2.9.4 Data filtering and sources

The cyclical components of all empirical series presented in this chapter have been obtain using the following procedure. First, the raw data (or the natural logarithm of it, whenever an exponential trend is present) is detrended by using the Hodrick-Prescott filter with a smoothing parameter of 1600 (see Hodrick and Prescott (1997)). As a second step, the resulting cyclical component is smoothed additionally by applying a moving average over 11 quarters (over 5 lags, the current observation and 5 leads). The second step emphasizes the persistent movements in the data and is done to make the patterns in the series more recognizable. In Figure 2.1 the fluctuations of the stock market index have been divided by 5, while those of the real base interest rate have been multiplied by 10 to make these comparable to the fluctuations of the output gap. In Figure 2.2 no re-scaling has been done. In Figure 2.5 the fluctuations of the risk premium have been multiplied by 5 to make these comparable to the fluctuations of the output gap. In Figure 2.6 the fluctuations of the stock market index have been divided by 5, while those of the real base interest rate have been multiplied by 10 to make these comparable to the fluctuations of the output gap. In Figure 2.8 no re-scaling has been done.

What follows is a list of the empirical series mentioned in the chapter together with their respective sources:

- The real gross value added of the non-financial sector is provided by the US. Bureau of Economic Analysis.
- The profit share in output is computed by using the National Income and Product Accounts (NIPA) Table 1.15 provided by the US. Bureau of Economic Analysis. We

divide the "Profit Per Unit of Real Gross Value Added of Nonfinancial Domestic Corporate Business (after tax with IVA and CCAdj)" by the "Price per unit of real gross value added of nonfinancial corporate business". Computing the profit share without considering taxes does not make a marked difference in terms of the dynamics of the profit share, only the level around which the profit share fluctuates changes.

Using data from the (NIPA) Table 1.14 yields very similar results. The profit share was computed in this way, for example, in the paper by Zipperer (2011).

- Different measures of Tobin's Q and various stock market indices have very similar dynamics over the business cycle. The historical data for the S&P 500 index was taken from the "Political calculations" blog (http://politicalcalculations.blogspot.com/2013/02/quarterly-data-for-s-500-since-1871.html) and in terms of the index in the month ending the respective quarter.

  Tobin's Q was computed by using data from the Federal Reserve Z.1 Statistical Release, section B.102 Balance Sheet of Non-farm Non-financial Corporate Business. Specifically, it is the ratio of Line 39 (Corporate Equities; Liability) divided by Line 36 (Corporate Business; Net Worth). Using other measure of Tobin's Q does not impact the overall dynamics much, since, in all cases, the most powerful source of variation is the price of equity (the stock prices). This is the intuition behind the very similar dynamics of stock price indices and measures of Tobin's Q over the business cycle.

- The real base interest rate – the quarterly series of the yearly "Effective Federal Funds Rate" divided by 4. It is taken from the Federal Reserve Economic Data (FRED).

- Inflation – the quarterly series of the yearly CPI inflation rate provided by the US. Bureau of Labor Statistics divided by 4.

- The risk premium – We take the BofA Merrill Lynch US High Yield Master II Option-Adjusted Spread divided by 4 as a proxy for the quarterly risk premium. The series are provided by BofA Merrill Lynch and are available only post 1996: https://research.stlouisfed.org/fred2/series/BAMLH0A0HYM2.

2.9.5 The parameter values used in the simulations

All simulations were done using a built-in numerical solver for systems of first-order of differential equations in Matlab. We always display or measure the simulation results after

the first 200 simulation quarters, when adjustments coming from the initial conditions have faded away. The model is calibrated for measurements at a quarterly frequency. This means that parameters like u^o, g^o, δ or π^* are set to reflect their empirical counterparts at a quarterly frequency.

The simulation producing the dynamics shown in Figure 2 (b) are based on the following parametrization of the model of the real sector:[44]

ν	ϕ_x	ϕ_r	c_2	h^o	ϑ_y	κ_{rw}	δ	g^o	u^o
0.3	0.008	0.5	0.3	0.3	23	0.1	0.025	0.005	0.25

The simulation producing the dynamics shown in Figure 4 are based on the following parametrization of the model of the real sector:

ν	ϕ_x	ϕ_r	c_2	h^o	ϑ_y	κ_{rw}	κ	α	γ
0.4	0.008	0.45	0.3	0.3	60	0.15	0.03	0.4	0.8

π^*	μ_i	μ_y	μ_π	ρ_q	ρ_ξ	ξ^c	δ	g^o	u^o
0.005	1	0.3	0.3	1	0	0.015	0.025	0.005	0.25

The values of the parameters underlying the final parametrization of the integrated model (see Section 2.6 and Figure 6) read as follows:

ν	ϕ_x	ϕ_r	c_2	h^o	ϑ_y	κ_{rw}	κ	α	γ
0.2	0.008	0.5	0.3	0.3	18.7	0.15	0.04	0.4	0.8

π^*	μ_i	μ_y	μ_π	ρ_q	ρ_ξ	ξ^c	δ	g^o	u^o
0.005	1	0.1	0.1	0.3	0.3	0.015	0.025	0.005	0.25

The two parametrizations differ in terms of the values of the parameters ν, ϕ_r, ϑ_y, μ_y, μ_π, ρ_q and ρ_ξ. The values of the parameters μ_y and μ_π are higher under the first parametrization to reflect the more aggressive monetary policy, while the values of the parameters ρ_ξ and ρ_q

[44]The "normal" output capital ratio might appear too high ($u^o = 0.25$). It should be noted that this ratio pertains to the non-financial sector and not to the whole economy. For the non-financial sector the average output capital ratio is higher than for the whole economy. See Franke (2015a, Section 5 and the Appendix) for more on this issue.

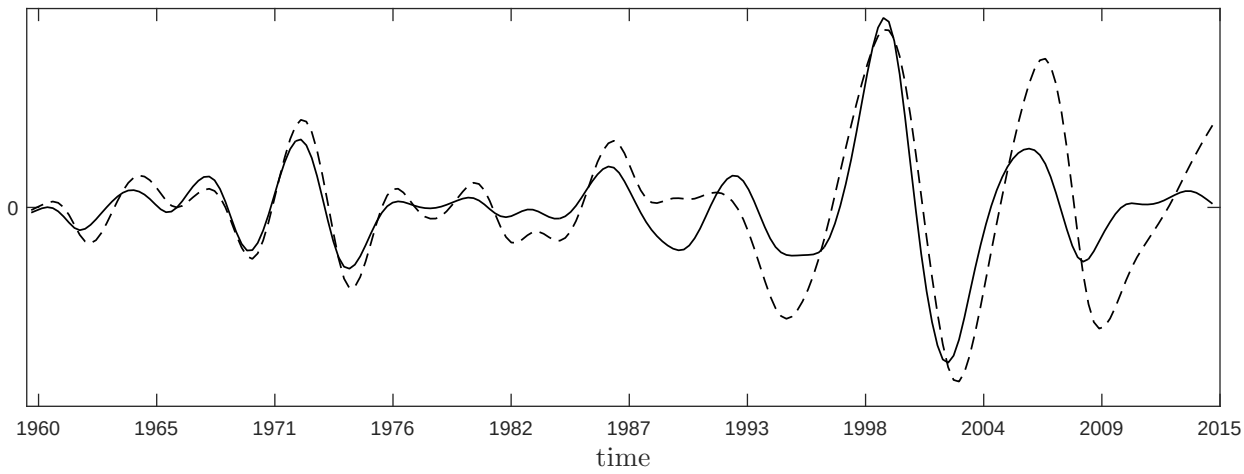

Figure 2.8: The filtered fluctuations of the stock price index S&P 500 (dashed line) and of a measure of Tobin's Q (solid line) around their respective long run trends for the US over the period (1960-2014). The fluctuations have been re-scaled to make them comparable by means of visual inspection.

reflect the introduction of an endogenous risk premium and an adjustment process for Tobin's Q. Adjustments in the parameters ν, ϕ_r and ϑ_y are needed to preserve the endogenous cycles produced by the model and to keep the desired amplitudes and cycle period of the variables fixed.

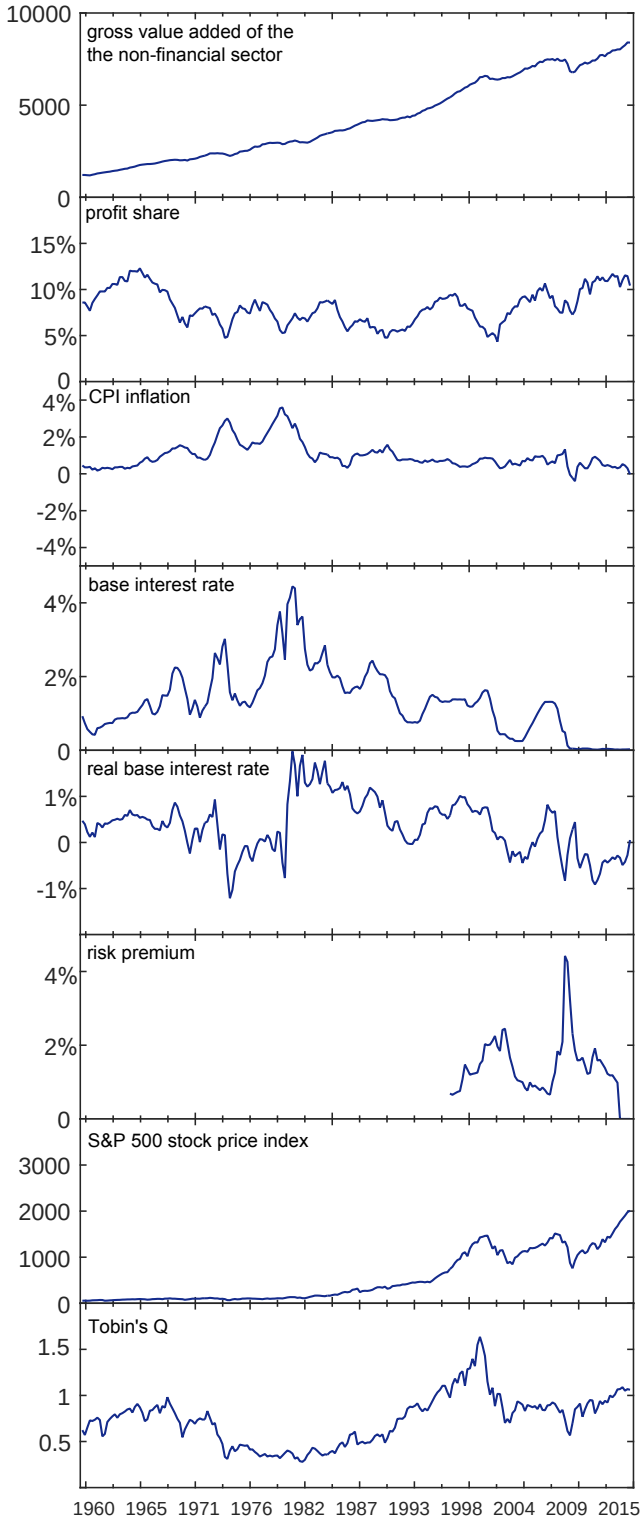

Figure 2.9: Plots of the raw data from which the fluctuations used for calibrating the model were extracted. All rates are yearly rates divided by 4 to approximate quarterly rates.

Chapter 3

On the long-run Equilibrium Value of Tobin's Average Q

Published in the European Journal of Economics and Economic Policies:

Intervention

Coauthored by: Boyan Yanovski and Reiner Franke.

Keywords: Tobin's average Q, debt and equity financing, no-arbitrage condition, fundamentalist traders.

3.1 Introduction

A central variable in macroeconomic growth models where firms finance their investment by debt and equities is the ratio of outside finance to the capital stock. This concept was first put forward by Kaldor (1966), who simply referred to it as the "valuation ratio", and then brought to prominence by Tobin (1969) and a number of subsequent writings, from when on it became known as Tobin's (average) Q.[1]

For Tobin himself and much of the literature, the obvious value for a long-run equilibrium was $Q = 1$ (for example, Tobin 1969: 23). Regarding possible reactions in the economy to deviations of Q from this benchmark, probably best known is the 'common sense' argument "that the incentive to make new capital investments is high when the securities giving title

[1] We write capital 'Q' in a purely descriptive context such as presently in the Introduction, and switch to lower case 'q' when we turn to the formal arguments.

to their future earnings can be sold for more than the investment cost, i.e., when q exceeds one" (Tobin 1996: 15), while arbitrage opportunities deter the production of new capital goods in the opposite case.[2] Considering the substantial delays in such a process, Tobin (1998: 107) interestingly adds later that "in a sense the stock market acts out in advance and in purely financial terms the subsequent and much slower adjustment of the physical stock of capital".[3]

Under closer scrutiny these arguments seem to apply to investment at the margin or, in more technical terms, with the notion of marginal rather than average Q.[4] This may be one of the reasons why contemporary structuralist, post-Keynesian modelling has practically no recourse to them. As a consequence, Q is here generally different from unity in a steady state; some representative examples are the stock-flow consistent models of a real-financial interaction by Godley and Lavoie (2007), Dos Santos and Zezza (2008), Le Heron and Mouakil (2008), Van Treeck (2008), or Bernardo et al. (2015). In these works, Q may actually attain any value in a steady state. It appears as the accidental result of the interplay of some components in the model that, however, bear no clear relation to the valuation ratio. That is, so far the models are not very thoroughly concerned with an explicit theory of the determination of the long-run equilibrium value of Q.

The present chapter sets out to provide some elementary insights that may prove useful for developing such a theory, which abstains from marginalist concepts. To this end, it characterizes Q by a ratio of certain rates of return on the real and financial assets, and this relationship serves to work out consistency conditions for a long-run equilibrium position. In particular, one condition with a suitable risk premium entering it is identified that, together with the others, would yield $Q=1$ in equilibrium. Because, however, it cannot be expected to hold true in general, we will also carry out a provisional numerical check to get a first feeling for possible deviations of Q from unity. It is found out in this way that typically these deviations will be of a fairly moderate order of magnitude.

[2] As far as Q may affect investment decisions, this reasoning was already essentially anticipated by Keynes (1936: 151): "the daily revaluations of the stock exchange … inevitably exert a decisive influence on the rate of current investment. For there is no sense in building up a new enterprise at a cost greater than that at which a similar existing enterprise can be purchased … if it can be floated off on the Stock Exchange at an immediate profit." (See also the footnote that Keynes adds to this quotation.)

[3] At the same place, Tobin also sketches other equilibrator mechanisms (pp. 106f).

[4] Marginal Q as a key determinant of investment was formally introduced in neoclassical models, which typically include adjustment costs. Marginal and average Q were shown to coincide if these costs exhibit constant returns (Hayashi, 1982).

3.2 Some basic relationships in the business sector

Consider an economy where besides retained earnings, firms finance fixed investment from external sources by issuing equities and raising credits. Accordingly, their accumulated liabilities are given by the loans outstanding L and by the evaluation p_eE of the firms on the stock market, E being the number of shares and p_e their price. The assets on the other side of the balance sheet of the firms are the stock of fixed capital K valued at the current price p.[5] Tobin's q is the ratio of the liabilities to the assets, and λ and e are the single ratios of the loans and equities, which add up to q:

$$q \;=\; \frac{L+p_eE}{pK}\,, \qquad \lambda \;=\; \frac{L}{pK}\,, \qquad e \;=\; \frac{p_eE}{pK} \tag{3.1}$$

Let a dot above a dynamic variable x denote its derivative with respect to time, $\dot{x}=dx/dt$, and a caret its growth rate $\hat{x}=\dot{x}/x$. Furthermore, denote the growth rates of loans and equities as $g_L=\hat{L}$ and $g_E=\hat{E}$, respectively, and by g and π the growth rate of the capital stock, $g=\hat{K}$, and the rate of goods price inflation, $\pi=\hat{p}$. The latter two may well be supposed to be positive, that is, the economy is generally growing in an inflationary environment.

Since $\dot{q}=\dot{\lambda}+\dot{e}=\lambda\,\hat{\lambda}+e\,\hat{e}$ and $\hat{\lambda}=g_L-g-\pi$, $\hat{e}=\hat{p}_e+g_E-g-\pi$, the motions of q are described by the equation

$$\dot{q} \;=\; \lambda\,g_L \;+\; e\,(\hat{p}_e+g_E) \;-\; q\,(g+\pi) \tag{3.2}$$

(the last term uses $\lambda+e=q$). In our discussion of the long-run equilibrium features in this framework, the values of the variables in a steady state are indicated by a superscript 'o'. To begin with, what is invariant in this position is not the stock prices but rather the ratio q, that is, $\dot{q}=0$ when the loan and stock markets are growing in step. Solving this equality in (3.2) for stock price inflation and writing from now on $\pi_e=\hat{p}_e$, the equilibrium value π_e^o is seen to be given by

$$\pi_e^o \;:=\; \pi_e\Big|_{\dot{q}=0} \;=\; \frac{1}{e}\Big[q\,(g+\pi) \;-\; \lambda\,g_L \;-\; e\,g_E\Big] \tag{3.3}$$

[5] The short-term as well as long-term financial assets in the corporate business are thus neglected, or the loans L may thought of net of them.

If in addition both markets themselves are on an equilibrium path, so that $\hat{\lambda} = g_L - \pi - g = 0$ (which also implies $\hat{e} = 0$), the prices on the stock market rise at a rate

$$\pi_e\Big|_{\dot{q}=\dot{\lambda}=0} \;=\; \pi \;+\; (g \;-\; g_E) \tag{3.4}$$

It is thus readily checked that stock prices rise at the same rate as goods prices if, and only if, the firms issue equities at the real rate of growth, $g_E = g$. Generally, stock price inflation exceeds the inflation rate for goods by the difference between g_E and g. To get an impression of a reasonable order of magnitude of such an equilibrium stock price inflation, we can refer to US data and observe that over the last three decades there was hardly ever a positive net issuance of equities. Firms rather followed a strategy of buying their shares back from the market, so that typically g_E was distinctly negative.[6] If in the (very) long term prices on the stock market show a tendency to rise faster than prices in the real sector, this is therefore not only due to a permanent speculative pressure.[7]

The core of the model is the finance equation of the firms. It says that the net investment $g\,pK$ is financed by internal and external sources. Internal financing is what the firms retain from their surplus $r\,pK$ (r being the rate of profit net of depreciation) after paying the interest costs iL (i the loan rate), the corporate income tax (based on a proportional tax rate τ_c levied on $r\,pK - iL$), and the dividends $d\,pK$ (d defined as the ratio of the dividends to the capital stock). External financing is given by (i) issuing new shares $\dot{E}$ at the going price p_e and (ii) raising new loans $\dot{L}$. Taken together, $g\,pK = (1-\tau_c)\,(r\,pK - i\,L) - d\,pK + \dot{L} + p_e\dot{E}$. The finance equation in intensive form is obtained by normalizing the variables by the capital stock pK. Using $\dot{L}/pK = (\dot{L}/L)\,(L/pK) = \lambda\, g_L$, $p_e\dot{E}/pK = (p_e\dot{E}/p_eE)\,(p_eE/pK) = e\, g_E$, it reads,

$$g \;=\; (1-\tau_c)(r \;-\; i\lambda) \;-\; d \;+\; \lambda\, g_L \;+\; e\, g_E \tag{3.5}$$

Given the limited scope of this chapter we need not discuss the determination of the variables in this identity; especially the profit rate may be treated as in the post-Keynesian or Kaleckian models of the real sector studying growth and income distribution. We dot not even need to make an assumption about the causality in this relationship. That is, it can be left open which of the variables is predetermined in some sense, by a function or a dynamic

[6] May it suffice to refer to Figures 2 and 3 in Skott and Ryoo (2008: 831) or, without their time aggregation, to Figure 1 in Ryoo (2010: 166).

[7] Equation (3.4) is put forward for making this elementary observation but it is not necessarily needed in the following analysis; working with eq. (3.3) will then already do.

adjustment equation, and which is then residually determined. For example, one may follow Hein (2013) and assume a constant proportion $\overline{d}_e$ of the dividend payments to the stock market value of the firms (rather than to their capital stock), so that $d = e\overline{d}_e$; or, what is more common in the literature, one may assume a constant after-tax retention rate s_f, so that the dividends normalized by the capital stock are determined as $d = (1-s_f)(1-\tau_c)(r-i\lambda)$ and therefore vary with r, i as well as λ.

3.3 The return on equities

To study the financial sector of the economy insofar as Tobin's q plays a role for its long-run equilibrium position, we begin with the rate of return r_e that the rentiers earn by holding equities. It is given by the dividends in relation to this investment $p_e E$, plus the capital gains π_e. Solving the finance equation (3.5) for d, the equilibrium value r_e^o when $\dot{q} = 0$ (and thus (3.3) holds true) is computed as

$$r_e^o \;:=\; \frac{d}{e} \;+\; \pi_e^o \;\;=\;\; \frac{1}{e}\Big[(1-\tau_c)(r-i\lambda) \;-\; g \;+\; q(\pi+g)\Big] \tag{3.6}$$

We next introduce a risk premium ξ_e of the equities. Given that loans and equities are not perfect substitutes, it is that premium that compensates the rentiers for the greater risk on the stock market and makes them indifferent between the returns from their investment in equities and the interest that they could earn from lending their money to the firms (directly or indirectly, intermediated by commercial banks). In such a situation, and only in such a situation, will the rentiers no longer reshuffle their portfolio and the two ratios e and λ can remain invariant. Let us thus formulate:[8]

Equilibrium Condition 1

With respect to a given risk premium ξ_e of the rentiers regarding their investment on the stock market,

$$r_e^o \;-\; \xi_e \;\;=\;\; i$$

prevails in a long-run equilibrium position.

[8] While the premium ξ_e is here treated as given, in a full-fledged dynamic model it may interact with q and other key variables. Also, for simplicity, we do not distinguish between the loan rate of the firms and a possibly different interest rate relevant to the rentiers.

To make it perfectly clear, Condition 1 is a necessary but by no means sufficient condition for a long-run equilibrium to come about.

Actually, eq. (3.6) indicates that r_e is inversely related to the equity ratio e (which also holds when $\dot{q} \neq 0$). Hence a relatively low e can be one reason for a situation where $r_e - \xi_e$ exceeds the interest rate i. The latter feature, however, will induce a larger group of rentiers to increase their demand on the stock market, which should then speed up the increase in stock prices and thus have a positive effect on the entire ratio $e = p_e E/pK$. This, in turn, introduces a negative feedback on the return rate r_e, so that the gap between $r_e - \xi_e$ and i is reduced. In this way we have sketched an elementary mechanism that may tend to restore Condition 1 in case it were violated.[9]

3.4 Tobin's q in the steady state: Model version A

The next two sections are directed at a characterization of the long-run equilibrium value of Tobin's q. Since, the ratios q, λ, e and the ratios in the desired portfolio of the rentiers are not independent of one another, their equilibrium values may generally be determined in a simultaneous manner. Before setting up a full-fledged model design it is, however, useful to treat some of them as parametrically given and examine the resulting implications.

In the present section we concentrate on a fixed value λ^o of the debt-asset ratio. It may even be argued that the firms borrow from commercial banks and λ^o comes about in an interaction of just these two parties, supposing that the banks do not particularly care about the firms' equity ratio as long as it remains within certain bounds.

The characterizations of q^o in which we are interested do not refer to the stock variables of the original definition of the valuation ratio. Loosely speaking, they are rather concerned with flow magnitudes, which include rates of return, of growth, and inflation. Proposition 1 presents two formulations, where the present setting with a given λ^o may be indicated by the letter 'A'.

Proposition 1

Suppose Condition 1 holds true. Then the long-run equilibrium values of q and

[9] Of course, this does not rule out that in a speculation dynamics there may also be other mechanisms at work, some of which could well be (locally) destabilizing.

λ are interrelated as follows,

$$q^o \;=\; \frac{r-\tau_c(r-i\lambda^o)+\lambda^o\xi_e-g}{i-\pi+\xi_e-g} \tag{3.7}$$

Equivalently, putting

$$\xi_f^A \;:=\; r-\tau_c(r-i\lambda^o)\;-\;(i-\pi) \tag{3.8}$$

and taking $e^o = q^o - \lambda^o$ into account,

$$q^o \;=\; \frac{r-\tau_c(r-i\lambda^o)-e^o\xi_e-g}{i-\pi-g} \;=\; 1 \;+\; \frac{\xi_f^A \;-\; e^o\xi_e}{i-\pi-g} \tag{3.9}$$

The proof is straightforward. Substitute (3.6) in Condition 1, multiply it by e, put $ei = qi - i\lambda$ and $e\xi_e = q\xi_e - \lambda\xi_e$, and solve the resulting equation for $q = q^o$. This yields eq. (3.7). The second part of the proposition is derived in the same manner, only the step $e\xi_e = q\xi_e - \lambda\xi_e$ is omitted.

We take it, of course, for granted that the denominator in (3.7) is positive. This equation sets up a pure functional relationship between the equilibrium values of λ and q. It is interesting to note that under a *ceteris paribus* condition an increase in the debt-asset ratio λ^o results in a higher q^o. The reaction is also economically plausible if we refer to the net worth of the firms, which is reduced by higher loans.[10] A possible counter-effect could be that therefore the stock market devalues the equities of the firms, but intuitively it should not be strong enough to offset the increase in loans. Equation (3.7) enables us to confirm this reasoning mathematically if $(1-\tau_c i)\,i > \pi + g$ is assumed. In fact, $\partial e^o/\partial\lambda^o < 0$ because $e^o = q^o - \lambda^o$ and $\partial q^o/\partial\lambda^o = (\tau_c i + \xi_e)/(i - \pi - g + \xi_e)$ is then less than one.[11]

Equation (3.9) in the second part of the proposition has q^o also appearing on the right-hand side, *via* $e^o = q^o - \lambda^o$, but on the other hand this relationship seems to make better economic sense. The fraction in the first equation in (3.9) relates two quasi-rates of return, we may say, which (given $\lambda = \lambda^o$) could be of some relevance to the managers of the firms. The

[10] The net worth is here defined as the difference between assets and total liabilities. The former are given by the capital stock valued at its replacement cost, the latter by the outstanding loans and equities. In the present notation, net worth $= (1-\lambda-e)\,pK = (1-q)\,pK$, which means that an increase in q is tantamount to a decrease in the firms' net worth.

[11] Recalling that i is not a riskless rate of interest but the firms' loan rate, which is higher, we will argue later that the inequality $(1-\tau_c i)\,i > \pi + g$ can indeed be considered to be empirically satisfied. Otherwise we would have $\partial e^o/\partial\lambda^o > 0$, the economic reason for which would not be so clear.

numerator displays the (after-tax) profit rate adjusted for growth and also discounted by the risk premium. As the latter only applies to equities, ξ_e is multiplied by the equity ratio $e = p_e E/pK$. The denominator is the real interest rate, likewise adjusted for growth.

An anonymous referee made us aware that the approach taken in Proposition 1 can be understood as an extension of a formula for q that Richard Kahn (1972) put forward already more than 40 years ago. In a framework without taxes and debt financing (i.e., $\tau_c = 0$, $\lambda^o = 0$), he expressed the valuation ratio as the difference between the profit rate and the growth rate divided by the difference between the rate of return on equity and the growth rate.

To use Tobin's expression in his famous article from 1969, the numerator in (3.9) might also be viewed as (a simple version of) the firms' marginal efficiency of capital (MEC), 'adjusted' for growth and risk. The benchmark $q^o = 1$ would be obtained if it were equated to the real interest cost, an equality which in these words is an old and venerable argument. The role that $e^o\xi_e$ should play for the managers in this specification of MEC is, however, not entirely clear, because it involves the risk premium of the share holders. In particular, this ξ_e also accounts for the risk from the price fluctuations on the stock market, which are of no direct concern to the operative business of the firms.

For a better distinction in this respect, the second equation in (3.9) introduces the specification of ξ_f^A. This difference between profits and real interest may be interpreted as risk premium for the irreversibility of fixed investment. ξ_f^A can furthermore serve as an evaluation of how successfully the managers are running the firms (therefore the index 'f'). Thus, it may be employed by the managers themselves or by the shareholders who assess their work.

A priori, ξ_f^A may or may not be equal to the other 'weighted' risk premium $e^o\xi_e$. The second part of eq. (3.9) reveals that $q^o = 1$ arises if and only if the two are equal, $\xi_f^A = e^o\xi_e$, while $q^o < 1$ prevails if $e^o\xi_e$ exceeds the irreversibility risk premium ξ_f^A (presupposing that $i - \pi > g$; cf. footnote 11). Because of the relatively small denominator $(i - \pi - g)$, the quantitative effects of these deviations are, however, not easy to assess; a little numerical check will therefore be provided below.

In the case that ξ_f^A and $e^o\xi_e$ are equal and also not affected by a *ceteris paribus* increase in the growth rate g, eq. (3.9) tells us that this change has no impact on q^o, either. This is in contrast to Kaldor's conclusion in his model (1966: 317) that higher accumulation rates yield

lower valuation ratios, which is a result that has also recently been obtained in a modern stock-flow consistent model with many more endogenous feedbacks (but still an exogenous growth rate); see Bernardo et al. (2015: 10).[12] In the simple setting underlying (3.9), the effect would come about if and only if $\xi_f^A < e^o \xi_e$, that is, if and only if the original q^o happens to be less than one.

3.5 Tobin's q in the steady state: Model version B

In this section we turn to a simultaneous determination of q^o, λ^o and e^o. To ease the discussion in a baseline version, suppose that the firms borrow directly from the rentiers by issuing corporate bonds (L), say, paying the interest rate i.[13] This setting implies that in a steady state the rentiers will also accept the debt-asset ratio λ^o of the firms. In addition to Condition 1, we put forward a second criterion for the portfolio decisions of the rentiers that is necessary for an invariance of e and λ. Besides comparing the returns from their alternative investment in loans and equities, the rentiers are explicitly supposed to entertain the notion of a balanced portfolio. That is, defining

$$\beta = \frac{L}{L + p_e E}, \qquad \varepsilon = \frac{p_e E}{L + p_e E} \tag{3.10}$$

the rentiers have target values $\beta^\star$, $\varepsilon^\star$ for the proportions of the corporate bonds and equities in which they wish to hold their wealth—in a situation where the two assets appear equally attractive in the sense of Condition 1. In other words, $\beta^\star$ and $\varepsilon^\star$ serve the role of an explicit anchor for the portfolio shares. Clearly, $\beta + \varepsilon = 1$ and $e = \varepsilon q$, $\lambda = \beta q = (1-\varepsilon) q$. Accordingly, even if Condition 1 is fulfilled but in a dynamic framework currently $\beta > \beta^\star$ and therefore $\varepsilon < \varepsilon^\star$, for example, the rentiers seek to decrease the share β of loans in their portfolio and to increase the share ε of equities. These adjustments should also introduce a tendency for the firms' debt-asset ratio λ to decline and for their equity ratio e to increase. Thus, the idea of the target proportions amounts to a second consistency requirement.

Equilibrium Condition 2

The actual portfolio of the rentiers is balanced in a long-run equilibrium position,

[12] On p. 6 the authors argue that there is also some empirical evidence for this result.

[13] Possible price variations from their trading on an extra market should have only weak effects, so that they can be safely ignored.

that is, with respect to their given target proportions $\beta^\star$, $\varepsilon^\star$,

$$\beta^o \;=\; \beta^\star, \qquad \varepsilon^o \;=\; \varepsilon^\star$$

In this way the equilibrium values of q, λ and e are linked by the target proportions of the rentiers, $e^o = \varepsilon^\star q^o$, $\lambda^o = \beta^\star q^o$. Adding the second assumption to the first one allows us to determine the steady state value of Tobin's q directly by $\beta^\star$ and $\varepsilon^\star$, where the modified setting in the present section may be identified by the letter 'B'.

Proposition 2

Suppose Conditions 1 and 2 hold true. Then the long-run equilibrium value of Tobin's q is determined from the rentiers' target proportions $\beta^\star$ and $\varepsilon^\star$ as

$$q^o \;=\; \frac{(1-\tau_c)\,r \;-\; g}{(1-\beta^\star\tau_c)\,i \;-\; \pi \;+\; \varepsilon^\star\xi_e \;-\; g} \tag{3.11}$$

Equivalently, putting

$$\xi_f^B \;:=\; r - \tau_c(r - i\beta^\star) - (i-\pi) \tag{3.12}$$

q^o can be expressed as

$$q^o \;=\; 1 \;+\; \frac{\xi_f^B \;-\; \varepsilon^\star\xi_e}{(1-\beta^\star\tau_c)\,i \;-\; \pi \;+\; \varepsilon^\star\xi_e \;-\; g} \tag{3.13}$$

To prove the first part of the proposition, consider the equation $q(i-\pi+\xi_e-g) = (1-\tau_c)r - g + (\tau_c i+\xi_e)\lambda$, which with the operations indicated in the remark on Proposition 1 is equivalent to Condition 1. Replacing λ with $(1-\varepsilon^\star)q$ and solving this equation for $q = q^o$ yields $q^o = [(1-\tau_c)\,r - g]\,/\,[(1-\tau_c)\,i + \varepsilon^\star(\tau_c i+\xi_e) - (\pi+g)]$ and thus, with $\varepsilon^\star\tau_c i = (1-\beta^\star)\tau_c i$, eq. (3.11). Equation (3.13) adds and subtracts the denominator in the numerator and rearranges these terms.

The expression in the numerator of (3.11) displays the growth-adjusted profit rate of the firms, where (somewhat strangely) the corporate tax rate is imputed on the entire gross profits. The denominator can be interpreted as a real interest rate pertaining to the rentiers, which is modified in three ways: (i) just like the profit rate, it is adjusted for growth; (ii) the risk premium of holding equities is added to the interest rate term, now multiplied by the weight $\varepsilon^\star = p_e E/(L+p_e E)$ of the equities in the total wealth of the rentiers; (iii) the corporate tax rate carries over to the nominal interest rate that the rentiers receive from the firms (although this is a mechanism that might perhaps seem somewhat artificial, too).

While $q^o = 1$ results if the two rates above and below the fraction line in (3.11) are equal, it is not clear what economic principle might equate them. Similar doubts hold for the representation of q^o in eq. (3.13), which compares the term ξ_f^B with the weighted risk premium $\varepsilon^\star\xi_e$. Regarding the former, in evaluating the performance of the firms it makes sense for the rentiers to relate the profit rate to the real interest rate, after the corporate taxes are accounted for. However, this is more appropriately done in the specification of ξ_f^A in Propo-

g	π	i	r	τ_c
2.50	2.50	8.00	14.64	25.00

Table 3.1: Benchmark values (in %) characterizing the real sector in the US.

sition 1, as $\tau_c \beta^\star i$ in the definition of ξ_f^B is of no direct significance for the after-tax profits earned by the firms. The distortions of ξ_f^B *vis-à-vis* ξ_f^A, or of the criterion in (3.13) *vis-à-vis* eq. (3.9), which both derive from the different denominators in Proposition 1 and 2, can be made more explicit by the relationships

$$\begin{aligned} \xi_f^B &= \xi_f^A - (q^o - 1)\,\tau_c i \beta^\star \\ q^o &= 1 + \frac{[\xi_f - e^o \xi_e] + (q^o - 1)\,[\varepsilon^\star \xi_e - \beta^\star \tau_c i]}{(1 - \beta^\star \tau_c)\, i - \pi + \varepsilon^\star \xi_e - g} \end{aligned}$$

(which are easily verified). In short, it may be said that eq. (3.9) in Proposition 1 is economically more meaningful than eq. (3.13) in Proposition 2, but at the price that its right-hand side is not independent of the value q^o on the left-hand side.

3.6 A numerical check

If reference is made to the differences between ξ_f^A and $e^o \xi_e$ or ξ_f^B and $\varepsilon^\star \xi_e$, respectively, it must be recognized that, irrespective of a more detailed story explaining them, the premia ξ_e and ξ_f^A, ξ_f^B are likely to be independent. Their equality in eqs (3.9) or (3.13) can therefore not be taken for granted and the long-run equilibrium value q^o may well be different from unity. In this section we want to get a feeling for a typical order of magnitude of these deviations, where we consider model versions A and B together.

Note that there are two reasons why our results cannot be directly related to the empirical time series for Tobin's q that can be found at various places. First, our ratios are the long-run equilibrium values, which might not necessarily be well captured by the empirical medium-term time averages. Second, the empirical specifications of what is called Tobin's q may be somewhat different from the present definition. Thus, our purpose is not so much an empirical assessment of Tobin's q but rather some hints that future calibrations of elaborate stock-flow consistent models may take into account.

We begin our little numerical study by putting forward reasonable values for the variables in the real sector, where we confine ourselves to US data.[14] With respect to an underlying time unit of one year, Table 3.1 presents the benchmark values we are working with. The 2.50% for the capital growth rate and goods price inflation are the approximate time averages for the US nonfinancial business sector over the years 1983 – 2007, a period that is often referred to as the Great Moderation. The value for the interest rate is close to the average of the prime rate over the same period; corporate AAA (BAA) bond rates are a little lower (somewhat higher, respectively). The profit rate $r = (1-\tau_v)hu - \delta$ is obtained from the following estimates: $\tau_v = 0.0875$ (the rate at which production is taxed), $h = 0.30$ (the profit share), $u = 0.90$ (the output-capital ratio), $\delta = 0.10$ (the capital depreciation rate); thus $r = 0.146375$. Lastly, the value for the corporate tax rate τ_c is another (grossly rounded) time average.[15]

The debt-asset ratio, which constitutes model A, is the statistic surrounded by the greatest uncertainty. Apart from data issues, one first has to clarify the conceptual problem whether in the specification of "net debt" only the firms' short-term financial assets are netted out or more. Because of these ambiguities we consider three alternative values of a given λ^o, namely 0.20, 0.30, 0.40.[16] The corresponding equity target proportions $\varepsilon^\star$ in model B are $\varepsilon^\star = 1-\beta^\star = 1-\lambda^o/q^o$, hence with respect to a benchmark $q^o = 1$ we consider $\varepsilon^\star = 0.80, 0.70, 0.60$.

Our benchmark risk premia are likewise based on $q^o = 1$. Together with the profit and real interest rates from above and taking $\lambda^o = 0.30$ as an example, the risk premium ξ_f results as $\xi_f^A = \xi_f^B = 0.060781250$ in (3.8) and (3.12). Putting $e^o = \varepsilon^\star$ and $\xi_f^A - e^o\xi_e = \xi_f^B - \varepsilon^\star\xi_e = 0$, the value of ξ_e that brings about $q^o = 1$ is computed as $\xi_e = 0.086830357$. It may be claimed that both premia do not seem very implausible. In particular, it makes sense that the stock market risk of the rentiers from the volatile prices exceeds the risk of the firms from the irreversibility of their fixed capital, and that in quantitative terms we have $\xi_f < \xi_e = \xi_f + 2.60\%$.

[14] Given our limited purpose and the problems of international data comparability, we abstain from considering other OECD countries. In particular, different tax conventions and the measurement of capital (to determine the output-capital ratio for the profit rate) would make things difficult. Furthermore, in the end these countries should not yield orders of magnitude that are drastically different from our benchmark values.

[15] For details on the data sources and the way in which especially the tax rates and the output-capital ratio Y/K were derived, the reader may be referred to Franke (2015, Section 5 and the Appendix). Regarding the perhaps somewhat unfamiliar value for Y/K it should be clarified that since we are concerned with the firm sector, the capital stock does not include housing or residential investment. Also, it can be misleading to relate nominal Y and K because their relative price underwent some systematic variation. Besides, lower values for Y/K might bring r too close to i or even below it.

[16] At first sight $\lambda^o = 0.20$ might appear very low. Hein and Schoder (2011: 702, 722), however, calculate ratios that are even five percentage points lower.

given λ^o	$\xi_f^A = \xi_f^B$	ξ_e	version A based on λ^o	version B $\varepsilon^\star = 1-\lambda^o$
			$q^o - 1$	
0.20 :		5.35	0.192	0.233
0.30 :		6.68	0.145	0.198
0.40 :		8.46	0.105	0.165
0.20 :	5.88	7.35	0.000	0.000
0.30 :	6.08	8.68	0.000	0.000
0.40 :	6.28	10.46	0.000	0.000
0.20 :		9.35	−0.130	−0.159
0.30 :		10.68	−0.102	−0.142
0.40 :		12.46	−0.078	−0.124

Table 3.2: The long-run equilibrium value of Tobin's Q in terms of deviations from one ($q^o - 1$) resulting from (3.7) and (3.11), respectively, for alternative values of the equity risk premium ξ_e (in %) and the ex-ante debt to asset ratio λ^o.

The middle block of Table 3.2 shows the same risk premia if we suppose $\lambda^o = 0.20$ and $\lambda^o = 0.40$. Both premia are seen to increase with the debt asset ratio, where the variation in ξ_f is rather minor and the one in ξ_e is somewhat larger, because according to Propositions 1 and 2 the benchmark $q^o = 1$ requires that $\xi_e = \xi_f^A/e^o = \xi_f^B/\varepsilon^\star = \xi_f/(1-\lambda^o)$.

On this basis, the remainder of Table 3.2 gives some examples of the impact on q^o when ξ_e differs from ξ_f^A/e^o or $\xi_f^B/e^\star$, respectively. We fix $\xi_f^A = \xi_f^B$ and decrease/increase the stock market risk premium by two percentage points; see the upper/lower part of the table. We see that the strongest changes in q^o are obtained for the lowest debt-asset ratio, and the changes in the framework of model B are somewhat more pronounced than in model A. It is also worth noting that the positive and negative reactions are not symmetric; depending on the given indebtedness λ^o the positive reactions of q^o are 1.33 or 1.48 times stronger than the negative reactions. Generally, however, the effects can be said to be rather limited, which is the main message from our numerical exploration.

3.7 Conclusion

The valuation ratio of Tobin's (average) Q is a venerable concept to describe the financial situation in the business sector. As a ratio that relates the stock of liabilities (equities and debt) of the firms to their fixed capital, a value $Q = 1$ is equivalent to a zero net worth (if the capital stock is valued at its replacement cost). Thus, $Q = 1$ is often viewed as being indicative of a financial equilibrium and one can find various arguments in the older literature why the economy may be driven in the direction of such a position. By contrast, several of the more recent and elaborated stock-flow consistent models of a post-Keynesian variety have no more recourse to them whatsoever.

As a consequence, the determination of a long-run equilibrium value $Q = Q^o$ is a side effect of the interplay of other model mechanisms and it is usually not carefully checked if the resulting Q^o and its implications are sufficiently meaningful. Still at a very general level, the present note may prove fruitful in this context because instead of a stock ratio, it characterizes Q^o as a ratio of several rates of return which, in particular, include two expressions that can be interpreted as risk premia pertaining to the firms and rentiers, respectively. These concepts can widen the horizon of contemporary models and may also be incorporated into some of their dynamic adjustment principles.

The special case $Q^o = 1$ can come about under certain precise conditions that may or may not be fulfilled. Typically, however, possible distortions from unity will be fairly moderate. Actually, an elementary numerical check yields values of Q^o between, say, 0.85 and 1.20 as a reasonable guideline for an ambitious numerical analysis. On the other hand, our approach can serve for a better understanding should larger deviations be obtained. It may then be discussed if such outcomes can still be accepted or if some modifications in the model or its numerical calibration may be necessary.

References

Bernardo, J.L., Stockhammer, E. and Martínez, F.L. (2015): A Post-Keynesian theory for Tobin's q in a stock-flow consistent framework. Post Keynesian Economics Study Group, Working Paper 1509.

Dos Santos, C. H. and Zezza, G. (2008): A simplified, "benchmark", stock-flow consistent Post-Keynesian growth model. *Metroeconomica*, 59, 441–478.

Franke, R. (2015): A simple approach to overcome the problems from the Keynesian stability condition. Working Paper, University of Kiel; `https://www.gwif.vwl.uni-kiel.de/de/working-papers-1`.

Godley, W. and Lavoie, M. (2007): *Monetary Economics*. Basingstoke: Palgrave MacMillan (1st ed.).

Hayashi, F. (1982): Tobin's marginal q and average q: A neoclassical interpretation. *Econometrica*, 50, 213–224.

Hein, E. (2013): On the importance of the retention ratio in a Kaleckian distribution and growth model with debt accumulation—A comment on Sasaki and Fujita (2012). *Metroeconomica*, 64, 186–196.

Hein, E. and Schoder, C. (2011): Interest rates, distribution and capital accumulation—A post-Kaleckian perspective on the US and Germany. *International Review of Applied Economics*, 25, 693–723.

Kahn, R. (1972): Notes on the rate of interest and the growth of firms. In *Selected Essays on Unemployment and Growth*. Cambridge: Cambridge University Press.

Kaldor, N. (1966): Marginal productivity and macro-economic theories of distribution. *Review of Economic Studies*, 33, 309–319.

Keynes, J.M. (1936): *The General Theory of Employment, Interest and Money*. London: Macmillan.

Le Heron, E. and Mouakil, T. (2008): A Post-Keynesian stock-flow consistent model for dynamic analysis of monetary policy shock on banking behaviour. *Metroeconomica*, 59, 405–440.

Ryoo, S. (2010): Long waves and short cycles in a model of endogenous financial fragility. *Journal of Economic Behavior and Organization*, 74, 163–186.

Sasaki, H. and Fujita, S. (2012): On the importance of the retention ratio in a Kaleckian model with debt accumulation. *Metroeconomica*, 63, 417–428.

Skott, P. and Ryoo, S. (2008): Macroeconomic implications of financialisation. *Cambridge Journal of Economics*, 32, 827–862.

Tobin, J. (1998): *Money, Credit, and Capital*. Boston: Irwin McGraw-Hill.

Tobin, J. (1996): *Volume 4: Essays in Economics: National and International*. Cambridge, Mass: MIT Press.

Tobin, J. (1969): A general equilibrium approach to monetary theory. *Journal of Money, Credit, and Banking*, 1, 15–29.

Van Treeck, T. (2008): A synthetic, stock-flow consistent macroeconomic model of "financialisation". *Cambridge Journal of Economics*, 33, 467–493.

Chapter 4

Structural Correlations in the Italian Overnight Money Market: An Analysis Based on Network Configuration Models

Published in Entropy

Coauthored by: Luu Duc Thi, Boyan Yanovski and Thomas Lux.

Keywords: Interbank Network; Structural Correlations; Mixing Natures; Clustering Coefficients; Configuration Models.

4.1 Introduction

Understanding the topological structure of complex systems is crucial in many areas, e.g. in ecology, physics, neuroscience, epidemiology, economics, and finance. Statistics pertaining to properties related to single nodes, linked node pairs and linked node triplets are often referred to as structural correlations of the first, second and third order respectively. The study of these structural correlations is one of the most common approaches for examining the properties of a network. The degree and strength sequences are examples of first order structural correlations. Statistics pertaining to properties related to linked node pairs reveal information about the type of mixing (assortative vs disassortative) that takes place in the network, while those related to linked node triplets are indicative of the clustering behavior.

In terms of second order correlations, a network would exhibit assortative mixing if its nodes are predominantly connected to other nodes having similar degrees or strengths. In contrast, disassortative mixing occurs when the connected nodes are dissimilar (see, for ex-

ample, Newman, 2002; Newman, 2003a). This concept can be extended to directed networks yielding four mixing categories, i.e. in-in, in-out, out-in, and in-in mixing as illustrated in Figure (4.1) (see, for example, Foster et al., 2010; Piraveenan et al., 2012; van der Hoorn and Litvak, 2015). It should be emphasized that, in many real world networks, the mixing behavior of the directed version can differ a lot from the one observed in the undirected version. Furthermore, the same directed network can have assortative and disassortative aspects related to the mixing categories mentioned above (see, for example, Foster et al., 2010).

At the level of a single node, in the binary case, second order structural correlations can be expressed in terms of a relationship describing the average degree of the nearest neighbors (ANND) of a node as a function of that node's own degree. If the ANND is an increasing function of degree, this can be considered evidence in favor of assortative mixing. In contrast, a decreasing function would signal disassortativity.

For the whole network, the Pearson correlation coefficient between the degrees of pairs of linked nodes is often used to assess whether a network displays disassortative or assortative mixing (Newman, 2002; Newman, 2003a). This indicator is nothing else but a function of node degree and can also be expressed in terms of the measures ANND collected for the whole network (see the Appendix for further details).

In addition, we can decompose the overall assortativity coefficient into the contributions of each node, i.e. we can measure the local assortativity associated with each node. Such a decomposition can reveal which nodes contribute to the overall observed mixing nature of the network and which are associated with the opposite type of mixing (see, for example, Piraveenan at al., 2012). For instance, a globally assortative network may be locally disassortative and vice versa. It is worth noting that two networks with the same degree distribution and the same global level of assortativity may display different patterns of local assortativity.

The analysis of the second order structural correlations in the binary case can be straightforwardly extended to weighted networks by employing a measure that takes the average strength of the nearest neighbors (ANNS) of a node or by computing the Pearson correlation coefficient between the strengths of pairs of linked nodes.

As is common in the literature, we use clustering coefficients as measures of the third order structural correlations in the network. A clustering coefficient measures the tendency of two neighbors of a particular node to also be connected to each other (e.g. Newman, 2003b). If we define a node triplet as three nodes connected by at least 2 edges, then,

considering a network as a whole, the transitivity ratio (T) is equal to the number of triplets in which all three nodes are directly connected (forming a triangle) as a fraction of all node triplets (e.g. Newman, 2003b). An alternative measure is proposed by Watts and Strogatz (1998), which can capture the observed local clustering. The average of these local clustering coefficients can be used as an alternative measure of clustering for the whole network. The difference between the transitivity ratio and the average clustering coefficient is that, while in the former we calculate the ratio of the means, in the latter we take the mean of the ratios. In addition, for the directed version of a network, it is useful to differentiate between different relationship types depending on the direction of the edges in a triangle, i.e. inward, outward, cyclic, and middleman relationships, since as shown in Figure (4.2), the different relationships have different implications in terms of the risk exposure the individual banks are facing and in terms of systemic risk (see, for example, Fagio, 2007; Tabak et al., 2014). In weighted networks, the weighted clustering coefficients can be formulated in several ways, depending on how we take into account the roles of the strengths and weights of the nodes in each triangle (see, for example, Barrat et al., 2004; Onnela et al., 2005; Zhang and Horvath, 2005; Holme et al., 2007 [1]).

To assess whether the observed higher order structural correlations in a network are typical of a network with the observed lower order structural correlations, we can employ a randomization procedure based on the observed lower order patterns in the attempt to arrive at a suitable null model to test against for non-random patterns. Such null models create a whole ensemble of networks out of a subset of the information necessary to completely define the observed network. This is why this technique can also be used for filling in unavailable information. The most basic null models are the random graph models (RGM), which specify only global constraints such as the node degree average in the binary case or the node strength average in the weighted case. Since in these models, all nodes are treated homogeneously, there is no difference between the expected topological properties across nodes, which does not happen often in real world networks. In order to capture the intrinsic heterogeneity in the capacity of the individual nodes, a popular approach is to generate the microcanonical ensemble of networks having exactly the same degree sequence (or the same strength sequence in weighted networks) as the one in the observed network (see, for example, Maslov and Sneppen, 2002; Maslov et al., 2004; Zlatic et al., 2011). However, this "hard" approach suffers from various limitations [2]. Based on the maximum-entropy and maximum-

[1] We refer the readers to Saramäki et al. (2007) for a comparison between different methods for calculating the local weighted clustering coefficients.

[2] See Squartini and Garlaschelli (2011) or Squartini et al. (2015) for a discussion of this "hard" approach

likelihood methods, recent advances in the specification of configuration models propose a "soft" approach that enforces the constraints on average over an ensemble of randomized networks (e.g. Garleschelli and Loffredo, 2008; Squartini and Garlaschelli, 2011; Squartini et al., 2011a; Squartini et al., 2011b; Mastrandrea et al., 2014; Squartini et al., 2015). This approach allows us to sample network ensembles more efficiently and in an unbiased manner (Squartini et al., 2015).

In this paper we analyze the structural correlations in a particular financial system, i.e. the Italian electronic market for interbank deposits (e-MID). While some of the network properties of the e-MID market have been previously studied (see, for example, De Masi et al., 2006; Fricke, 2012; Fricke et al., 2013; Finger et al., 2013; Fricke and Lux, 2015a; Fricke and Lux, 2015b; Squartini et al., 2015; Cimini et al., 2015a), what is novel in our paper is that: (i) we provide a more comprehensive analysis of the structural correlations in all versions of the network, and employ both local as well as global measures for analyzing such patterns; (ii) we employ configuration models to investigate whether the intrinsic node heterogeneity represented by the degree sequence (in the binary network) and/or strength sequence (in the weighted network) can explain higher order structural correlations observed in the system; (iii) we utilize the so called Directed Enhanced Configuration Model as a null model for the directed weighted version of the network, which makes use of the available information about the direction of the edges in the network.

We use quarterly data for the e-MID network over the period 1999-2010 and restrict our analysis to the Italian banks participating in this market, because foreign banks are not frequently active in the market. Particularly, from the onset of the financial crisis in 2008 onward, non-Italian banks have basically withdrawn from this electronic market (e.g. see Fricke et al., 2013) [3].

The remainder of this paper is structured as follows. In Sec. 4.2 we provide a general framework for analyzing the structural correlations in different versions of the observed network as well as the algorithm for generating an ensemble of randomized networks from given constraints. In Sec. 4.3, we analyze the structural correlations in the undirected and directed binary versions of the e-MID network, and then compare the results to those obtained from the associated null models. In Sec. 4.4, we provide a similar analysis of the undirected as well as directed weighted versions of the network. Sec. 4.5 contains a

and its limitations.

[3]The transactions between banks are aggregated into quarterly data, since at the higher frequencies the matrix of the trades between banks is really sparse. For a more detailed description of the e-MID dataset, we refer the readers to the studies of Fricke et al. (2013) and Finger et al. (2013), or to the e-MID website http://www.e-mid.it/.

discussion of the results as well as directions for future research. At the end of this paper, the Appendix provides additional details concerning the measures of structural correlations.

4.2 Structural correlations in complex networks

4.2.1 For undirected networks

General notation

In the undirected version, suppose we have a network (of size n) characterized by a symmetric adjacency matrix $A = \{a_{ij}\}_{nxn}$ and a symmetric weighted matrix $W = \{w_{ij}\}_{nxn}$ ($a_{ii} = w_{ii} = 0$). The degree and strength sequences for each node i are respectively defined as

$$k_i^{un} = \sum_{j=1}^{n} a_{ij}, \tag{4.1}$$

and

$$s_i^{un} = \sum_{j=1}^{n} w_{ij}. \tag{4.2}$$

The total degree and total strength over all nodes in the network are given by

$$m = \frac{1}{2}\sum_{i=1}^{n} k_i^{un}, \tag{4.3}$$

and

$$w_{tol} = \frac{1}{2}\sum_{i=1}^{n} s_i^{un}. \tag{4.4}$$

Structural correlations in undirected networks

Assortativity Analysis

Regarding assortativity, we use two measures, i.e. the average degree (strength in the weighted case) of the nearest neighbors as well as the Pearson correlation coefficient (hereafter: Pearson coefficient) between degrees (strengths in the weighted case).

The average degree and strength of the nearest neighbors

The average degree of the nearest neighbors (ANND) of node i in the binary version of a network is given by

$$k_{nn,i}^{un} = \frac{\sum_{j=1}^{n} a_{ij} k_j^{un}}{k_i^{un}}. \tag{4.5}$$

For the weighted version, the average strength of the nearest neighbors (ANNS) of node i is

defined as

$$s_{nn,i}^{un} = \frac{\sum_{j=1}^{n} a_{ij} s_j^{un}}{k_i^{un}}. \tag{4.6}$$

Treating k_{nn}^{un} as a function of k^{un}, an overall positive (negative) correlation between k_{nn}^{un} and k^{un} suggests assortative (disassortative) mixing in the binary version of the network. In the weighted case, a positive (negative) correlation between s_{nn}^{un} and s^{un} evidences assortative (disassortative) mixing.

We can also compute the averages of ANND and ANNS over the whole network respectively as

$$\bar{k}_{nn}^{un} = \frac{1}{n} \sum_{i=1}^{n} k_{nn,i}^{un} \tag{4.7}$$

and

$$\bar{s}_{nn}^{un} = \frac{1}{n} \sum_{i=1}^{n} s_{nn,i}^{un}. \tag{4.8}$$

Pearson correlation coefficient of the node degrees and of the node strengths

The second measure of mixing computes the Pearson's correlation between two degree sequences (see the Appendix for further details). Practically, the main idea to measure such a correlation is that, from the adjacency matrix, first, we obtain a list of m edges, that is the list of pairs of nodes (i_e, j_e) where $a_{i_e j_e} = 1$, (for $e = 1, 2, ..., m$, $1 \leq i_e, j_e \leq n$). Next, for each e, we get two degrees $k_{i_e}^{un}$, $k_{j_e}^{un}$, and two strengths $s_{i_e}^{un}$, $s_{j_e}^{un}$ associated with the pair of nodes (i_e, j_e). The correlation coefficient of the degrees (r_{bin}^{un}) is equal to the Pearson correlation coefficient between the degrees at either ends of an edge (e.g. Newman, 2002; Newman, 2003a). Similarly, we can define the correlation coefficient of the strengths (r_w^{un}) as the Pearson correlation coefficient between the strengths at either ends of an edge. In the binary case, if r_{bin}^{un} is negative, it signals the presence of disassortativity, while a positive value implies the opposite. The same interpretation holds for r_w^{un} in the weighted case, but r_{bin}^{un} and r_w^{un} are not necessary equal.

Clustering coefficients

According to Watts and Strogatz (1998), the undirected binary clustering associated with node i is defined as

$$C_{bin,i}^{un} = \frac{\sum_{j \neq i} \sum_{k \neq i,j} a_{ij} a_{jk} a_{jk}}{\sum_{j \neq i} \sum_{k \neq i,j} a_{ij} a_{ik}}. \tag{4.9}$$

Following Onnela et al. (2005), we obtain the local weighted clustering associated with node i in undirected version of the network as

$$C_{w,i}^{un} = \frac{\sum_{j \neq i} \sum_{k \neq i,j} w_{ij}^{\frac{1}{3}} w_{jk}^{\frac{1}{3}} w_{jk}^{\frac{1}{3}}}{\sum_{j \neq i} \sum_{k \neq i,j} a_{ij} a_{ik}}. \tag{4.10}$$

Note that $C^{un}_{w,i}$ in Eq. (4.10) is invariant to weight permutation for each triangle and it takes into account the weights of all associated edges. In addition, it is easy to show that if $A = W$, we will have $c^{un}_{w,i} = c^{un}_{bin,i}$.

To analyze the evolution of the third order correlations over time, we define the average of $\{C^{un}_{bin,i}\}^n_{i=1}$ as

$$\bar{C}^{un}_{bin} = \frac{1}{n}\sum_{i=1}^{n} C^{un}_{bin,i}, \tag{4.11}$$

and the average of $\{C^{un}_{w,i}\}^n_{i=1}$ as

$$\bar{C}^{un}_{w} = \frac{1}{n}\sum_{i=1}^{n} C^{un}_{w,i}. \tag{4.12}$$

4.2.2 For directed networks

General definitions

In a directed network, the two matrices A and W are not symmetric (i.e. $\mathrm{A} \neq \mathrm{A}^{\mathrm{T}}$ and $\mathrm{W} \neq \mathrm{W}^{\mathrm{T}}$). We distinguish between in-degree and out-degree for every node i as

$$\mathrm{k}^{in}_{\mathrm{i}} = \sum_{j=1}^{n} \mathrm{a}_{\mathrm{ji}}, \tag{4.13}$$

and

$$\mathrm{k}^{out}_{\mathrm{i}} = \sum_{j=1}^{n} \mathrm{a}_{\mathrm{ij}}. \tag{4.14}$$

Similarly, in-strength and out-strength for every node i are given by

$$\mathrm{s}^{in}_{\mathrm{i}} = \sum_{j=1}^{n} \mathrm{w}_{\mathrm{ji}}, \tag{4.15}$$

and

$$\mathrm{s}^{out}_{\mathrm{i}} = \sum_{j=1}^{n} \mathrm{w}_{\mathrm{ij}}. \tag{4.16}$$

The total in-degree and total out-degree over all nodes in the network are equal to

$$\mathrm{M} = \sum_{i\neq j} \mathrm{a}_{\mathrm{ij}} = \sum_{j\neq i} \mathrm{a}_{\mathrm{ji}}. \tag{4.17}$$

The total in-strength and total out-strength over all nodes in the network are defined as

$$\mathrm{w}_{tol} = \sum_{i\neq j} \mathrm{w}_{\mathrm{ij}} = \sum_{j\neq i} \mathrm{w}_{\mathrm{ji}}. \tag{4.18}$$

Structural correlations in directed networks

Assortativity Analysis

The average degree and strength of the nearest neighbors in directed networks

Taking the directions of edges into account (as in Figure (4.1)), two types of nodes (giving and receiving) give rise to four types of relationships and four versions of ANND for each node i:

$$k_{nn,i}^{in-in} = \frac{\sum_{j=1}^{n} a_{ji} k_j^{in}}{k_i^{in}}, \tag{4.19}$$

$$k_{nn,i}^{in-out} = \frac{\sum_{j=1}^{n} a_{ji} k_j^{out}}{k_i^{in}}, \tag{4.20}$$

$$k_{nn,i}^{out-in} = \frac{\sum_{j=1}^{n} a_{ij} k_j^{in}}{k_i^{out}}, \tag{4.21}$$

$$k_{nn,i}^{out-out} = \frac{\sum_{j=1}^{n} a_{ij} k_j^{out}}{k_i^{out}}. \tag{4.22}$$

Similarly we define different versions of ANNS for each node i:

$$s_{nn,i}^{in-in} = \frac{\sum_{j=1}^{n} a_{ji} s_j^{in}}{k_i^{in}}, \tag{4.23}$$

$$s_{nn,i}^{in-out} = \frac{\sum_{j=1}^{n} a_{ji} s_j^{out}}{k_i^{in}}, \tag{4.24}$$

$$s_{nn,i}^{out-in} = \frac{\sum_{j=1}^{n} a_{ij} s_j^{in}}{k_i^{out}}, \tag{4.25}$$

$$s_{nn,i}^{out-out} = \frac{\sum_{j=1}^{n} a_{ij} s_j^{out}}{k_i^{out}}. \tag{4.26}$$

In each version, the interpretation of the relationship between the ANND and node degree and between the ANNS and node strength is similar to the one for the measures discussed in the undirected case. That is, a negative (positive) relationship signals disassortativity (assortativity) in the respective class of relationships.

The averages of the different versions of ANND are given by

$$\bar{k}_{nn}^{in-in} = \frac{1}{n} \sum_{i=1}^{n} k_{nn,i}^{in-in}, \tag{4.27}$$

$$\bar{k}_{nn}^{in-out} = \frac{1}{n} \sum_{i=1}^{n} k_{nn,i}^{in-out}, \tag{4.28}$$

$$\bar{k}_{nn}^{out-in} = \frac{1}{n}\sum_{i=1}^{n} k_{nn,i}^{out-in}, \tag{4.29}$$

$$\bar{k}_{nn}^{out-out} = \frac{1}{n}\sum_{i=1}^{n} k_{nn,i}^{out-out}. \tag{4.30}$$

For a directed and weighted network, the averages of the different versions of ANNS are defined as

$$\bar{s}_{nn}^{in-in} = \frac{1}{n}\sum_{i=1}^{n} s_{nn,i}^{in-in}, \tag{4.31}$$

$$\bar{s}_{nn}^{in-out} = \frac{1}{n}\sum_{i=1}^{n} s_{nn,i}^{in-out}, \tag{4.32}$$

$$\bar{s}_{nn}^{out-in} = \frac{1}{n}\sum_{i=1}^{n} s_{nn,i}^{out-in}, \tag{4.33}$$

$$\bar{s}_{nn}^{out-out} = \frac{1}{n}\sum_{i=1}^{n} s_{nn,i}^{out-out}. \tag{4.34}$$

Directed Pearson correlation coefficient of the node degrees and of the node strengths

Similarly, the four possible combinations between giving and receiving nodes are associated with four global assortativity coefficients, i.e. r_{bin}^{in-in}, r_{bin}^{in-out}, r_{bin}^{out-in}, and $r_{bin}^{out-out}$ (see the Appendix for further details). Their weighted counterparts are r_{w}^{in-in}, r_{w}^{in-out}, r_{w}^{out-in}, and $r_{w}^{out-out}$. The algorithm for calculating these binary (weighted) coefficients is still similar to the one used for r_{bin}^{un} (or r_{w}^{un} for the weighted case), except for the requirement that the directions of edges (see Figure (4.1)) must be taken into account.

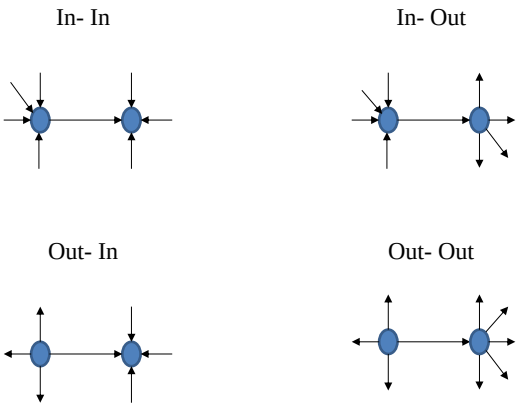

Figure 4.1: Degree-degree dependencies in the directed version.

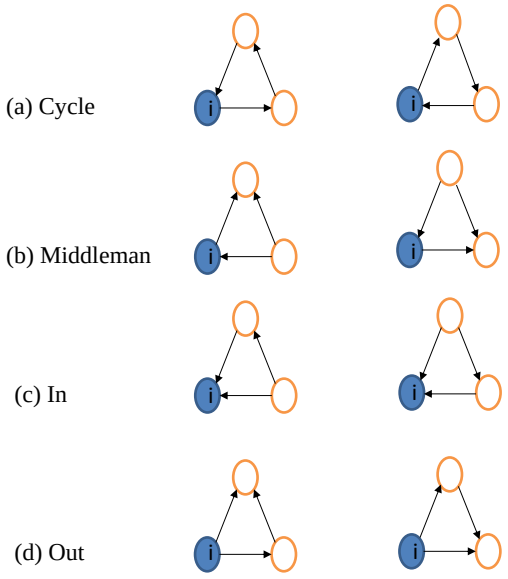

Figure 4.2: Directed triangles and the corresponding (binary) clusterings associated with a node *i*. (a) Cycle clustering, (b) Middleman clustering, (c) In clustering, (d) Out clustering.

Clustering coefficients

Directed binary clustering coefficients

As shown in Figure (4.2), for each node i, we define four local binary clustering coefficients in a directed network associated with the respective type of relationship:

$$C_{bin,i}^{in} = \frac{\sum_{j\neq i}\sum_{k\neq i,j} a_{jk}a_{ji}a_{ki}}{(\sum_{j\neq i} a_{ji})^2 - (\sum_{j\neq i} a_{ji}^2)}, \tag{4.35}$$

$$C_{bin,i}^{out} = \frac{\sum_{j\neq i}\sum_{k\neq i,j} a_{ik}a_{ij}a_{jk}}{(\sum_{j\neq i} a_{ij})^2 - (\sum_{j\neq i} a_{ij}^2)}, \tag{4.36}$$

$$C_{bin,i}^{cyc} = \frac{\sum_{j\neq i}\sum_{k\neq i,j} a_{ij}a_{jk}a_{ki}}{(\sum_{j\neq i} a_{ij}\sum_{j\neq i} a_{ji}) - (\sum_{j\neq i} a_{ij}a_{ji})}, \tag{4.37}$$

$$C_{bin,i}^{mid} = \frac{\sum_{j\neq i}\sum_{k\neq i,j} a_{ik}a_{jk}a_{ji}}{(\sum_{j\neq i} a_{ij}\sum_{j\neq i} a_{ji}) - (\sum_{j\neq i} a_{ij}a_{ji})}. \tag{4.38}$$

Note that, in the binary case we have $a_{ij}^2 = a_{ij}$ $(\forall i, j)$, therefore from Eqs. (4.35), (4.36), (4.37), (4.38) we have

$$C_{bin,i}^{in} = \frac{\sum_{j\neq i}\sum_{k\neq i,j} a_{jk}a_{ji}a_{ki}}{k_i^{in}(k_i^{in}-1)}, \tag{4.39}$$

$$C_{bin,i}^{out} = \frac{\sum_{j\neq i}\sum_{k\neq i,j} a_{ik}a_{ij}a_{jk}}{k_i^{out}(k_i^{out}-1)}, \tag{4.40}$$

$$C_{bin,i}^{cyc} = \frac{\sum_{j\neq i}\sum_{k\neq i,j} a_{ij}a_{jk}a_{ki}}{k_i^{in}k_i^{out} - k_i^{\leftrightarrow}}, \tag{4.41}$$

$$C_{bin,i}^{mid} = \frac{\sum_{j\neq i}\sum_{k\neq i,j} a_{ik}a_{jk}a_{ji}}{k_i^{in}k_i^{out} - k_i^{\leftrightarrow}}, \tag{4.42}$$

where $k_i^{\leftrightarrow}$ is the number of nodes j in the neighborhood of the node i such that $a_{ij} = a_{ji} = 1$.

The averages over the local binary clustering coefficients are defined as

$$\bar{C}_{bin}^{in} = \frac{1}{n}\sum_{i=1}^{n} C_{bin,i}^{in}, \tag{4.43}$$

$$\bar{C}_{bin}^{out} = \frac{1}{n}\sum_{i=1}^{n} C_{bin,i}^{out}. \tag{4.44}$$

$$\bar{C}_{bin}^{cyc} = \frac{1}{n}\sum_{i=1}^{n} C_{bin,i}^{cyc}, \tag{4.45}$$

$$\bar{C}_{bin}^{mid} = \frac{1}{n}\sum_{i=1}^{n} C_{bin,i}^{mid}, \tag{4.46}$$

Directed weighted clustering coefficients

In a weighted directed network, among various measures, following Onnela et al. (2005), we define the local weighted clustering coefficients for each node i as

$$C_{w,i}^{in} = \frac{\sum_{j\neq i}\sum_{k\neq i,j} w_{jk}^{\frac{1}{3}} w_{ji}^{\frac{1}{3}} w_{ki}^{\frac{1}{3}}}{(\sum_{j\neq i} a_{ji})^2 - (\sum_{j\neq i} a_{ji}^2)}, \tag{4.47}$$

$$C_{w,i}^{out} = \frac{\sum_{j\neq i}\sum_{k\neq i,j} w_{ik}^{\frac{1}{3}} w_{ij}^{\frac{1}{3}} w_{jk}^{\frac{1}{3}}}{(\sum_{j\neq i} a_{ij})^2 - (\sum_{j\neq i} a_{ij}^2)}, \tag{4.48}$$

$$C_{w,i}^{cyc} = \frac{\sum_{j\neq i}\sum_{k\neq i,j} w_{ij}^{\frac{1}{3}} w_{jk}^{\frac{1}{3}} w_{ki}^{\frac{1}{3}}}{(\sum_{j\neq i} a_{ij}\sum_{j\neq i} a_{ji}) - (\sum_{j\neq i} a_{ij}a_{ji})}, \tag{4.49}$$

$$C_{w,i}^{mid} = \frac{\sum_{j\neq i}\sum_{k\neq i,j} w_{ik}^{\frac{1}{3}} w_{jk}^{\frac{1}{3}} w_{ji}^{\frac{1}{3}}}{(\sum_{j\neq i} a_{ij}\sum_{j\neq i} a_{ji}) - (\sum_{j\neq i} a_{ij}a_{ji})}. \tag{4.50}$$

We can see that in all local weighted clustering coefficients, the denominators are identical to those in the binary counterparts. Obviously, it is easy to show that for $A = W$, the binary clustering coefficients from Eqs. (4.35), (4.36), (4.37), (4.38) can be recovered respectively from Eqs. (4.47), (4.48), (4.49), (4.50).

Note that, similar to the binary case, one can also rewrite Eqs. (4.47), (4.48), (4.49), (4.50) as

$$C_{w,i}^{in} = \frac{\sum_{j\neq i}\sum_{k\neq i,j} w_{jk}^{\frac{1}{3}} w_{ji}^{\frac{1}{3}} w_{ki}^{\frac{1}{3}}}{k_i^{in}(k_i^{in}-1)}, \tag{4.51}$$

$$C_{w,i}^{out} = \frac{\sum_{j\neq i}\sum_{k\neq i,j} w_{ik}^{\frac{1}{3}} w_{ij}^{\frac{1}{3}} w_{jk}^{\frac{1}{3}}}{k_i^{out}(k_i^{out}-1)}, \tag{4.52}$$

$$C_{w,i}^{cyc} = \frac{\sum_{j\neq i}\sum_{k\neq i,j} w_{ij}^{\frac{1}{3}} w_{jk}^{\frac{1}{3}} w_{ki}^{\frac{1}{3}}}{k_i^{in}k_i^{out} - k_i^{\leftrightarrow}}, \tag{4.53}$$

$$C_{w,i}^{mid} = \frac{\sum_{j\neq i}\sum_{k\neq i,j} w_{ik}^{\frac{1}{3}} w_{jk}^{\frac{1}{3}} w_{ji}^{\frac{1}{3}}}{k_i^{in}k_i^{out} - k_i^{\leftrightarrow}}. \tag{4.54}$$

For the analysis of the evolution of the prevalence of a particular type of relationship

observed in node triangles over time, we compute the averages of the local weighted clustering coefficients across all nodes as

$$\bar{C}_w^{in} = \frac{1}{n}\sum_{i=1}^{n} C_{w,i}^{in}, \tag{4.55}$$

$$\bar{C}_w^{out} = \frac{1}{n}\sum_{i=1}^{n} C_{w,i}^{out}, \tag{4.56}$$

$$\bar{C}_w^{cyc} = \frac{1}{n}\sum_{i=1}^{n} C_{w,i}^{cyc}, \tag{4.57}$$

$$\bar{C}_w^{mid} = \frac{1}{n}\sum_{i=1}^{n} C_{w,i}^{mid}. \tag{4.58}$$

4.2.3 Configuration models

In this subsection we will summarize the main ideas behind the algorithm involved in the extraction of hidden (latent) variables from an observed network and their role in the network randomization process (see, for example, Squartini and Garlaschelli, 2011; Squartini et al., 2011a; Squartini et al., 2011b; Mastrandrea et al., 2014; Squartini et al., 2015). For a more detailed explanation of the derivation of the family of Exponential Random Graph Model based on the maximum-entropy method, as well as on how to use the maximum-likelihood method to solve for the hidden variables under given constraints, we refer readers to the studies by Park and Newman (2004), Squartini and Garlaschelli (2011), and Squartini et al. (2015).

Undirected Binary Configuration model (UBCM)

In the UBCM, briefly, the entropy of a randomized ensemble of networks is maximized under the constraint that the node degrees in the observed network $\{k_i^{un}\}_{i=1}^{n}$ should match the averages of node degrees in the randomized ensemble. Mathematically, we need to solve the following system of n equations to obtain the non-negative hidden variables $\{x_i^*\}_{i=1}^{n}$ that carry the information from the constraints and allow us to perform an efficient unbiased sampling of the ensemble

$$\sum_{j\neq i} \frac{x_i^* x_j^*}{1+x_i^* x_j^*} = k_i^{un}, \forall i = 1,2,...,n. \tag{4.59}$$

Once obtained, the hidden variable can be used to compute the probability p_{ij} of a link between any two nodes i and j, which in turn allows us to easily sample the ensemble associated with the above constraints

$$p_{ij} = \langle a_{ij} \rangle = \frac{x_i^* x_j^*}{1+x_i^* x_j^*}, \tag{4.60}$$

where $\langle a_{ij} \rangle$ is the notation for the expectation of a_{ij} over the ensemble.

Directed Binary Configuration model (DBCM)

In the DBCM, the constraints are the observed out-degree and in-degree sequences $\{k_i^{out}\}_{i=1}^n$ and $\{k_i^{in}\}_{i=1}^n$. We need to solve the following system of 2n equations to obtain the associated non-negative hidden variables $\{x_i^*\}_{i=1}^n$ and $\{y_i^*\}_{i=1}^n$

$$\begin{cases} \sum_{j \neq i} \frac{x_i^* y_j^*}{1+x_i^* y_j^*} = k_i^{out}, \forall i = 1,2,...,n, \\ \sum_{j \neq i} \frac{x_j^* y_i^*}{1+x_j^* y_i^*} = k_i^{in}, \forall i = 1,2,...,n. \end{cases} \tag{4.61}$$

The probability of a link from node i to j is given by

$$p_{ij} = \langle a_{ij} \rangle = \frac{x_i^* y_j^*}{1+x_i^* y_j^*}, \tag{4.62}$$

and the probability of a link from node j to i is given by

$$p_{ji} = \langle a_{ji} \rangle = \frac{x_j^* y_i^*}{1+x_j^* y_i^*}. \tag{4.63}$$

Undirected Weighted Configuration model (UWCM)

Similarly, suppose that in an undirected weighted network we want to extract n hidden variables $\{x_i^*\}_{i=1}^n$ associated with the observed strength sequence $\{s_i^{un}\}_{i=1}^n$, $(\{x_i^*\}_{i=1}^n \in [0,1))$. The maximum likelihood method involves solving the following system of n equations for the hidden variables

$$\sum_{j \neq i} \frac{x_i^* x_j^*}{1-x_i^* x_j^*} = s_i^{un}, \forall i = 1,2,...,n. \tag{4.64}$$

The expected link weight between node i and node j is given by

$$\langle w_{ij} \rangle = \frac{x_i^* x_j^*}{1-x_i^* x_j^*}. \tag{4.65}$$

The probability of a link weight w_{ij} between node i and node j in the UWCM is

$$q(w_{ij}) = (p_{ij})^{w_{ij}}(1-p_{ij}), \tag{4.66}$$

for $w_{ij} > 0$, where $p_{ij} = \langle a_{ij} \rangle$ is the probability of a link between two nodes (i, j), which is given by

$$p_{ij} = \langle a_{ij} \rangle = x_i^* x_j^*. \tag{4.67}$$

Directed Weighted Configuration model (DWCM)

In the DWCM, the constraints are the observed out-strength and in-strength sequences (i.e. $\{s_i^{out}\}_{i=1}^n$ and $\{s_i^{in}\}_{i=1}^n$). Mathematically, we need to solve the following system of 2n equations to obtain the hidden variables $\{x_i^*\}_{i=1}^n$ and $\{y_i^*\}_{i=1}^n \in [0,1)$, which are respectively associated with $\{s_i^{out}\}_{i=1}^n$ and $\{s_i^{in}\}_{i=1}^n$

$$\begin{cases} \sum_{j\neq i} \frac{x_i^* y_j^*}{1-x_i^* y_j^*} = s_i^{out}, \forall i = 1,2,...,n, \\ \sum_{j\neq i} \frac{x_j^* y_i^*}{1-x_j^* y_i^*} = s_i^{in}, \forall i = 1,2,...,n. \end{cases} \tag{4.68}$$

The expected link weights between node i and node j are given by

$$\langle w_{ij} \rangle = \frac{x_i^* y_j^*}{1-x_i^* y_j^*}, \tag{4.69}$$

and

$$\langle w_{ji} \rangle = \frac{x_j^* y_i^*}{1-x_j^* y_i^*}. \tag{4.70}$$

The probability of a link weight w_{ij} from node i to node j in the DWCM is

$$q(w_{ij}) = (p_{ij})^{w_{ij}}(1-p_{ij}), \tag{4.71}$$

for $w_{ij} > 0$, where $p_{ij} = \langle a_{ij} \rangle$ is the probability of a link between two nodes (i,j), given by

$$p_{ij} = \langle a_{ij} \rangle = x_i^* y_j^*. \tag{4.72}$$

Undirected Enhanced Configuration model (UECM)

In the UECM, we use both the degree sequence $\{k_i^{un}\}_{i=1}^n$ as well as the strength sequence $\{s_i^{un}\}_{i=1}^n$ as constraints. The associated non-negative hidden variables $\{x_i^*\}_{i=1}^n$ and $\{y_i^*\}_{i=1}^n$ ($\{y_i^*\}_{i=1}^n \in [0,1)$) are then the solution to the following system of 2n equations

$$\begin{cases} \sum_{j\neq i} \frac{x_i^* x_j^* y_i^* y_j^*}{1-y_i^* y_j^* + x_i^* x_j^* y_i^* y_j^*} = k_i^{un}, \forall i = 1,2,...,n, \\ \sum_{j\neq i} \frac{x_i^* x_j^* y_i^* y_j^*}{(1-y_i^* y_j^*)(1-y_i^* y_j^* + x_i^* x_j^* y_i^* y_j^*)} = s_i^{un}, \forall i = 1,2,...,n. \end{cases} \tag{4.73}$$

It should be noted that, in the UECM, the probability of a link (i.e. $\langle a_{ij}\rangle$) and the expected weight (i.e. $\langle w_{ij}\rangle$) between node i and node j depend on the information encoded in the strengths as well as in the degrees. More specifically, they are given by

$$p_{ij} = \langle a_{ij}\rangle = \frac{x_i^* x_j^* y_i^* y_j^*}{1-y_i^* y_j^* + x_i^* x_j^* y_i^* y_j^*}, \tag{4.74}$$

and

$$\langle w_{ij}\rangle = \frac{x_i^* x_j^* y_i^* y_j^*}{(1-y_i^* y_j^*)(1-y_i^* y_j^* + x_i^* x_j^* y_i^* y_j^*)}. \tag{4.75}$$

In this model the probability of a link weight w_{ij} between two nodes (i,j) is given by

$$q(w_{ij}) = \begin{cases} 1-p_{ij}, & \text{if } w_{ij} = 0 \\ p_{ij}(r_{ij})^{w_{ij}-1}(1-r_{ij}), & \text{if } w_{ij} > 0, \end{cases} \tag{4.76}$$

where $r_{ij} = y_i^* y_j^*$, and p_{ij} is defined by Eq. (4.74).

Directed Enhanced Configuration model (DECM)

In the DECM, the non-negative hidden variables $\{x_i^*\}_{i=1}^n$, $\{y_i^*\}_{i=1}^n$, $\{z_i^*\}_{i=1}^n$, $\{t_i^*\}_{i=1}^n$ ($\{z_i^*\}_{i=1}^n$, $\{t_i^*\}_{i=1}^n \in [0,1)$) extracted from the four sequences of constraints $\{k_i^{out}\}_{i=1}^n$, $\{k_i^{in}\}_{i=1}^n$, $\{s_i^{out}\}_{i=1}^n$, and $\{s_i^{in}\}_{i=1}^n$ are the solution to the following system of 4n equations

$$\begin{cases} \sum_{j\neq i} \frac{x_i^* y_j^* z_i^* t_j^*}{1-z_i^* t_j^* + x_i^* y_j^* z_i^* t_j^*} = k_i^{out}, \forall i = 1,2,...,n, \\ \sum_{j\neq i} \frac{x_j^* y_i^* z_j^* t_i^*}{1-z_j^* t_i^* + x_j^* y_i^* z_j^* t_i^*} = k_i^{in}, \forall i = 1,2,...,n, \\ \sum_{j\neq i} \frac{x_i^* y_j^* z_i^* t_j^*}{(1-z_i^* t_j^*)(1-z_i^* t_j^* + x_i^* y_j^* z_i^* t_j^*)} = s_i^{out}, \forall i = 1,2,...,n, \\ \sum_{j\neq i} \frac{x_j^* y_i^* z_j^* t_i^*}{(1-z_j^* t_i^*)(1-z_j^* t_i^* + x_j^* y_i^* z_j^* t_i^*)}) = s_i^{in}, \forall i = 1,2,...,n. \end{cases} \tag{4.77}$$

Similar to the UECM, in the DECM, the probability of a link (i.e. $\langle a_{ij}\rangle$) and the expected weight (i.e. $\langle w_{ij}\rangle$) from node i to node j depend on information encoded in the two sequences of observed degrees as well as in the two sequences of observed strengths. More specifically,

we have

$$p_{ij} = \langle a_{ij} \rangle = \frac{x_i^* y_j^* z_i^* t_j^*}{1 - z_i^* t_j^* + x_i^* y_j^* z_i^* t_j^*}, \tag{4.78}$$

$$\langle w_{ij} \rangle = \frac{x_i^* y_j^* z_i^* t_j^*}{(1 - z_i^* t_j^*)(1 - z_i^* t_j^* + x_i^* y_j^* z_i^* t_j^*)}, \tag{4.79}$$

Similarly,

$$p_{ji} = \langle a_{ji} \rangle = \frac{x_j^* y_i^* z_j^* t_i^*}{1 - z_j^* t_i^* + x_j^* y_i^* z_j^* t_i^*}, \tag{4.80}$$

$$\langle w_{ji} \rangle = \frac{x_j^* y_i^* z_j^* t_i^*}{(1 - z_j^* t_i^*)(1 - z_j^* t_i^* + x_j^* y_i^* z_j^* t_i^*)}. \tag{4.81}$$

The probability of a link weight w_{ij} from node i to node j is now given by

$$q(w_{ij}) = \begin{cases} 1 - p_{ij}, & \text{if } w_{ij} = 0, \\ p_{ij}(r_{ij})^{w_{ij}-1}(1 - r_{ij}), & \text{if } w_{ij} > 0, \end{cases} \tag{4.82}$$

where $r_{ij} = z_i^* t_j^*$, and p_{ij} is defined by Eq. (4.78).

Note that, the expected values of the second and third structural correlations in the randomized networks can be analytically computed via the hidden variables extracted from each configuration model or numerically computed by taking the average over a simulated ensemble. In our study, for each considered null model, we generate an ensemble of 1000 randomized networks, and then take the averages of the measures in question over the ensemble.

4.3 Findings for the binary network

4.3.1 Structural correlations in the undirected binary e-MID network

We first investigate the degree dependencies in the undirected binary e-MID network by examining the relationship between the node degree (k^{un}) and the average degree of its neighbors (k_{nn}^{un}). The overall disassortativity in this version of the network is evidenced by the negative relationship between these two quantities as shown in panels (a) and (b) of Figure (4.3), in which the measures for the networks from Q1 (the first quarter in our data set) and from Q48 (the last quarter in our data set) are plotted as an example. Note that the overall negative correlation between k_{nn}^{un} and k^{un} is also observed in all 48 quarters from 1999 to 2010. In addition, generally, we find that the absolute value of this correlation is

declining over time. This also seems to be true for other observed dependencies.

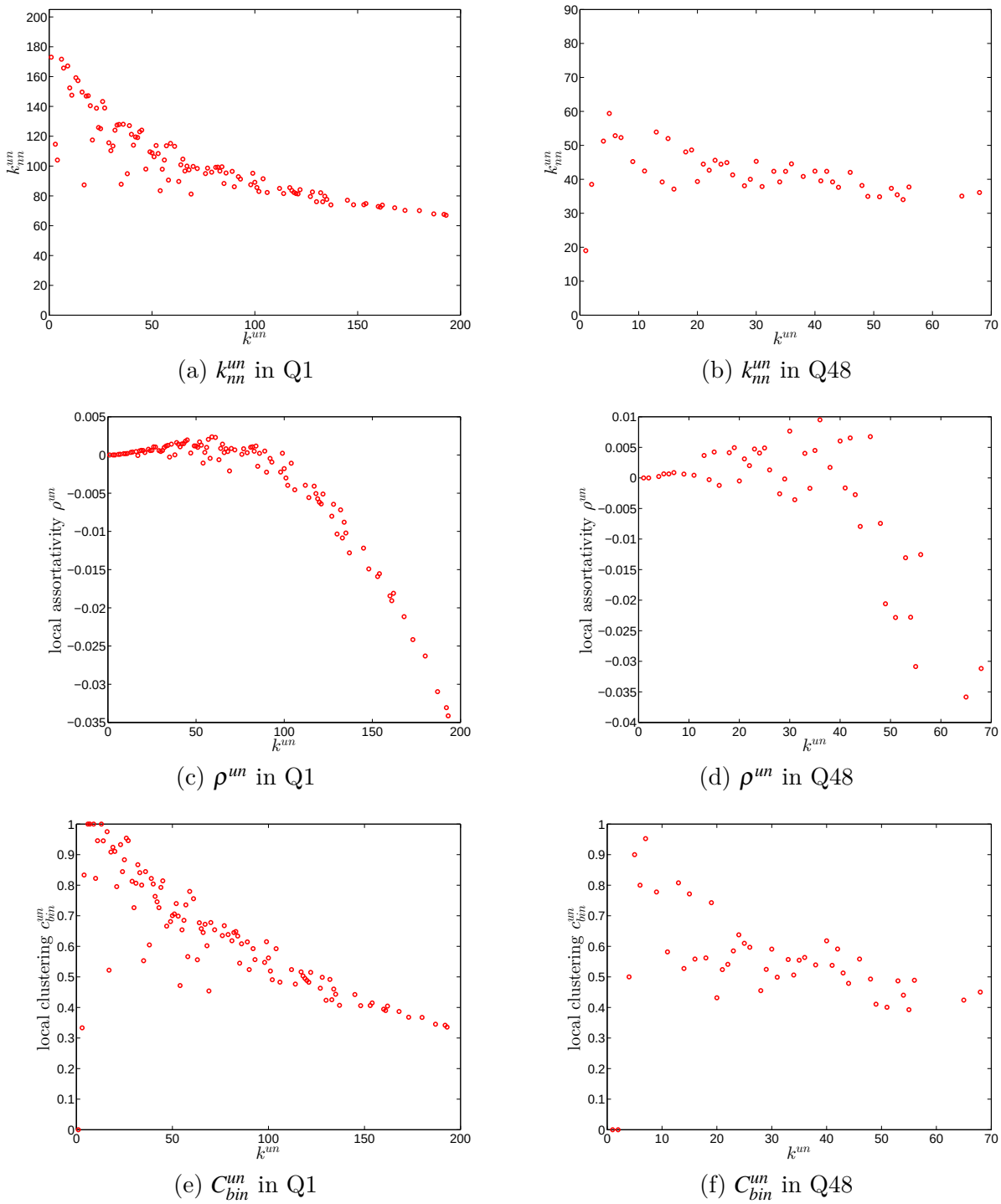

(a) k_{nn}^{un} in Q1

(b) k_{nn}^{un} in Q48

(c) ρ^{un} in Q1

(d) ρ^{un} in Q48

(e) C_{bin}^{un} in Q1

(f) C_{bin}^{un} in Q48

Figure 4.3: ANND (panels a, b), local assortativity ρ^{un} (panels c, d), and local clustering coefficients C_{bin}^{un} (panels e, f) in the undirected binary e-MID network, in Q1 and Q48.

Next, we now turn to the Pearson correlation coefficient of degrees r_{bin}^{un} as an overall

indicator of degree dependencies in the network. As shown in Figure (4.4), over time, overall, the network exhibits disassortativity as signaled by the negative coefficient. Consistent with what we discovered in our analysis of the measure ANND, the absolute value of r_{bin}^{un} is also declining from 1999 to 2010.

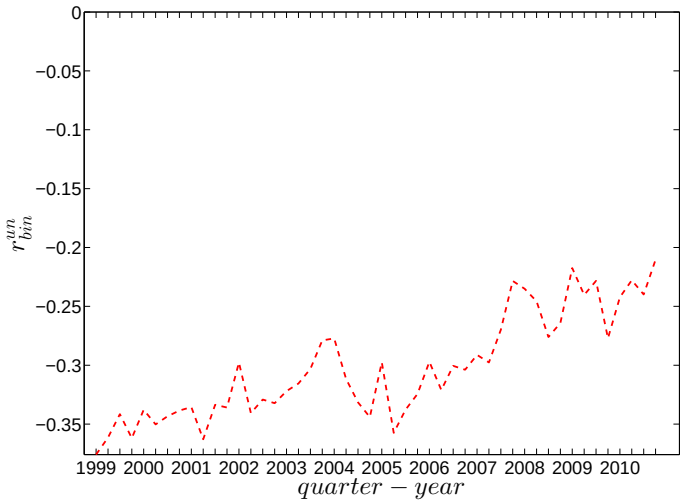

Figure 4.4: Evolution of the overall assortativity indicator r_{bin}^{un} in the undirected binary e-MID network.

For a more comprehensive assessment of the degree dependencies in the network, we employ the local assortativity coefficients ρ^{un} that expose the contribution of each node to the global level of assortativity r_{bin}^{un} (see the Appendix for further details). The basic idea is that the numerator in the Pearson correlation coefficient proposed by Newman (2002, 2003a) can be reformulated based on the contribution of the individual nodes instead of in term of the edges (see, for example, Piraveenan et al., 2010). It should be emphasized that we always have

$$r_{bin}^{un} = \sum_{i=1}^{n} \rho_i^{un}. \tag{4.83}$$

In panels (c) and (d) of Figure (4.3) we plot ρ^{un} against k^{un} to investigate which nodes (in terms of their degrees) contribute most to r_{bin}^{un}. It is clear that the hubs are the primarily contributors to the overall disassortativity of the network, while smaller degree nodes sometimes exhibit assortativity. This also reveals that adding or removing a hub from a network may have a large impact on its overall mixing nature.

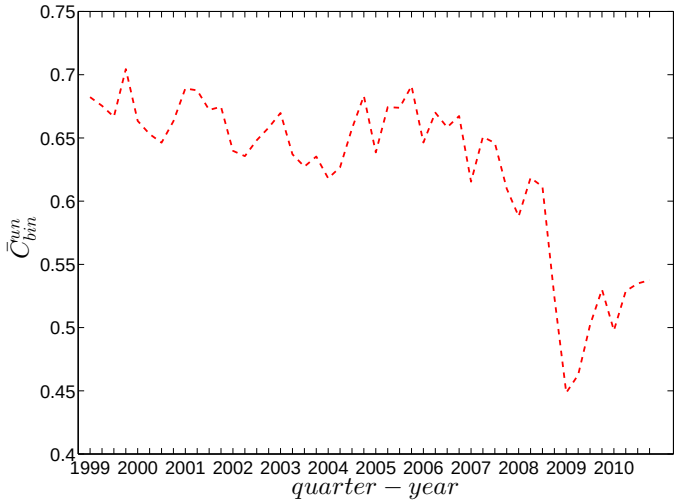

Figure 4.5: Evolution of the average of local clustering coefficients (i.e. $\bar{C}^{un}_{bin}$) in the undirected binary e-MID network.

For the third order correlations, we employ the local clustering coefficient proposed by Watts and Strogatz (1998). In this simple version of the network (undirected binary case) clustering refers to the extent to which two connected nodes in the network have common neighbors. We observe that, overall, the undirected local clustering is a decreasing function of degree (panels (e) and (f) of Figure (4.3)), meaning that the neighbors of highly (poorly) connected banks are poorly (highly) interconnected. In fact, this relationship is typically found in many real world networks exhibiting a high heterogeneity in the degrees and a disassortative mixing nature (e.g. see Newman, 2003b). In our network, the bank degrees are highly heterogeneous, and the small (large) degree banks seem to have larger (smaller) local clustering coefficients because they are mostly connected to large (small) degree banks.

The evolution of the average of the undirected local binary clustering coefficients over all nodes is shown in Figure (4.5), where we can see a significant reduction in $\bar{C}^{un}_{bin}$ around the time the financial crisis spreads to Europe.

4.3.2 Structural correlations in the directed binary e-MID network

We now extend our analysis to the directed version of the binary network. Figures (4.6) and (4.7) show the relationship between ANND and node degree for the four types of mixing, i.e. in-in, in-out, out-in, and out-out. In the same network some types of mixing can be assortative, while others disassortative. For instance, while in Q1, overall, ANND is a decreasing function of the associated degree in all four cases, this relationship breaks down for the in-in and out-out mixing in Q48. In contrast, the overall negative correlation between ANND and the associated degree for the in-out and out-in mixing is observed in almost all quarters.

For a more general assessment of the overall mixing nature in the directed binary network, we calculate the Pearson correlation coefficient in each category of mixing and show its evolution over time (see Figure (4.8)). In comparison to the undirected version, the directed binary network displays more complicated degree dependencies. We can see that r_{bin}^{out-in} and r_{bin}^{in-out} display a different behavior than r_{bin}^{in-in} and $r_{bin}^{out-out}$. More specifically, while in the out-in and out-in categories we persistently observe disassortativity in all quarters, the other two categories switch between displaying assortativity and disassortativity over time. The interpretation of the mixing observed in the various categories is similar to the interpretation of mixing in an undirected binary network. For instance, a negative value of r_{bin}^{out-in}, signaling disassortativity in the out-in category, indicates that a high out-degree bank tends to have out-going links to low in-degree banks, and/or that a low out-degree bank tends to have out-going links to high in-degree banks. The mixing we observe in the out-in category (r_{bin}^{out-in}) comes closest to the one observed in the undirected network captured by r_{bin}^{un}. The similarity between these two quantities was mathematically proven by van der Hoorn and Litvak (2015). In addition, although the in-out mixing category exhibits disassortativity, in many quarters the coefficient r_{bin}^{in-out} is very close to zero.

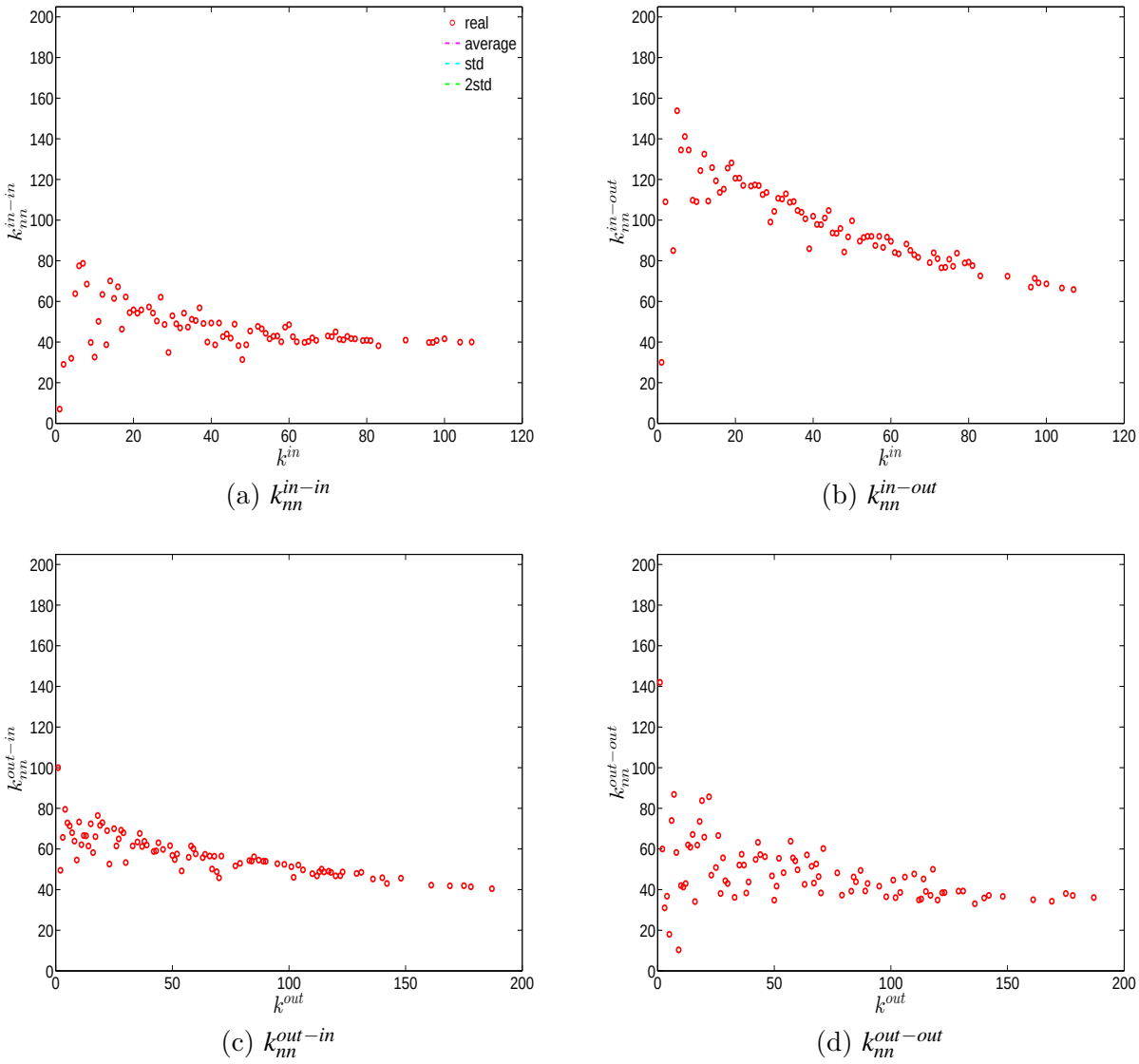

(a) k_{nn}^{in-in} (b) k_{nn}^{in-out}

(c) k_{nn}^{out-in} (d) $k_{nn}^{out-out}$

Figure 4.6: ANND in the directed binary e-MID network, in Q1. k_{nn}^{in-in} (panel a), k_{nn}^{in-out} (panel b), k_{nn}^{out-in} (panel c), $k_{nn}^{out-out}$ (panel d).

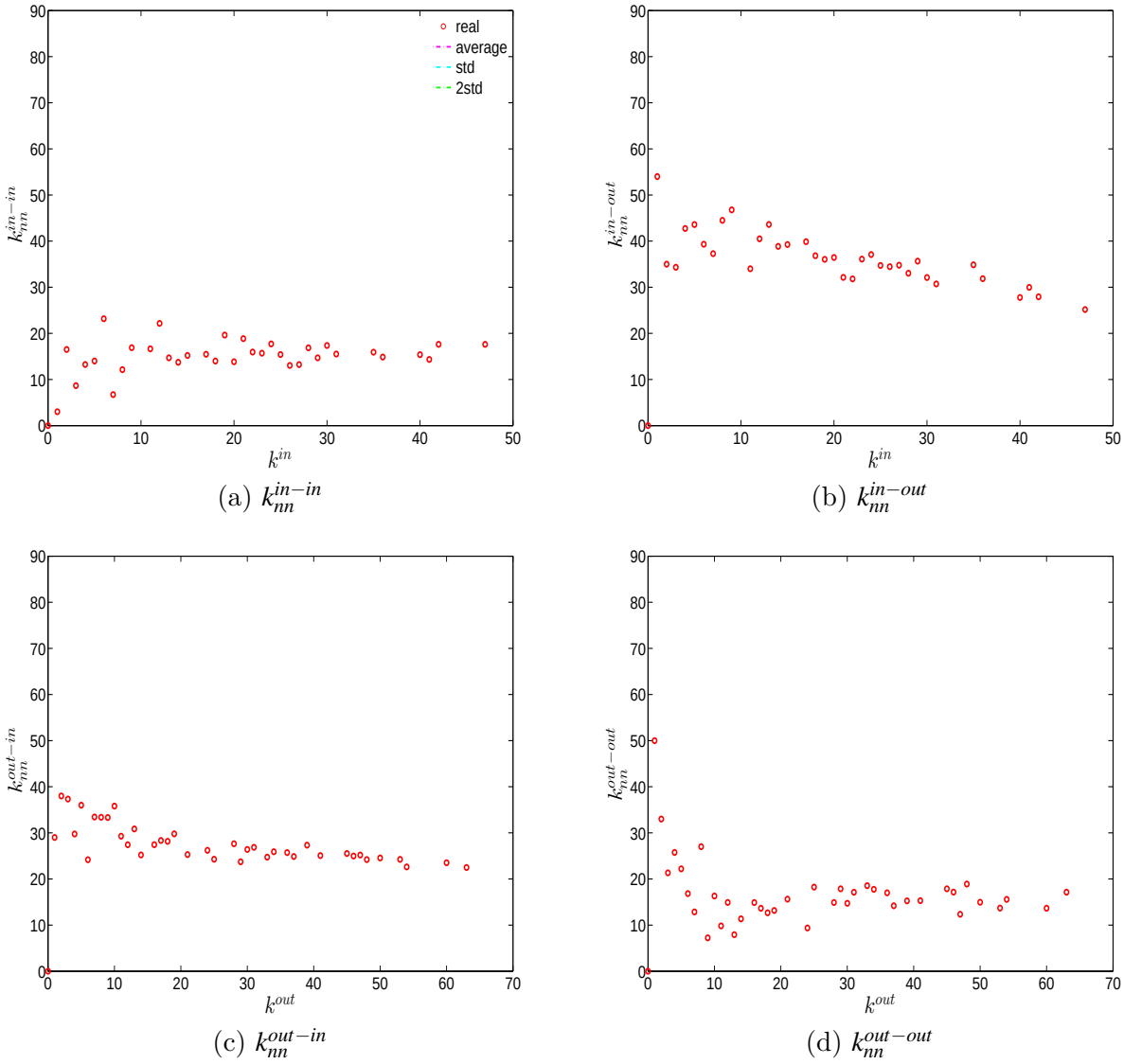

(a) k_{nn}^{in-in} (b) k_{nn}^{in-out}

(c) k_{nn}^{out-in} (d) $k_{nn}^{out-out}$

Figure 4.7: ANND in the directed binary e-MID network, in Q48. k_{nn}^{in-in} (panel a), k_{nn}^{in-out} (panel b), k_{nn}^{out-in} (panel c), $k_{nn}^{out-out}$ (panel d).

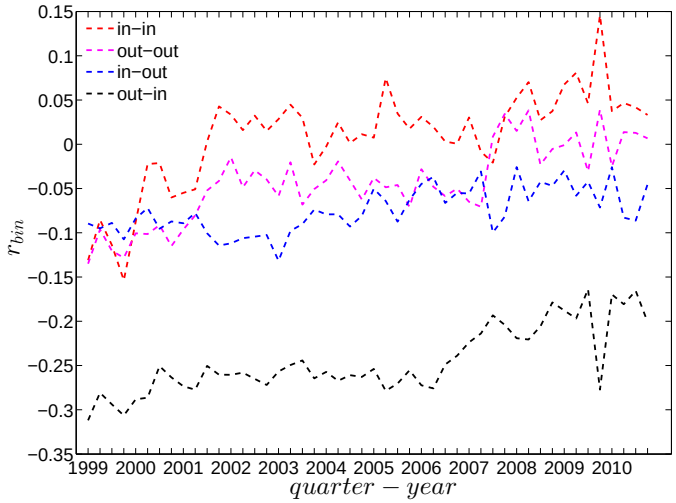

Figure 4.8: Evolution of the overall assortativity indicators in the directed binary e-MID network.

Similarly to the undirected case, we define the local assortativity measures for a given node i as ρ_i^{in-in}, ρ_i^{in-out}, ρ_i^{out-in}, and $\rho_i^{out-out}$ corresponding to the four mixing categories in the directed version of the network. Note that the following equalities must hold:

$$r_{bin}^{in-in} = \sum_{i=1}^{n} \rho_i^{in-in}, \tag{4.84}$$

$$r_{bin}^{in-out} = \sum_{i=1}^{n} \rho_i^{in-out}, \tag{4.85}$$

$$r_{bin}^{out-in} = \sum_{i=1}^{n} \rho_i^{out-in}, \tag{4.86}$$

$$r_{bin}^{out-out} = \sum_{i=1}^{n} \rho_i^{out-out}. \tag{4.87}$$

The measures ρ_i^{in-in}, ρ_i^{in-out}, ρ_i^{out-in}, and $\rho_i^{out-out}$ give us useful information about the contribution of each node to the respective overall assortativity indicators.

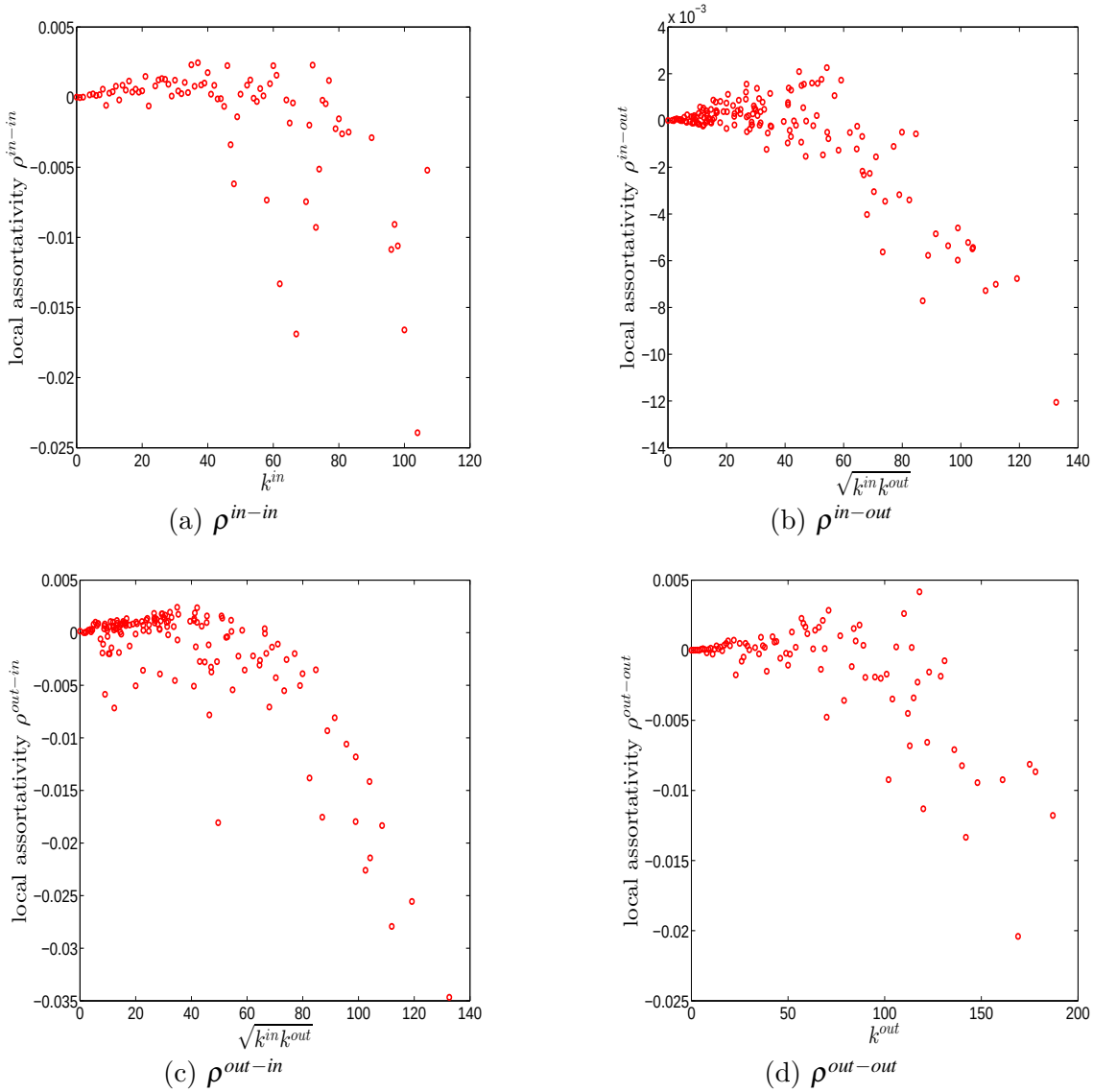

(a) ρ^{in-in} (b) ρ^{in-out}

(c) ρ^{out-in} (d) $\rho^{out-out}$

Figure 4.9: Local assortativity in the directed binary e-MID network, in Q1. ρ^{in-in} (panel a), ρ^{in-out} (panel b), ρ^{out-in} (panel c), $\rho^{out-out}$ (panel d).

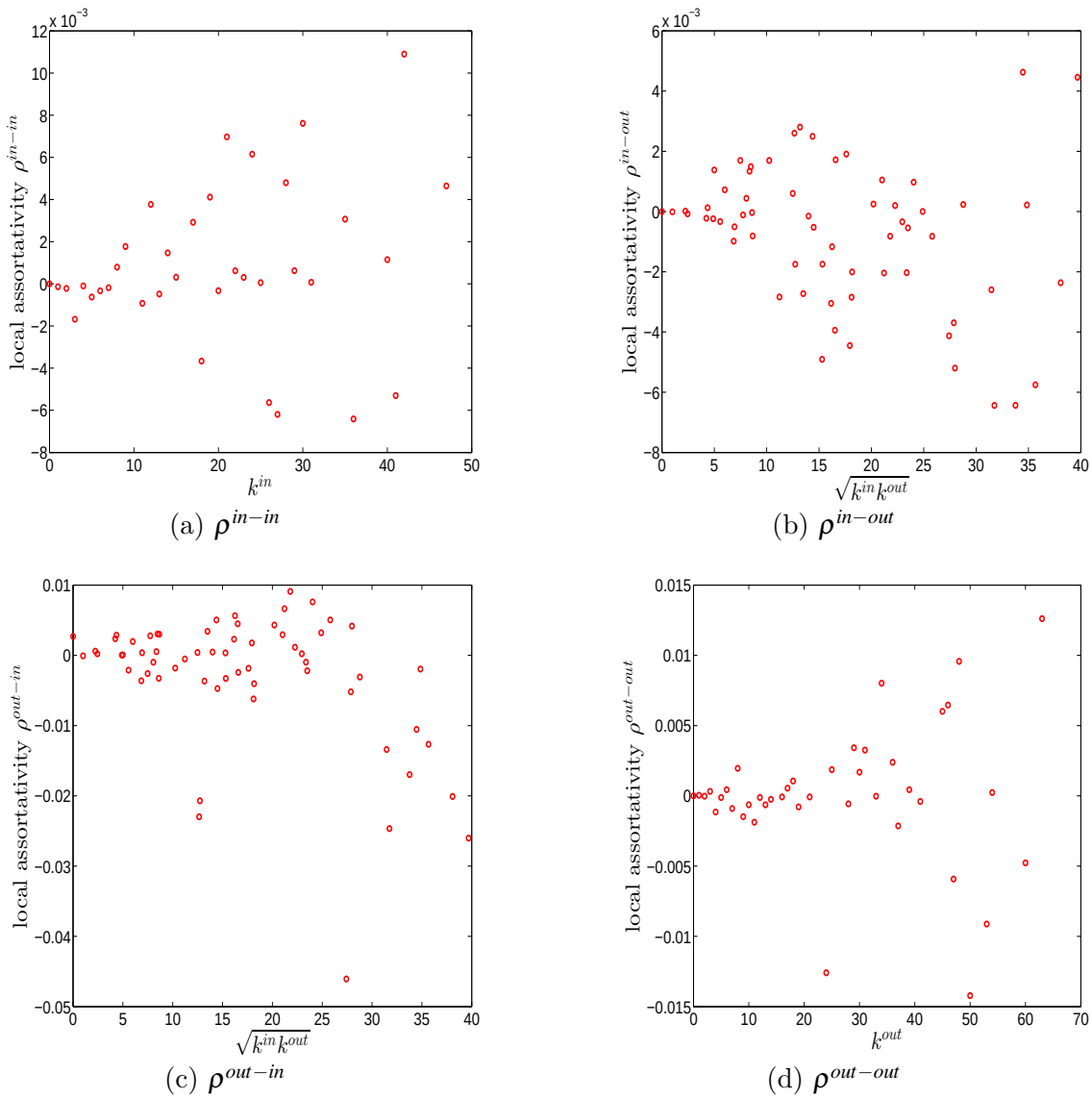

Figure 4.10: Local assortativity in the directed binary e-MID network, in Q48. ρ^{in-in} (panel a), ρ^{in-out} (panel b), ρ^{out-in} (panel c), $\rho^{out-out}$ (panel d).

The local assortativity indicators in the two quarters Q1 and Q48 are respectively shown in Figures (4.9) and (4.10). Note that for each local assortativity indicator, we consider it as the function of the corresponding degree [4]. The results indicate that, first, given an overall level of assortativity in a particular category, the contribution of nodes of different degrees varies across the four mixing categories. In the out-in mixing category, we observe that, on the one hand, the hubs contribute most to the overall level of assortativity; on the other hand, small degree nodes can be associated with slight assortativity or disassortativity. In

[4] In the cases of ρ^{in-out} and ρ^{out-in}, we plot them against $k^{in-out} = \sqrt{k^{in}k^{out}}$, since each of them depends on both k^{in} and k^{out} (see the Appendix for more detailed derivations).

addition, the contributions of medium degree nodes are more volatile than those of the small degree nodes. This is very similar to what we found in the undirected version of the network. However, the behavior of the local assortativity indicators becomes more complicated for the other mixing categories. For example, the contributions of hubs and medium degree nodes can fluctuate a lot, so that it becomes difficult to classify which type of nodes plays an important role for the overall level of assortativity.

Next, we turn to the third order correlations between banks in the directed binary network. We focus on investigating local clustering as a function of degree for the four cases shown in Figure (4.2) (see, for example, Fagiolo, 2007). In the following discussion we will be referring to nodes i, j, k as an example of three vertices in a network building a triangle. It is clear that the directions of the edges now matter for the clustering analysis. The measures C^{mid}, C^{cyc}, C^{out} and C^{in} summarize the prevalence of a particular type of relationship that a node has with its neighbors. For instance, larger values of C^{mid} (see panel (b) of Figure (4.2)) may represent a higher systemic risk associated with that node, since bank i can be a source of risk as well as be exposed to risk from other banks. Clustering relationships of the type shown in panel (c) of Figure (4.2) are also conducive to systemic risk since a default of bank i would affect both its partners. Larger values of C^{in} therefore indicate a higher systemic risk related to overlapping portfolios in the banking system. This is, however, not the case for cyclical clustering relationships (captured by C^{cyc}) since in this type of relationships exposures can cancel each other out (see panel (a) of Figure (4.2)). Finally, large values of C^{out} associated with bank i tell a story about risk exposure affecting bank i itself, since both banks j and k can affect bank i in case either of them would default (see panel (d) of Figure (4.2).

For each type of clustering relationship, we first consider the local clustering coefficient as the function of the corresponding degree [5]. Typically, in each case, a general negative relationship is observed in the first quarters, but for later quarters this relationship becomes flatter (see, for example, Figures (4.11) and (4.12)).

[5] In the cases of C^{cyc}_{bin} and C^{mid}_{bin}, we plot them against $k^{in-out} = \sqrt{k^{in}k^{out}}$.

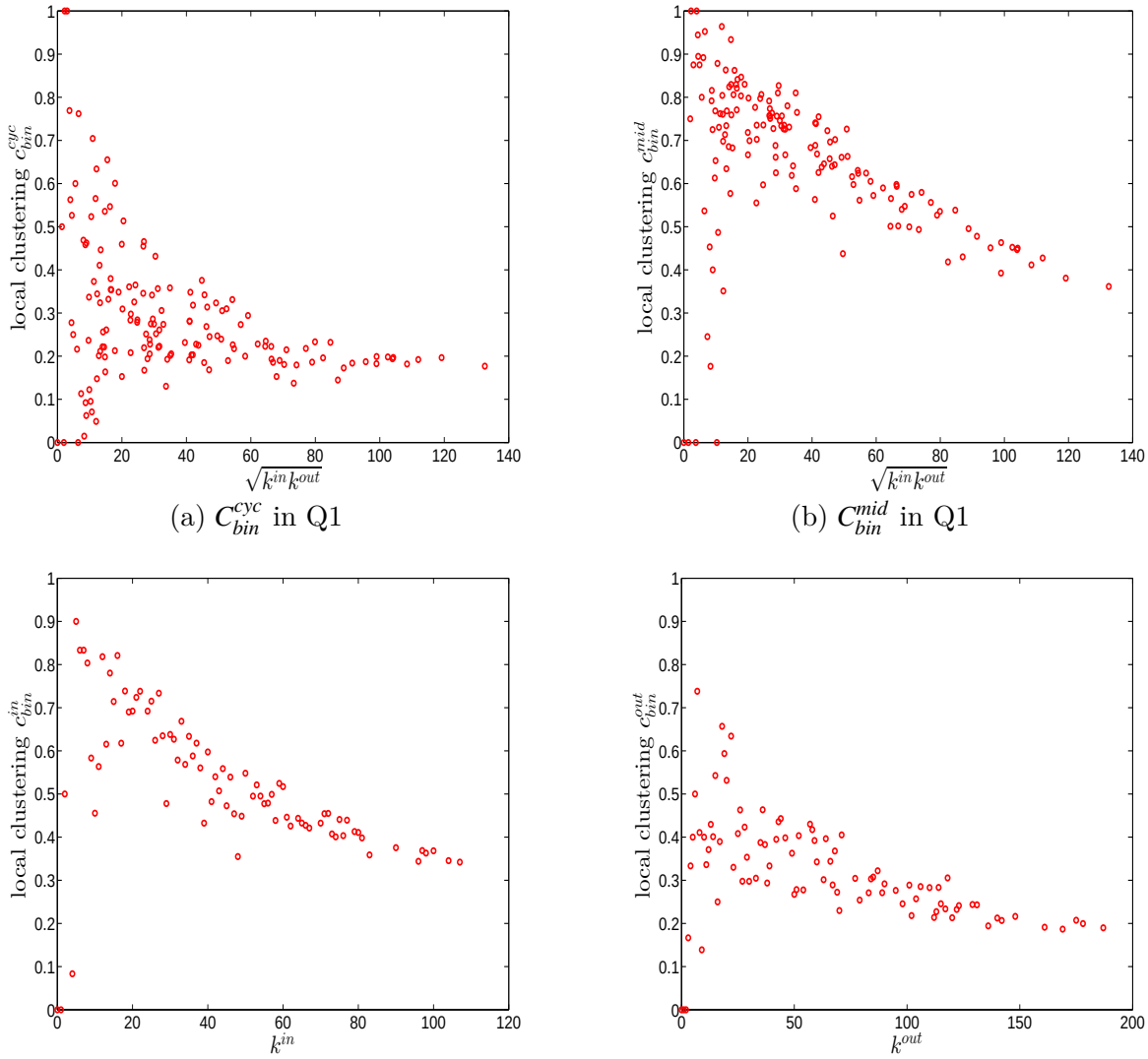

(a) C_{bin}^{cyc} in Q1

(b) C_{bin}^{mid} in Q1

(c) C_{bin}^{in} in Q1

(d) C_{bin}^{out} in Q1

Figure 4.11: Local clustering coefficients C_{bin}^{cyc} (panel a), C_{bin}^{mid} (panel b), C_{bin}^{in} (panel c), C_{bin}^{out} (panel d) in the directed binary e-MID network, in Q1.

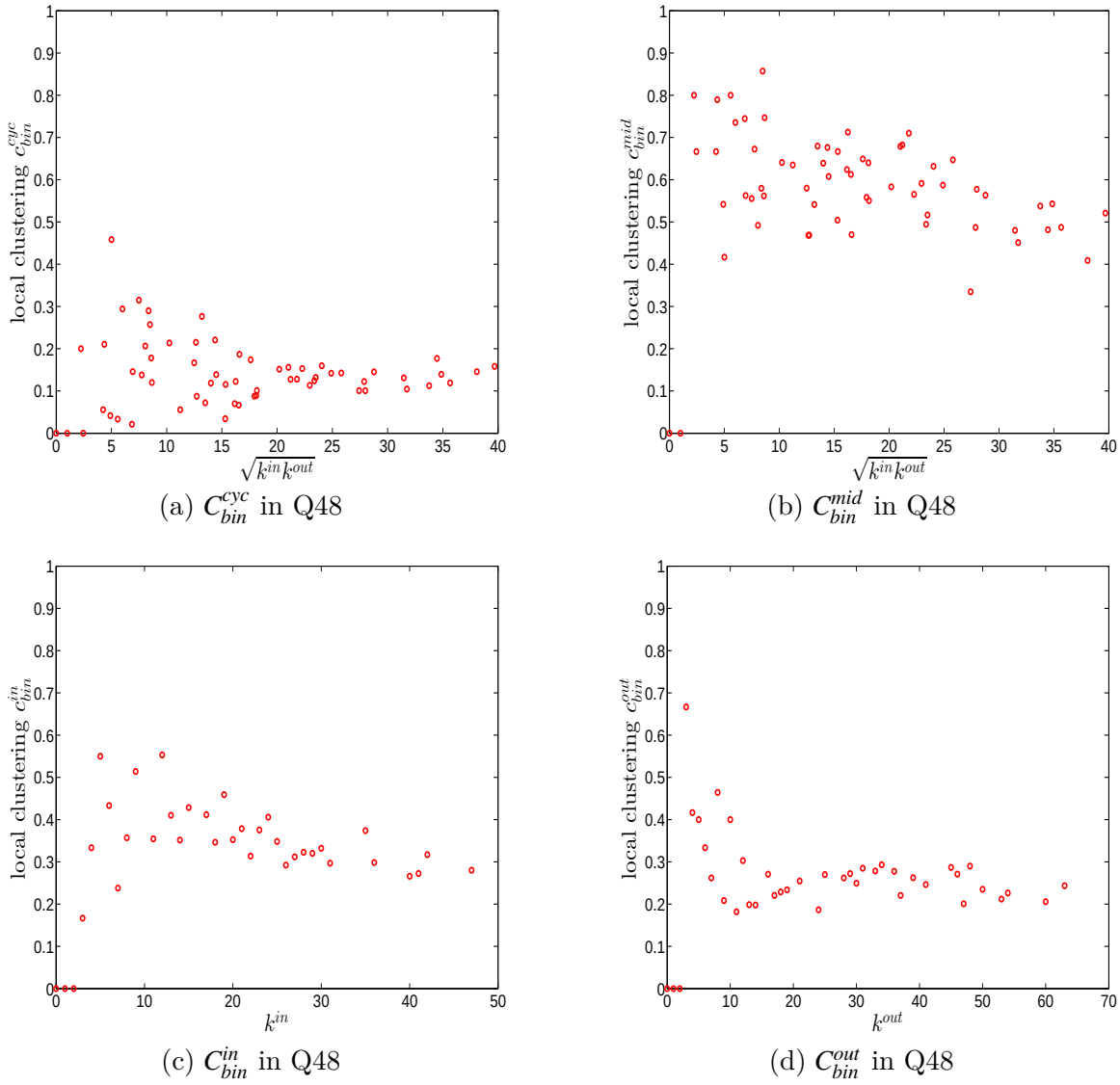

(a) C_{bin}^{cyc} in Q48

(b) C_{bin}^{mid} in Q48

(c) C_{bin}^{in} in Q48

(d) C_{bin}^{out} in Q48

Figure 4.12: Local clustering coefficients C_{bin}^{cyc} (panel a), C_{bin}^{mid} (panel b), C_{bin}^{in} (panel c), C_{bin}^{out} (panel d) in the directed binary e-MID network, in Q48.

We now take the averages of the local clustering coefficients across all nodes and then investigate their evolution over time. We observe that, first, for the most part, the averages $\bar{C}^{mid}$, $\bar{C}^{in}$, $\bar{C}^{out}$, and $\bar{C}^{cyc}$ are in descending order, with clustering relationships of the cyclical and out-type being much less common than the other two. We consider this prevalence of the middleman and in-type clustering relationships as evidence of the presence of systemic risk in the network. Second, similarly to what we observed in the undirected network for $\bar{C}_{bin}^{un}$, the averages of the local clustering coefficients for all four clustering types dramatically decrease around the time of the financial crisis, evidencing structural change in the third

order correlations between banks.

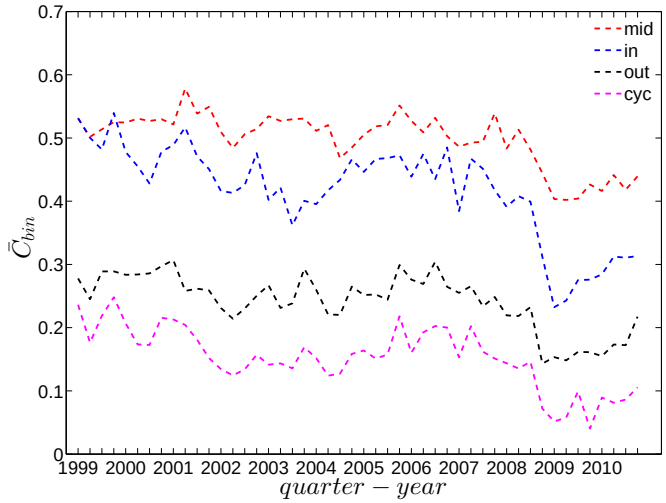

Figure 4.13: Evolution of the averages of local clustering coefficients (i.e. $\bar{C}^{mid}$, $\bar{C}^{in}$, $\bar{C}^{out}$, and $\bar{C}^{cyc}$) in the directed binary e-MID network.

4.3.3 Comparisons to the configuration models

Undirected Binary Network

We first employ the undirected binary configuration model (UBCM), which maintains the intrinsic heterogeneity in the degree sequence of the undirected binary version of the observed e-MID network. Figure (4.14) shows a comparison between various higher order structural correlations observed in the e-MID network and the same structural correlations observed in the randomized ensemble for the first and last quarters. Note that, in each panel of Figure (4.14), besides the observed and the expected values (over the randomized ensemble), we also report the regions of ± 1 standard deviation (std.) and $\pm$ 2 std. away from the expectations. In most cases, as shown in panels (a) to (f), the local behavior of the structural correlations is well replicated by the UBCM. As shown in panel (a) of Figure (4.15), the average of the ANNDs over all nodes ($\bar{k}^{un}_{nn}$) is also located inside the ± 2 std. band when plotted over time. In contrast, in terms of our measure of global assortativity (r^{un}_{bin}), in almost all of the quarters, the observed values lie outside the ± 2 std. band (see panel (b) of Figure (4.15)). A similar result is obtained for the evolution of the average of the local clustering coefficients ($\bar{C}^{un}_{bin}$) with many significant deviations, but the main trends of the observed and the expected values are similar (see panel (c) of Figure (4.15)).

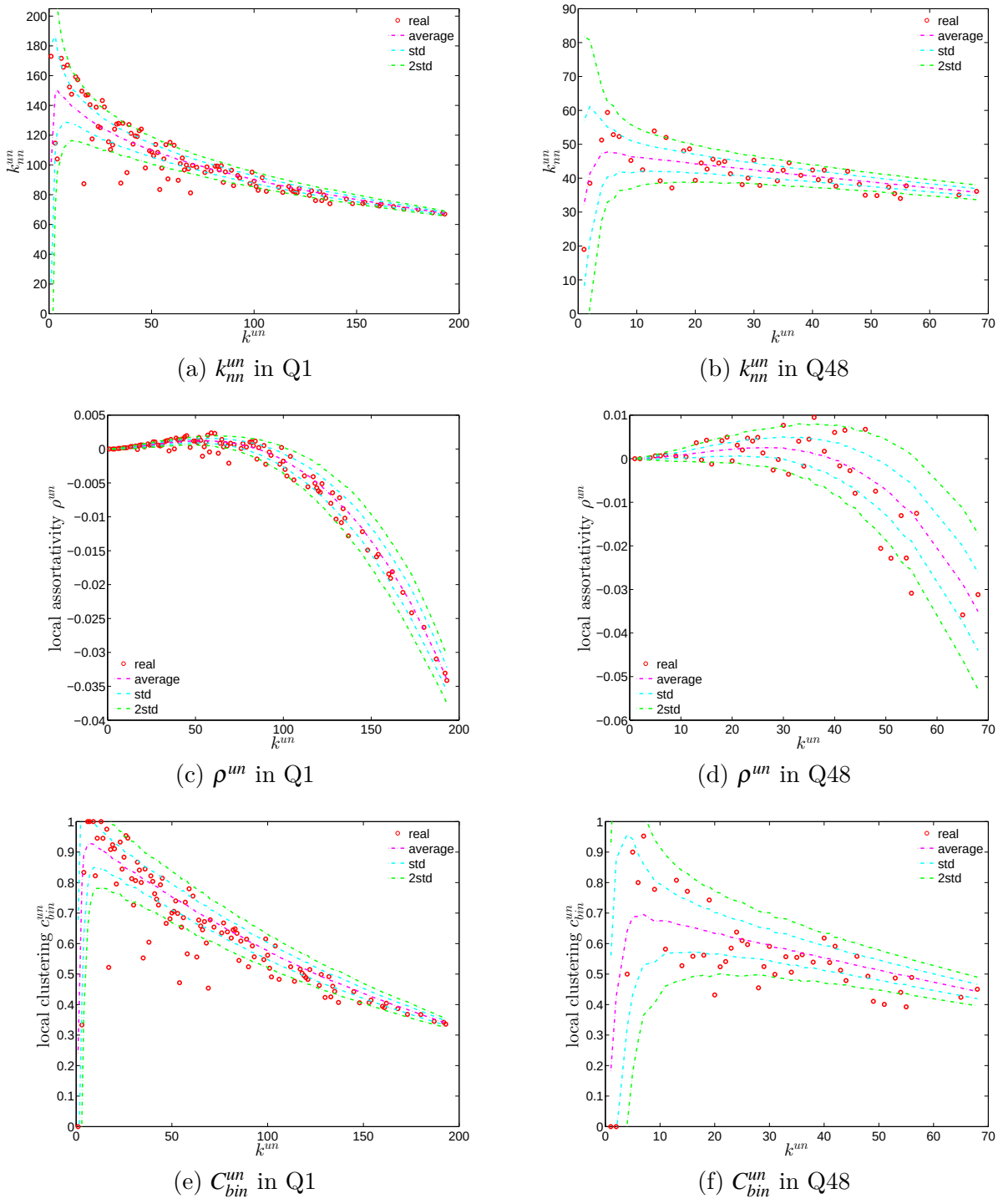

(a) k^{un}_{nn} in Q1

(b) k^{un}_{nn} in Q48

(c) ρ^{un} in Q1

(d) ρ^{un} in Q48

(e) C^{un}_{bin} in Q1

(f) C^{un}_{bin} in Q48

Figure 4.14: ANND (panels a, b), local assortativity ρ^{un} (panels c, d), local clustering coefficients C^{un}_{bin} (panels e, f) in the observed e-MID network and in the UBCM, in Q1 and Q48.

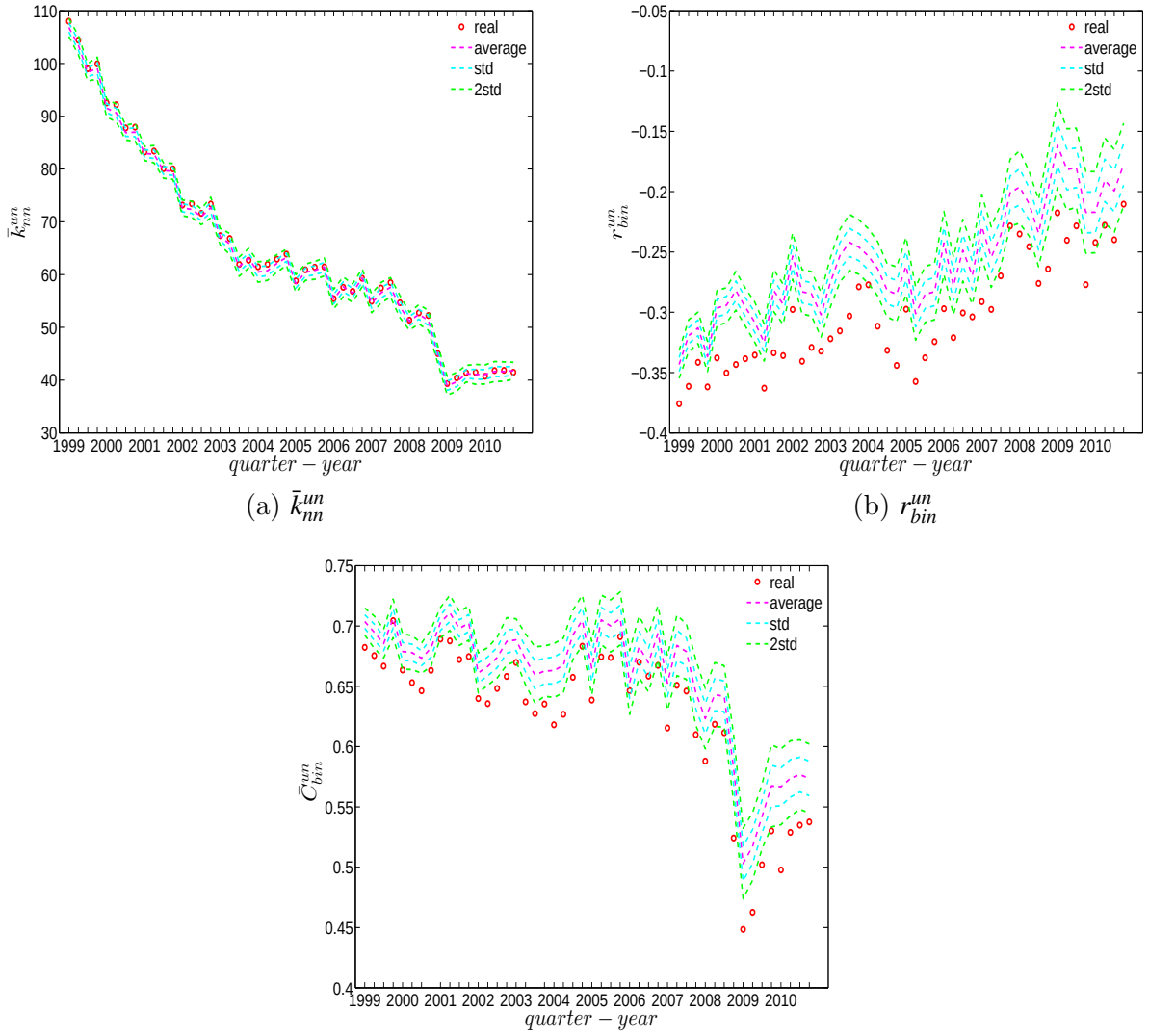

(a) $\bar{k}^{un}_{nn}$ (b) r^{un}_{bin}

(c) $\bar{C}^{un}_{in}$

Figure 4.15: Evolution of $\bar{k}^{un}_{nn}$ (panel a), r^{un}_{bin} (panel b), and $\bar{C}^{un}_{in}$ (panel c) in the observed e-MID network and in the UBCM.

Directed Binary Network

Recalling that under the directed binary configuration model (DBCM), both out-going and in-coming degrees are enforced on average over the ensemble, we show the comparisons between the structural correlations of observed network and those obtained from that model in Figures (4.16) and (4.17) (for ANND), Figures (4.18) and (4.19) (for the local assortativity indicators), and Figures (4.20) and (4.21) (for the local clustering coefficients).

In addition, as for the undirected version, we also compare the evolution of the global indicators with the evolution of their expected values obtained from the DBCM. We show the results for the averages of the ANNDs (i.e. $\bar{k}^{in-in}_{nn}$, $\bar{k}^{in-out}_{nn}$, $\bar{k}^{out-in}_{nn}$, $\bar{k}^{out-out}_{nn}$) in Figure

(4.22), for the global assortativity indicators (r_{bin}^{in-in}, r_{bin}^{in-out}, r_{bin}^{out-in}, $r_{bin}^{out-out}$) in Figure (4.23), and for the averages of the local clustering coefficients ($\bar{C}_{bin}^{in-in}$, $\bar{C}_{bin}^{in-out}$, $\bar{C}_{bin}^{out-in}$, $\bar{C}_{bin}^{out-out}$) in Figure (4.24).

First, regarding the local indicators (see from Figure (4.16) to Figure (4.21)), in most cases, the observed ANNDs, local assortativity indicators, and local clustering coefficients are in agreement with those evaluated under the DBCM. Since the few observed points significantly deviating from the expected ones might not reveal any patterns (under the DBCM), they might be seen as the expected rejections one obtains for a large sequence of simultaneous tests.

Second, regarding the evolution of the averages of the ANNDs, Figure (4.22) shows that, $\bar{k}_{nn}^{in-in}$, $\bar{k}_{nn}^{in-out}$, and $\bar{k}_{nn}^{out-in}$ always lie within the ± 2 std. band, while $\bar{k}_{nn}^{out-out}$ is underestimated for most of the time.

Third, in terms of the global assortativity indicators, for the most part, r_{bin}^{in-in} and r_{bin}^{out-in} are located inside the $\pm$ 2 std. band, while r_{bin}^{in-out} and $r_{bin}^{out-out}$ are mostly being overestimated (see Figure (4.23)).

Finally, over time, the averages of the local clustering coefficients $\bar{C}_{bin}^{in-in}$, $\bar{C}_{bin}^{in-out}$, $\bar{C}_{bin}^{out-in}$, and $\bar{C}_{bin}^{out-out}$ are generally in agreement with their expected values from the DBCM, as shown in Figure (4.24).

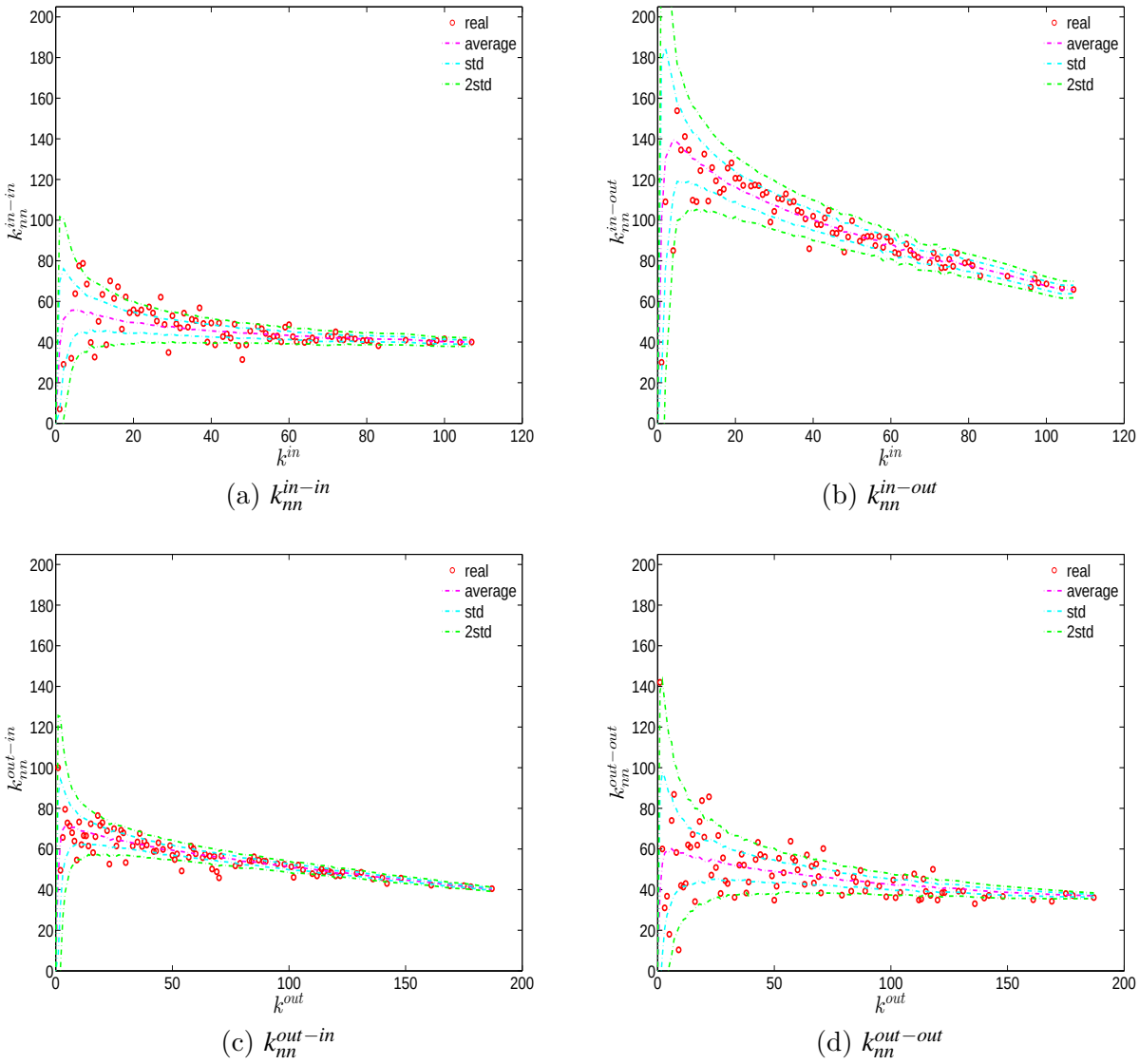

(a) k_{nn}^{in-in} (b) k_{nn}^{in-out}

(c) k_{nn}^{out-in} (d) $k_{nn}^{out-out}$

Figure 4.16: ANND in the observed e-MID network and in the DBCM, in Q1. k_{nn}^{in-in} (panel a), k_{nn}^{in-out} (panel b), k_{nn}^{out-in} (panel c), $k_{nn}^{out-out}$ (panel d).

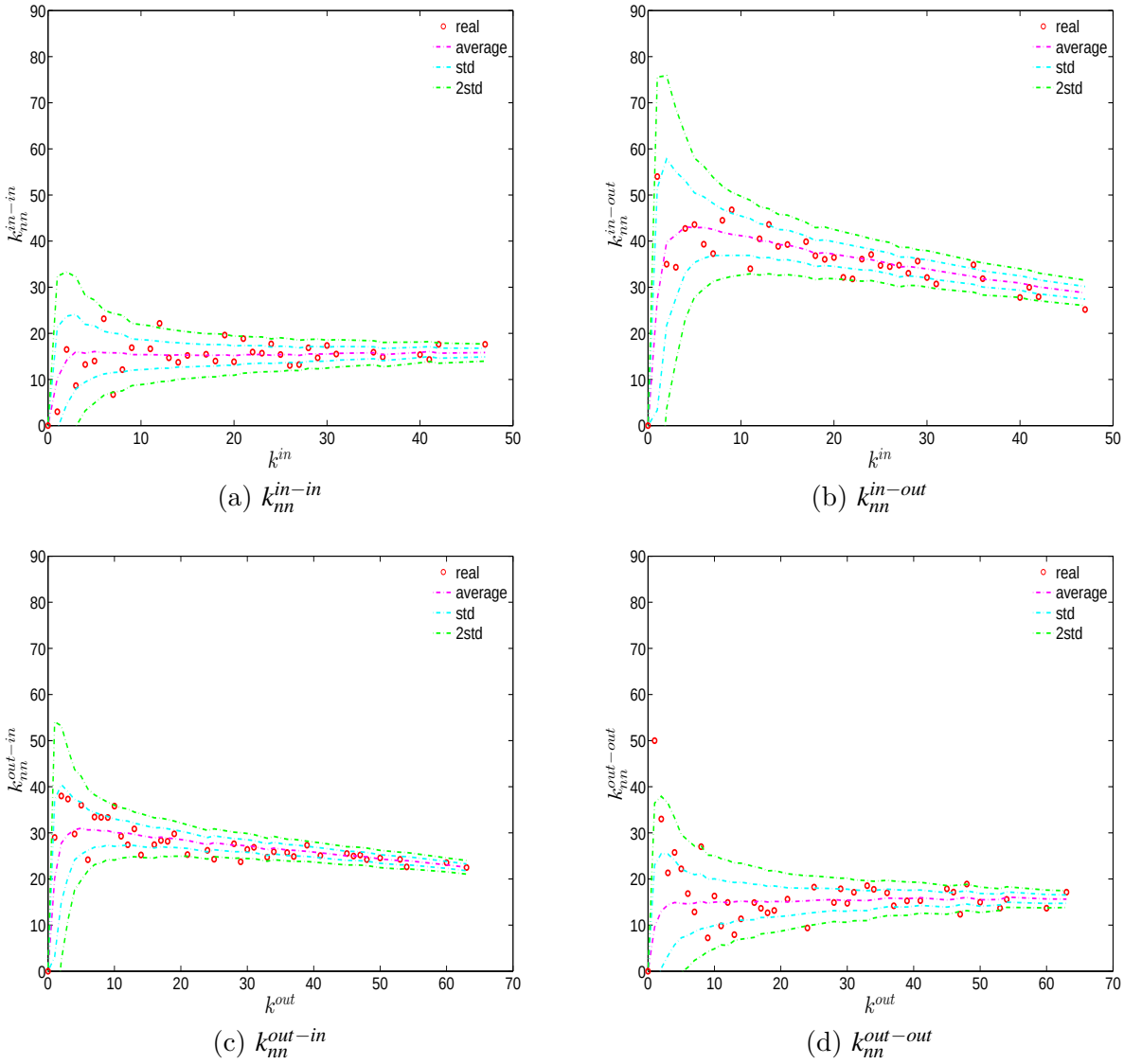

(a) k_{nn}^{in-in} (b) k_{nn}^{in-out}

(c) k_{nn}^{out-in} (d) $k_{nn}^{out-out}$

Figure 4.17: ANND in the observed e-MID network and in the DBCM, in Q48. k_{nn}^{in-in} (panel a), k_{nn}^{in-out} (panel b), k_{nn}^{out-in} (panel c), $k_{nn}^{out-out}$ (panel d).

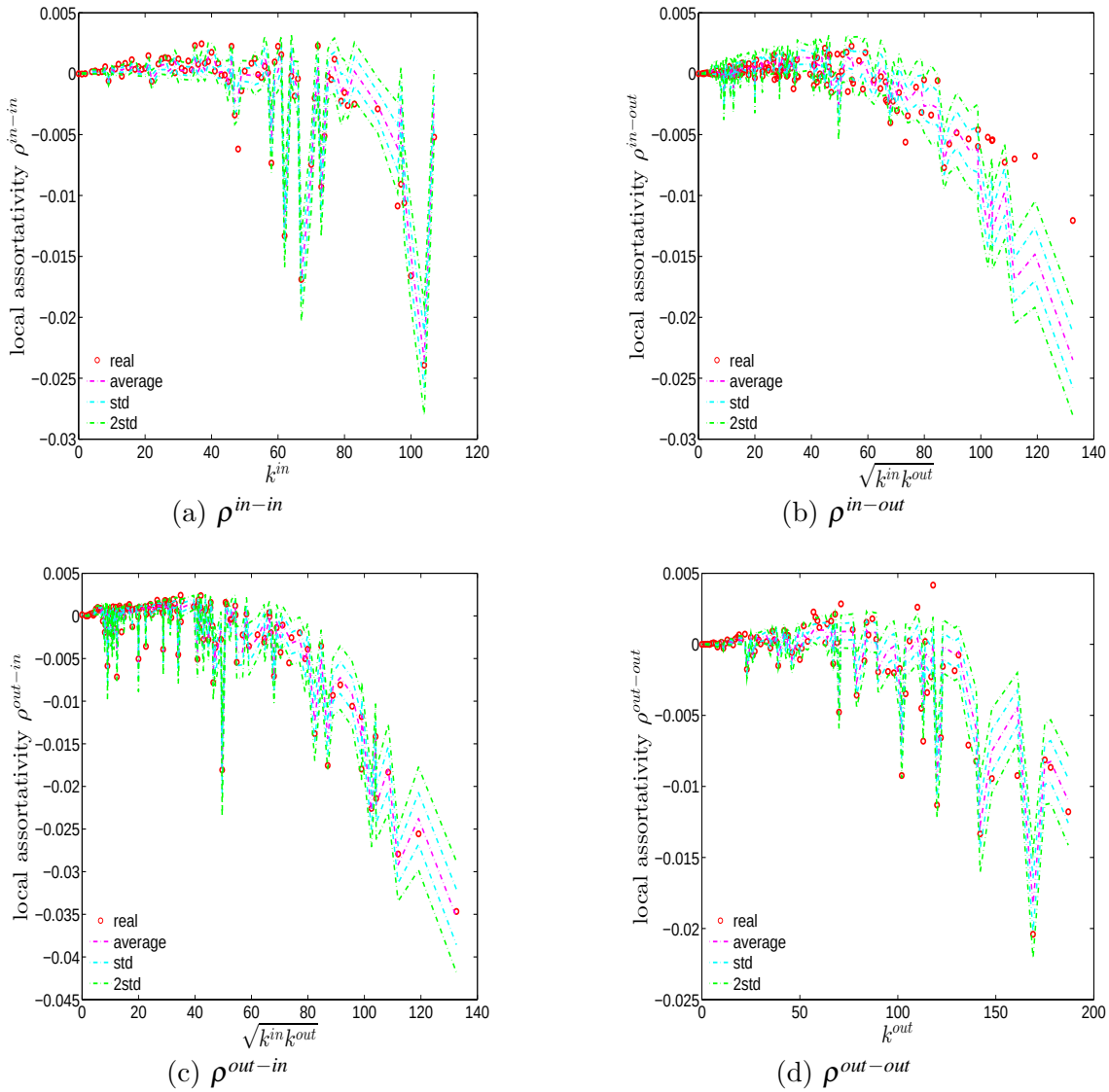

Figure 4.18: Local assortativity in the observed e-MID network and in the DBCM, in Q1. ρ^{in-in} (panel a), ρ^{in-out} (panel b), ρ^{out-in} (panel c), $\rho^{out-out}$ (panel d).

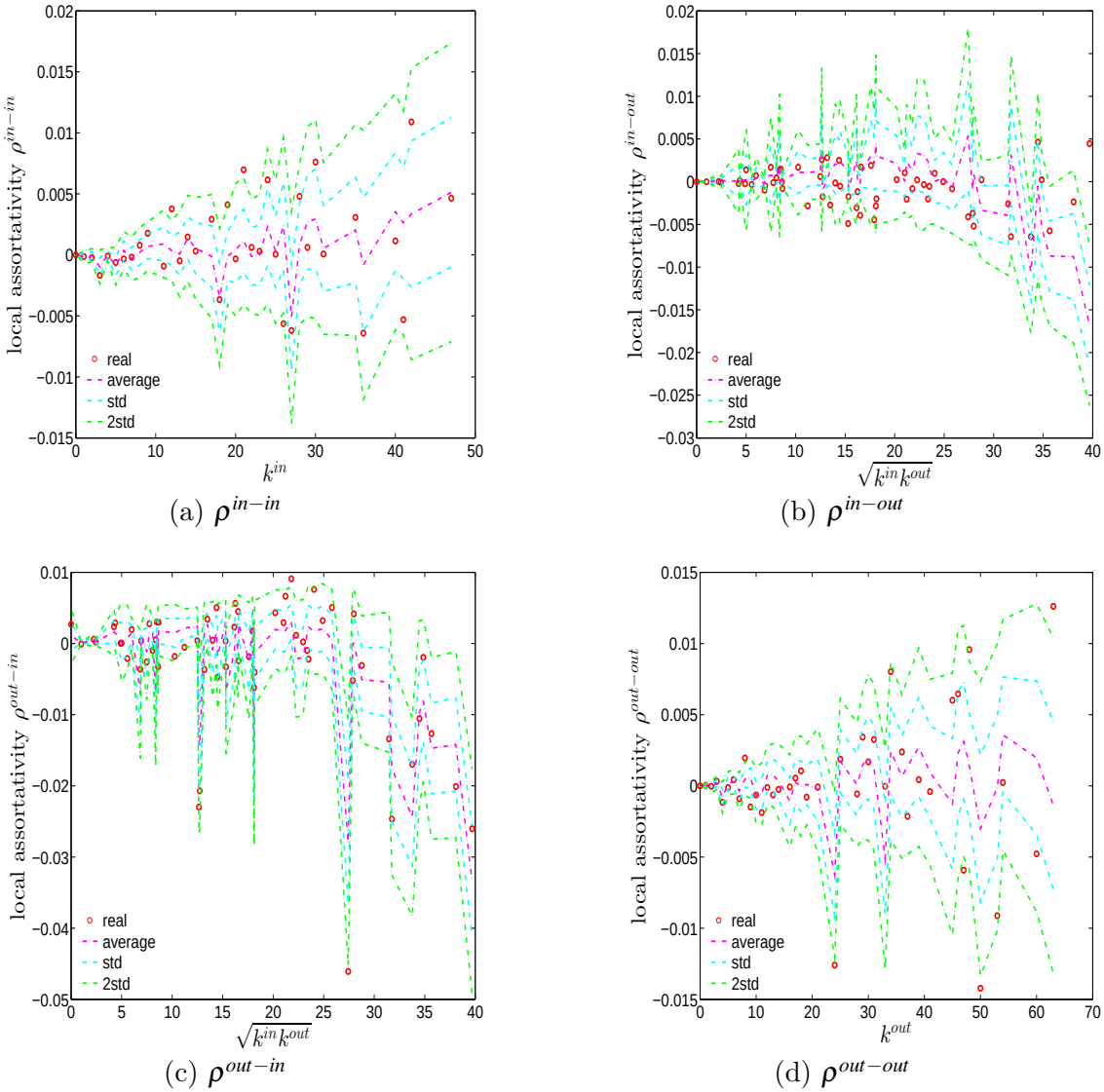

(a) ρ^{in-in} (b) ρ^{in-out}

(c) ρ^{out-in} (d) $\rho^{out-out}$

Figure 4.19: Local assortativity in the observed e-MID network and in the DBCM, in Q48. ρ^{in-in} (panel a), ρ^{in-out} (panel b), ρ^{out-in} (panel c), $\rho^{out-out}$ (panel d).

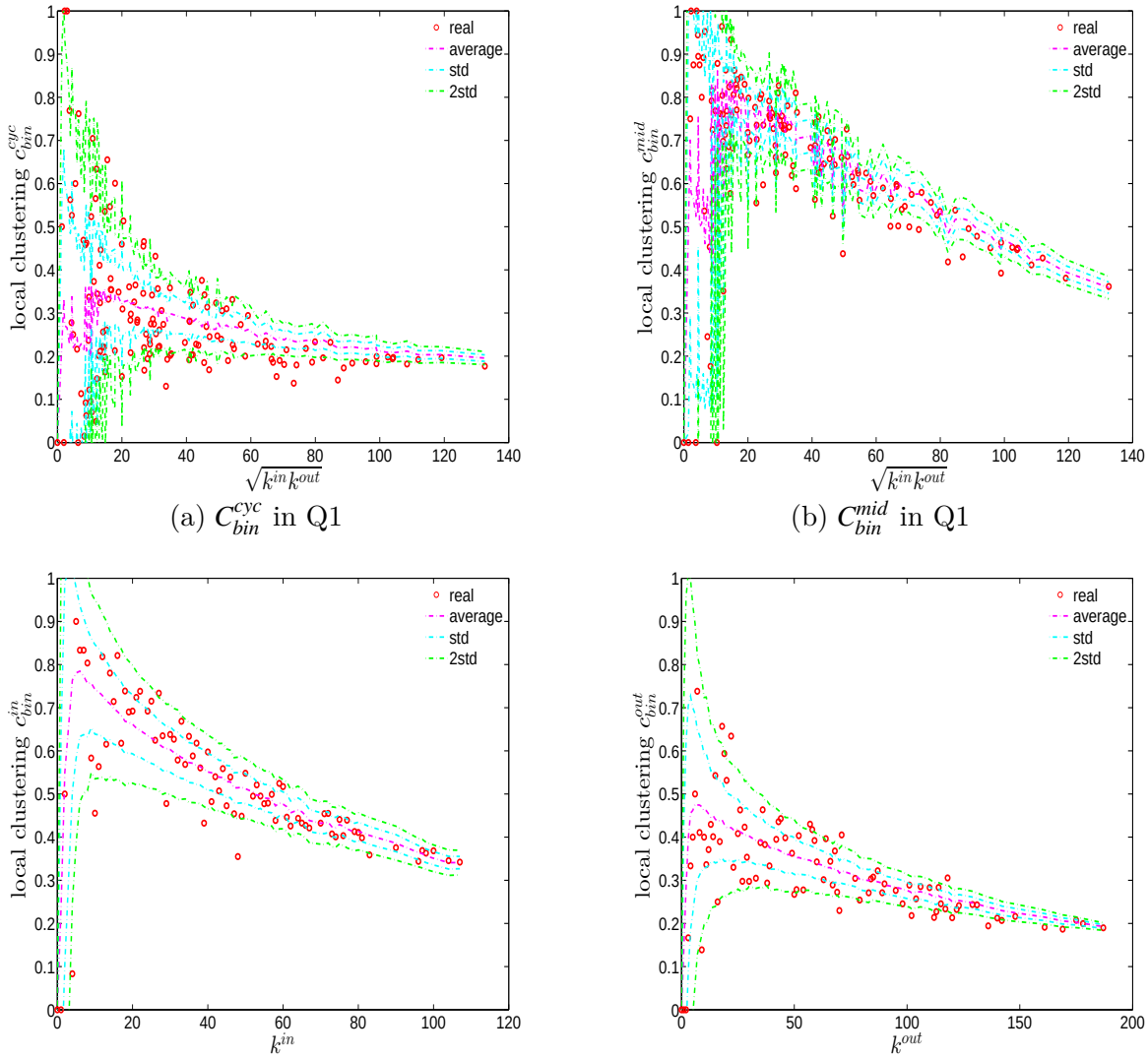

(a) C_{bin}^{cyc} in Q1

(b) C_{bin}^{mid} in Q1

(c) C_{bin}^{in} in Q1

(d) C_{bin}^{out} in Q1

Figure 4.20: Local clustering coefficients C_{bin}^{cyc} (panel a), C_{bin}^{mid} (panel b), C_{bin}^{in} (panel c), C_{bin}^{out} (panel d) in the observed e-MID network and in DBCM, in Q1.

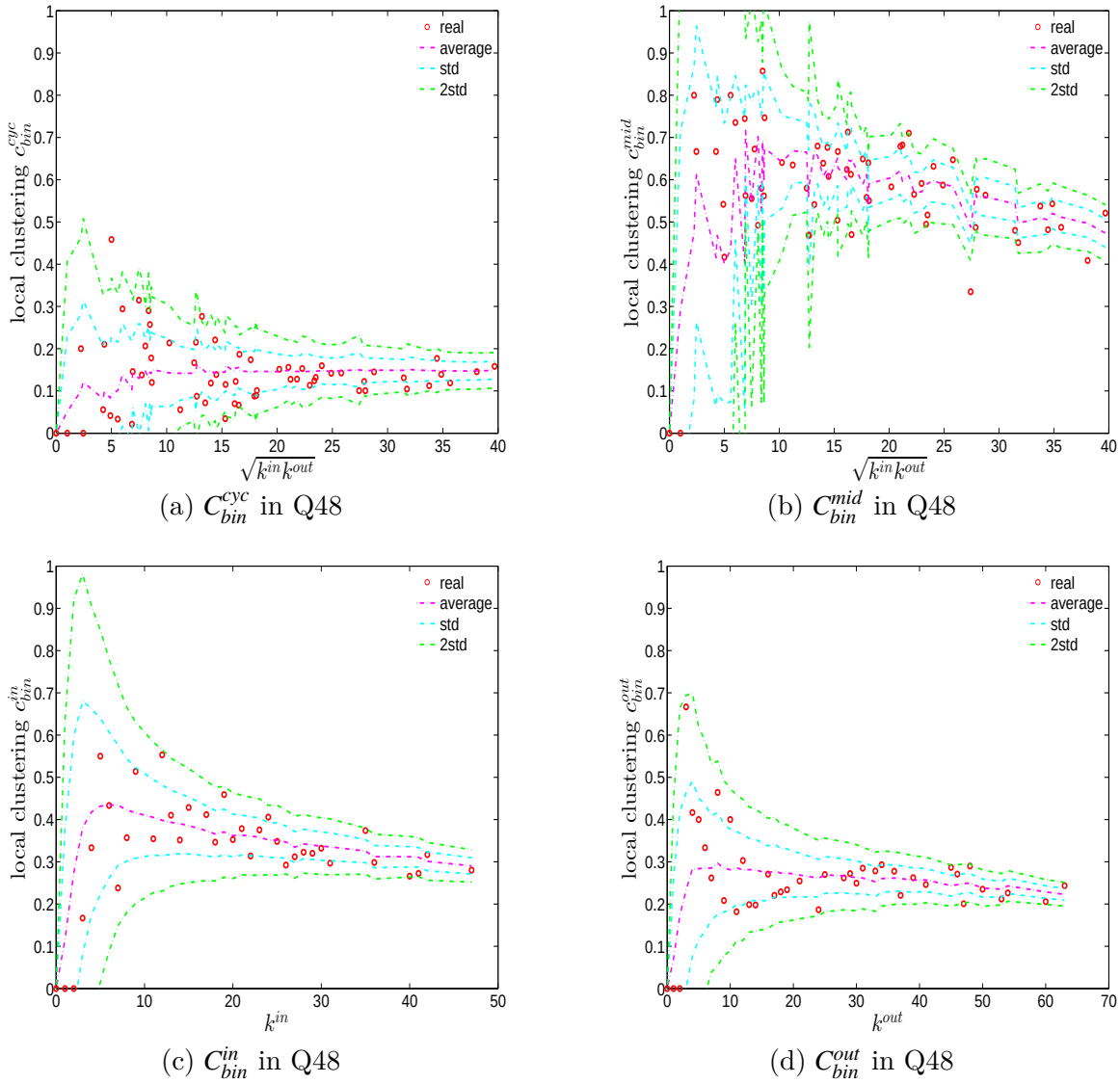

(a) C^{cyc}_{bin} in Q48

(b) C^{mid}_{bin} in Q48

(c) C^{in}_{bin} in Q48

(d) C^{out}_{bin} in Q48

Figure 4.21: Local clustering coefficients C^{cyc}_{bin} (panel a), C^{mid}_{bin} (panel b), C^{in}_{bin} (panel c), C^{out}_{bin} (panel d) in the observed e-MID network and in DBCM, in Q48.

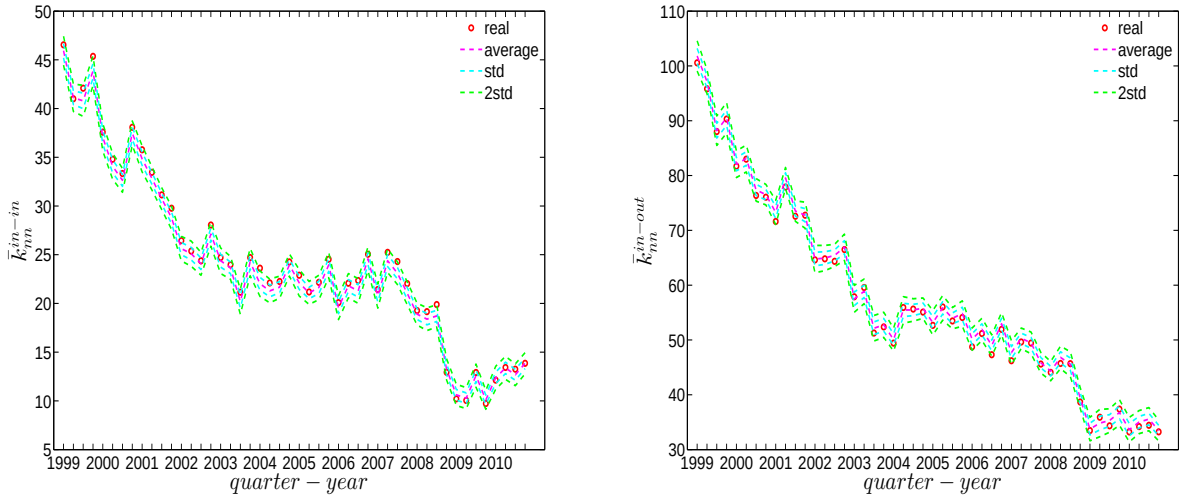

(a) $\bar{k}_{nn}^{in-in}$

(b) $\bar{k}_{nn}^{in-out}$

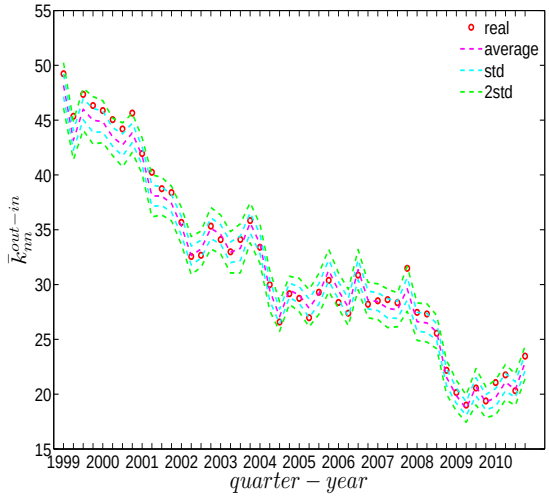

(c) $\bar{k}_{nn}^{out-in}$

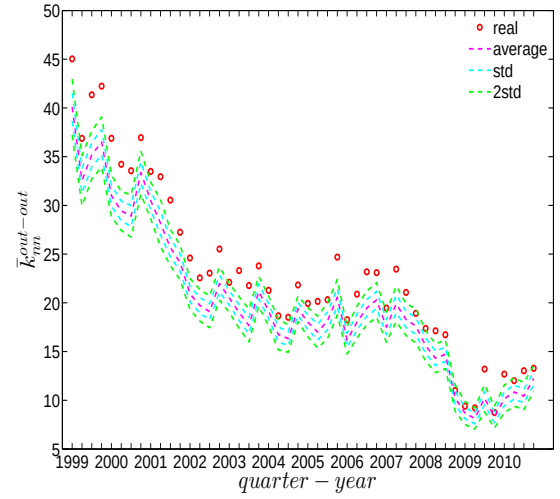

(d) $\bar{k}_{nn}^{out-out}$

Figure 4.22: Evolution of the averages of ANNDs in the observed e-MID network and in the DBCM. $\bar{k}_{nn}^{in-in}$ (panel a), $\bar{k}_{nn}^{in-out}$ (panel b), $\bar{k}_{nn}^{out-in}$ (panel c), $\bar{k}_{nn}^{out-out}$ (panel d).

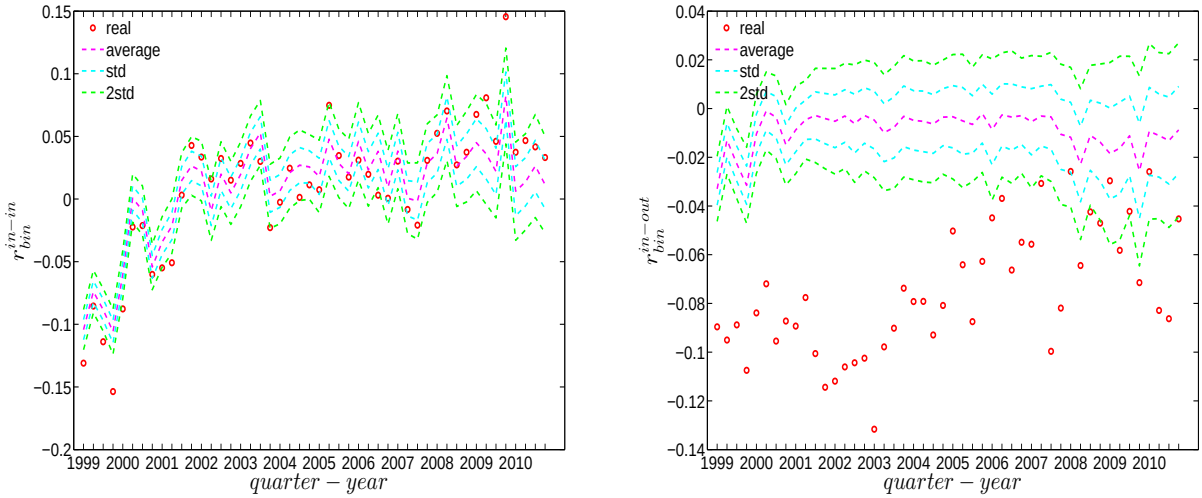

(a) r_{bin}^{in-in}

(b) r_{bin}^{in-out}

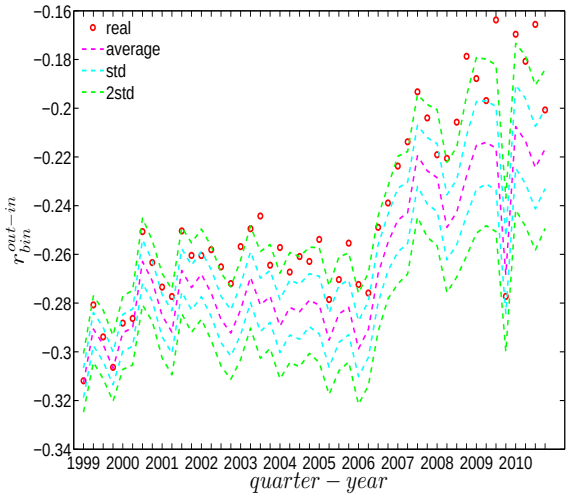

(c) r_{bin}^{out-in}

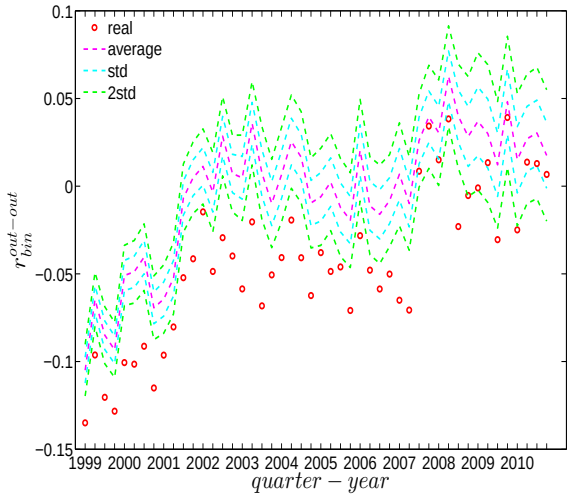

(d) $r_{bin}^{out-out}$

Figure 4.23: Evolution of the global assortativity indicators in the observed e-MID network and in the DBCM. r_{bin}^{in-in} (panel a), r_{bin}^{in-out} (panel b), r_{bin}^{out-in} (panel c), $r_{bin}^{out-out}$ (panel d).

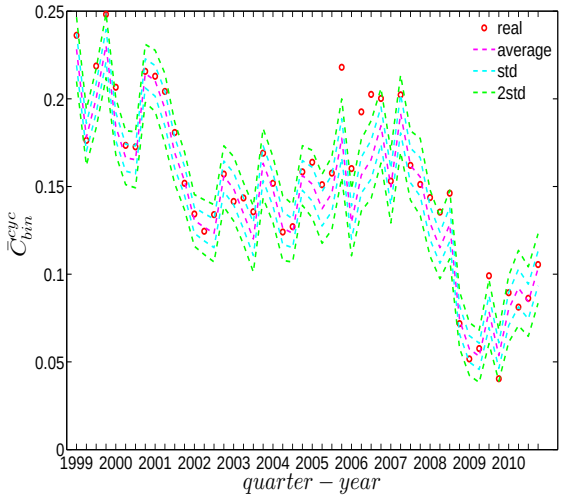

(a) $\bar{C}^{cyc}_{bin}$

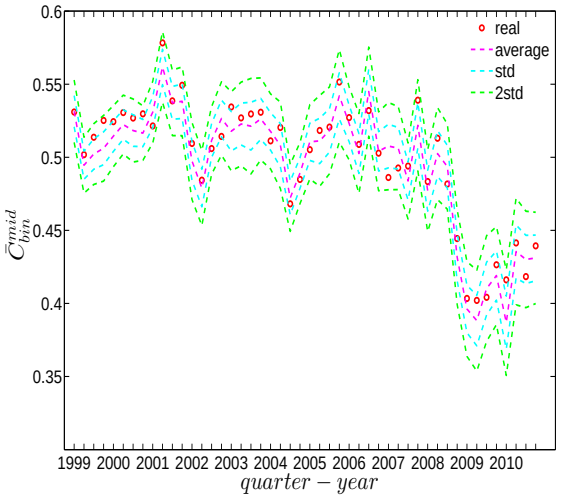

(b) $\bar{C}^{mid}_{bin}$

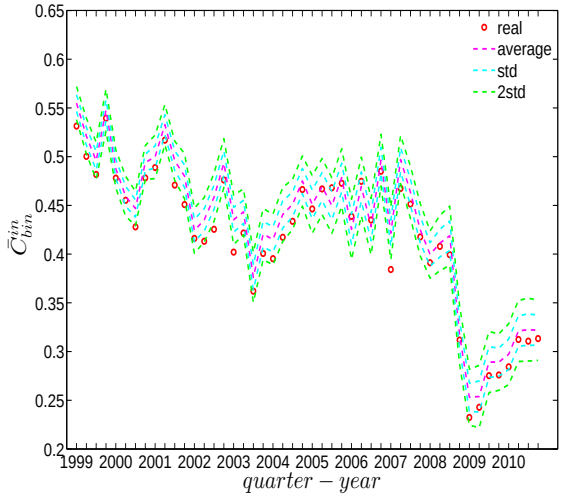

(c) $\bar{C}^{in}_{bin}$

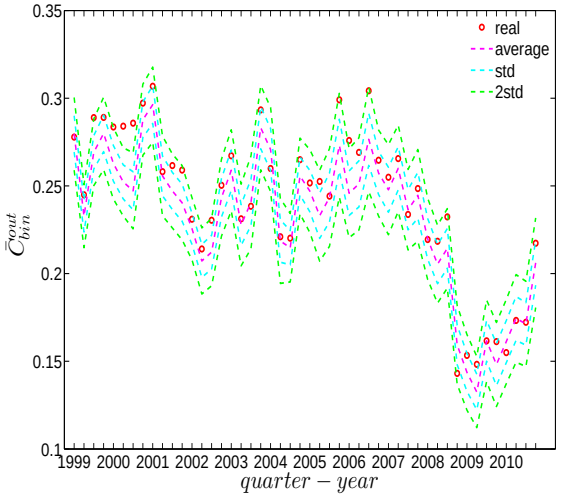

(d) $\bar{C}^{out}_{bin}$

Figure 4.24: Evolution of the averages of clustering coefficients in the observed e-MID network and in the DBCM. $\bar{C}^{cyc}_{bin}$ (panel a), $\bar{C}^{mid}_{bin}$ (panel b), $\bar{C}^{in}_{bin}$ (panel c), $\bar{C}^{out}_{bin}$ (panel d).

4.4 Findings for the weighted network

In the binary version of the observed network, we treat all edges as if they were homogeneous. However, in reality, the capacity and intensity of the relations between banks can be very heterogeneous, consequently the weighted version can have different properties compared to its binary counterpart. In this section, we investigate the structural correlations in the weighted e-MID network. For the sake of simplicity, we do not consider the local weighted assortativity in this section, since breaking down the overall weighted assortativity measure into the contributions of the individual nodes is much more complicated than in the binary case.

Regarding the null models, instead of preserving the observed degree sequence(s) as in the Binary Configure Models (i.e. UBCM, DBCM), first, we employ the weighted configuration model preserving the observed strength sequence(s) (i.e. the UWCM model in the undirected case and the DWCM model in the directed case) and examine whether the chosen null models can replicate the structural correlations in the observed weighted network. As a second step, we consider the enhanced configuration models which maintain both the observed degree as well as strength sequences (i.e. the UECM and the DECM respectively in the undirected and directed cases) and repeat the same exercise.

4.4.1 Structural correlations in the undirected weighted e-MID network

We report the strength dependencies in Figure (4.25) by considering the relationship between s^{un}_{nn} (ANNS) and s^{un} in the first and last quarters. We observe that s^{un}_{nn} is generally a declining function of s^{un}. This relationship is confirmed by the negative value of the global weighted assortativity measure r^{un}_{w} (see Figure (4.26)). This signals the prevalence of disassortative mixing in the undirected weighted e-MID network, meaning that, in general, high strength banks tend to have relations with low strength banks. Furthermore, it should be emphasized that, in comparison to the undirected binary version of the network, the undirected weighted network exhibits less disassortativity overall, since r^{un}_{w} is smaller than r^{un}_{bin} in absolute value.

In our analysis of the third order correlations, in contrast to what we discovered in the binary version, we find that, on average the higher strength banks also have higher local clustering coefficients (see Figure (4.27)). This is mainly because the heterogeneity in the transaction volumes across banks in every triangle is now taken into account and the average transactions of high strength banks are much larger than those of low strength

banks. Furthermore, we observe three phases in the evolution of the average of the local weighted clustering coefficients, i.e. before 2002, from 2002 to 2006, and from 2007 onward, which might reflect effects arising from the adoption of the euro as well as from the recent financial crisis (see Figure (4.28)). In particular, we find that $\bar{C}_w^{un}$ is strongly elevated from 2002 to 2006. The same results still hold if we normalize all weights by the total weight average.

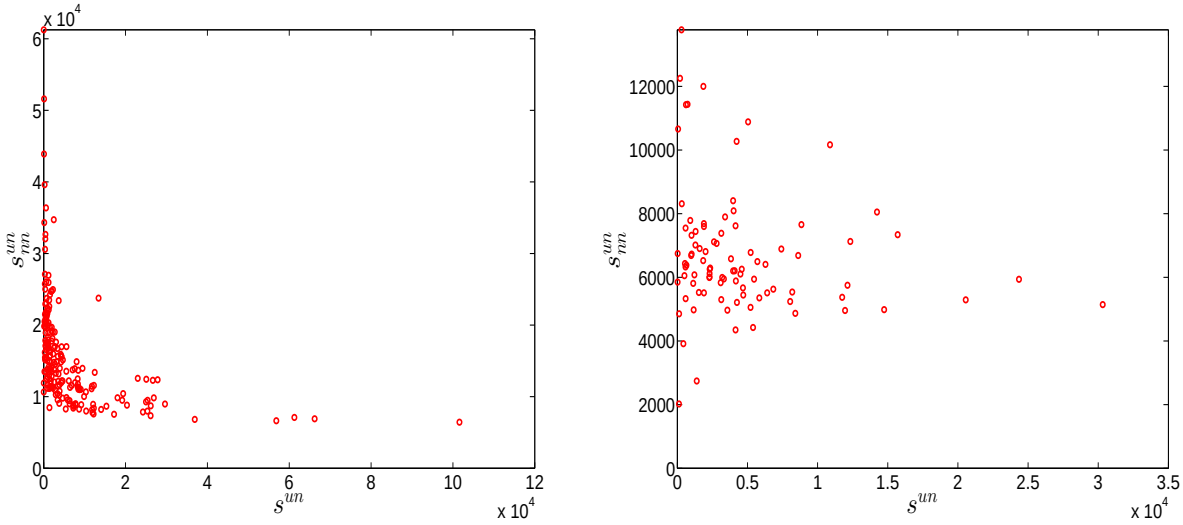

(a) s_{nn}^{un} in Q1 (b) s_{nn}^{un} in Q48

Figure 4.25: ANNS in the undirected weighted e-MID network, in Q1 and Q48.

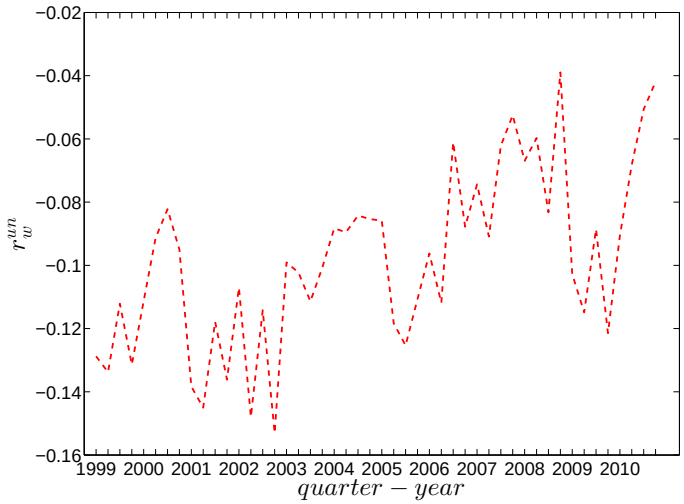

Figure 4.26: Evolution of global weighted assortativity r_w^{un} in the undirected weighted e-MID network.

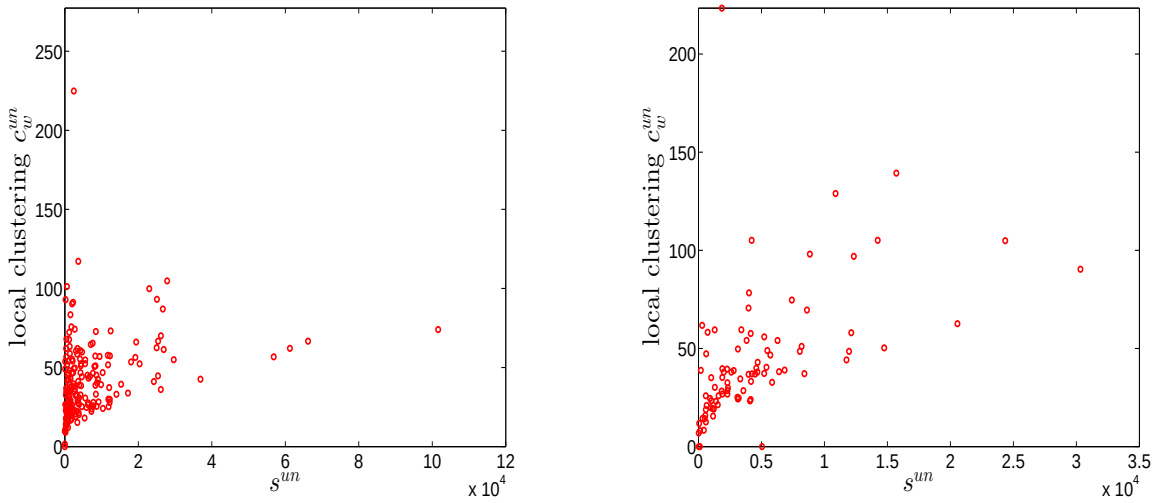

(a) C_w^{un} in Q1 (b) C_w^{un} in Q48

Figure 4.27: Local clustering coefficients C_w^{un} in the undirected weighted e-MID network, in Q1 and Q48.

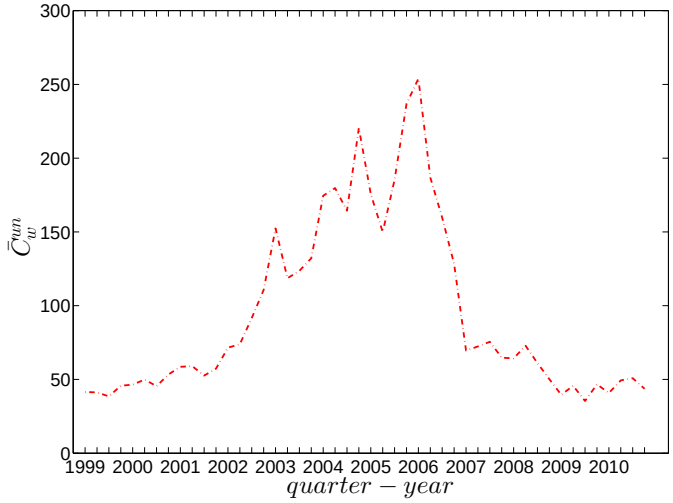

Figure 4.28: Evolution of the average of local weighted clustering coefficients (i.e. $\bar{C}_w^{un}$) in the undirected weighted e-MID network.

4.4.2 Structural correlations in the directed weighted e-MID network

In the directed weighted version of the e-MID network, to analyzing the structural correlations, we employ average nearest neighbor strength measures for the various mixing categories ($s_{nn,i}^{in-in}$, $s_{nn,i}^{in-out}$, $s_{nn,i}^{out-in}$, $s_{nn,i}^{out-out}$), global weighted assortativity indicators (r_w^{in-in}, r_w^{in-out},

r_w^{out-in}, $r_w^{out-out}$), and weighted clustering coefficients (C_w^{cyc},C_w^{mid},C_w^{in},C_w^{out}).

First, Figures (4.29) and (4.30) show the relationship between the ANNSs and the associated strengths for all four mixing categories in Q1 and Q48. Over time, while in the first quarters, the ANNSs are a declining function of the associated strengths (after certain truncated values of the associated strengths), in many later quarters these relationships break down, especially for the mixing categories in-in, in-out, and out-out. To obtain the overall level of strength dependency of bank interactions for each mixing category, we calculate the global assortativity indicators r_w^{in-in},r_w^{in-out},r_w^{out-in},$r_w^{out-out}$, and show their evolution over time in Figure (4.31). The results indicate that, while the out-in mixing is disassortative for the most part, the other three categories do not seem to exhibit a distinct mixing nature. In comparison to the directed binary version, the absolute values of r_w^{in-in},r_w^{in-out},r_w^{out-in},$r_w^{out-out}$ are smaller than those of r_{bin}^{in-in},r_{bin}^{in-out},r_{bin}^{out-in},$r_{bin}^{out-out}$. An interesting observation is that, among the four mixing categories, the weighted assortativity in the out-in category is closest to the undirected weighted assortativity, i.e. $r_w^{un} \sim r_w^{out-in}$. For the binary versions of the network, when comparing the mixing patterns in the directed and undirected case, we made the same observation.

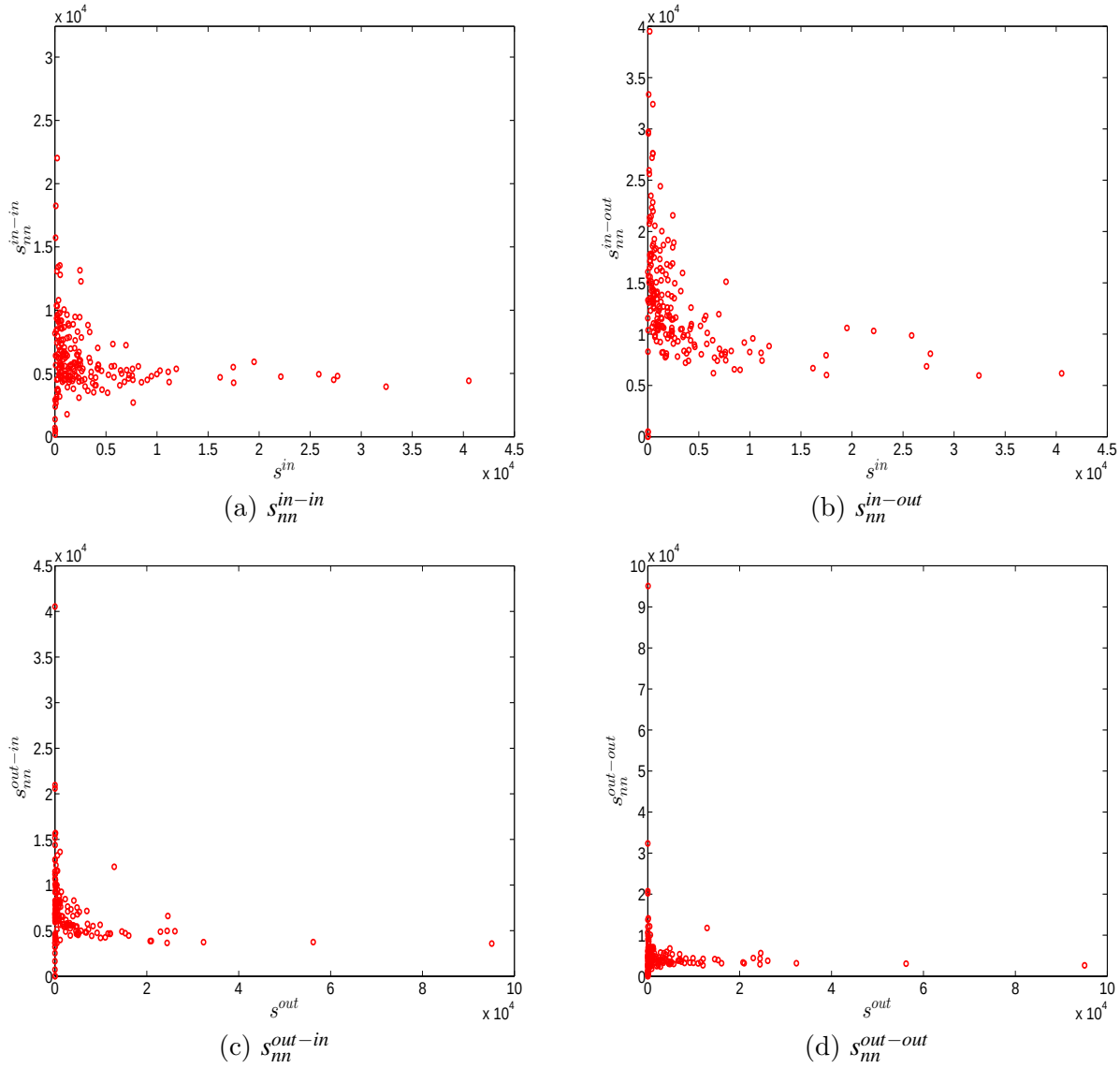

(a) s_{nn}^{in-in} (b) s_{nn}^{in-out}

(c) s_{nn}^{out-in} (d) $s_{nn}^{out-out}$

Figure 4.29: ANNSs in the directed weighted e-MID network, in Q1. s_{nn}^{in-in} (panel a), s_{nn}^{in-out} (panel b), s_{nn}^{out-in} (panel c), $s_{nn}^{out-out}$ (panel d).

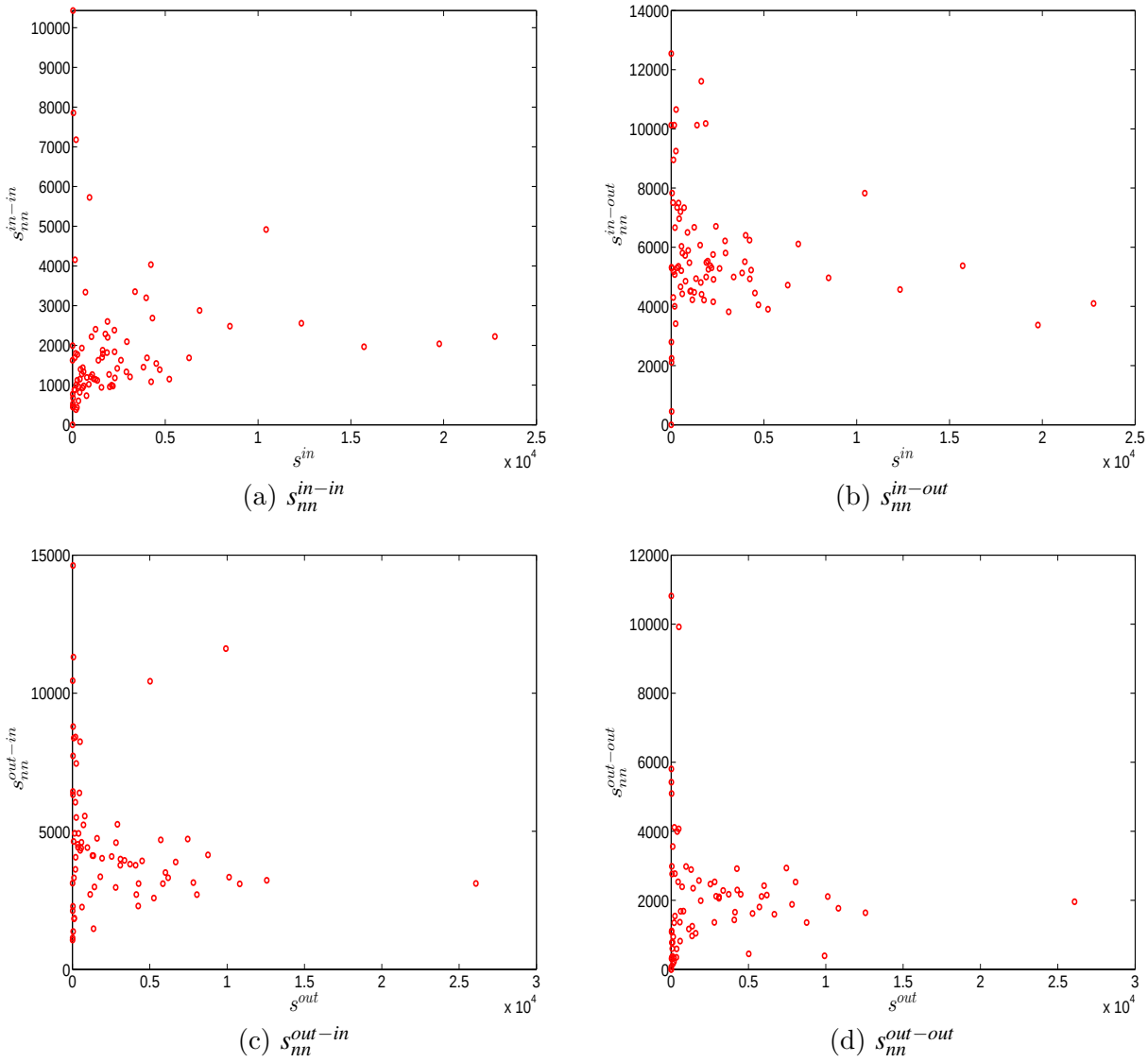

(a) s_{nn}^{in-in} (b) s_{nn}^{in-out}

(c) s_{nn}^{out-in} (d) $s_{nn}^{out-out}$

Figure 4.30: ANNSs in the directed weighted e-MID network, in Q48. s_{nn}^{in-in} (panel a), s_{nn}^{in-out} (panel b), s_{nn}^{out-in} (panel c), $s_{nn}^{out-out}$ (panel d).

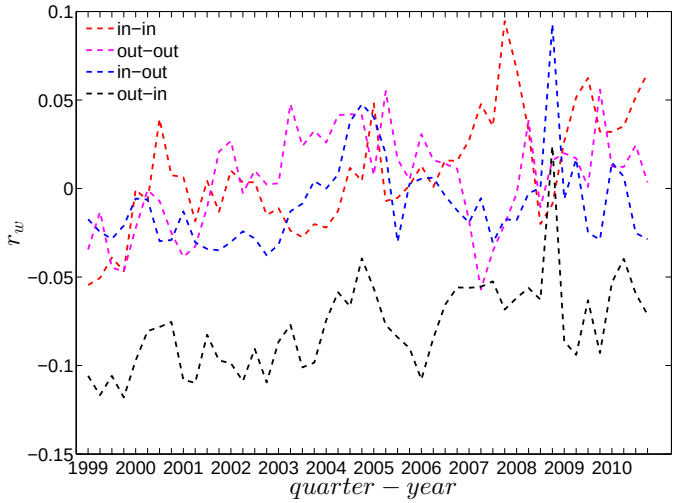

Figure 4.31: Evolution of the directed weighted assortativity indicators, i.e. r_w^{in-in}, r_w^{in-out}, r_w^{out-in}, and $r_w^{out-out}$ in the directed weighted e-MID network.

Second, the local weighted clustering coefficients for the four clustering types C_w^{cyc}, C_w^{mid}, C_w^{in}, C_w^{out} are plotted against the associated strengths in Figures (4.32) and (4.33) [6]. We observe that, generally, higher (lower) strengths correspond to higher (lower) local weighted clustering coefficients.

The evolution of the averages of the local weighted clustering coefficients also exhibits three different phases, i.e. before 2002, from 2002 to 2006, and from 2007 onward. For all types of clustering, the averages in the period from 2002 to 2006 are higher than those in the other two periods. Recall that, on average, larger values of $\bar{C}_w^{mid}$, $\bar{C}_w^{in}$ imply higher systemic risk, while larger values of $\bar{C}_w^{out}$ reveal the high exposure of the associated bank to risk. The order and magnitude of different combinations of $\bar{C}_w$ shown in Figure (4.34) thus reveal the importance of both types of risk in the period from 2002 to 2006 in the weighted version of the network. It should be emphasized that, even when all weights are normalized by the average weight over the whole network, we still observe a similar trend, signaling that the evolution of the averages of the directed local weighted clustering coefficients is not only driven by changes in the overall transaction volume (overall strength of the interactions) but also by changes in the frequency of aforementioned tripartite relations among banks.

[6] In the cases of C_w^{cyc} and C_w^{mid}, we plot them against $s^{in-out} = \sqrt{s^{in} s^{out}}$.

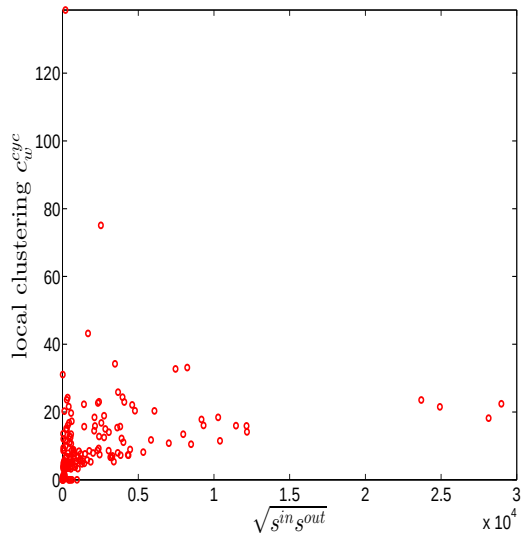

(a) C_w^{cyc} in Q1

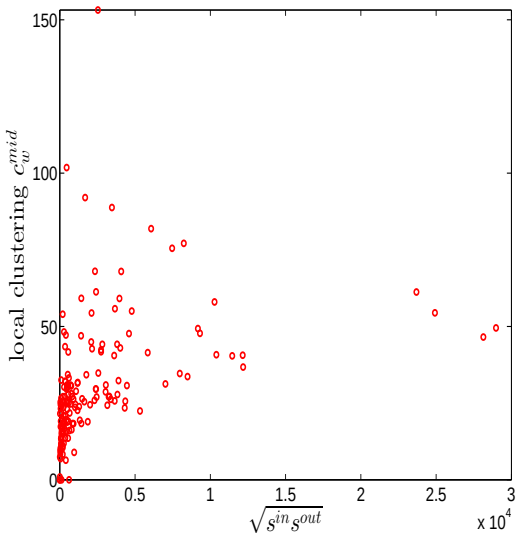

(b) C_w^{mid} in Q1

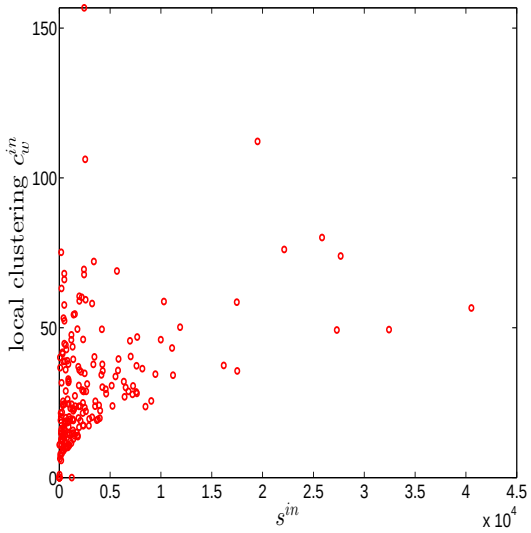

(c) C_w^{in} in Q1

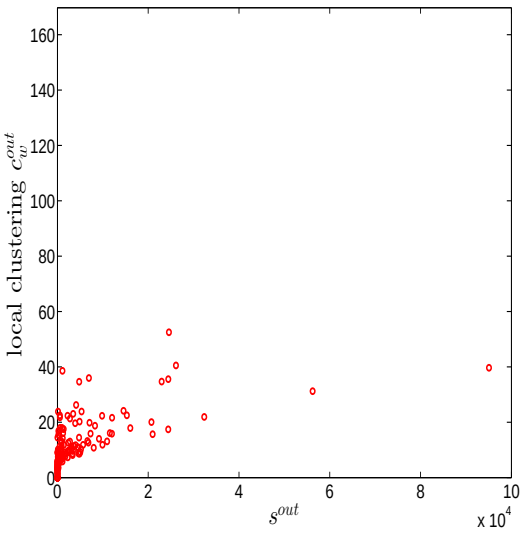

(d) C_w^{out} in Q1

Figure 4.32: Local weighted clustering coefficients in the directed weighted e-MID network, in Q1. C_w^{cyc} (panel a), C_w^{mid} (panel b), C_w^{in} (panel c), C_w^{out} (panel d).

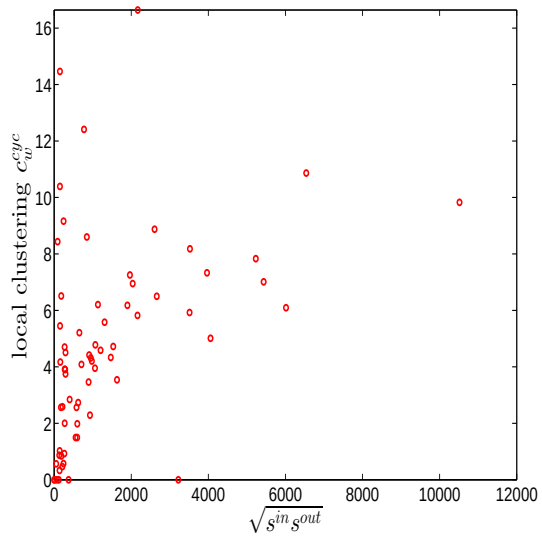

(a) C_w^{cyc} in Q48

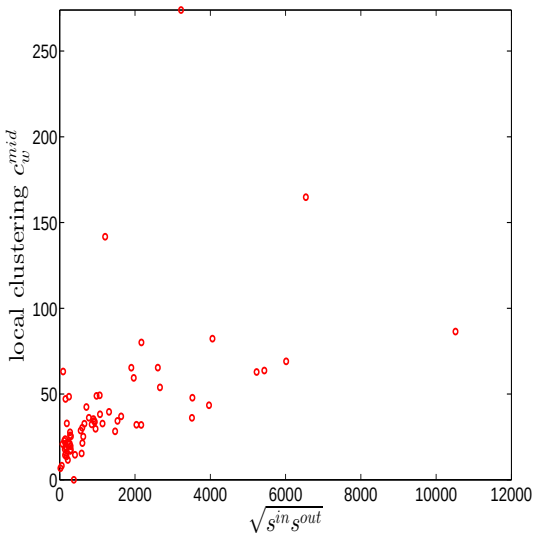

(b) C_w^{mid} in Q48

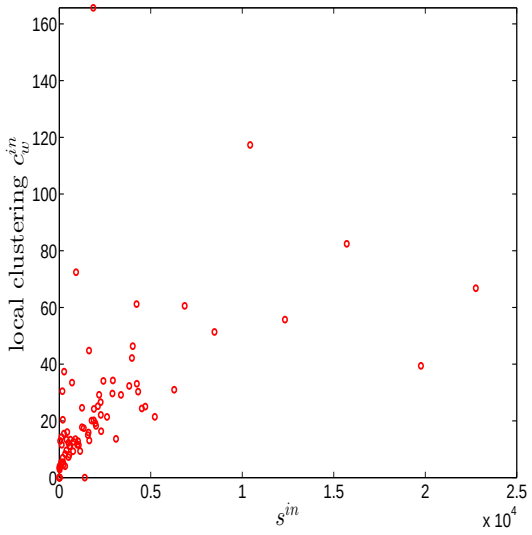

(c) C_w^{in} in Q48

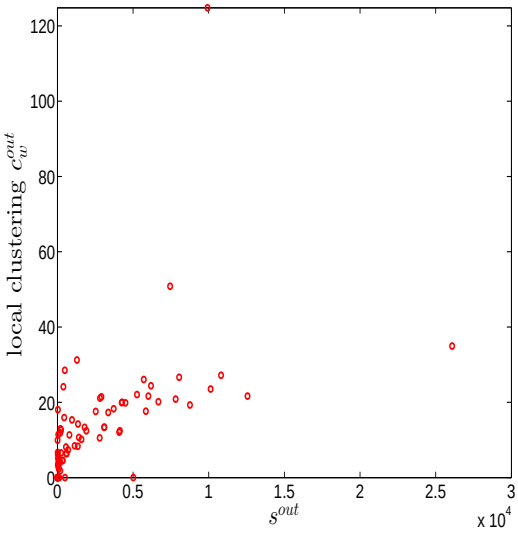

(d) C_w^{out} in Q48

Figure 4.33: Local weighted clustering coefficients in the directed weighted e-MID network, in Q48. C_w^{cyc} (panel a), C_w^{mid} (panel b), C_w^{in} (panel c), C_w^{out} (panel d).

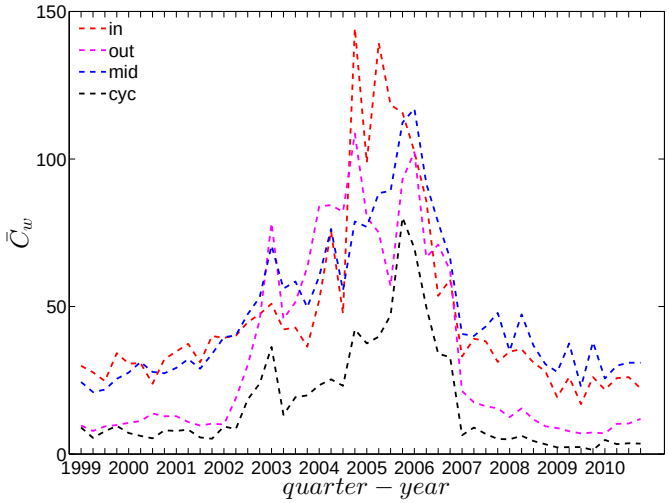

Figure 4.34: Evolution of the averages of local weighted clustering coefficients, i.e. $\bar{C}_w^{cyc}$, $\bar{C}_w^{mid}$, $\bar{C}_w^{in}$, and $\bar{C}_w^{out}$ in the directed weighted e-MID network.

4.4.3 Comparisons to the weighted configuration models

Undirected Weighted Network

To examine the role of the heterogeneity in the local constraints for the emergence of higher order structural correlations in the weighted version of the observed network, we employ the UWCM, which preserves the observed strength sequence, and the UECM, which enforces both the observed degree as well as strength sequences on to the randomized ensemble.

First, the observed values of the measure ANNS as well as of the local weighted clustering coefficients (as can be seen in Figures (4.35) and (4.36)) strongly deviate from their respective expectations under the UWCM. In contrast, we find that the UECM model is able to reproduce the main features of such measures (see Figures (4.37) and (4.38)).

For a more detailed comparison between the two models, we compare the z-scores of the measure ANNS as well as of the local weighted clustering coefficients evaluated under the UWCM with those for the same measures evaluated under the UECM (see subsection B of the Appendix for a more detailed explanation). More specifically, for every bank i, we define the z-scores

$$z_{\mathrm{ANNS}}^{\mathrm{UWCM}}(i) = \frac{\mathrm{ANNS}(i) - \langle \mathrm{ANNS}(i) \rangle_{\mathrm{UWCM}}}{\sigma[\mathrm{ANNS}(i)]_{\mathrm{UWCM}}}, \tag{4.88}$$

and

$$z_{\mathrm{ANNS}}^{\mathrm{UECM}}(i) = \frac{\mathrm{ANNS}(i) - \langle \mathrm{ANNS}(i) \rangle_{\mathrm{UECM}}}{\sigma[\mathrm{ANNS}(i)]_{\mathrm{UECM}}}, \tag{4.89}$$

where $\mathrm{ANNS}(i)\rangle_{\mathrm{UWCM}}$ and $\mathrm{ANNS}(i)\rangle_{\mathrm{UECM}}$ are respectively the expected values of the measure ANNS for bank i evaluated under the UWCM and the UECM; and $\sigma(\mathrm{ANNS}(i))_{\mathrm{UWCM}}$ and $\sigma(\mathrm{ANNS}(i))_{\mathrm{UECM}}$ are respectively the standard deviations of ANNS(i) evaluated under the UWCM and the UECM [7].

Similarly, the z-scores for the local weighted clustering coefficients for bank i evaluated under the UWCM and the UECM are defined as

$$z_{C_w}^{\mathrm{UWCM}}(i) = \frac{C_w^{un}(i) - \langle C_w^{un}(i) \rangle_{\mathrm{UWCM}}}{\sigma[C_w^{un}(i)]_{\mathrm{UWCM}}}, \tag{4.90}$$

and

$$z_{C_w}^{\mathrm{UECM}}(i) = \frac{C_w^{un}(i) - \langle C_w^{un}(i) \rangle_{\mathrm{UECM}}}{\sigma[C_w^{un}(i)]_{\mathrm{UECM}}}. \tag{4.91}$$

We show the comparisons between the z-scores under the two considered configuration

[7] Throughout this paper, the notation $\langle \mathrm{X} \rangle_{\text{null model}}$ and $\sigma[\mathrm{X}]_{\text{null model}}$ are respectively the expected value and standard deviation of X evaluated under the referenced null model.

models in Figure (4.39) and Figure (4.40). For almost all banks, we find that $|z^{\text{UECM}}_{\text{ANNS}}| < |z^{\text{UWCM}}_{\text{ANNS}}|$ and $|z^{\text{UECM}}_{C^{un}_w}| < |z^{\text{UWCM}}_{C^{un}_w}|$.

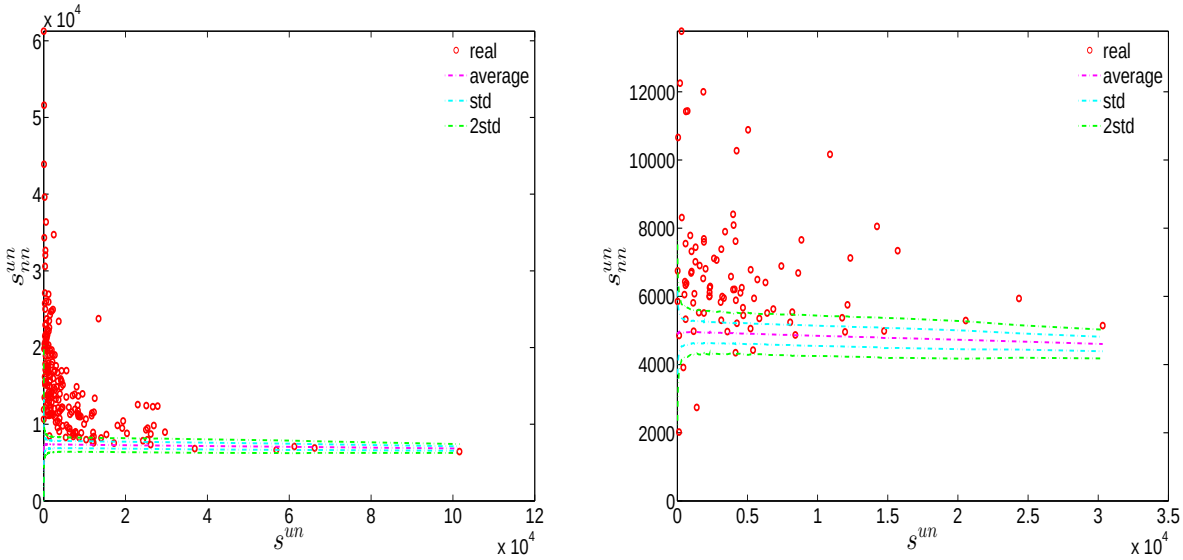

(a) s^{un}_{nn} in Q1 (b) s^{un}_{nn} in Q48

Figure 4.35: ANNS in the observed e-MID network and in the UWCM, in Q1 and Q48.

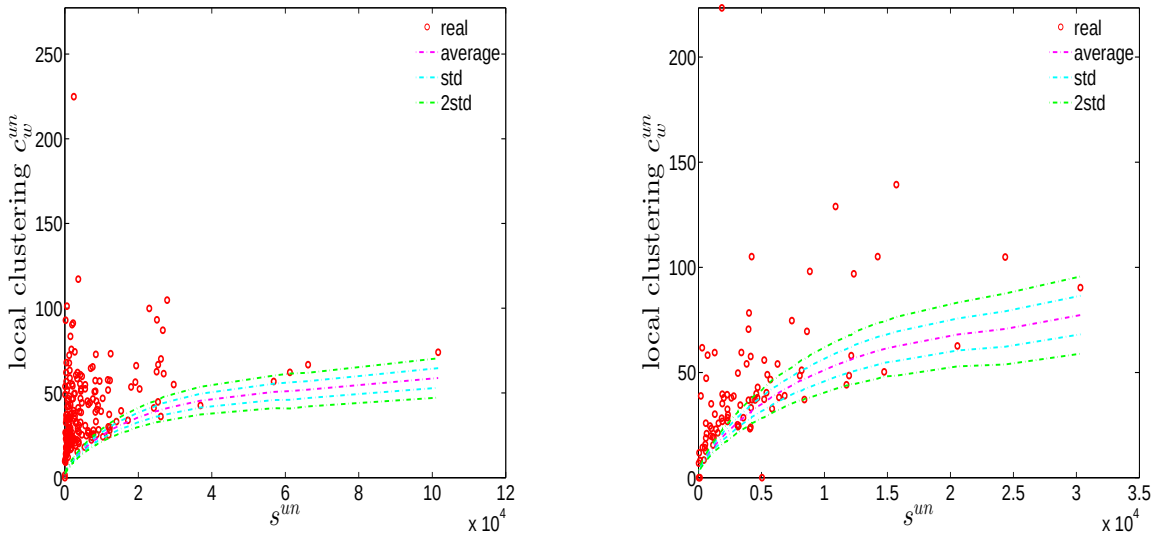

(a) C^{un}_w in Q1 (b) C^{un}_w in Q48

Figure 4.36: Local weighted clustering coefficients C^{un}_w in the observed e-MID network and in the UWCM, in Q1 and Q48.

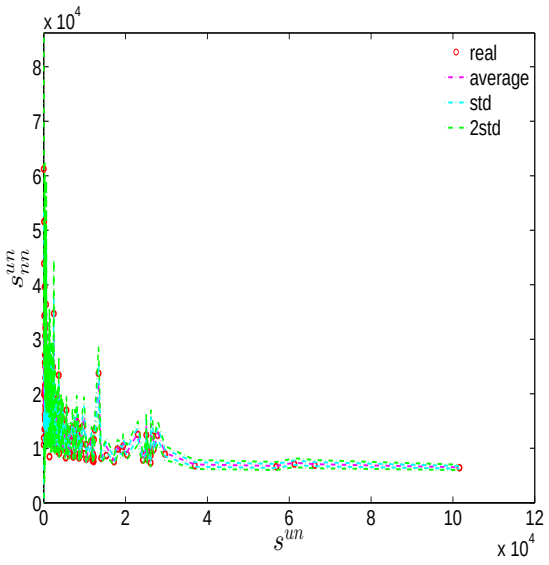

(a) s_{nn}^{un} in Q1

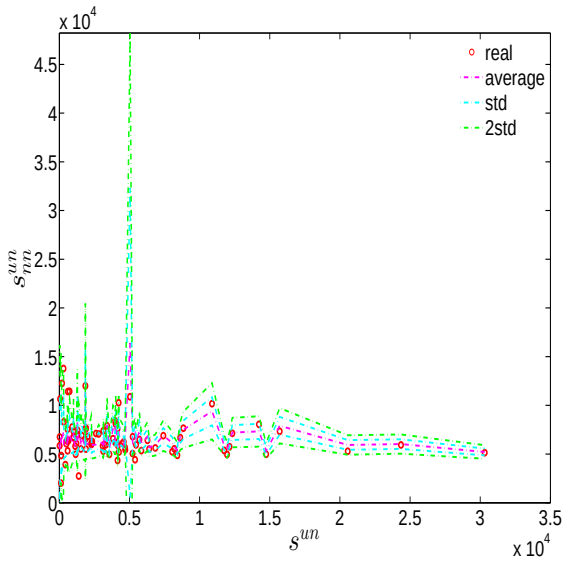

(b) s_{nn}^{un} in Q48

Figure 4.37: ANNS in the observed e-MID network and in the UECM, in Q1 and Q48.

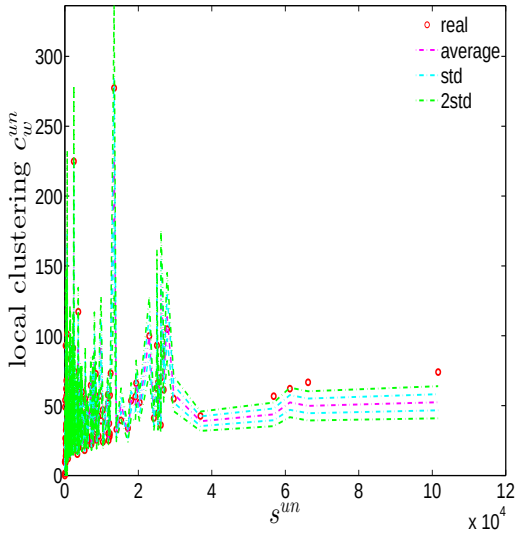

(a) C_w^{un} in Q1

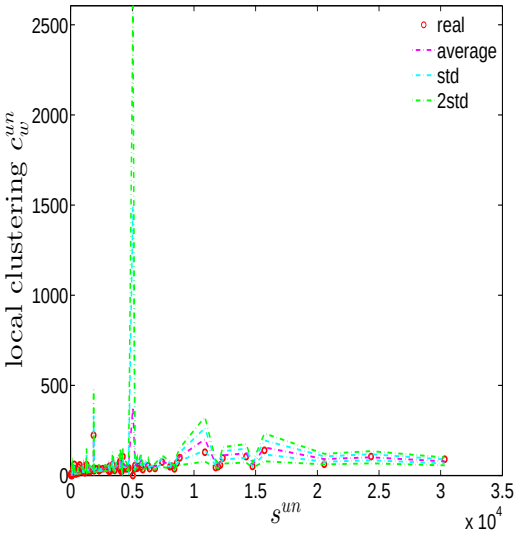

(b) C_w^{un} in Q48

Figure 4.38: Local weighted clustering coefficients C_w^{un} in the observed e-MID network and in the UECM, in Q1 and Q48.

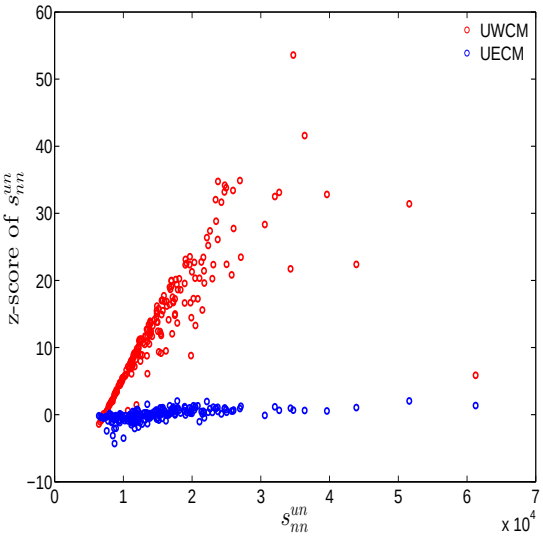

(a) z-scores of s_{nn}^{un} in Q1

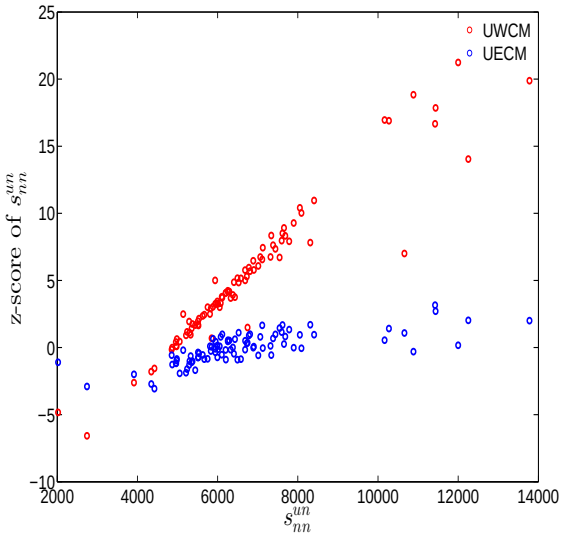

(b) z-scores of s_{nn}^{un} in Q48

Figure 4.39: z-scores of s_{nn}^{un} vs. s_{nn}^{un} in the UWCM and the UECM, in Q1 and in Q48. Panel (a) for z-scores of s_{nn}^{un} in Q1, panel (b) for z-scores of s_{nn}^{un} in Q48.

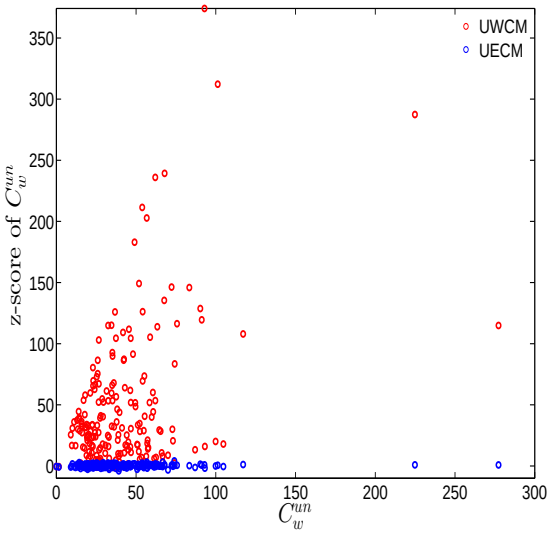

(a) z-scores of C_w^{un} in Q1

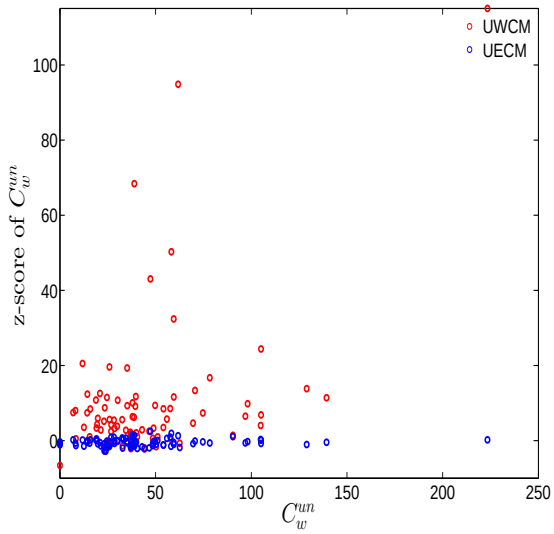

(b) z-scores of C_w^{un} in Q48

Figure 4.40: z-scores of C_w^{un} vs. C_w^{un} in the UWCM and the UECM. Panel (a) for z-scores of C_w^{un} in Q1, panel (b) for z-scores of C_w^{un} in Q48.

We now compare the evolution of $\bar{s}_{nn}^{un}$, r_w^{un}, and $\bar{C}_w^{un}$ for the observed network with the one obtained for these measures under the UWCM and the UECM. In Figure (4.41), we see that for most of the time, the observed values of $\bar{s}_{nn}^{un}$, r_w^{un}, and $\bar{C}_w^{un}$ lie outside the $\pm$ 2 bands associated with the UWCM. In contrast, in Figure (4.42), we see that the evolution

of these measures is well captured by the ECM. The observed values of $\bar{s}_{nn}^{un}$ and $\bar{C}_{w}^{un}$ and the expected ones obtained from the ECM are in very close agreement. Even in the case of r_{w}^{un}, for which several significant deviations are found, the main features of its evolution are well reproduced by the ECM.

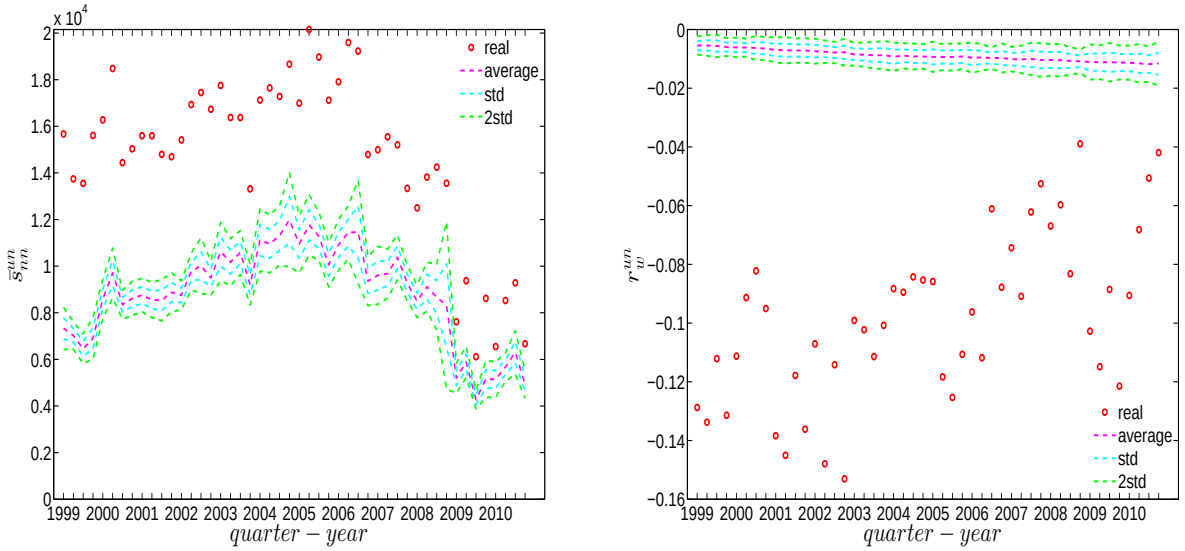

(a) $\bar{s}_{nn}^{un}$

(b) r_{w}^{un}

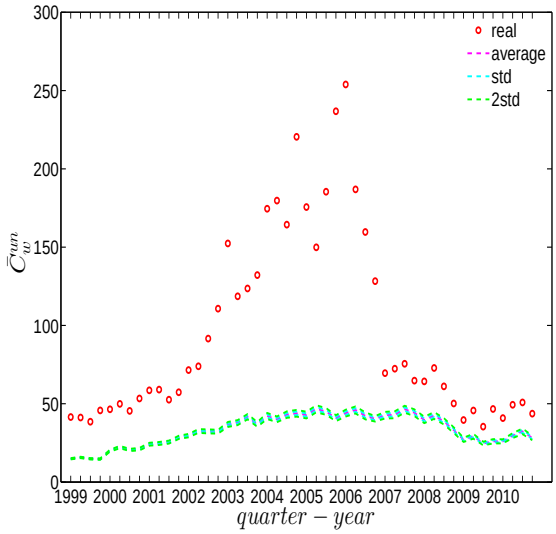

(c) $\bar{C}_{w}^{un}$

Figure 4.41: Evolution of $\bar{s}_{nn}^{un}$ (panel a), r_{w}^{un} (panel b), and $\bar{C}_{w}^{un}$ (panel c) in the observed e-MID network and in the UWCM.

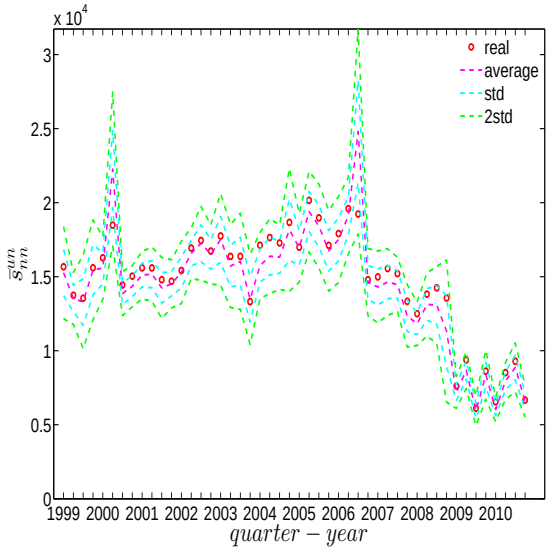

(a) $\bar{s}_{nn}^{un}$

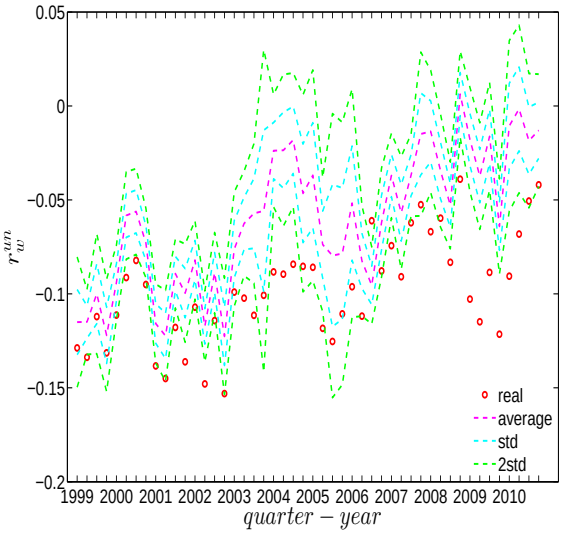

(b) r_w^{un}

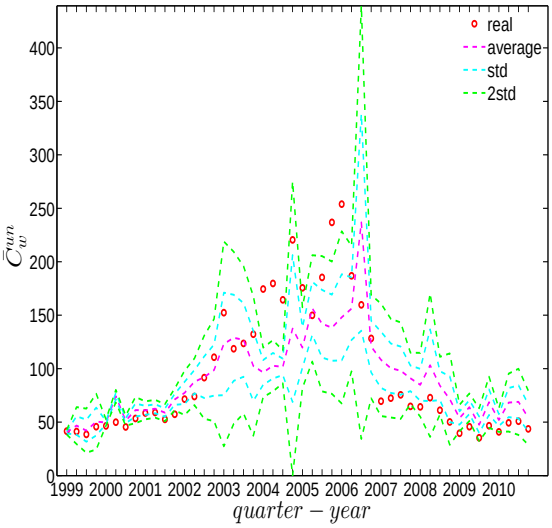

(c) $\bar{C}_w^{un}$

Figure 4.42: Evolution of $\bar{s}_{nn}^{un}$ (panel a), r_w^{un} (panel b), and $\bar{C}_w^{un}$ (panel c) in the observed e-MID network and in the UECM.

Directed Weighted Network

We now extend our comparison between the observed network and the configuration models to the directed weighted version. For this purpose, two null models are employed, i.e. the DWCM and the DECM.

First, regarding the directed versions of the measure ANNS, we compare s_{nn}^{in-in}, s_{nn}^{in-out}, s_{nn}^{out-in}, and $s_{nn}^{out-out}$ of the observed network in the two chosen quarters with those obtained from the DWCM in Figures (4.43) and (4.44), and with those obtained from the DECM

in Figures (4.45) and (4.46). Similar to the undirected weighted case, the z-scores of the directed weighted versions of the measure ANNS evaluated under these two models are also reported in Figures (4.47) and (4.48). Overall, we see that the main features of the measure ANNS are replicated much better by the DECM than by the DWCM. Furthermore, typically for almost all banks, we find that $|z_{\mathrm{ANNS}}^{\mathrm{DECM}}| < |z_{\mathrm{ANNS}}^{\mathrm{DWCM}}|$.

In terms of the third order structural correlations, the DECM again outperforms the DWCM in terms of reproducing the main features of local weighted clustering coefficients. This is visualized in Figures (4.49), (4.50), (4.51), and (4.52). In addition, for each type of local weighted clustering coefficients we also calculate the z-scores evaluated under the DWCM and the DECM. As shown in Figures (4.53) and (4.54), we typically observe that $|z_{C_w^{cyc}}^{\mathrm{DECM}}| < |z_{C_w^{cyc}}^{\mathrm{DWCM}}|$, $|z_{C_w^{mid}}^{\mathrm{DECM}}| < |z_{C_w^{mid}}^{\mathrm{DWCM}}|$, $|z_{C_w^{in}}^{\mathrm{DECM}}| < |z_{C_w^{in}}^{\mathrm{DWCM}}|$, and $|z_{C_w^{out}}^{\mathrm{DECM}}| < |z_{C_w^{out}}^{\mathrm{DWCM}}|$.

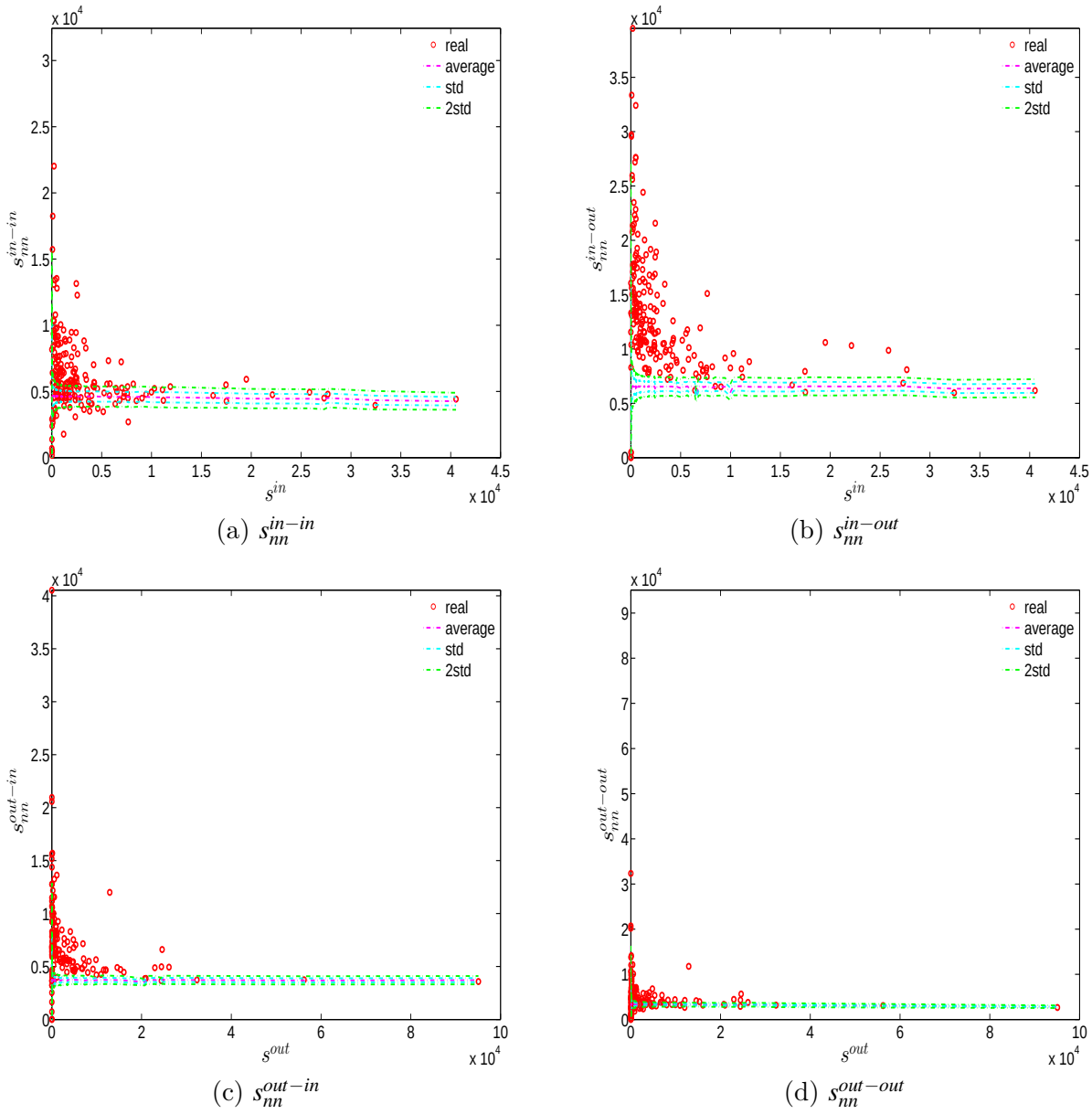

(a) s_{nn}^{in-in} (b) s_{nn}^{in-out}

(c) s_{nn}^{out-in} (d) $s_{nn}^{out-out}$

Figure 4.43: ANNSs in the observed e-MID network and in the DWCM, in Q1. s_{nn}^{in-in} (panel a), s_{nn}^{in-out} (panel b), s_{nn}^{out-in} (panel c), $s_{nn}^{out-out}$ (panel d).

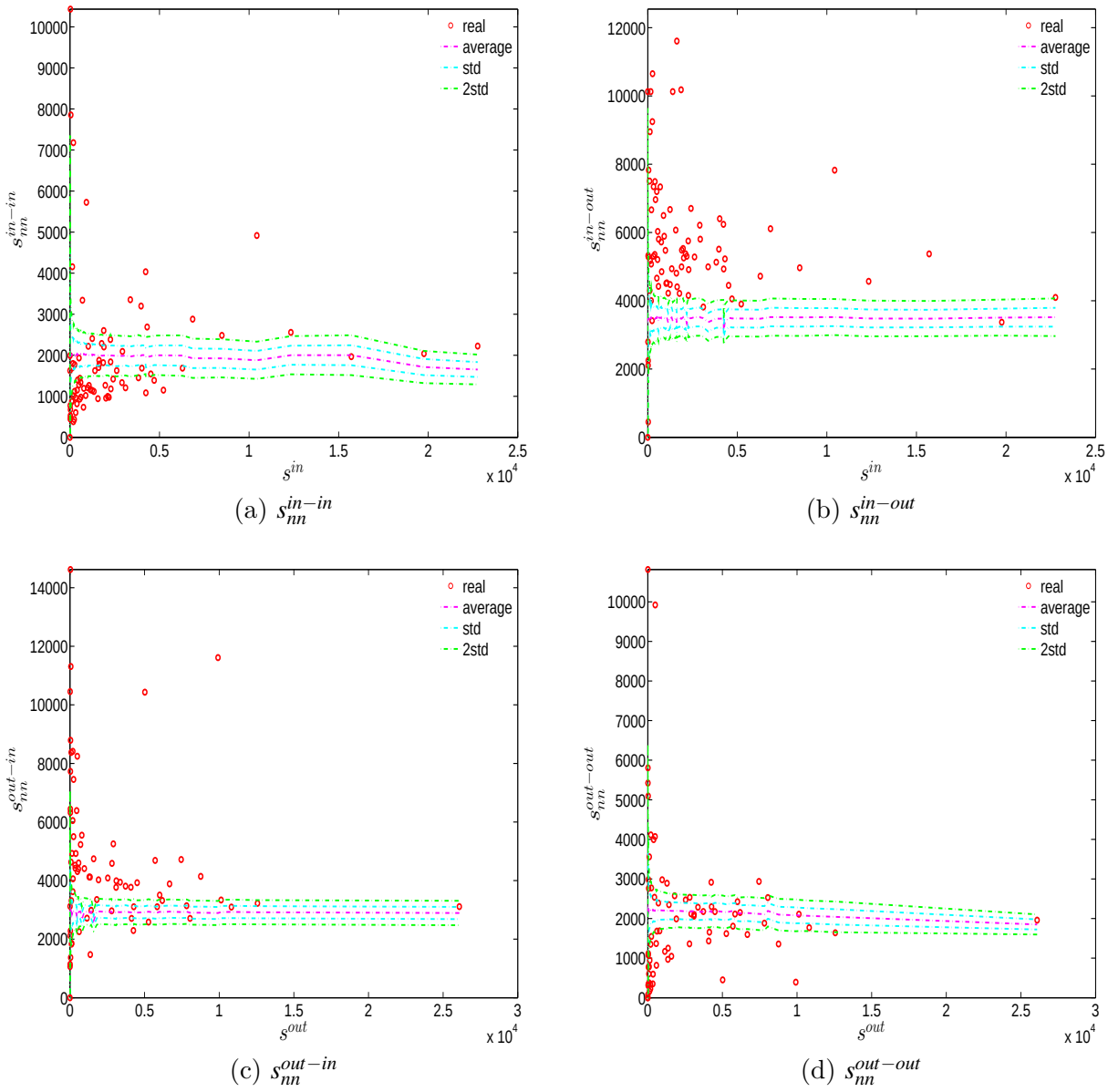

(a) s_{nn}^{in-in} (b) s_{nn}^{in-out}

(c) s_{nn}^{out-in} (d) $s_{nn}^{out-out}$

Figure 4.44: ANNSs in the observed e-MID network and in the DWCM, in Q48. s_{nn}^{in-in} (panel a), s_{nn}^{in-out} (panel b), s_{nn}^{out-in} (panel c), $s_{nn}^{out-out}$ (panel d).

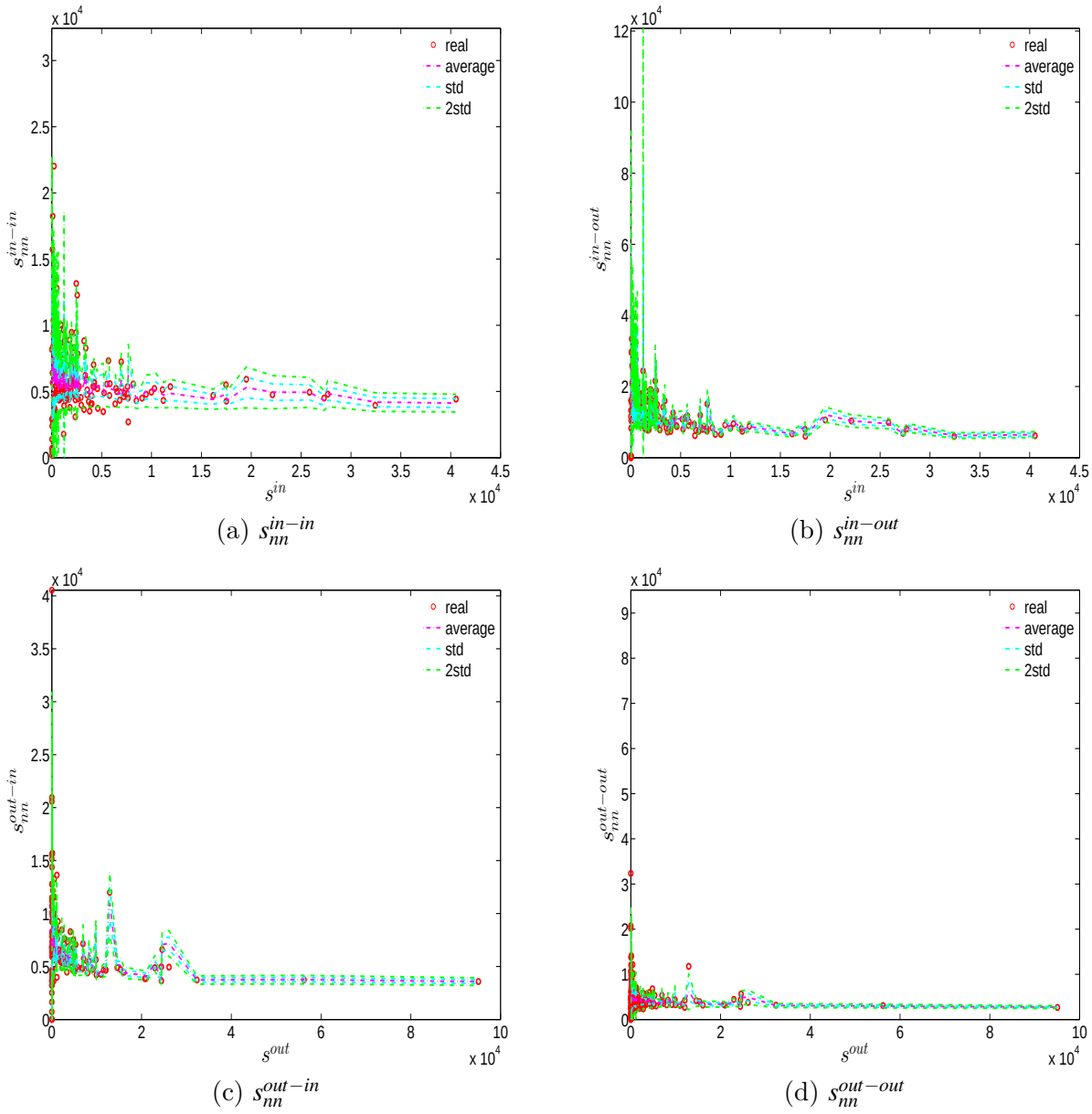

(a) s_{nn}^{in-in} (b) s_{nn}^{in-out}

(c) s_{nn}^{out-in} (d) $s_{nn}^{out-out}$

Figure 4.45: ANNSs in the observed e-MID network and in the DECM, in Q1. s_{nn}^{in-in} (panel a), s_{nn}^{in-out} (panel b), s_{nn}^{out-in} (panel c), $s_{nn}^{out-out}$ (panel d).

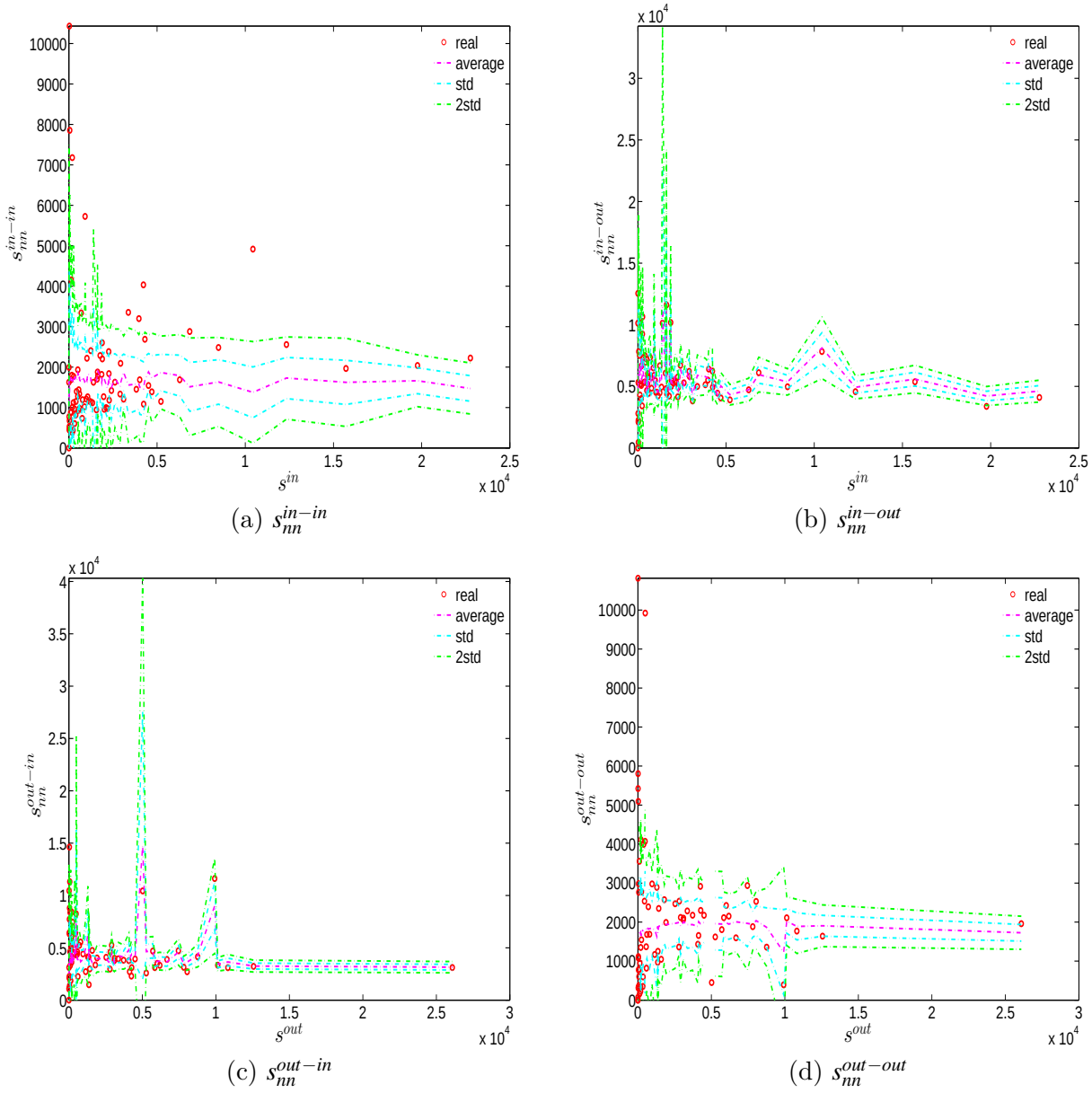

(a) s_{nn}^{in-in} (b) s_{nn}^{in-out}

(c) s_{nn}^{out-in} (d) $s_{nn}^{out-out}$

Figure 4.46: ANNSs in the observed e-MID network and in the DECM, in Q48. s_{nn}^{in-in} (panel a), s_{nn}^{in-out} (panel b), s_{nn}^{out-in} (panel c), $s_{nn}^{out-out}$ (panel d).

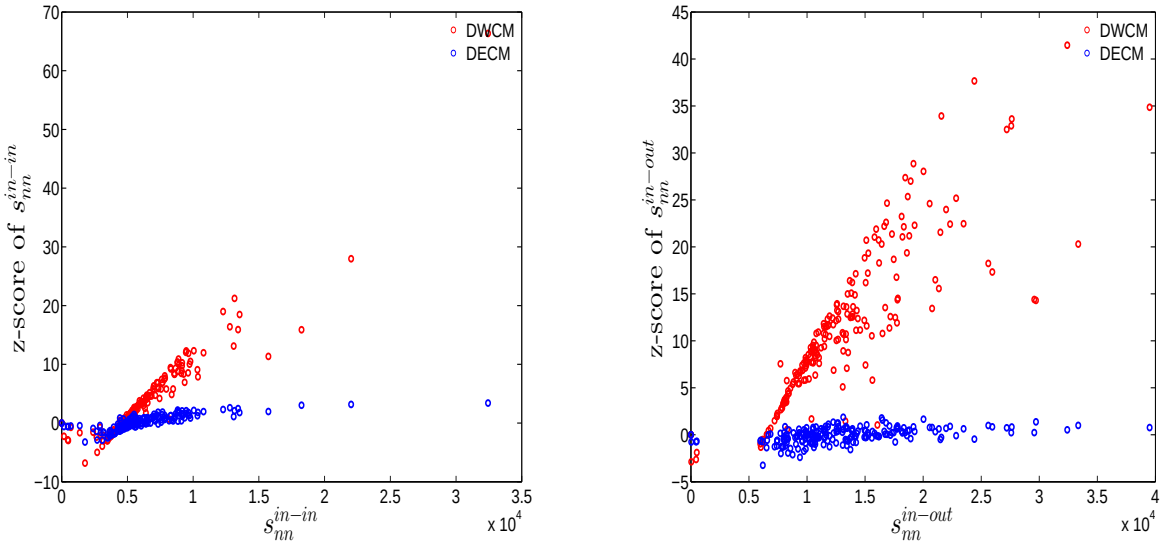

(a) z-scores of s_{nn}^{in-in}

(b) z-scores of s_{nn}^{in-out}

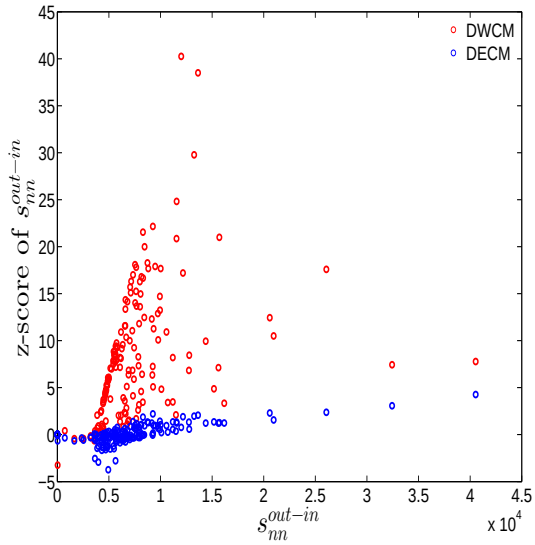

(c) z-scores of s_{nn}^{out-in}

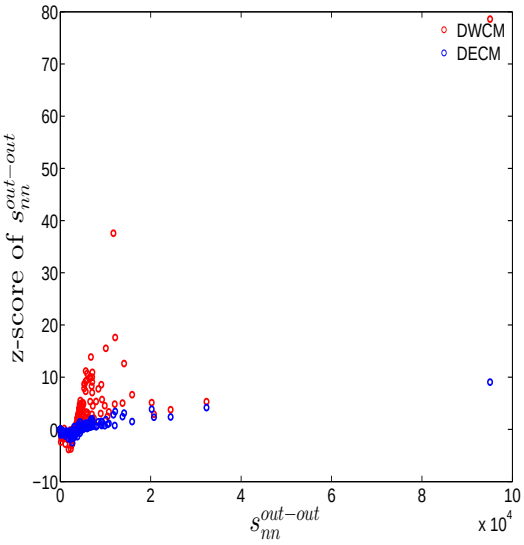

(d) z-scores of $s_{nn}^{out-out}$

Figure 4.47: z-scores of ANNSs vs. ANNSs, in the DWCM and DECM models, in Q1. Panels (a) for s_{nn}^{in-in}, (b) for s_{nn}^{in-out}, (c) for s_{nn}^{out-in}, (d) for $s_{nn}^{out-out}$.

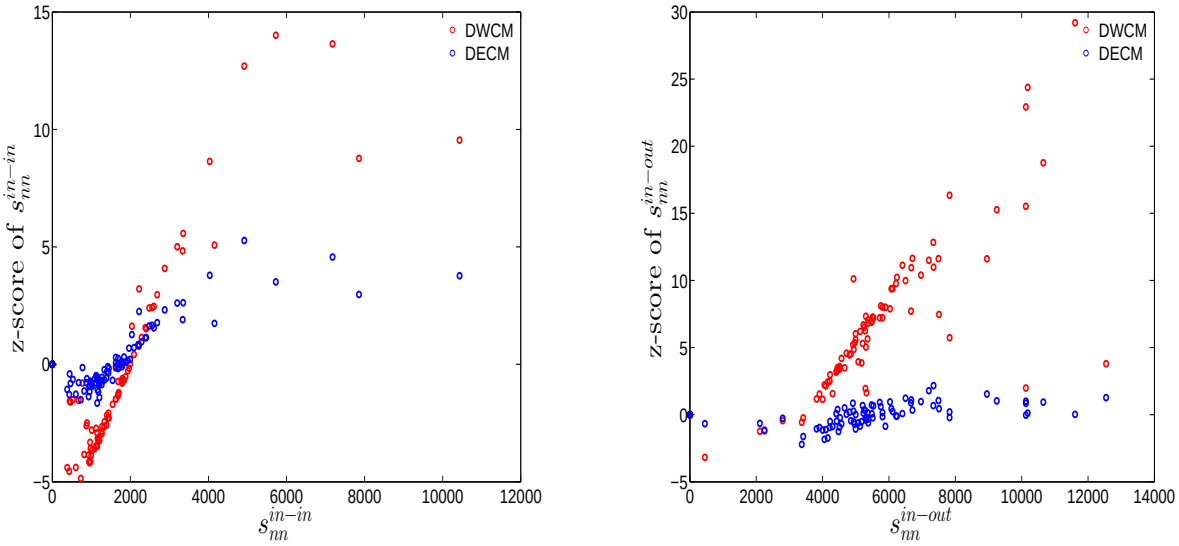

(a) z-scores of s_{nn}^{in-in} (b) z-scores of s_{nn}^{in-out}

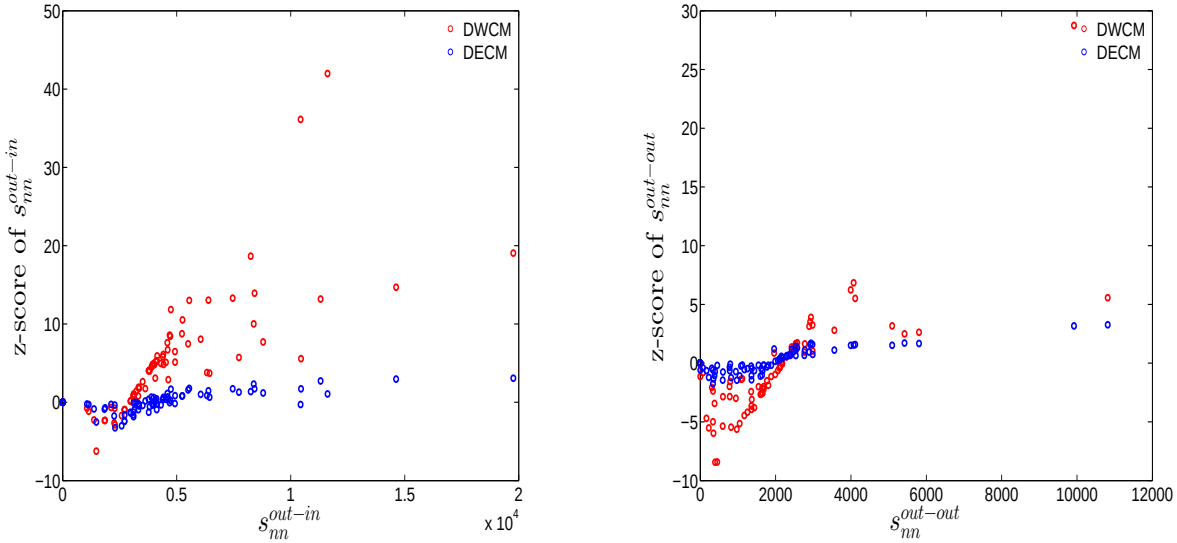

(c) z-scores of s_{nn}^{out-in} (d) z-scores of $s_{nn}^{out-out}$

Figure 4.48: z-scores of ANNSs vs. ANNSs, in the DWCM and DECM models, in Q48. Panels (a) for s_{nn}^{in-in}, (b) for s_{nn}^{in-out}, (c) for s_{nn}^{out-in}, (d) for $s_{nn}^{out-out}$.

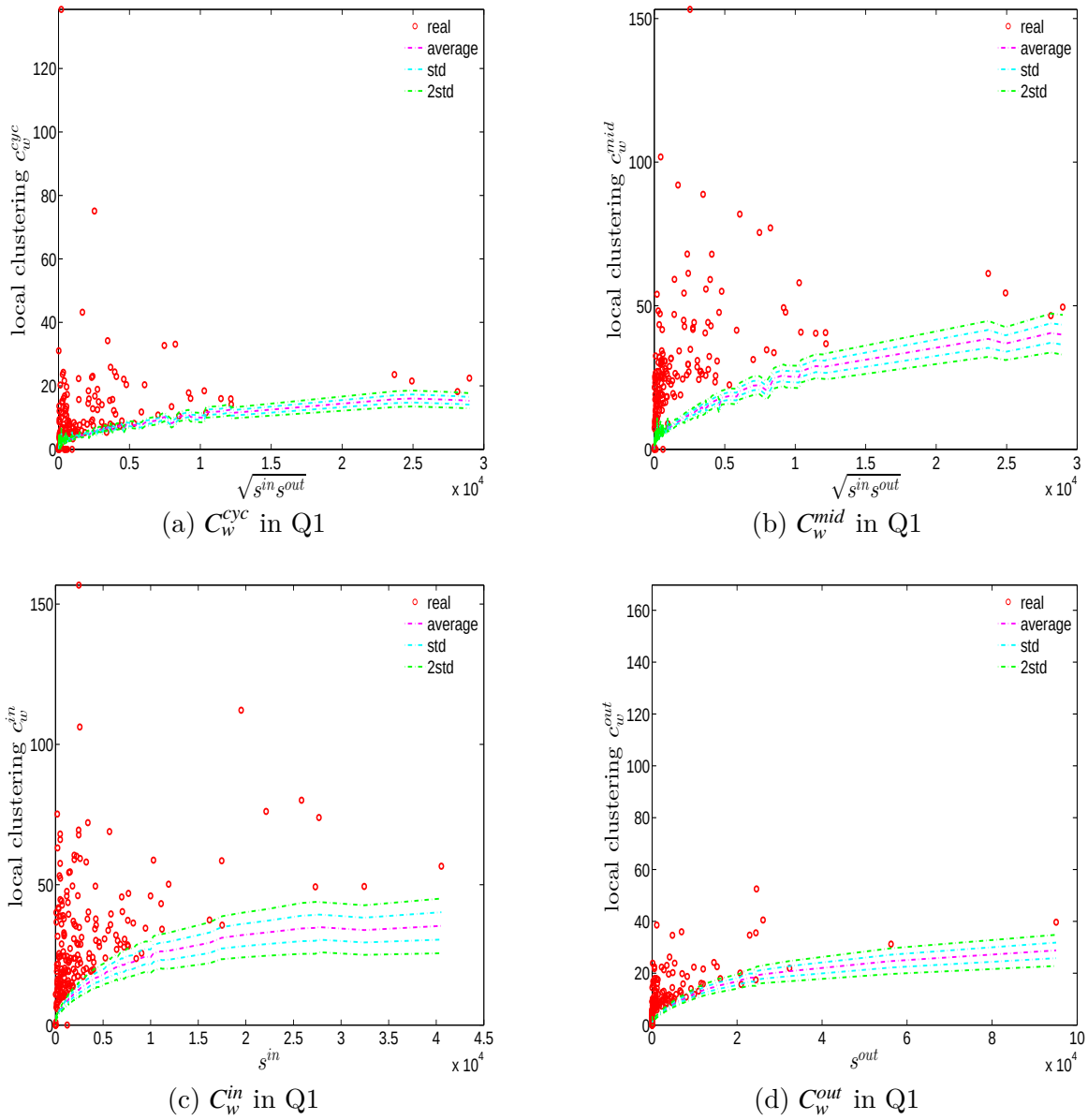

(a) C_w^{cyc} in Q1

(b) C_w^{mid} in Q1

(c) C_w^{in} in Q1

(d) C_w^{out} in Q1

Figure 4.49: Local weighted clustering coefficients in the observed e-MID network and in the DWCM, in Q1. C_w^{cyc} (panel a), C_w^{mid} (panel b), C_w^{in} (panel c), C_w^{out} (panel d).

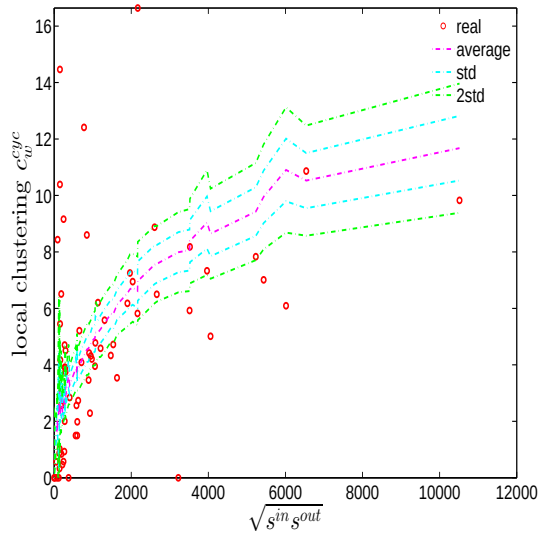

(a) C_w^{cyc} in Q48

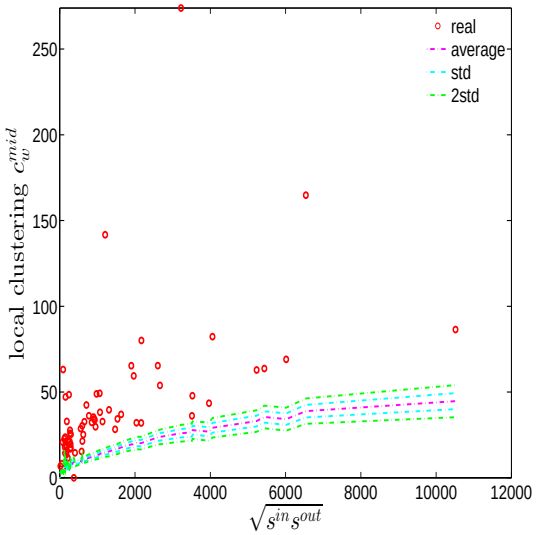

(b) C_w^{mid} in Q48

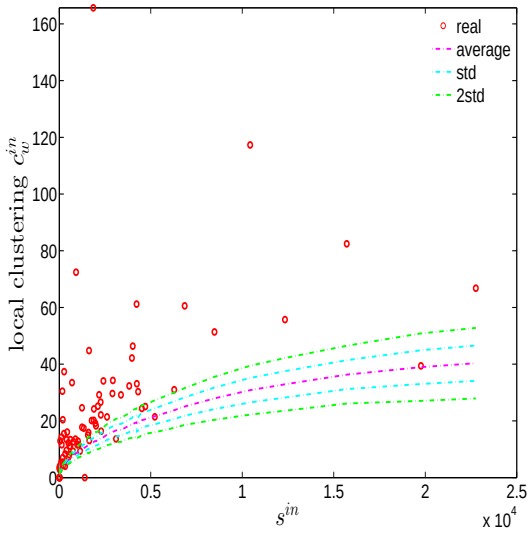

(c) C_w^{in} in Q48

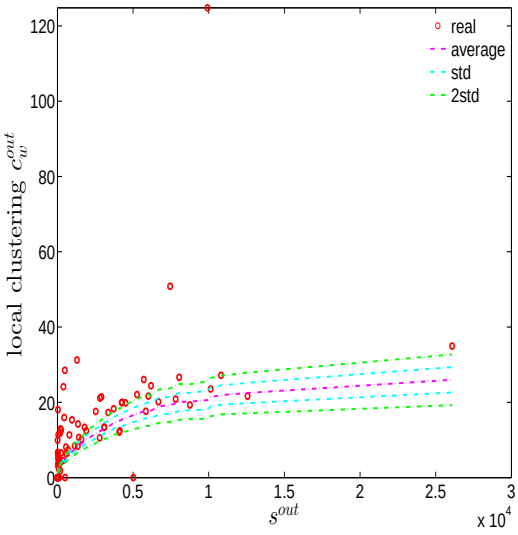

(d) C_w^{out} in Q48

Figure 4.50: Local weighted clustering coefficients in the observed e-MID network and in the DWCM, in Q48. C_w^{cyc} (panel a), C_w^{mid} (panel b), C_w^{in} (panel c), C_w^{out} (panel d).

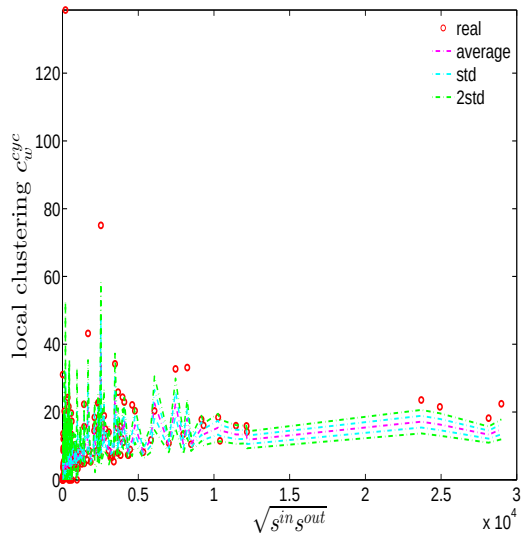

(a) C_w^{cyc} in Q1

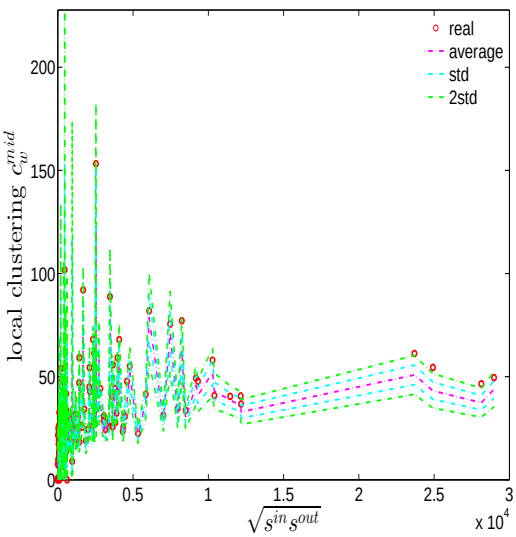

(b) C_w^{mid} in Q1

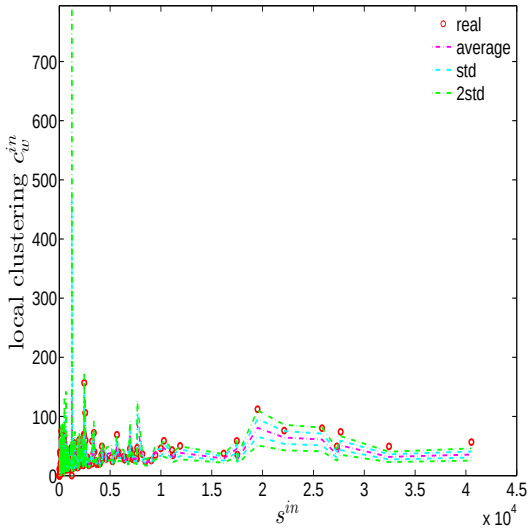

(c) C_w^{in} in Q1

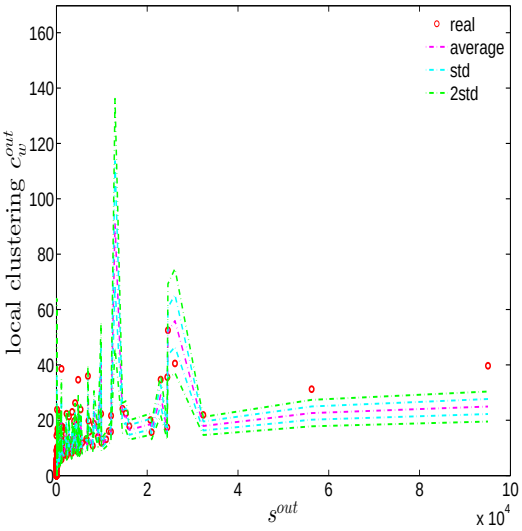

(d) C_w^{out} in Q1

Figure 4.51: Local weighted clustering coefficients in the observed e-MID network and in the DECM, in Q1. C_w^{cyc} (panel a), C_w^{mid} (panel b), C_w^{in} (panel c), C_w^{out} (panel d).

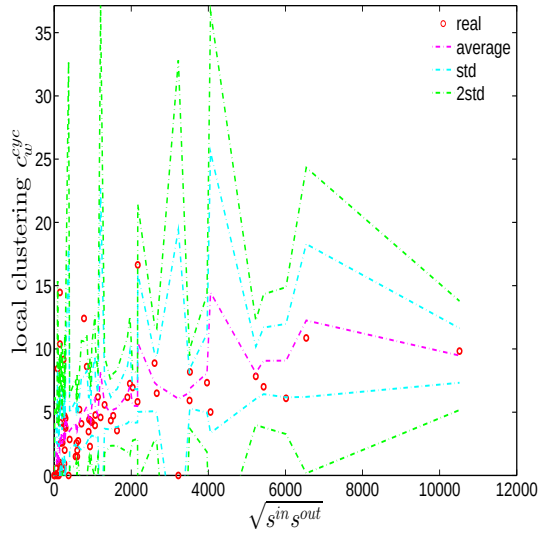

(a) C_w^{cyc} in Q48

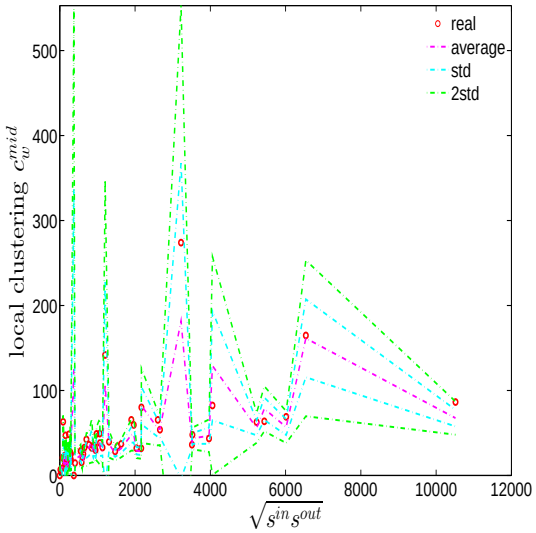

(b) C_w^{mid} in Q48

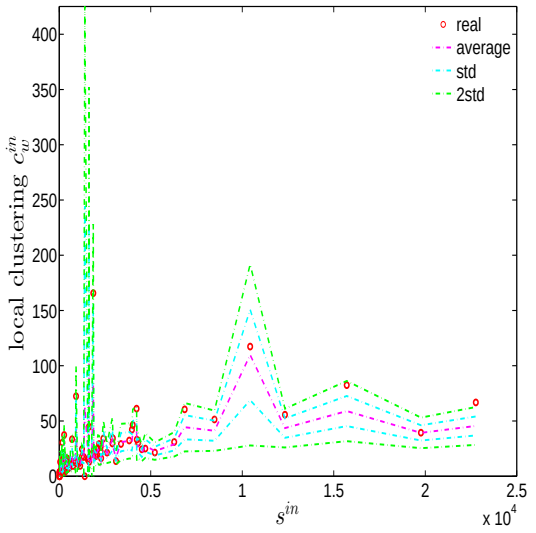

(c) C_w^{in} in Q48

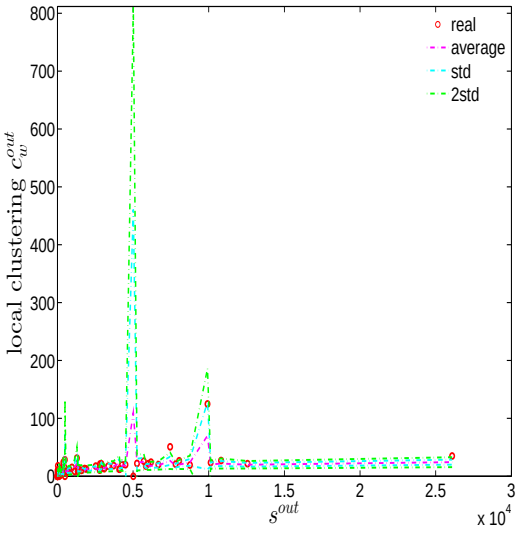

(d) C_w^{out} in Q48

Figure 4.52: Local weighted clustering coefficients in the observed e-MID network and in the DECM, in Q48. C_w^{cyc} (panel a), C_w^{mid} (panel b), C_w^{in} (panel c), C_w^{out} (panel d).

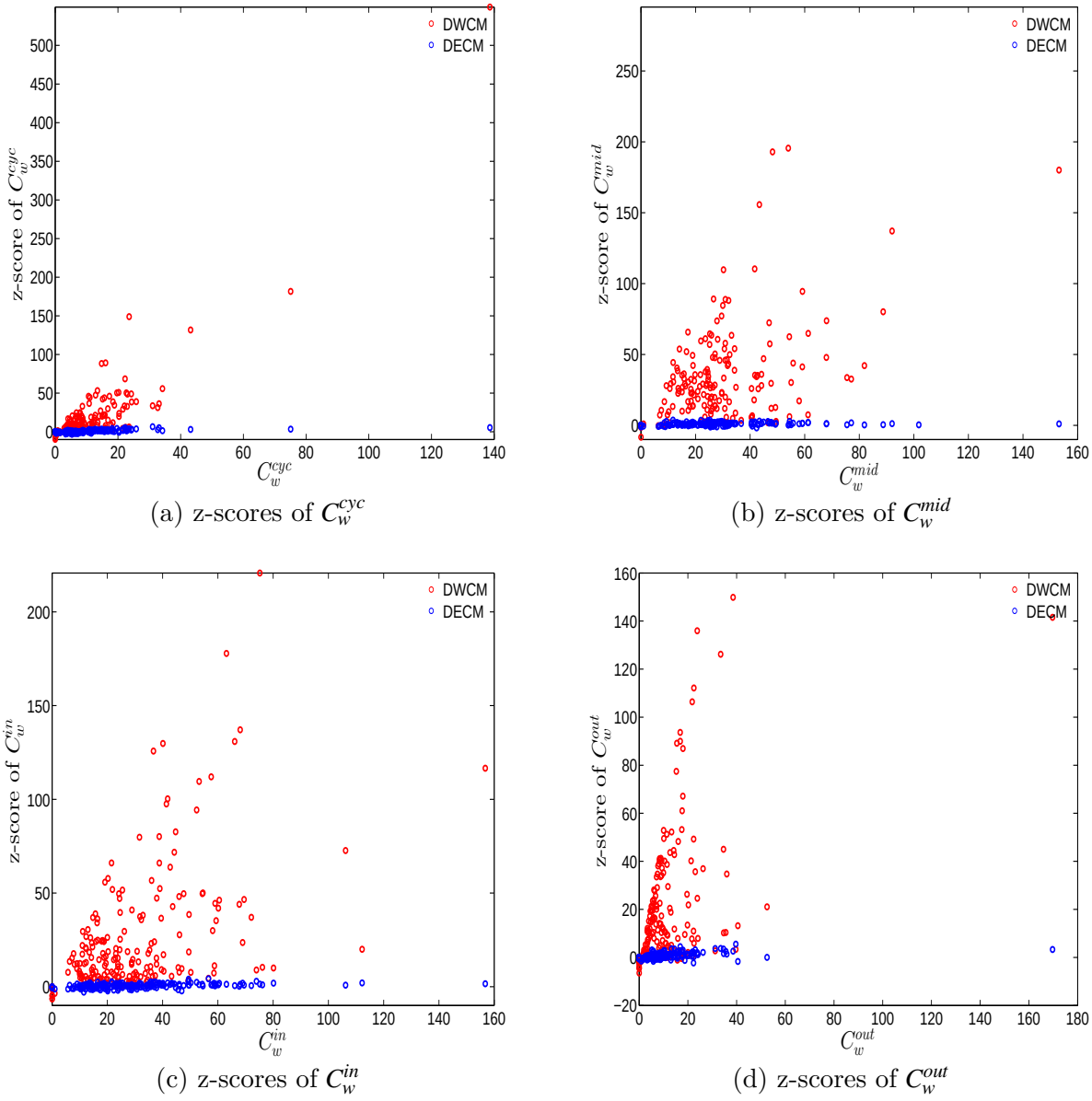

(a) z-scores of C_w^{cyc}

(b) z-scores of C_w^{mid}

(c) z-scores of C_w^{in}

(d) z-scores of C_w^{out}

Figure 4.53: z-scores of C_w vs. C_w, evaluated under the DWCM and DECM models, in Q1. Panel (a) for C_w^{cyc}, panel (b) for C_w^{mid}, panel (c) for C_w^{in}, panel (d) for C_w^{out} .

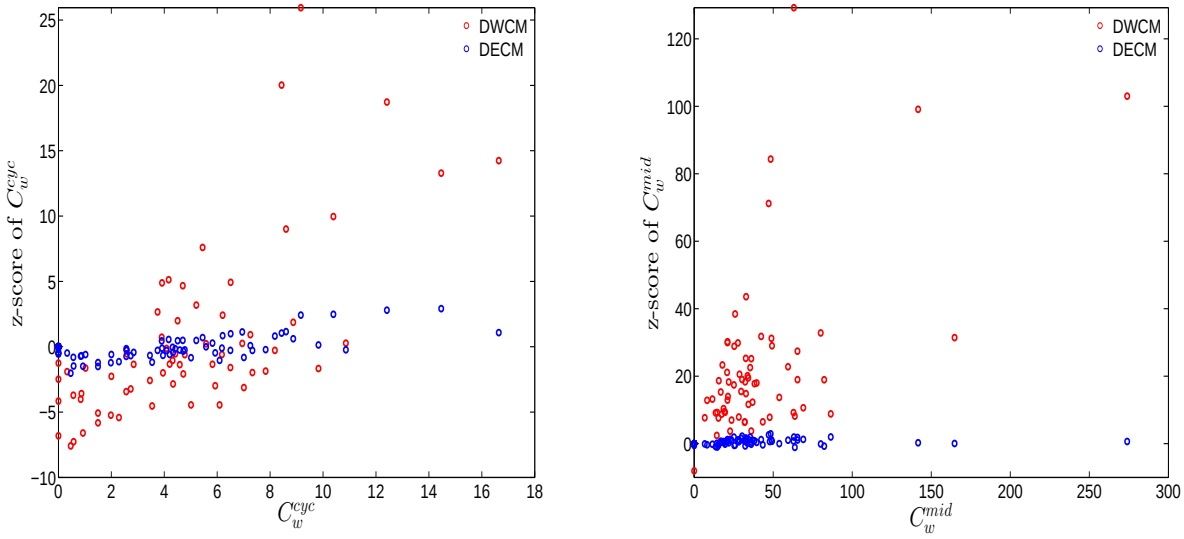

(a) z-scores of C_w^{cyc} (b) z-scores of C_w^{mid}

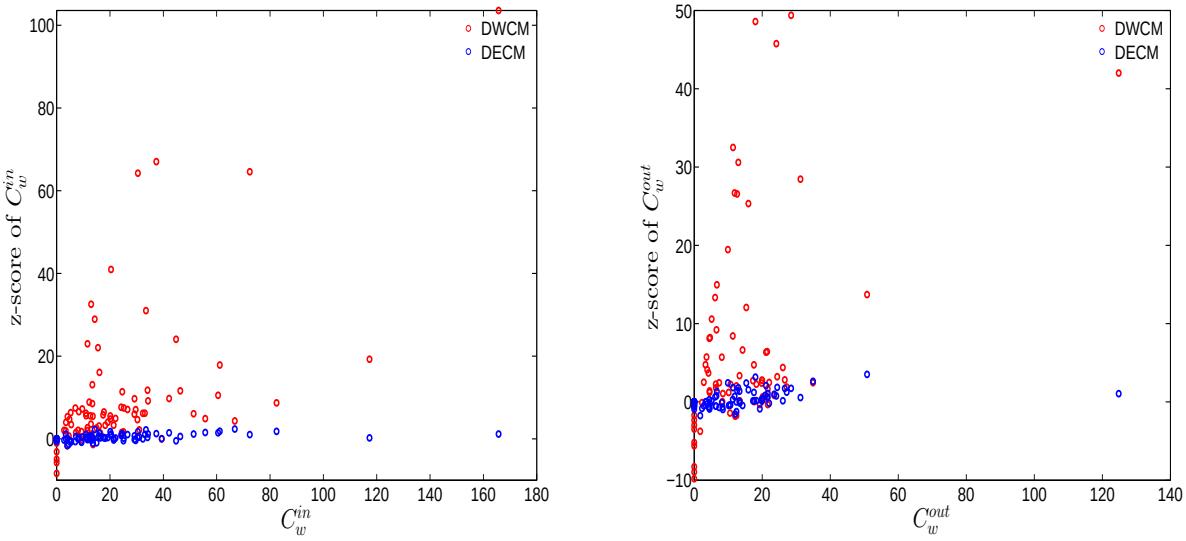

(c) z-scores of C_w^{in} (d) z-scores of C_w^{out}

Figure 4.54: z-scores of C_w vs. C_w, evaluated under the DWCM and DECM models, in Q48. Panel (a) for C_w^{cyc}, panel (b) for C_w^{mid}, panel (c) for C_w^{in}, panel (d) for C_w^{out} .

Finally, we now analyze the predictive power of the two considered null models in terms of the evolution of the averages of the various versions of the measure ANNSs (i.e. $\bar{s}_{nn}^{in-in}$, $\bar{s}_{nn}^{in-out}$, $\bar{s}_{nn}^{out-in}$ and $\bar{s}_{nn}^{out-out}$), the global weighted assortativity indicators (i.e. r_w^{in-in}, r_w^{in-out}, r_w^{out-in} and $r_w^{out-out}$), and the averages of the local weighted clustering coefficients (i.e. $\bar{C}_w^{cyc}$, $\bar{C}_w^{mid}$, $\bar{C}_w^{in}$ and $\bar{C}_w^{out}$) (see also the next subsection section for a further comparison).

Figures (4.55), (4.56), and (4.57) show significant deviations of the observed network from the DWCM over time. A comparison between the DECM and the observed network in terms

of the aforementioned measures is shown in Figures (4.58), (4.59), and (4.60). Overall, we observe that, on the one hand, the DWCM is clearly dominated by the DECM, on the other hand, significant deviations from the DECM are still present in several quarters, regarding such as the average of the measure ANNS in the mixing category out-out ($\bar{s}_{nn}^{out-out}$), the global weighted assortativity indicators in the in-in and in-out categories, the average of the local weighted clustering coefficients $\bar{C}_w^{cyc}$ and the average of the local weighted clustering coefficients $\bar{C}_w^{out}$.

We emphasize that one of the main features not explained by the sequences of degrees and strengths of the network nodes themselves is the high level of clustering in the years preceding the crisis, i.e. the huge increase in various indirect exposures generated via more intensive interbank credit links.

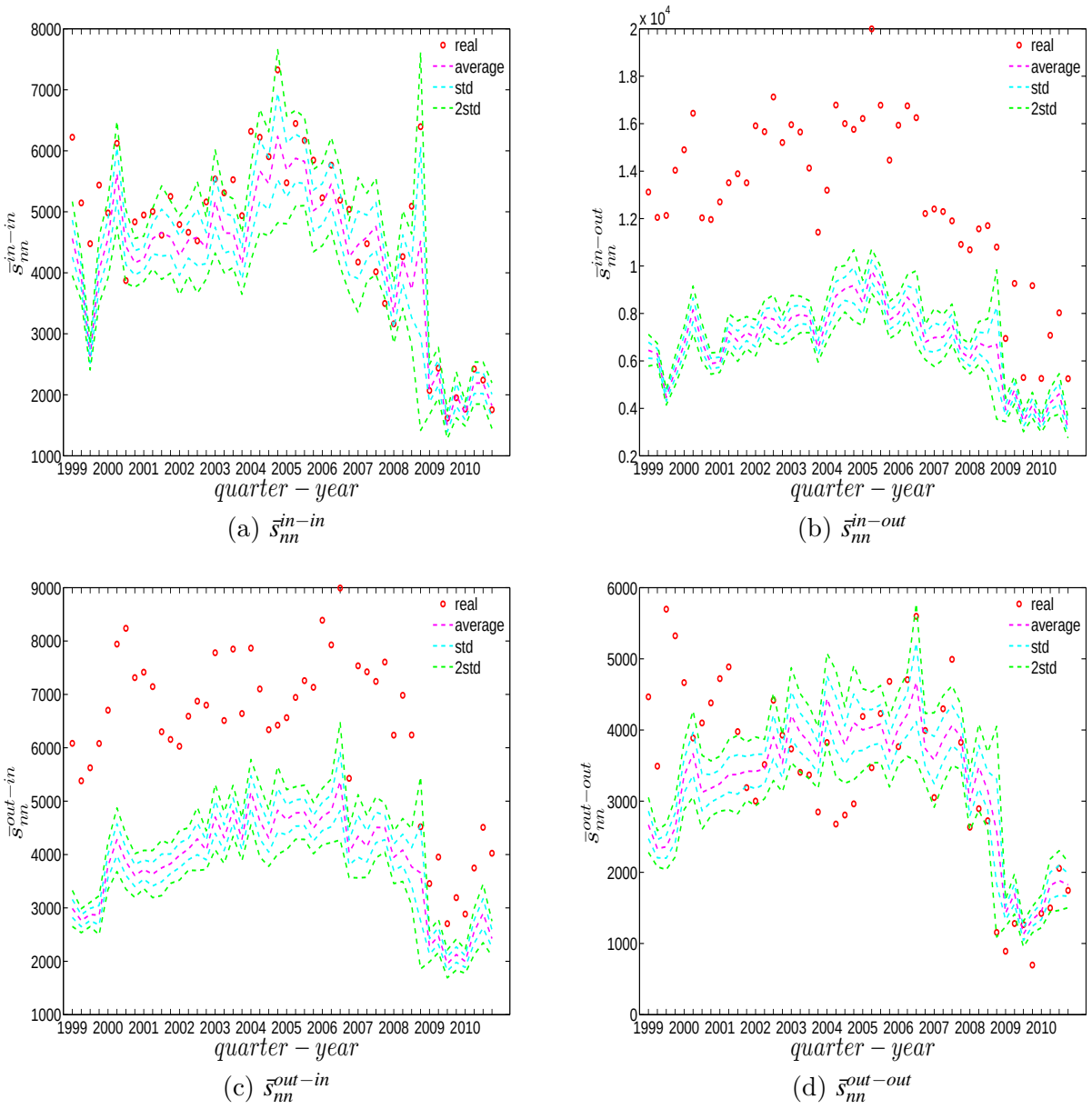

(a) $\bar{s}_{nn}^{in-in}$ (b) $\bar{s}_{nn}^{in-out}$

(c) $\bar{s}_{nn}^{out-in}$ (d) $\bar{s}_{nn}^{out-out}$

Figure 4.55: Evolution of the averages of ANNSs in the observed e-MID network and in the DWCM. $\bar{s}_{nn}^{in-in}$ (panel a), $\bar{s}_{nn}^{in-out}$ (panel b), $\bar{s}_{nn}^{out-in}$ (panel c), $\bar{s}_{nn}^{out-out}$ (panel d).

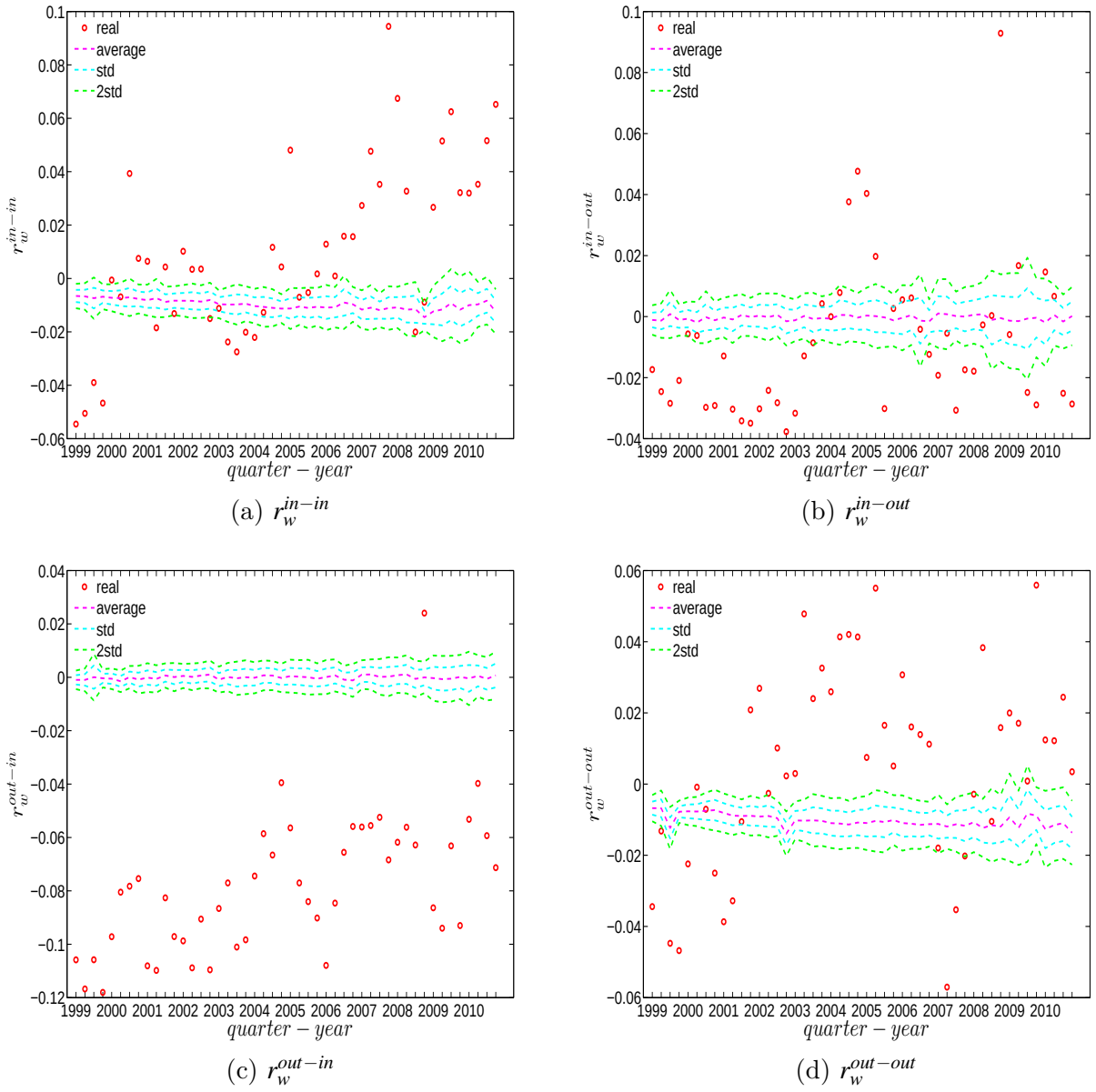

(a) r_w^{in-in} (b) r_w^{in-out}

(c) r_w^{out-in} (d) $r_w^{out-out}$

Figure 4.56: Evolution of the global weighted assortativity indicators in the observed e-MID network and in the DWCM. r_w^{in-in} (panel a), r_w^{in-out} (panel b), r_w^{out-in} (panel c), $r_w^{out-out}$ (panel d).

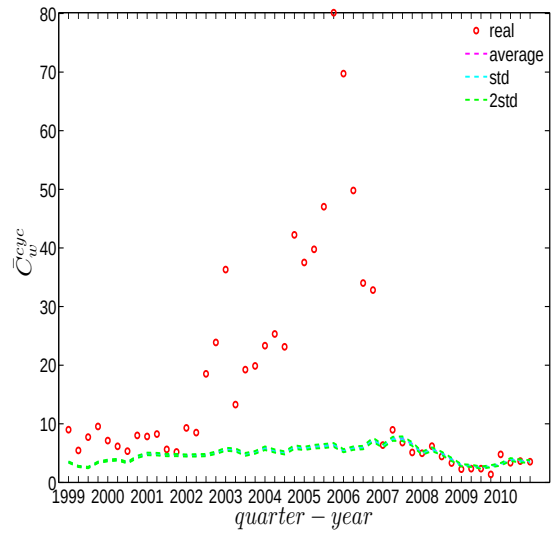

(a) $\bar{C}_w^{cyc}$

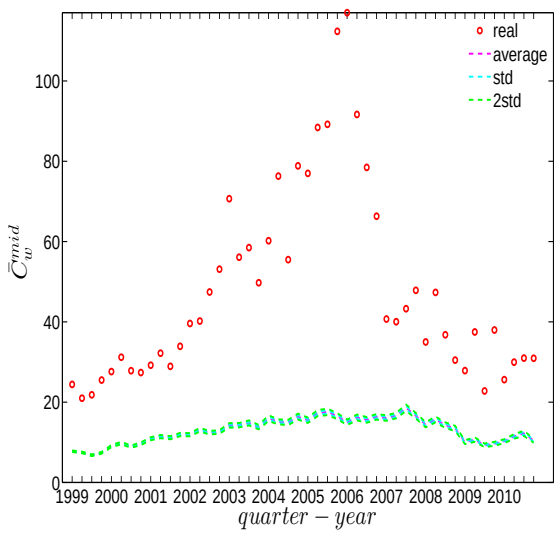

(b) $\bar{C}_w^{mid}$

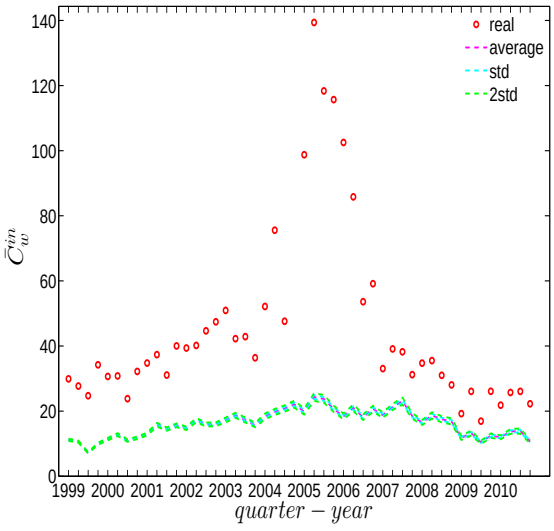

(c) $\bar{C}_w^{in}$

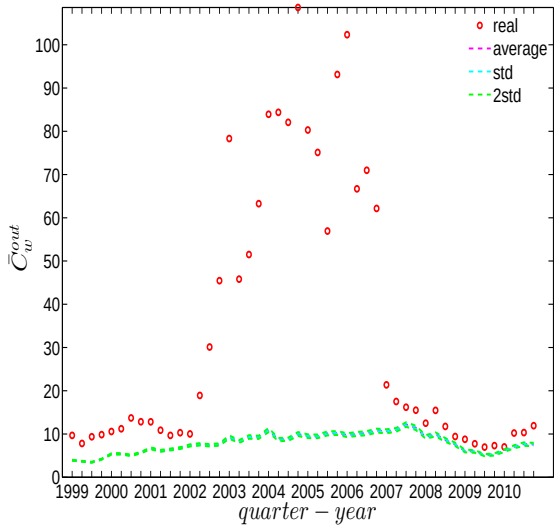

(d) $\bar{C}_w^{out}$

Figure 4.57: Evolution of the averages of local weighted clustering coefficients in the observed e-MID network and in the DWCM. $\bar{C}_w^{cyc}$ (panel a), $\bar{C}_w^{mid}$ (panel b), $\bar{C}_w^{in}$ (panel c), $\bar{C}_w^{out}$ (panel d).

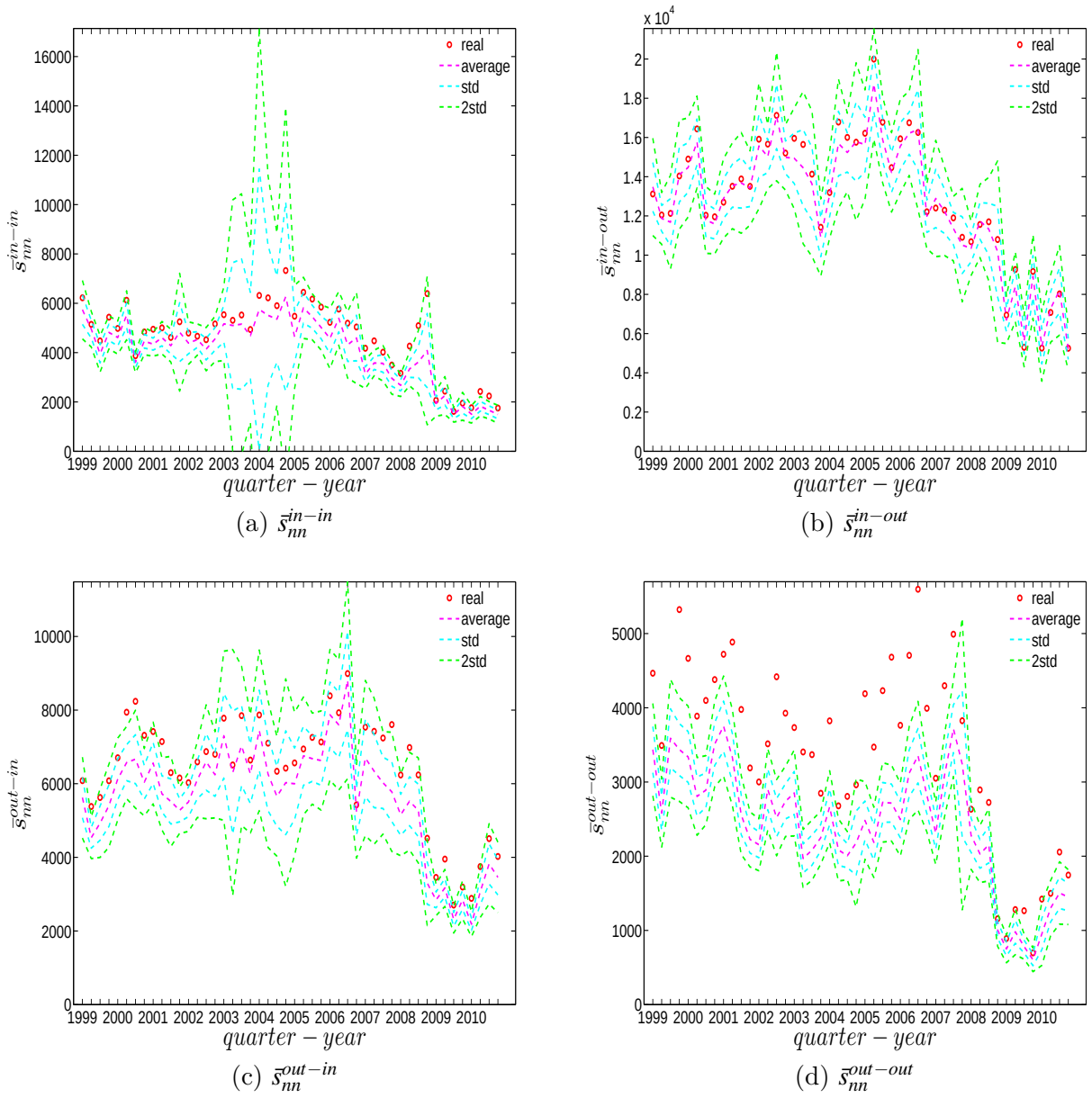

(a) $\bar{s}_{nn}^{in-in}$ (b) $\bar{s}_{nn}^{in-out}$

(c) $\bar{s}_{nn}^{out-in}$ (d) $\bar{s}_{nn}^{out-out}$

Figure 4.58: Evolution of the averages of ANNSs in the observed e-MID network and in the DECM. $\bar{s}_{nn}^{in-in}$ (panel a), $\bar{s}_{nn}^{in-out}$ (panel b), $\bar{s}_{nn}^{out-in}$ (panel c), $\bar{s}_{nn}^{out-out}$ (panel d).

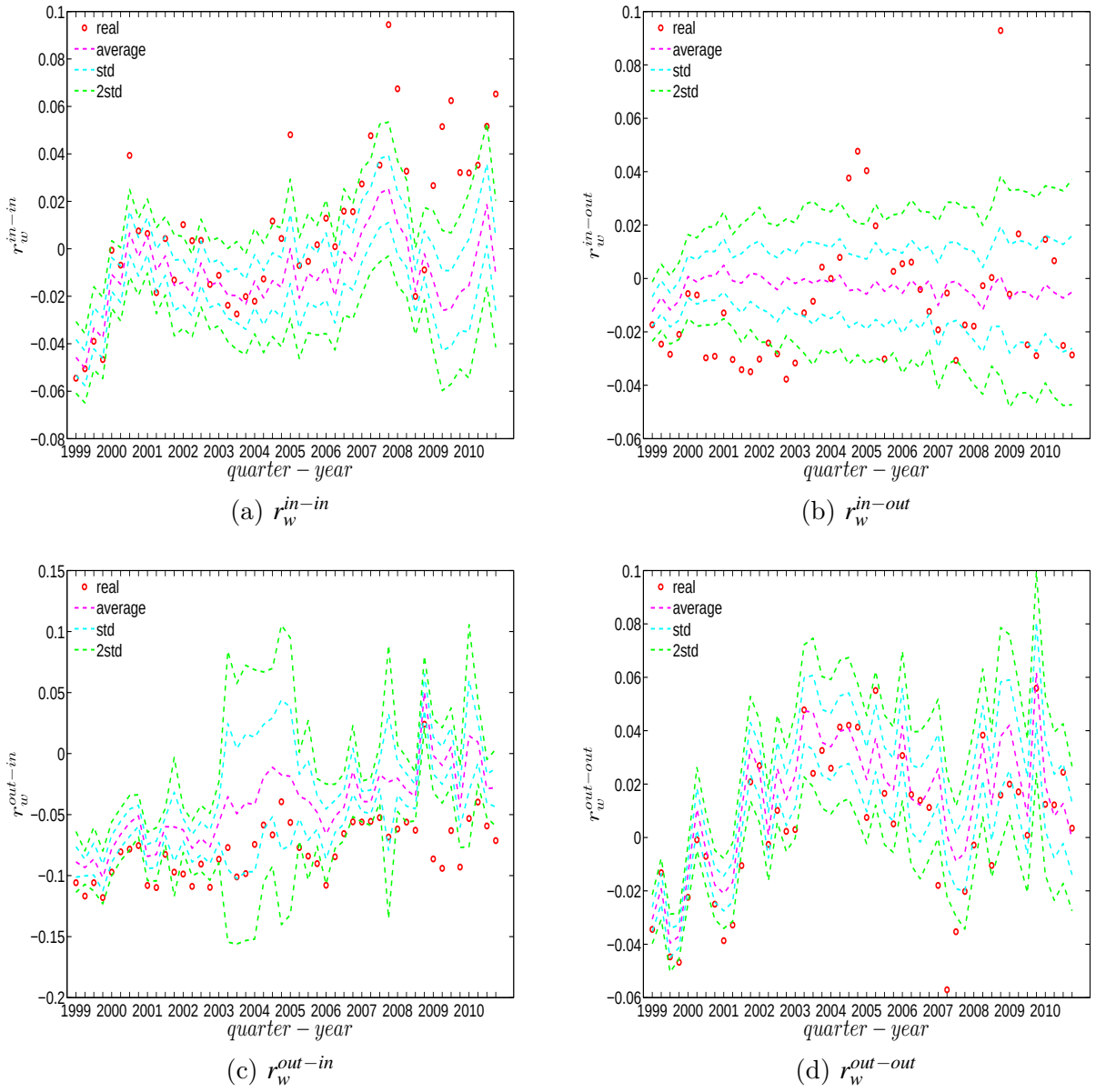

(a) r_w^{in-in} (b) r_w^{in-out}

(c) r_w^{out-in} (d) $r_w^{out-out}$

Figure 4.59: Evolution of the global weighted assortativity indicators in the observed e-MID network and in the DECM. r_w^{in-in} (panel a), r_w^{in-out} (panel b), r_w^{out-in} (panel c), $r_w^{out-out}$ (panel d).

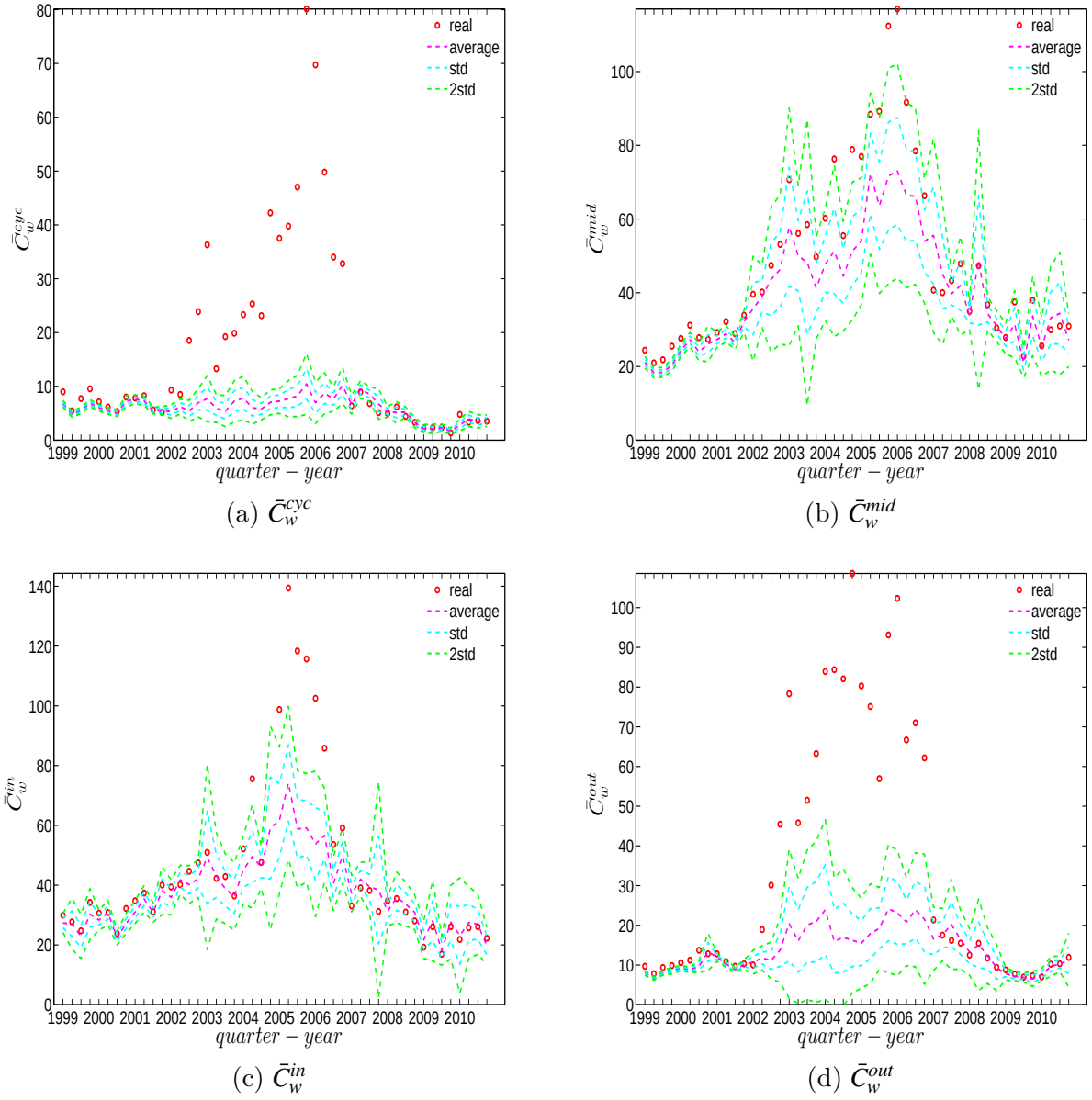

(a) $\bar{C}_w^{cyc}$ (b) $\bar{C}_w^{mid}$

(c) $\bar{C}_w^{in}$ (d) $\bar{C}_w^{out}$

Figure 4.60: Evolution of the averages of local weighted clustering coefficients in the observed e-MID network and in the DECM. $\bar{C}_w^{cyc}$ (panel a), $\bar{C}_w^{mid}$ (panel b), $\bar{C}_w^{in}$ (panel c), $\bar{C}_w^{out}$ (panel d).

Note that, although, in general, we find that the family of Enhanced Configuration Models outperforms the family of Weighted Configuration Models in terms of replicating the main features of the structural correlations in the weighted version of the observed network, solving the system (4.77) to extract the hidden variables in the DECM (or system (4.73) in the UECM for the undirected version of the network) is much more computationally demanding than solving the system (4.68) for the DWCM (or sys. (4.64) for the UWCM for

the undirected version of the network) [8,9].

4.4.4 z-scores analysis revealing structural changes in the weighted system

To analyze the evolution of the discrepancies between the referenced models and the observed network, we define z-scores for the global indicators, i.e. for $\bar{s}^{un}_{nn}, r^{un}_{w}, \bar{C}^{w}_{un}$ in the undirected weighted network (evaluated under the UWCM and the UECM) and for $\bar{s}^{in-in}_{nn}, \bar{s}^{in-out}_{nn}$, $\bar{s}^{out-in}_{nn}, \bar{s}^{out-out}_{nn}$, $r^{in-in}_{w}, r^{in-out}_{w}, r^{out-in}_{w}, r^{out-out}_{w}$, $\bar{C}^{cyc}_{w}, \bar{C}^{mid}_{w}, \bar{C}^{in}_{w}$, and $\bar{C}^{out}_{w}$ in the directed weighted network (evaluated under the DWCM and the DECM) (see subsection 4.7.2 in the Appendix for further details).

Before going into details, it should be noted that from Figure (4.61) to Figure (4.64), when comparing the UECM with the UWCM in the undirected version or the DECM with the DWCM in the directed version, some of the high z-scores under the UECM (or under the DECM) are blurred because of the presence of much larger z-scores under the UWCM (or under the DWCM).

In the undirected weighted case, two important findings are obtained. First, overall, the z-scores are mostly smaller in absolute value under the UECM than under the UWCM (see Figure (4.61)). This is consistent with what we found for the local indicators and re-emphasizes the finding that the UECM out-performs the UWCM. Second, interestingly, in panel (c) of Figure (4.61) we see that, the distance between the z-scores for $\bar{C}^{un}_{w}$ evaluated under the UWCM and the UECM increases over the period from 2002 to 2006, and then decreases sharply after the financial crisis. This suggests that the importance of particular basic features of a network (like its degree sequence or its strength sequence) for the emergence of higher order correlations structures can vary over time.

In the directed weighted case, similarly, we find that the z-scores under the DECM are much smaller in absolute value than those evaluated under the DWCM (see Figures (4.62), (4.63), and (4.64)). The third order correlations among banks in the directed case still seem to be much more informative than the second order ones if one would like to detect the effects of critical events on the topology of the network. As we can see in Figure (4.64), similar to

[8] According to Squartini et al. (2015), solving system (4.77) for the DECM and solving the system (4.73) for the UECM may be very time consuming if the strength distribution contains big outliers and the degree distribution is narrow. This also happens in our study, and in fact our data set shows that the strength distribution is much wider than the degree distribution.

[9] Following Mastrandrea et al. (2014) and Squartini et al. (2015), in order to speed up the process of solving system (4.73) for the UECM and system (4.77) for the DECM, we have to employ the iteration method, which uses the output of the previous iteration as the initial value for the current one. However, it remains a very time consuming process to obtain an acceptable solution for the hidden variables.

the undirected version, the distance between the z-scores for each of the $\bar{C}_w$ evaluated under the DWCM and the DECM continuously increases during the period 2002 to 2006, and then decreases dramatically after the financial crisis.

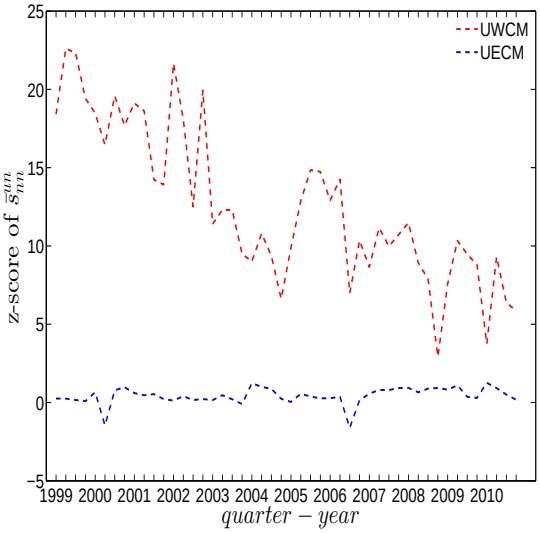

(a) z-score of $\bar{s}^{un}_{nn}$

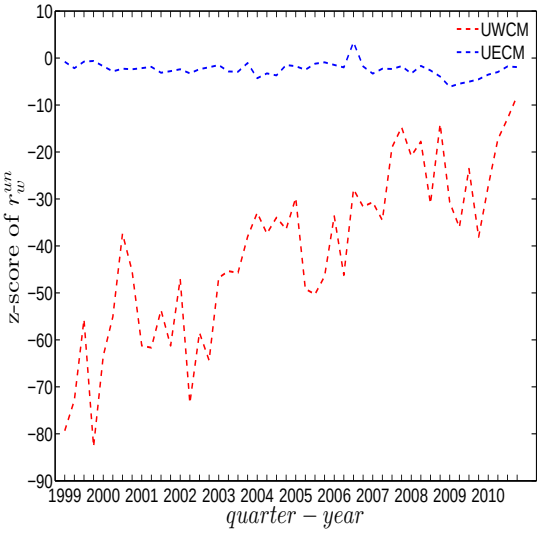

(b) z-score of r^{un}_{w}

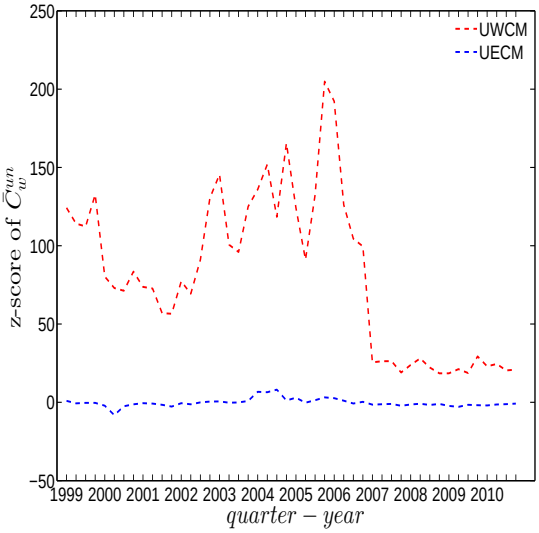

(c) z-score of $\bar{C}^{un}_{w}$

Figure 4.61: Evolution of z-scores for $\bar{s}^{un}_{nn}$ (panel a), r^{un}_{w} (panel b), and $\bar{C}^{un}_{w}$ (panel c) evaluated under the UWCM (red dashed lines) and the UECM (blue dashed lines).

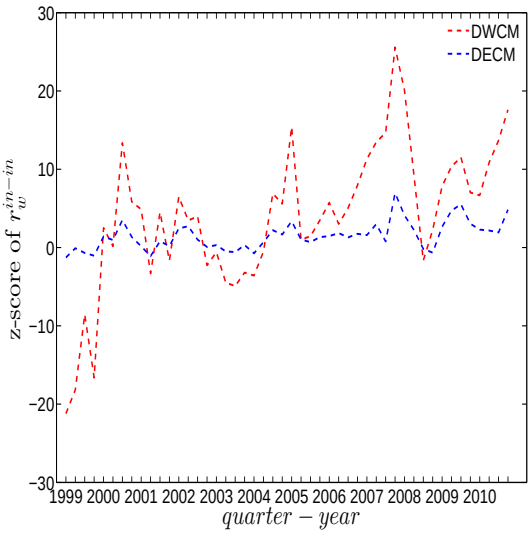

(a) z-score of r_w^{in-in}

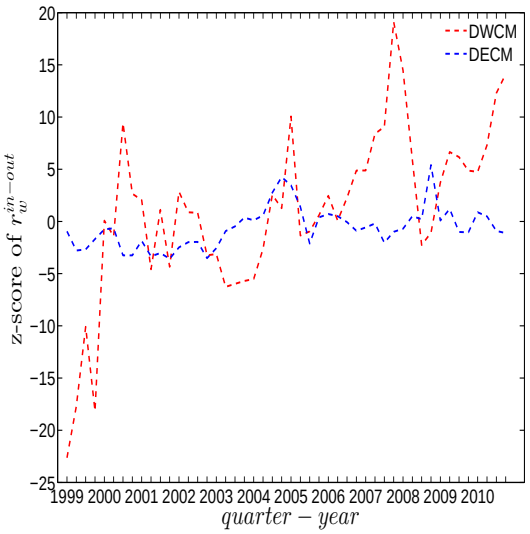

(b) z-score of r_w^{in-out}

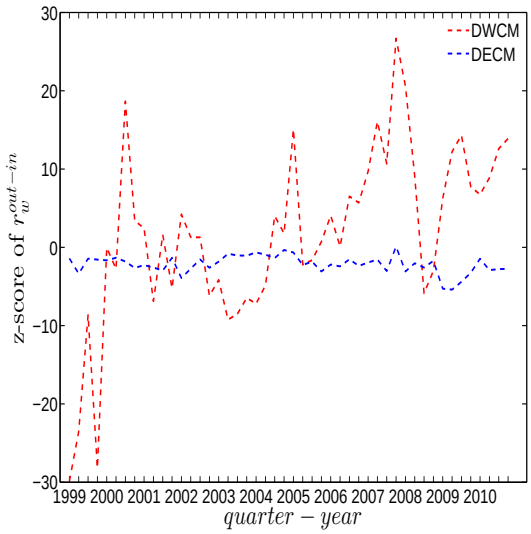

(c) z-score of r_w^{out-in}

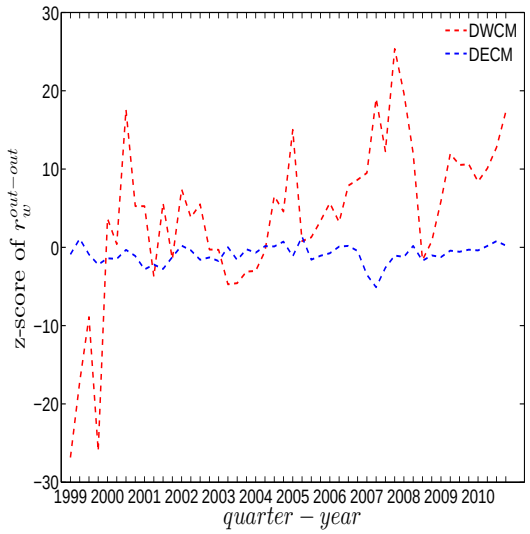

(d) z-score of $r_w^{out-out}$

Figure 4.62: Evolution of z-scores for r_w^{in-in} (panel a), r_w^{in-out} (panel b), r_w^{out-in} (panel c), and $r_w^{out-out}$ evaluated under the DWCM (red dashed lines) and the DECM (blue dashed lines).

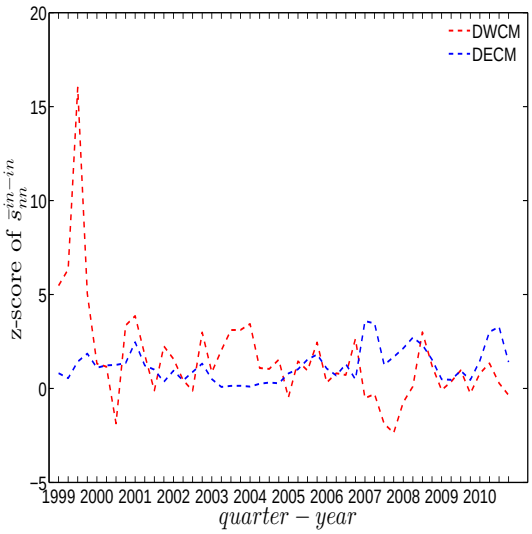

(a) z-score of $\bar{s}_{nn}^{in-in}$

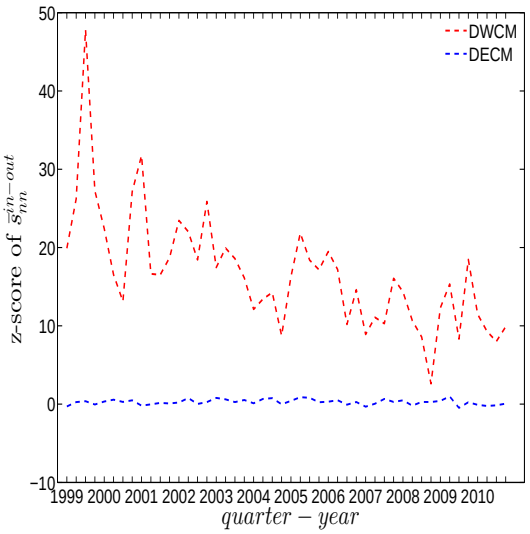

(b) z-score of $\bar{s}_{nn}^{in-out}$

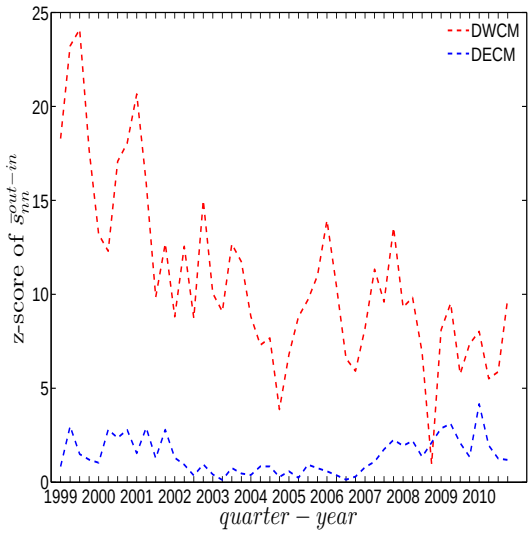

(c) z-score of $\bar{s}_{nn}^{out-in}$

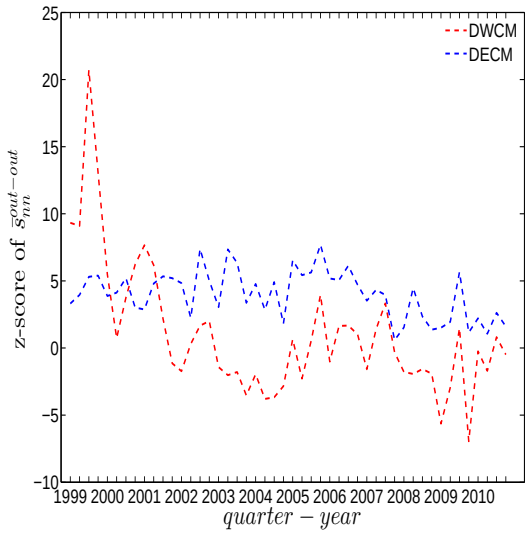

(d) z-score of $\bar{s}_{nn}^{out-out}$

Figure 4.63: Evolution of z-scores for $\bar{s}_{nn}^{in-in}$ (panel a), $\bar{s}_{nn}^{in-out}$ (panel b), $\bar{s}_{nn}^{out-in}$ (panel c), and $\bar{s}_{nn}^{out-out}$ evaluated under the DWCM (red dashed lines) and the DECM (blue dashed lines).

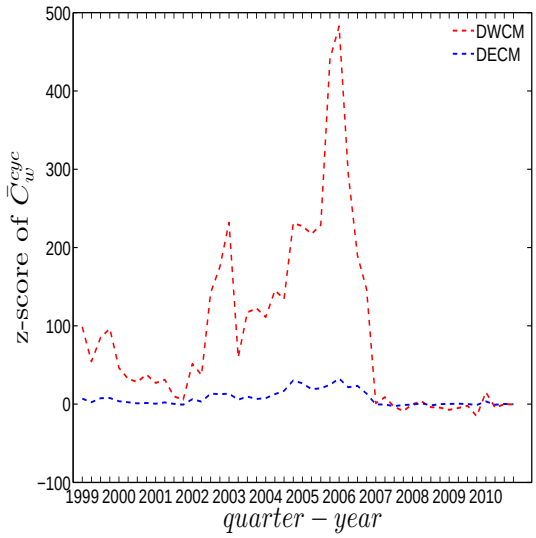

(a) z-score of $\bar{C}_w^{cyc}$

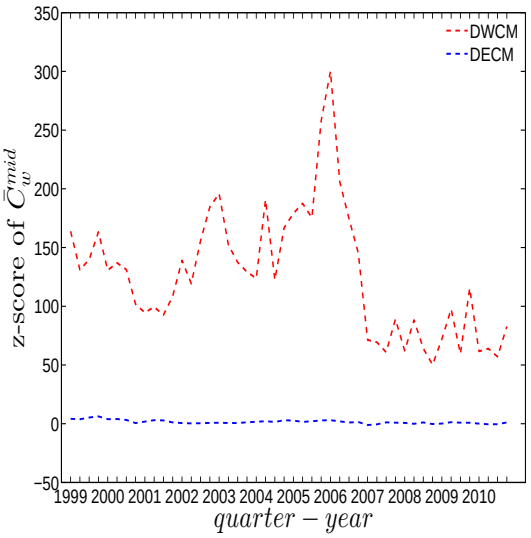

(b) z-score of $\bar{C}_w^{mid}$

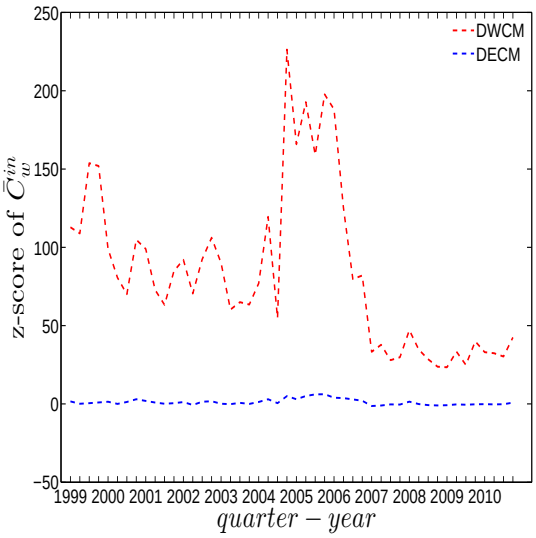

(c) z-score of $\bar{C}_w^{in}$

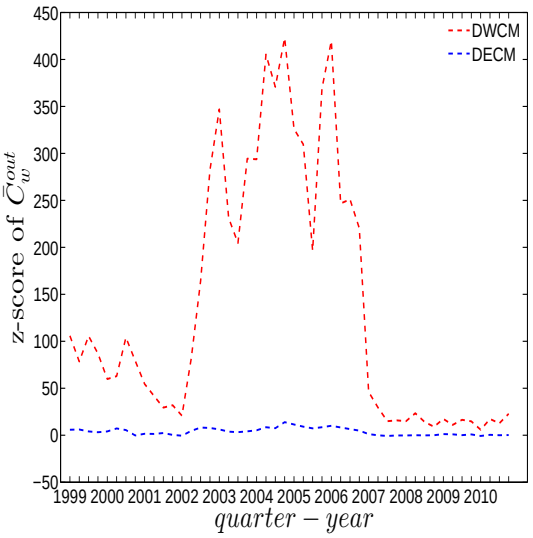

(d) z-score of $\bar{C}_w^{out}$

Figure 4.64: Evolution of z-scores for $\bar{C}_w^{cyc}$ (panel a), $\bar{C}_w^{mid}$ (panel b), $\bar{C}_w^{in}$ (panel c), and $\bar{C}_w^{out}$ evaluated under the DWCM (red dashed lines) and the DECM (blue dashed lines).

4.5 Conclusions

In this study, we investigated the structural correlations in the e-MID network. We find that the observed structural correlations can vary across different versions of the network (binary vs weighted and undirected vs directed). In the undirected version of the network, the mixing is disassortative in both the binary and the weighted case. In addition, when the directions of the edges are taken into account, we find that among the four mixing categories (i.e. in-in, in-out, out-in, and out-out), the global assortativity in the out-in category comes closest to the mixing observed in the undirected network. The similarity between these two quantities is suggested in the study by van der Hoorn and Litvak (2015). Due to the fact that only in the out-in mixing category the considered edge (see the out-in category in Figure (4.1)) contributes to the node degrees on both of its sides, this mixing category can be considered a generalization of the mixing in undirected networks. During our analysis of the evolution of the third order correlations among banks over time, we detected dramatic changes in the network structure surrounding the recent financial crisis in 2007. More specifically, in the weighted network, the averages of the local weighted clustering coefficients appear elevated from the adoption of the Euro up until 2006, and then decrease dramatically around the time of the financial crisis. We also report strong indications of elevated systemic risk in the network, evidenced by the prevalence of the "middleman" and "inward" types of clustering in the network.

Moreover, by employing the various configuration models, we examined whether the information encoded in the local constraints (like the observed degree sequence and/or the strength sequence of a network) can explain higher order structural correlations. We find that, in the binary case, the degree sequence is informative in terms of explaining the main features of the structural correlations in the e-MID network. However, under scrutiny, the binary e-MID network does display some non-random patterns that cannot simply be explained by the degree sequence in conjunction with the configuration model.

In the weighted version of the network, for the most part, the structural correlations in the observed e-MID network are deviating strongly from their respective expectations evaluated under the Weighted Configuration Models, which capture only the heterogeneity in the strength sequence(s) (i.e. the UWCM in the undirected version and the DWCM in the directed version). One possible explanation is that while all measures of structural correlations used in the weighted network depend on the elements of both the adjacency as well as the weighting matrices, neither the UWCM or DWCM utilize information about the node degrees (degree sequence), which is, in fact, found to be more important than the

strength sequence in reproducing the topological properties of real world networks (see, for example, Squartini et al., 2011a, Squartini et al., 2011b; Squartini et al., 2015).

Due to the failures of the UWCM and the DWCM, we consider the family of Enhanced Configuration Models, which constrains the degree as well as the strength sequences of the randomized ensemble to match those of the observed network on average (i.e. UECM in the undirected case and the DECM in the directed case). Our findings indicate that the randomized ensembles produced by the Enhanced Configuration Model have a much greater predictive power. This is in line with what was found in previous studies such as Mastrandrea et al. (2014) and Squartini et al. (2015), and is not very surprising since the Enhanced Configuration Models utilize more information when replicating the structural correlations of the observed network. The results obtained from the analysis of the DECM confirms the role that the distribution of the in-coming and out-going degrees in directed weighted networks plays for the emergence of higher order structural correlations.

Still, a detailed comparison between the observed network and the Enhanced Configuration Models reveals that even this family of Configuration Models is not able to produce accurate estimates for all the measures of structural correlations we used, meaning that some of the patterns can be considered non-random or unexplained by the models. For instance, in the undirected network, we find that even when using the UECM, the weighted assortativity deviates significantly from the respective expected value in a couple of times. In the directed weighted network, the global weighted assortativity in the in-in as well as in the in-out mixing categories and the average of the local weighted clustering coefficients of "inward","outward", and "cyclical" clustering also display non-random patterns in several quarters, mainly from 2002 to 2006. The high degree of clustering in this episode is the one characteristic that can not be explained satisfactorily via the influence of lower-order characteristics like the degree and strength sequences. Hence, this finding points to a behavioral change in the formation of the credit network: A deliberate increase of indirect exposure through multiple credit relations. Interestingly, with the crisis year 2007, we find an abrupt reduction of all clustering coefficients to their "normal" levels implied by the degree and strength sequences.

The Enhanced Configuration Models also fail to reproduce the local behavior of certain banks captured by the local indicators of structural correlations. Unfortunately, because of the lack of more detailed information about the banks in the system, we can not identify the factors for the formations of such non-random patterns.

Interestingly, similar to the study of Squartini et al. (2013) [10], we also observe the evidence for structural changes when comparing the weighted version of the e-MID network with the weighted configuration models. More specifically, the distance between the predictions of the Weighted Configuration Models and of the Enhanced Configuration Models for the averages of local weighted clustering coefficients continuously increases from the adoption of the Euro up until the financial crisis in 2007 and then sharply decreases after that. This result can be interpreted as an indication of structural changes in the network associated with these two critical events. It also suggests that the importance of particular basic features of a network (like its degree sequence or its strength sequence) for the emergence of higher order correlation structures can vary over time.

Due to issues of confidentiality, in many cases, the biggest challenge in the analysis of complex real financial systems lies in the utilization of the limited available information. Our results can be understood as an evaluation of the potential of configuration models to reconstruct higher order topological properties of a network from limited information (e.g. see Mastrandrea et al., 2014; Cimini et al., 2015a). Successful information intensive network analysis, like, for example, systemic risk evaluation, can be conducted on reconstructed networks only to the extent to which the reconstruction is reliable (see, for example, Cimini et al., 2015b).

In addition, the configuration models translate the local constraints in the observed network into hidden variables associated with the individual banks. It would be interesting to investigate whether some individual node characteristics (i.e. non-topological properties) correlate with the extracted hidden variables (see, for example, Garlaschelli and Loffredo, 2004; Garlaschelli et al., 2007; Garlaschelli and Loffredo, 2008; Almog et al., 2015), however, such additional information is unfortunately not available in our data set. This can be a fruitful direction for future research into financial networks.

Moreover, since the Exponential Random Graph Model is generic and flexible enough, one may want to investigate the extent to which it can be useful to use other statistics of the observed network as ensemble constraints. For instance, the average degree of the nearest neighbors or the local clustering coefficients might also prove informative in explaining particular topological properties of the observed network (see, for example, Park and Newman (2004) and Bianconi (2009) for employing different constraints). In addition, since the second and third order structural correlations are the main focus of this study, we suggest that the role of various constraints for the emergence of higher order correlations (or motifs) and

[10] Squartini et al. (2013) focus on the analysis of the binary version of the network of interbank exposures among Dutch banks over the period 1998-2008.

for the meso-scale network structures such as the core-periphery and community structures should be studied further.

4.6 References

Almog A., Squartini T., Garlaschelli D. 2015. A GDP-driven model for the binary and weighted structure of the international trade network. *New Journal of Physics 17.*

Barrat A., Barthélemy M., Pastor-Satorras R., Vespignani A. 2004. The architecture of complex weighted networks. *Proc. Natl. Acad. Sci. 101 (11), pp. 3747-3752.*

Bianconi G. 2009. Entropy of network ensembles. *Physical Review E 79 (3).*

Cimini G., Squartini T., Garlaschelli D., Gabrielli A. 2015a. Estimating topological properties of weighted networks from limited information. *Physical Review E 92 (4).*

Cimini G., Squartini T., Garlaschelli D., Gabrielli A. 2015b. Systemic risk analysis on reconstructed economic and financial networks. *Scientific Reports 5.*

De Masi G., Iori G., Caldarelli G. 2006. Fitness model for the Italian interbank money market. *Physical Review E 74 (6).*

Fagiolo G. 2007. Clustering in complex directed networks. *Physical Review E 76 (2).*

Finger K., Fricke D., Lux T. 2013. Network analysis of the e-MID overnight money market: the informational value of different aggregation levels for intrinsic dynamic processes. *Computational Management Science 10 (2), pp. 187-211.*

Foster J. G., Foster D. V., Grassberger P., Paczuski M. 2010. Edge direction and the structure of networks. *Proc. Natl. Acad. Sci. 107 (24), pp. 10815-10820.*

Fricke D. 2012. Trading strategies in the overnight money market: Correlations and clustering on the e-MID trading platform. *Physica A: Statistical Mechanics and its Applications, 391 (24), pp. 6528-6542.*

Fricke D., Finger K., Lux T. 2013. On assortative and disassortative mixing scale-free networks: The case of interbank credit networks. *Kiel Working Papers 1830*, Kiel Institute for the World Economy. Available at:

https://www.ifw-members.ifw-kiel.de/publications/on-assortative-and-disassortative-mixing-scale-free-networks-the-case-of-interbank-credit-networks/1830_KWP.pdf.

Fricke D., Lux T. 2015a. On the distribution of links in the interbank network: evidence from the e-MID overnight money market. *Empirical Economics 49 (4), pp. 1463-1495.*

Fricke D., Lux T. 2015b. Core-periphery structure in the overnight money market: Evidence from the e-MID trading platform. *Computational Economics. 45 (3), pp. 359-395.*

Garlaschelli D., Loffredo M. I. 2004. Fitness-dependent topological properties of the world trade web. *Physical Review Letters 93 (18).*

Garlaschelli D., Di Matteo T., Aste T., Caldarelli G., Loffredo M. 2007. Interplay between topology and dynamics in the world trade web. *The European Physical Journal B 57 (2), pp. 159-164.*

Garlaschelli D., Loffredo M. I. 2008. Maximum likelihood: Extracting unbiased information from complex networks. *Physical Review E 78 (1).*

Holme P., Park S. M., Kim B. J., Edling C. R. 2007. Korean university life in a network perspective: Dynamics of a large affiliation network. *Physica A: Statistical Mechanics and its Applications 373, pp. 821-830.*

Maslov S., Sneppen K. 2002. Specificity and stability in topology of protein networks. *Science 296 (5569), pp. 910-913.*

Maslov S., Sneppen K., Zaliznyak A. 2004. Detection of topological patterns in complex networks: Correlation profile of the internet. *Physica A: Statistical Mechanics and its Applications 333, pp. 529-540.*

Mastrandrea R., Squartini T., Fagiolo G., Garlaschelli D. 2014. Enhanced reconstruction of weighted networks from strengths and degrees. *New Journal of Physics 16.*

Newman M. E. J. 2002. Assortative mixing in networks. *Physical Review Letters 89 (20).*

Newman M. E. J. 2003a. Mixing patterns in networks. *Physical Review E 67 (2).*

Newman M. E. J. 2003b. The structure and function of complex networks. *Society for Industrial and Applied Mathematics Review 45 (2), pp. 167-256.*

Onnela J. -P., Saramäki J., Kertész J., Kaski K. 2005. Intensity and coherence of motifs in weighted complex networks. *Physical Review E 71 (6).*

Park J., Newman M. E. J. 2003. Origin of degree correlations in the Internet and other networks. *Physical Review E 68 (2).*

Park J., Newman M. E. J. 2004. Statistical mechanics of networks. *Physical Review E 70 (6).*

Piraveenan M., Prokopenko M., Zomaya A. 2010. Classifying complex networks using unbiased local assortativity. In Fellermann H., Dörr M., Hanczyc M. M., Ladegaard Laursen L., Maurer S., Merkle D., Monnard P. -A., Stoy K., Rasmussen S. (Eds.), *Artificial Life XII, Proc. 12th Int'l Conf. Synthesis and Simulation of Living Systems* (pp. 329-336).

Piraveenan M., Prokopenko M., Zomaya A. 2012. Assortative mixing in directed biological networks. *IEEE/ACM Transactions on Computational Biology and Bioinformatics 9 (1), pp. 66-78.*

Saramäki J., Kivelä M., Onnela J., Kaski K., Kertész J. 2007. Generalizations of the clustering coefficient to weighted complex networks. *Physical Review E 75 (2).*

Squartini T., Fagiolo G., Garlaschelli D. 2011a. Randomizing world trade. I. A binary network analysis. *Physical Review E 84 (4).*

Squartini T., Fagiolo G., Garlaschelli D. 2011b. Randomizing world trade. II. A weighted network analysis. *Physical Review E 84 (4).*

Squartini T., Garlaschelli D. 2011. Analytical maximum-likelihood method to detect patterns in real networks. *New Journal of Physics 13.*

Squartini T., van Lelyveld I., Garlaschelli D. 2013. Early-warning signals of topological collapse in interbank networks.*Scientific Reports 3.*

Squartini T., Mastrandrea R., Garlaschelli D. 2015. Unbiased sampling of network ensembles. *New Journal of Physics 17.*

Tabak B. M., Takami M., Rocha J. M. C., Cajueiro D. O., Souza S. R. S. 2014. Directed clustering coefficient as a measure of systemic risk in complex banking networks. *Physica A: Statistical Mechanics and its Applications 394, pp. 211-216.*

van der Hoorn P., Litvak N. 2015. Degree-degree dependencies in directed networks with heavy-tailed degrees. *Internet Mathematics 11 (2), pp. 155-179.*

Watts D. J., Strogatz S. H. 1998. Collective dynamics of "small-world" networks. *Nature 393, pp. 440-442.*

Zlatic V., Bianconi G., Díaz-Guilera A., Garlaschelli D., Rao F., Caldarelli G. 2009. On the rich-club effect in dense and weighted networks. *The European Physical Journal B 67 (3), pp. 271-275.*

Zhang B., Horvath S. 2005. A general framework for weighted gene co-expression network analysis. *Statistical Applications in Genetics and Molecular Biology 4 (1).*

4.7 Appendix

4.7.1 Assortativity Coefficients

Overall Assortativity

In an undirected network, define the list of m edges $\{A_eB_e\}_{e=1}^m$, where for each index e, the two nodes A_e, B_e stand for the ends of an edge. Note that, the overall assortativity indicator r_{bin}^{un} can be calculated via $\{k_i^{un}\}_{i=1}^n$ and $\{k_{nn,i}^{un}\}_{i=1}^n$ as

$$r_{bin}^{un} = \frac{\sum_{i=1}^n (k_i^{un})^2 k_{nn,i}^{un} - \frac{1}{2m}[\sum_{i=1}^n (k_i^{un})^2]^2}{\sum_{i=1}^n (k_i^{un})^3 - \frac{1}{2m}[\sum_{i=1}^n (k_i^{un})^2]^2}, \tag{4.92}$$

where $m = \frac{1}{2}\sum_{i=1}^n k_i^{un}$ (e.g. Park and Newman, 2003).

In a directed network, suppose that we have a list of M edges $\{A_eB_e\}_{e=1}^M$, where for each index e, the two nodes A_e, B_e respectively stand for the source and target nodes (note that $M = \sum_{i=1}^n k_i^{in} = \sum_{i=1}^n k_i^{out}$).

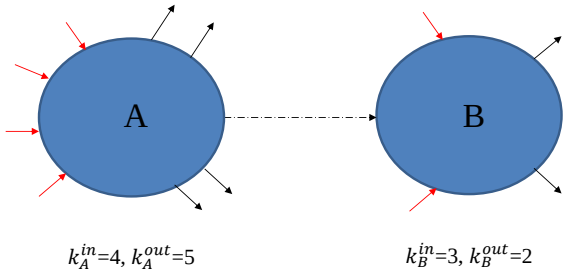

Four combinations of correlations over all edges (A-B):
$k_A^{in} - k_B^{in}, k_A^{in} - k_B^{out}, k_A^{out} - k_B^{in}$, and $k_A^{out} - k_B^{out}$

Figure 4.65: In-coming, out-going degrees to two vertices of an edge in directed networks.

Each node A_e or B_e has an in-coming degree and an out-going degree (see Figure (4.65). Consequently, we have four combinations of degrees associated with each edge as mentioned in Figure (4.1). Therefore, regarding the degree dependencies, four separate indicators can be obtained, i.e. $r_{bin}^{in-in}, r_{bin}^{out-in}, r_{bin}^{in-out}, r_{bin}^{out-out}$. Similar to the undirected case, mathematically, these measures of overall assortativity actually depend on the degree sequences $\{k^{in}\}_{i=1}^n$, $\{k^{out}\}_{i=1}^n$ as well as the sequences of the average nearest neighbor degrees $k_{nn,i}^{in-in}, k_{nn,i}^{in-out}, k_{nn,i}^{out-in}, k_{nn,i}^{out-out}$ (e.g. Piraveenan et al., 2012; van der Hoorn and Litvak, 2015). More specifically, accordingly, they are given by

$$r_{bin}^{in-in} = \frac{\frac{1}{2}[\sum_{i=1}^n (k_i^{in})^2 k_{nn,i}^{in-in} + k_i^{in} k_i^{out} k_{nn,i}^{out-in}] - \frac{1}{M}[\sum_{i=1}^n (k_i^{in})^2 \sum_{i=1}^n (k_i^{in} k_i^{out})]}{\sqrt{\{\sum_{i=1}^n (k_i^{in})^3 - \frac{1}{M}[\sum_{i=1}^n (k_i^{in})^2]^2\}\{\sum_{i=1}^n (k_i^{in})^2 k_i^{out} - \frac{1}{M}[\sum_{i=1}^n (k_i^{in} k_i^{out})]^2\}}}, \tag{4.93}$$

$$r_{bin}^{in-out} = \frac{\frac{1}{2}\sum_{i=1}^n k_i^{in} k_i^{out} (k_{nn,i}^{in-in} + k_{nn,i}^{out-out}) - \frac{1}{M}[\sum_{i=1}^n (k_i^{in} k_i^{out})]^2}{\sqrt{\{\sum_{i=1}^n (k_i^{in})^2 k_i^{out} - \frac{1}{M}[\sum_{i=1}^n (k_i^{in} k_i^{out})]^2\}\{\sum_{i=1}^n (k_i^{out})^2 k_i^{in} - \frac{1}{M}[\sum_{i=1}^n (k_i^{out} k_i^{in})]^2\}}}, \tag{4.94}$$

$$r_{bin}^{out-in} = \frac{\frac{1}{2}\sum_{i=1}^n [(k_i^{out})^2 k_{nn,i}^{out-in} + (k_i^{in})^2 k_{nn,i}^{in-out}] - \frac{1}{M}[\sum_{i=1}^n (k_i^{in})^2 \sum_{i=1}^n (k_i^{out})^2]}{\sqrt{\{\sum_{i=1}^n (k_i^{in})^3 - \frac{1}{M}[\sum_{i=1}^n (k_i^{in})^2]^2\}\{\sum_{i=1}^n (k_i^{out})^3 - \frac{1}{M}[\sum_{i=1}^n (k_i^{out})^2]^2\}}}, \tag{4.95}$$

and

$$r_{bin}^{out-out} = \frac{\frac{1}{2}\sum_{i=1}^{n}[(k_i^{out})^2 k_{nn,i}^{out-out} + k_i^{out} k_i^{in} k_{nn,i}^{in-out}] - \frac{1}{M}[\sum_{i=1}^{n}(k_i^{out})^2 \sum_{i=1}^{n}(k_i^{in} k_i^{out})]}{\sqrt{\{\sum_{i=1}^{n}(k_i^{out})^3 - \frac{1}{M}[\sum_{i=1}^{n}(k_i^{out})^2]^2\}\{\sum_{i=1}^{n}(k_i^{out})^2 k_i^{in} - \frac{1}{M}[\sum_{i=1}^{n}(k_i^{in} k_i^{out})]^2\}}}. \quad (4.96)$$

Local Assortativity

The concept of local assortativity stems from the demand to calculate the (unbiased) contribution of individual nodes to the overall (global) assortativity. The basic idea is that the numerator in the Pearson correlation coefficient proposed by Newman (2003) can be reformulated based on the contribution of individual nodes instead of edges (e.g. Piraveenan et al., 2010; Piraveenan et al., 2012).

It should be emphasized that, for the directed version of the measure of local assortativity primarily introduced in Piraveenan et al. (2012), the two in-out and out-in degree dependencies are not differentiated, when in fact they exhibit totally different behaviors (as found in Foster et al. (2010) and in Sec. 4.3 of our study). In our study, the contributions to the in-out and out-in degree dependencies are distinguishable.

We denote the local assortativity measures for a given node i as ρ_i^{in-in}, ρ_i^{in-out}, ρ_i^{out-in}, and $\rho_i^{out-out}$ corresponding to the four mixing categories in the directed version and ρ_i^{un} is used for the undirected version. Note that the following equalities must hold:

$$r_{bin}^{un} = \sum_{i=1}^{n} \rho_i^{un}, \quad (4.97)$$

$$r_{bin}^{in-in} = \sum_{i=1}^{n} \rho_i^{in-in}, \quad (4.98)$$

$$r_{bin}^{in-out} = \sum_{i=1}^{n} \rho_i^{in-out}, \quad (4.99)$$

$$r_{bin}^{out-in} = \sum_{i=1}^{n} \rho_i^{out-in}, \quad (4.100)$$

$$r_{bin}^{out-out} = \sum_{i=1}^{n} \rho_i^{out-out}. \quad (4.101)$$

First, we define

$$\mu_{un} = \frac{1}{2m}\sum_{i=1}^{n}(k_i^{un})^2, \quad (4.102)$$

$$\mu_{in-in} = \frac{1}{M}\sum_{i=1}^{n}(k_i^{in})^2, \quad (4.103)$$

$$\mu_{out-out} = \frac{1}{M}\sum_{i=1}^{n}(k_i^{out})^2, \tag{4.104}$$

and

$$\mu_{in-out} = \mu_{out-in} = \frac{1}{M}\sum_{i=1}^{n}(k_i^{in}k_i^{out}). \tag{4.105}$$

Note that, in the undirected case, it can be shown that μ_{un} is equal to the average of the degrees of the target and source nodes in the edge list $\{A_eB_e\}_{e=1}^{m}$, i.e. $\mu_{un} = \frac{1}{2m}(\sum_{e=1}^{m} k_{A_e}^{un} + \sum_{e=1}^{m} k_{B_e}^{un})$. Similarly, in the directed case, given the edge list the edge list $\{A_eB_e\}_{e=1}^{M}$, it can be shown that μ_{in-in} and $\mu_{out-out}$ are respectively equal to the averages of the in-coming and out-going degrees from target and source nodes in the edge list. Mathematically, $\mu_{in} = \frac{1}{M}\sum_{e=1}^{M} k_{B_e}^{in}$ and $\mu_{out} = \frac{1}{M}\sum_{e=1}^{M} k_{A_e}^{out}$. In contrast, μ_{in-out} (μ_{out-in}) tells us the average of out-going (in-coming) degrees of the target (source) nodes in the edge list. We have that $\mu_{in-out} = \frac{1}{M}\sum_{e=1}^{M} k_{A_e}^{in}$ and $\mu_{out-in} = \frac{1}{M}\sum_{e=1}^{M} k_{B_e}^{out}$.

Second, we define

$$\sigma_{un}^2 = \sum_{i=1}^{n}(k_i^{un})^3 - \frac{1}{2m}[\sum_{i}(k_i^{un})^2]^2. \tag{4.106}$$

$$\sigma_{in}^2 = \sum_{i=1}^{n}(k_i^{in})^3 - \frac{1}{M}[\sum_{i}(k_i^{in})^2]^2 \tag{4.107}$$

$$\sigma_{out}^2 = \sum_{i=1}^{n}(k_i^{out})^3 - \frac{1}{M}[\sum_{i=1}^{n}(k_i^{out})^2]^2, \tag{4.108}$$

$$\sigma_{in'}^2 = \sum_{i=1}^{n}(k_i^{in})^2 k_i^{out} - \frac{1}{M}[\sum_{i=1}^{n}(k_i^{in}k_i^{out}]^2, \tag{4.109}$$

and

$$\sigma_{out'}^2 = \sum_{i=1}^{n}(k_i^{out})^2 k_i^{in} - \frac{1}{M}[\sum_{i=1}^{n}(k_i^{in}k_i^{out}]^2. \tag{4.110}$$

The denominators in Eqs. (4.92), (4.93), (4.94), (4.95), (4.96) are respectively equal to σ_{un}^2, $\sigma_{in}\sigma_{in'}$, $\sigma_{in'}\sigma_{out'}$, $\sigma_{out}\sigma_{in}$, and $\sigma_{out}\sigma_{out'}$.

By decomposing the overall assortativity coefficient r_{bin}^{un} in Eq. (4.92), we obtain the local assortativity indicators. More specifically, the contribution of node i to r is

$$\rho_i^{un} = \frac{(k_i^{un})^2 k_{nn,i}^{un} - (k_i^{un})^2\mu_{un}}{\sigma_{un}^2}. \tag{4.111}$$

Similarly, in the directed case, for each node i, we have four local assortativity indicators:

$$\rho_i^{in-in} = \frac{k_i^{in}[k_i^{in} * (k_{nn,i}^{in-in} - \mu_{in-out}) + k_i^{out}(k_{nn,i}^{out-in} - \mu_{in-in})]}{2\sigma_{in}\sigma_{in'}}, \tag{4.112}$$

$$\rho_i^{in-out} = \frac{[k_i^{in}k_i^{out}(k_{nn,i}^{out-out} + k_{nn,i}^{in-in}) - 2k_i^{in}k_i^{out} * \mu_{in-out}]}{2\sigma_{out'}\sigma_{in'}}, \tag{4.113}$$

$$\rho_i^{out-in} = \frac{[(k_i^{out})^2 * (k_{nn,i}^{out-in} - \mu_{in-in}) + (k_i^{in})^2(k_{nn,i}^{in-out} - \mu_{out-out})]}{2\sigma_{out}\sigma_{in}}, \tag{4.114}$$

$$\rho_i^{out-out} = \frac{k_i^{out}[k_i^{out} * (k_{nn,i}^{out-out} - \mu_{out-in}) + k_i^{in}(k_{nn,i}^{in-out} - \mu_{out-out})]}{2\sigma_{out}\sigma_{out'}}. \tag{4.115}$$

4.7.2 z-scores analysis of the indicators of structural correlations

In the main text, in the undirected weighted network, the UWCM is compared with the UECM. Similarly, in the directed weighted network, the DWCM is compared with the DECM. For that purpose, we employ z-scores evaluated under each referenced null model, generally defined as

$$z_X^{\text{null model}} = \frac{X - \langle X \rangle_{\text{null model}}}{\sigma[X]_{\text{null model}}} \tag{4.116}$$

where X is a measured quantity of the observed network, $\langle X \rangle_{\text{null model}}$ and $\sigma[X]_{\text{null model}}$ are respectively the expected value and the standard deviation of X evaluated under the referenced null model. Obviously, the interpretation of the statistical significance of the discrepancy between quantity X and its expected value is valid if and only if X follows a Gaussian; however, the value of $z_X^{\text{null model}}$ can still tell us by how many standard deviations the value of X in the observed network differs from the expected one (see, for example, Squartini et al., 2013).

As shown in the main text, one can define z-scores for the local indicators such as for the ANNSs as well as the local weighted clustering coefficients, and can then compare different models for every bank (e.g. Eqs. (4.88), (4.89), (4.90), (4.91) in the main text). We can also define such scores for global indicators such as $\vec{s}_{nn}^{un}, r_w^{un}, \bar{C}_{un}^w$ in the undirected weighted network (under the UWCM and the UECM), and for $\vec{s}_{nn}^{in-in}, \vec{s}_{nn}^{in-out}, \vec{s}_{nn}^{out-in}, \vec{s}_{nn}^{out-out}$, $r_w^{in-in}, r_w^{in-out}, r_w^{out-in}, r_w^{out-out}$, $\bar{C}_w^{cyc}, \bar{C}_w^{mid}, \bar{C}_w^{in}$, and $\bar{C}_w^{out}$ in the directed weighted network (under the DWCM and the DECM).

Chapter 5

An Analysis of Systemic risk in Worldwide Economic Sentiment Indices

Coauthored by: Luu Duc Thi, Boyan Yanovski and Thomas Lux.

Keywords: Sentiment Index; Correlations; Random Matrix Theory; Principal Components.

5.1 Introduction

The analysis of business cycles in different countries is one of the fundamental issues in international economics. So far, much of the analysis is often directed at investigating the synchronization and convergence of "tangible" macroeconomic variables like GDP growth rates, unemployment rates, and so forth (e.g. Bordo and Hebling, 2003; Bordo and Hebling, 2011; Artis et al., 2011; Kose at al., 2012; Ferroni and Klaus, 2015). However, up until now, issues related to the correlations between the expectation structures across different countries have been receiving less attention.

Expectations are a key driver of fluctuations in economic activity since most economically relevant decisions have a strong inter-temporal component (e.g. investment, consumption or saving decisions). This was emphasized, in particular, by Keynes (1936), and later by Minsky (1977) and Akerlof and Shiller (2009). Empirically, such claims are supported by studies by authors like Santero and Westerlund (1996), Howrey (2001), Taylor and McNabb (2007), Carriero and Marcellino (2011), Milani (2011), van Aarle and Kappler (2012), or Milani (2014) in which the structure of the expectations is measured by sentiment or confidence indices. The expectations themselves are formed on the basis of past experience or on cur-

rently incoming information signals from the economy. We argue that "global" information signals, like the collapse of the US housing market in 2007, can lead to a homogenization of the expectation structure around the world, as such information can provide a coordination signal for a global phase of pessimistic expectations. Here we confine ourselves to the phenomenological analysis of coordination of expectations. Whether this synchronization is justified in fundamental terms by the spillovers between countries in real economic activity, or whether it constitutes another, psychological factor of contagion, should be investigated in subsequent research.

This study contributes to the understanding of cross- correlations between economic and business sentiment indices worldwide. We aim to answer three main research questions: (i) how many statistically significant common factors can we extract from the joint dynamics of the sentiment indices worldwide; (ii) how well do these common factors account for the dynamics of the individual indices; and (iii) how does the weight of these factors change over time?

We analyze two data sets, i.e. the Business Confidence Index (BCI) and the Economic Sentiment Indices (ESI) [1]. In terms of methods, instead of using traditional approaches based on econometric models, we employ Random Matrix Theory (see, for example, Laloux et al., 1999; Bouchaud and Potters, 2009) and Principal Component Analysis (see, for example, Jolliffe, 1986; Billio et al., 2012; Wang et al., 2011) to investigate the dynamics of the correlation matrix of country-specific sentiment/confidence indices. We extract the hidden factors encoded in the empirical correlations across countries by analyzing the group of eigenvalues (and their corresponding eigenvectors) deviating from the random bulk. In this way, we can capture the evolution of the statistically significant factors underlying the dynamics of the correlation matrix. The extent to which different countries are affected by these factors can be thought of as the risk of sentiment contagion that the individual countries are facing during a particular period.

This paper is structured as follows. In Sec. 5.2 we briefly describe the data and methods employed in our study. Sec. 5.3 reports our main findings. Discussions and concluding remarks are found in Sec. 5.4.

[1] See the next section for a more detailed description of the two data sets.

5.2 Data and Methods

5.2.1 Data

We consider two data sets containing country-specific sentiment indices. The first data set is collected by the OECD, which consists of all the OECD members and several other countries including China, Russia, India, Turkey, and Brazil. We name this data set OECD$^+$. The data set captures the Business Confidence Index (BCI) measured monthly for each country. The index is based on the entrepreneurs' assessments of their current production, orders and stocks, as well as on their expectations for the immediate future (e.g. OECD, 2016, [2]). To avoid the problem of missing data in some reported countries, we confine our analysis to the period from January 2002 until the end of 2015. This gives us data on the monthly business confidence indices in 33 countries.

The second data set reports the Economic Sentiment Indices (ESI) of Eurozone members and other European countries. The ESI summarizes consumer confidence, as well as the developments and expectations in the other surveyed sectors, i.e. industry (manufacturing), services, retail trade and construction sectors (e.g. EC, 2016, [3]). In our analysis, we name this group of countries EU$^+$. We use this data set for the period from January 1997 to December 2015, which gives us 24 monthly economic sentiment indices associated with 24 European countries.

5.2.2 Methods

Correlation matrix

Given the reported N indices for every month $\{\mathrm{SI}_{i,t}\}_{i=1:N}$ from time t =1 to t= T, we apply a standard normalization procedure to the data [4]. First, we consider the difference in logs across periods

$$\mathrm{I}_{i,t} = \ln(\mathrm{SI}_{i,t+1}) - \ln(\mathrm{SI}_{i,t}). \tag{5.1}$$

As a second step, we define the normalized log-sentiment index for the time horizon T as

$$\mathrm{X}_{i,t} = \frac{I_{i,t} - \langle I_{i,t} \rangle}{\sigma_{i,t}}, \tag{5.2}$$

where $\langle I_i(t) \rangle$ and $\sigma_i(t)$ are respectively the time average and the standard deviation of $I_i(t)$

[2] See OECD. 2016. Business Confidence Index (indicator). doi:10.1787/3092dc4f-en (Accessed on 29 January 2016).

[3] See EC. 2016. Economic Sentiment Index (ESI). http://ec.europa.eu/economy_finance/db_indicators/surveys/index_en.htm (Accessed on 29 January 2016).

[4] In our study, we choose T=36 (months), which satisfies the condition that T>N.

over the time horizon T. Now we have $\langle X_i \rangle = 0$ and $\mathrm{Var}(X_i) = 1$. Next, we consider the rectangular matrix $X = \{X_{i,t}\}_{N\mathrm{x}T}$ and the associated correlation matrix of the N normalized log-sentiment indices

$$\mathrm{C} = \{\mathrm{C}_{ij}\}_{N\mathrm{x}N} = \frac{1}{T} X X^T, \tag{5.3}$$

where the notation X^T stands for the matrix transposition of X. The value of C_{ij} denotes the correlation between country index i and j, where $-1 < \mathrm{C}_{ij} < 1$, for $1 \leq i < j \leq N$. Note that, for any i we always have $\mathrm{C}_{ii} = 1$. In case $\mathrm{C}_{ij} > 0$ (< 0) the two countries i and j are positively (negatively) empirically correlated, while $\mathrm{C}_{ij} = 0$ indicates a lack of any correlation.

Similarity matrix

One of the methods we use, to study the central question of the evolution of the sentiment correlation matrix over time, is the method proposed in Münnix et al. (2012), which is often applied when identifying states of stock markets [5]. The main idea is to come up with a measure of the similarity between correlation matrices from different periods. Suppose we observe two correlation matrices $\mathrm{C}(t_1)$ and $\mathrm{C}(t_2)$ associated with the two distinct periods t_1 and t_2 from the sample $\{1, 2, ...\mathscr{T}\}$, then the similarity S between those two matrices is defined as

$$\mathrm{S}_{t_1,t_2} = \langle |\mathrm{C}(t_1) - \mathrm{C}(t_2)| \rangle, \tag{5.4}$$

where $|...|$ is the notation for the absolute value. Note that a higher value of S_{t_1,t_2} indicates that the "distance" between two correlation matrices is higher; in contrast, a smaller value of S_{t_1,t_2} reveals a higher level of similarity between the two matrices.

Random Matrix Theory

RMT, which was originally developed in nuclear physics by Wigner and Dirac to explain complex quantum systems, has emerged as one of the most important techniques for extracting latent information embedded in empirical correlations from the financial sector (e.g. Laloux et al., 1999; Laloux et al., 2000; Plerou et al., 2002; Kim and Jeong, 2005; Meng et al., 2014; Jiang et al., 2014; Uechi et al., 2015; MacMahon and Garlaschelli, 2015) [6]. Surprisingly, the applications of RMT in macroeconomic time series are very limited. Only a few studies, such as the studies by Ormerod and Mounfield (2002) and Ormerod (2008), have employed that technique to investigate the phenomenon of business cycle synchronization over time.

Define $\{\lambda_i\}_{i=1}^{i=N}$ to be the eigenvalues of the correlation matrix C and consider the prob-

[5] One can also use other similarity measures such as the one proposed in Münnix et al. (2010).

[6] We suggest the readers to, for instance, Bouchaud and Potters (2009) for a more detailed review of the financial applications of RMT.

ability density function of these eigenvalues

$$\rho C(\lambda) = \frac{dn(\lambda)}{d(\lambda)}, \tag{5.5}$$

where $n(\lambda)$ is the number of eigenvalues of C less than λ.

According to RMT, if all $X_{it} \overset{iid}{\sim} \mathcal{N}(0, \sigma^2)$, for $N, T \to \infty$ and $Q = \frac{T}{N} \to a = \text{constant} > 1$, the probability density function $\rho C(\lambda)$ of eigenvalue λ will follow the Marchenko-Pastur (M-P) law

$$\rho C(\lambda) = \frac{Q}{2\pi\sigma^2} \frac{\sqrt{(\lambda_{max}^{RMT} - \lambda)(\lambda - \lambda_{min}^{RMT})}}{\lambda}, \text{for } \lambda_{min}^{RMT} \leq \lambda \leq \lambda_{max}^{RMT}, \tag{5.6}$$

and $\rho C(\lambda) = 0$ elsewhere, with λ_{max}^{RMT} and λ_{min}^{RMT} are respectively the upper and lower bounds of eigenvalues associated with a random correlation matrix with the same variance and the same Q. According to RMT these bounds are given by

$$\lambda_{max}^{RMT} = \sigma^2(1 + \sqrt{1/Q})^2, \text{and } \lambda_{min}^{RMT} = \sigma^2(1 - \sqrt{1/Q})^2. \tag{5.7}$$

We are interested in the latent information encoded in the eigenvectors corresponding to the largest eigenvalues deviating from the bulk of eigenvalues associated with a random correlation matrix with the same variance and the same Q. Suppose $\lambda_1 > ... > \lambda_k > \lambda_{max}^{RMT} > ... > \lambda_N$ are the eigenvalues of the empirical correlation matrix C in descending order and their corresponding eigenvectors are $u_1, u_2, ..., u_N$. The elements of the eigenvector u_1 can be interpreted as the effect of the strongest factor (extracted from the correlation matrix) on all country-specific indices (see, for example, Plerou et al., 2002). In the following, we will be referring to this factor as the "market mode" or the "market factor". In our study, we will investigate the temporal dynamics of the largest eigenvalues (larger than λ_{max}^{RMT}) and their corresponding eigenvectors, in order to identify periods with distinct cross-country sentiment correlation structures, as well as, to quantify the systemic risk associated with these periods (see, for example, Billio et al., 2012; Zheng et al., 2012; Meng et al., 2014; Nobi and Lee, 2016).

Decomposition and noise filtering

Note that we can diagonalize the correlation matrix C as

$$\mathrm{C} = \mathrm{U}\Lambda\mathrm{U}^T, \tag{5.8}$$

where $\Lambda = \text{diag}\{\lambda_1, ..., \lambda_N\}$ and the matrix $\{\mathrm{U}\}_{N\mathrm{x}N}$ is orthonormal, whose i^{th} column is the

normalized eigenvector u_i associated with λ_i. From Eq. (5.8) we have

$$\lambda_i = \mathrm{u}_i^T \mathrm{C}\mathrm{u}_i = \mathrm{u}_i^T \mathrm{Cov}(\mathrm{X}_t)\mathrm{u}_i = \mathrm{Var}(\mathrm{u}_i^T \mathrm{X}_t). \tag{5.9}$$

The total variance of X_t is then

$$\sum_{i=1}^{N} \mathrm{Var}(X_{i,t}) = N = \sum_{i=1}^{N} \lambda_i = \sum_{i=1}^{N} \mathrm{Var}(\mathrm{u}_i^T \mathrm{X}_t). \tag{5.10}$$

Now we can see that λ_i indicates the portion of total variance of X_t contributed by the principal component $y_{i,t} = \mathrm{u}_i^T \mathrm{X}_t$ (e.g. Jolliffe, 1986).

We can rewrite Eq. (5.8) as

$$\mathrm{C} = \sum_{i=1}^{i=N} \lambda_i \mathrm{u}_i \mathrm{u}_i^T. \tag{5.11}$$

The expression $\mathrm{C}^m = \lambda_1 \mathrm{u}_1 \mathrm{u}_1^T$ represents the part of the sentiment correlation structure accounted for by the market mode (recall that the eigenvalues are indexed in descending order). We can filter the market mode away from C. Following Kim and Jeong (2005), we define the filtered correlation matrix

$$\mathrm{M} = \mathrm{C} - \mathrm{C}^m. \tag{5.12}$$

From Eq. (5.11), we can express M in the following way

$$\mathrm{M} = \mathrm{C} - \lambda_1 \mathrm{u}_1 \mathrm{u}_1^T = \sum_{i=2}^{i=N} \lambda_i \mathrm{u}_i \mathrm{u}_i^T. \tag{5.13}$$

The latent information encoded in the eigenvectors of the second largest eigenvalue can also be useful if it is still large enough not to fall within the random bulk (i.e. if $\lambda_2 > \lambda_{max}^{RMT}$). In general, information embedded in other eigenvalues larger than λ_{max}^{RMT} is associated with important factors other than the market mode. In that case, the correlation matrix can be decomposed as

$$\mathrm{C} = \mathrm{C}^m + \mathrm{C}^g + [\mathrm{C} - \mathrm{C}^m + \mathrm{C}^g], \tag{5.14}$$

where C^g accounts for correlations captured by the second most important factor. For instance, in the analysis of stock markets, it is repeatedly suggested that the sectoral component can be captured by the eigenvectors associated with the second largest eigenvalues. In our study, we can think of the cultural and economic peculiarities of particular countries or groups of countries (e.g. emerging markets) as being such a factor.

Absorption ratio

From Eq. (5.8) and Eq. (5.9), the absorption ratios are given by

$$\mathrm{E}_i = \sum_{j=1}^{i} \lambda_j / N \ \text{(for } i = 1, 2, ...N). \tag{5.15}$$

E_i represents the fraction of the total variance of X_t explained by the first i principal components (since $\sum_{j=1}^{N} \lambda_j / N = \frac{\mathrm{trace(C)}}{N} = 1$, we always have $E_N = 1$). What we are interested in, are comparisons between $E_1, ..., E_k$ and $E_N = 1$ (i.e. E_N stands for 100% of the variance as shown in Eq. (5.10)), where k is the largest integer for which $\lambda_k > \lambda_{max}^{RMT}$ is true. Besides using the average of correlations, the absorption ratios can be used to infer the systemic risk in the market (see, for example, Pukthuanthong and Roll, 2009; Billio et al., 2012; Zheng et al., 2012; Meng et al., 2014). For instance, high values of E_1 associated with a high λ_1 signal a strong co-movement of the individual sentiment indices, which implies a high systemic risk.

Inverse Partition Ratio

The inverse of the Inverse Partition Ratio (IPR) measures the number of eigenvector components (i.e. countries) strongly associated with a particular factor (the market mode, for example). It is defined as

$$\mathrm{IPR}(i) = \sum_{j=1}^{N} u_i(j)^4. \tag{5.16}$$

Recalling that the elements of each eigenvector are normalized, i.e. $\sum_{j=1}^{N} u_i(j)^2 = 1$ $(\forall i = 1, 2, ...N)$, it is easy to show that for all i =1 ,2,...N, we have

$$\frac{1}{N} \leq \mathrm{IPR}(i) \leq 1, \tag{5.17}$$

where $\mathrm{IPR}(i) = \frac{1}{N}$ if and only if $u_i(j)^2 = \frac{1}{N}$ for all j =1 ,2,...N; while $\mathrm{IPR}(i) = 1$ if and only if only one element of the eigenvector u_i is different than zero, which implies that only this element (country) contributes to this particular factor. Overall, the inverse of the IPR indicates the number of eigenvector components that contribute significantly to that eigenvector. More specifically, a low IPR indicates that countries contribute more equally. In contrast, a large IPR would imply that the factor is driven by the dynamics of a small number of countries.

5.3 Findings

We report the temporal dynamics of the distribution of correlations between sentiment indices in Figure (5.1) for the BCI data (OECD$^+$ group) and in Figure (5.2) for the ESI data

(EU$^+$ group) [7]. Our first observation is that the distribution of C_{ij} is generally asymmetric, and its shape is not stable over time. A noticeable change can be easily detected for the period of the financial crisis (2007 to 2009). More specifically, the average of correlations and the kurtosis increase during that time, while the skewness decreases significantly. In addition, we find that for all years, in the case of the BCI data, the average of correlations is always positive and the distribution always is left-skewed, signaling that the mass of the distribution of correlations is concentrated on the positive side. This implies that, overall, countries tend to be more positively than negatively correlated (see, for example, Plerou et al., 2002). A similar observation can be made for the ESI data, except for several years, during which a positive skewness is observed (in particular, around the period when the Eurozone was implemented). We provide the following potential explanation for the increased number of negative correlations during that period. Before the introduction of the Euro the interest rates in the "periphery" (Spain, Italy, Portugal, etc.) were much higher than those in the "core" (Germany, Netherlands, France, etc.) of the monetary union. Thus, during the implementation of the Eurozone, the sentiment in the "periphery" of the union might have been positively affected by the convergence of the interest rates across the Eurozone members, while the effect on the sentiment in the "core" might have been negative [8]. In other words, the convergence implies an increase of interest rates in the "core" and a fall in the "periphery", which might result in opposing sentiment dynamics in the two areas of the union. In this rare case, the global information signal can have implications that differ across countries.

Since we observe that the sentiment correlation matrix is not stable over time, the question of how to identify the different states of C comes to the fore. In the previous section, we have introduced a method to quantify the similarity between correlation matrices (see Eq. (5.4)). This method allows us to identify particular states of the sentiment correlation matrix.

Figure (5.3) shows the similarity between the temporal correlation matrices for the BCI data and for the ESI data, respectively in panels (a) and (b). Three states can be identified from these panels, i.e. before 2007, from 2007 to 2009, and after 2009. We can see that the period from 2007 to 2009 is very homogeneous with respect to the correlation structures observed. The correlation matrices from the years 2007, 2008 and 2009 are very similar to each other compared to matrices from other periods. This is consistent with what we

[7] The entries of the correlation matrix for each year have simply been pooled, after which a kernel density estimator has been used to arrive at a distribution in a particular year.

[8] For a discussion of the interest rate convergence in Eurozone see, for example, Arghyrou et al., 2009.

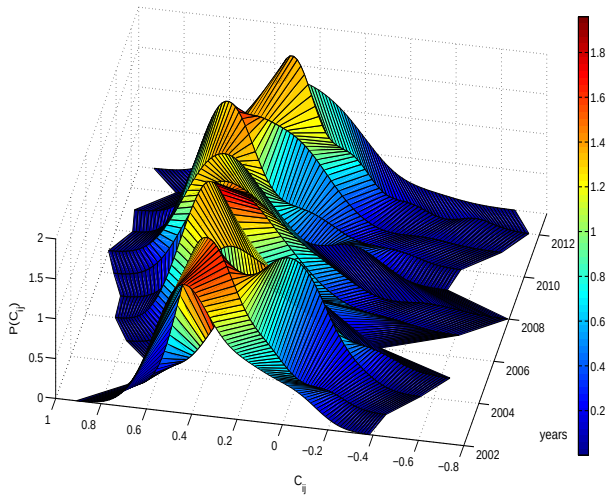

(a) Distribution of C, BCI data, OECD$^+$ group

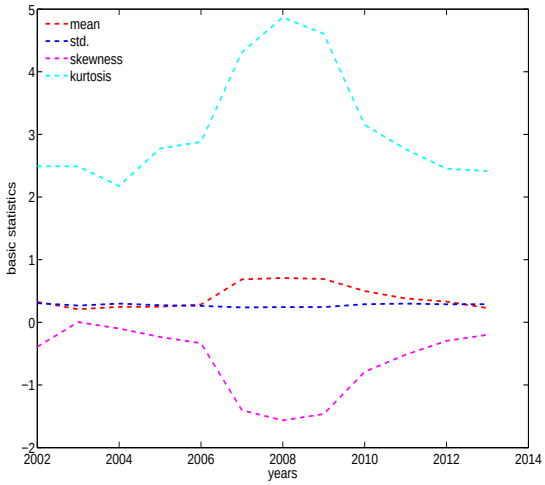

(b) Statistics of C, BCI data, OECD$^+$ group

Figure 5.1: Evolution of the distribution of the elements of C, for BCI data in the OECD$^+$ group. Panel (a) shows the distribution of the elements of C from 2002 to 2013. Panel (b) reports the basic statistical indicators of the elements of C including the mean, standard deviation (std.), skewness, and kurtosis.

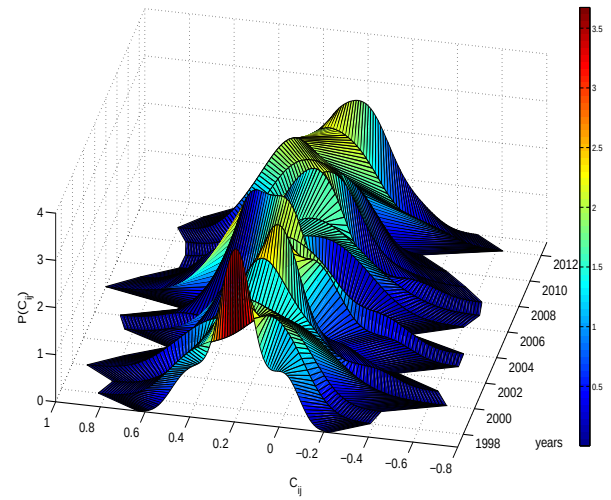

(a) Distribution of C, ESI data, EU$^+$ group

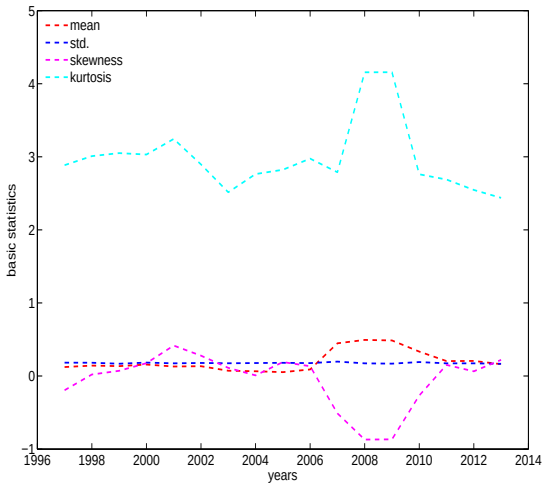

(b) Statistics of C, ESI data, EU$^+$ group

Figure 5.2: Evolution of the distribution of the elements of C, for ESI data in the EU$^+$ group. Panel (a) shows the distribution of the elements of C from 1997 to 2013. Panel (b) reports the basic statistical indicators of the elements of C including the mean, standard deviation, skewness, and kurtosis.

have found during our analysis of the evolution of the basic statistics of the correlation matrices over time. In addition, in panel (b) we see that the correlation matrices for the EU$^+$ group associated with the period of the European debt crisis (2011 to 2013) exhibit strong

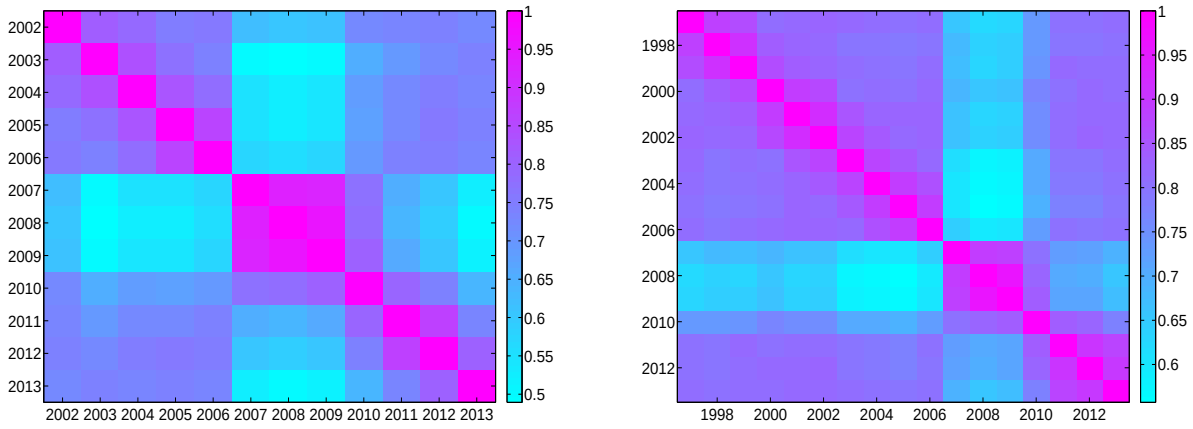

(a) Similarity among C, BCI data, OECD$^+$ group (b) Similarity among C, ESI data, EU$^+$ group

Figure 5.3: Identifying states of correlation matrix using similarity-based analysis. Panel (a) shows the similarity among correlation matrices C from 2002 to 2013, for BCI data in the OECD$^+$ group. Panel (b) shows the similarity among correlation matrices C from 1997 to 2013, for ESI data in the EU$^+$ group.

similarities relative to correlation matrices from other periods. We can thus conclude that for the EU$^+$ we can detect an additional distinct state of the correlation matrix associated with the time of the debt crisis in Europe. In the following, we are going to look more closely at what these distinct states are characterized by.

We start by investigating the spectrum of the correlation matrix and its evolution over time. In Figure (5.4) and Figure (5.5), panel (a) we see that the largest eigenvalue λ_1 is typically more than three times larger than the upper bound λ_{max}^{RMT} for the OECD$^+$ group, and more than 1.3 times larger for the EU$^+$ group. In all years, λ_1 always deviates from the random bulk associated with the M-P law. Figure (5.6) shows the distribution of the eigenvalues of a random correlation matrix (with the same variance and the same Q) compared to the actual distribution of the eigenvalues in 2007 for both groups of countries. For the EU$^+$ group, during the whole sample period, only the first eigenvalue λ_1 is larger than the upper bound $\lambda_{\max}^{RMT}$, while for the OECD$^+$ group, in some years, a second eigenvalue λ_2 crosses this upper bound [9]. The second factor may be interpreted as a group factor. On some rare occasions (e.g. like in the years 2003, 2004 and 2010), particular countries (including some "emerging markets") can have sentiment dynamics opposing those of the rest of the world. We can detect this by looking at the eigenvector elements associated with countries like Mexico, Turkey, Slovakia, Russia, China for in some years and recognizing that these

[9]We also observe that λ_1 is always very similar to $N\langle C_{ij}\rangle$ (where $\langle C_{ij}\rangle$ stands for the pooled average of C), which supports the presence of one common factor affecting all indices.

elements have the opposite sign of the elements associated with countries from the rest of the world. Some developed countries like New Zealand and Australia for instance, also show a similar behavior. All this suggests that the cross-country sentiment dynamics are driven primarily by a single factor (the market mode) and only on rare occasions does a second factor become marginally significant. In the following, we will thus be concentrating on the market mode and on the relationship that countries or groups of countries have with it.

The evolution of the importance of the market factor for the cross-country sentiment dynamics can also be observed in Figure (5.4) and Figure (5.5). We see that during the financial crisis the importance of the market factor becomes overwhelming since both the largest eigenvalue and the associated absorption ratio jump by approximately 100%. Since the largest eigenvalue and the associated absorption ratio increase together, we can say that the systemic worldwide component of sentiment was high during the period 2007 to 2009. We can also see that, for the EU^+ group, the absorption ratios after 2009 are still higher than during the period before the financial crisis. The perceived threat to the Eurozone's stability stemming from the risk of sovereign default of some member states might have prevented individual sentiment indices in Europe from diverging from the market mode.

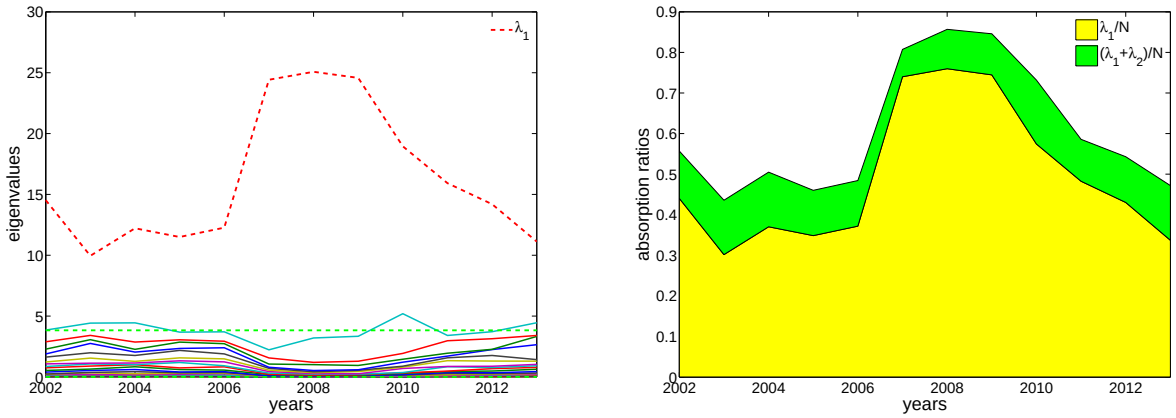

(a) Eigenvalues (b) Absorption ratios

Figure 5.4: Evolution of eigenvalues and absorption ratios for BCI data in the $OECD^+$ group. In panel (a), the red dashed line stands for the largest eigenvalue, the green dashed lines stand for the interval $[\lambda_{min}^{RMT}, \lambda_{max}^{RMT}]$ explained by RMT. Panel (b) shows the absorption ratios associated with the first and the second largest eigenvalues.

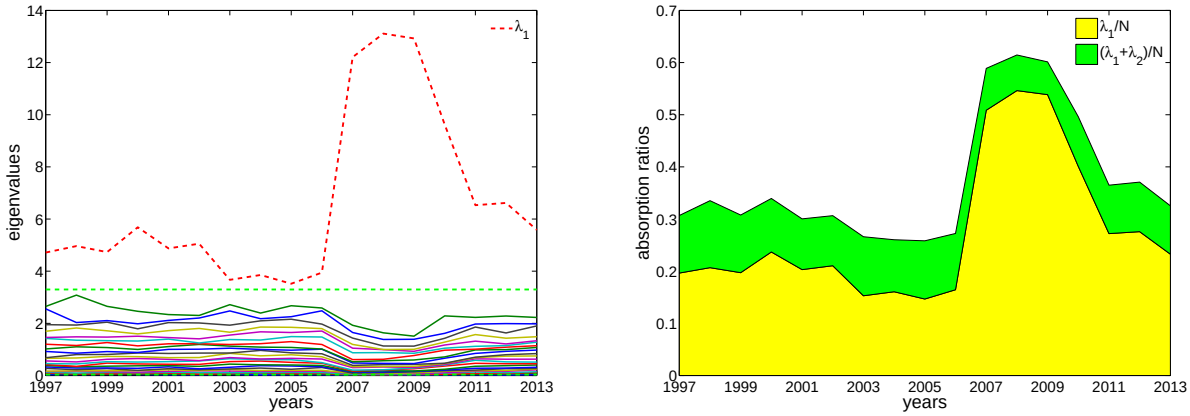

(a) Eigenvalues (b) Absorption ratios

Figure 5.5: Evolution of eigenvalues and absorption ratios for ESI data in the EU$^+$ group. In panel (a), the red dashed line stands for the largest eigenvalue, the green dashed lines stand for interval $[\lambda_{min}^{RMT}, \lambda_{max}^{RMT}]$ explained by RMT. Panel (b) shows the absorption ratios associated with the first and the second largest eigenvalues.

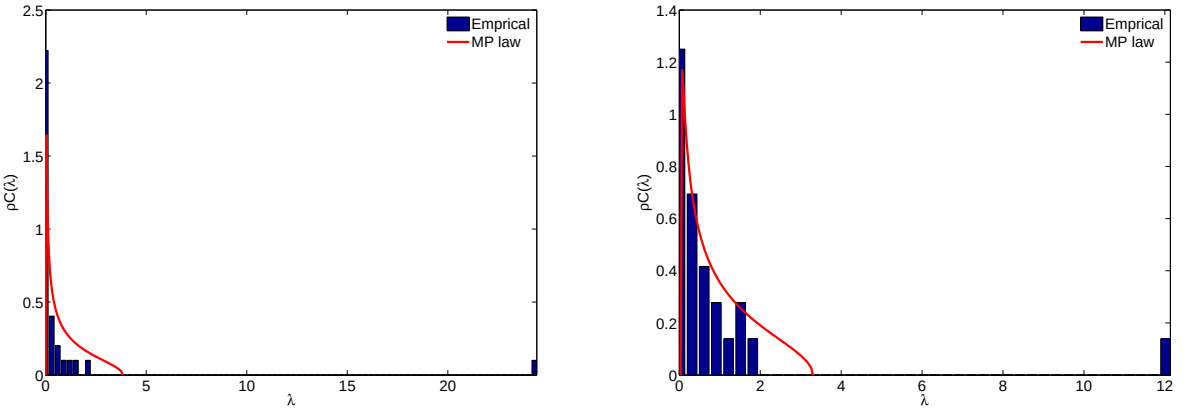

(a) Dist. of eigenvalues, BCI data (b) Dist. of eigenvalues, ESI data

Figure 5.6: Distribution of eigenvalues of C in 2007, compared with RMT. Panel (a) for BCI data in the OECD$^+$ group. Panel (b) for ESI data in the EU$^+$ group.

Next, let us look in more detail at the components of the eigenvector u_1 associated with the market mode. We find that in the period of financial crisis (2007 to 2009), the components of u_1 become more homogeneous, evidencing the synchronization of the sentiment indices around the world (see Figures (5.7), (5.8), and (5.9)). This result holds true for both the EU$^+$ and OECD$^+$ groups. Still, a few countries like China, South Africa or New Zealand seem to be somewhat less influenced by the market mode during the crisis. During normal times, much more divergent behavior is observed. More specifically, in case of the OECD$^+$ group,

countries like Italy, France, Belgium, Hungary, U.K., Austria, Slovenia, Denmark, Chile, Netherlands or Germany contribute the most to the market mode, while the sentiment dynamics in other countries like Finland, Korea, Mexico, New Zealand, Turkey, Slovakia, Australia, Russia, China or India can be divergent to a certain extent. For the EU^{+} group, countries like Belgium, Denmark, Germany, France, Italy, Netherlands or Sweden contribute the most to the market mode, while the sentiment dynamics in other countries like Bulgaria, Latvia, Poland, Romania, Slovakia or Finland can be divergent to a certain extent.

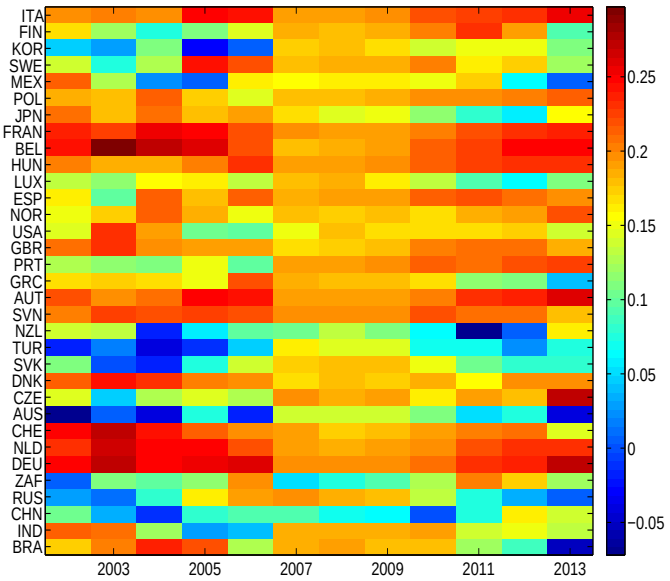

Figure 5.7: Evolution of the eigenvector components of the largest eigenvalue (λ_1), for BCI data in the $OECD^{+}$ group. Without loss of generality, we assume that the sign of the eigenvector element that has the largest absolute value is non-negative. The financial crisis from 2007 to 2009 is captured by drastic changes in the the largest eigenvector components, i.e. they become more homogeneous during that period.

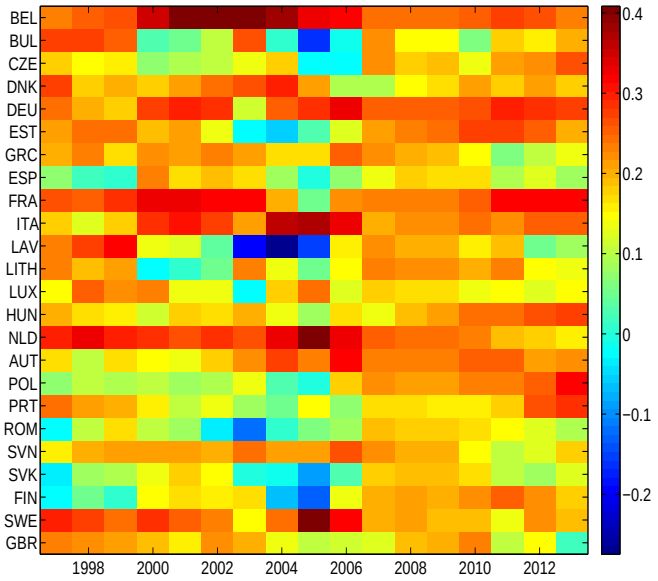

Figure 5.8: Evolution of the eigenvector components of the largest eigenvalue (λ_1), for ESI data in the EU$^+$ group. Without loss of generality, we assume that the sign of the eigenvector element that has the largest absolute value is non-negative. The financial crisis from 2007 to 2009 is captured by drastic changes in the the largest eigenvector components, i.e. they become more homogeneous during that period.

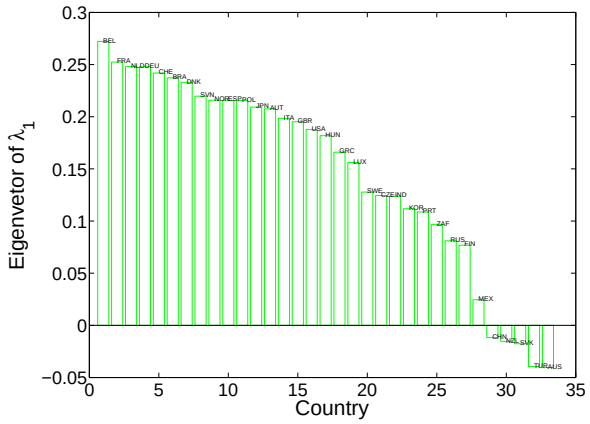

(a) Eivec1 in 2003, BCI

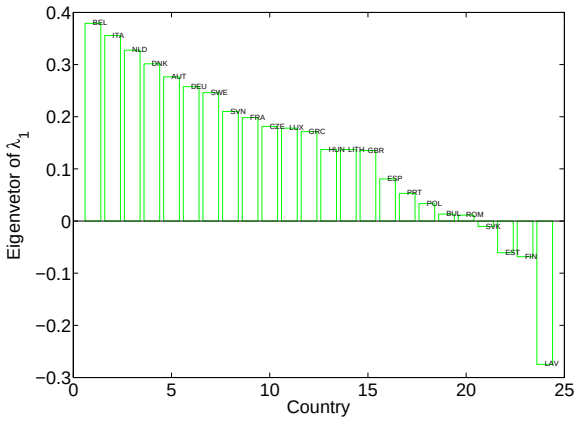

(b) Eivec1 in 2003, ESI

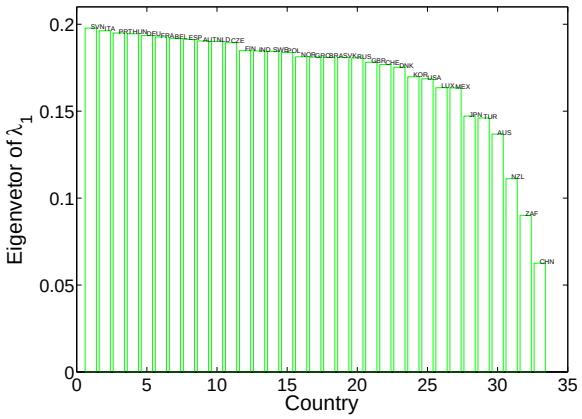

(c) Eivec1 in 2007, BCI

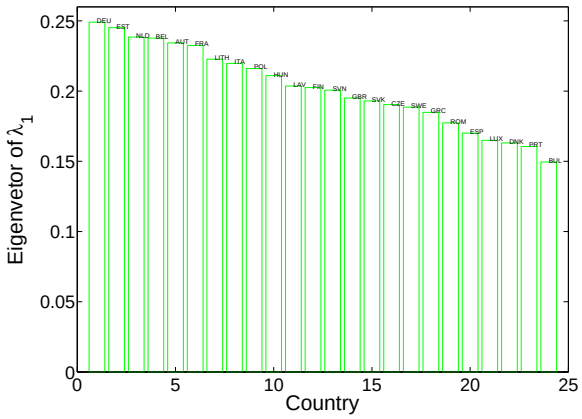

(d) Eivec1 in 2007, ESI

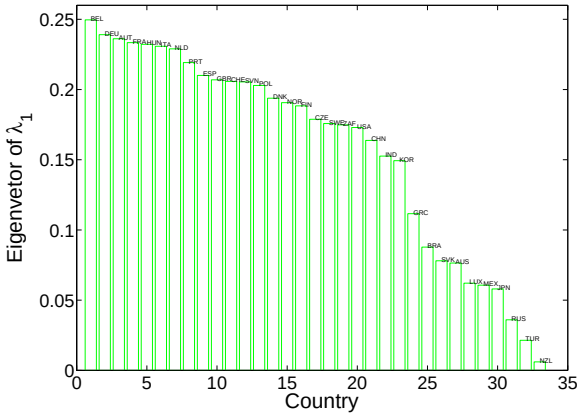

(e) Eivec1 in 2011, BCI

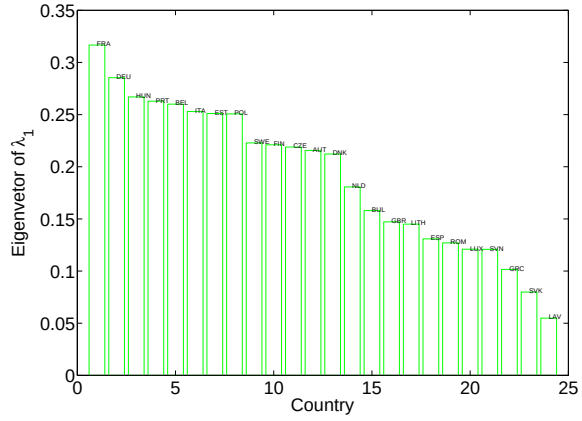

(f) Eivec1 in 2011, ESI

Figure 5.9: Eigenvector components of $\boldsymbol{\lambda}_1$ (Evec1). Without loss of generality, we assume that the sign of the eigenvector element that has the largest absolute value is non-negative. The three left panels (a), (c), and (e) are for BCI data in the OECD$^+$ group, in 2003, 2007, and 2011. The three right panels (b), (d), and (f) are for ESI data in the EU$^+$ group, in 2003, 2007, and 2011. The country code associated with each eigenvector component is also reported. We can see that in the three example years, the eigenvector components of $\boldsymbol{\lambda}_1$ are more homogeneous in 2007.

We further analyze the eigenvectors by calculating the IPR. Figure (5.10) shows the IPR versus the corresponding eigenvalues for the years 2003, 2007, and 2011 as examples. Panels (a) and (b) do this for the OECD$^+$ and for the EU$^+$ groups, respectively. We find that for those years, in which if the largest eigenvalue strongly deviates from the random bulk, the associated eigenvector also exhibits the largest inverse of IPR, meaning that the sentiment dynamics in the majority of the countries is influenced by the market mode.

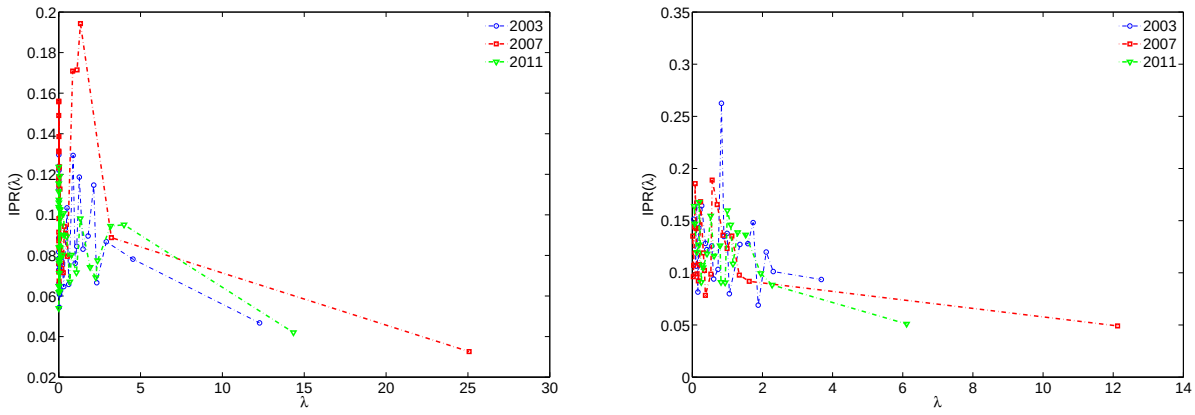

(a) BCI, OECD$^+$ data (b) ESI, EU$^+$ data

Figure 5.10: Comparison of Inverse Participation Ratios of the eigenvectors of the correlation matrix for periods before the financial crisis, during the financial crisis, and after the financial crisis. Panel (a) shows the IPR for BCI in the OECD$^+$ group, panel (b) shows the IPR for ESI in the EU$^+$ group. In both panels, three years, (i) 2003, (ii) 2007, and (iii) 2011, are chosen as the examples.

Above, we have detected a common factor underlying the dynamics of the sentiment indices. Now, we will compare the sentiment correlation matrix over time before and after filtering the effect of that factor. The results are shown in Figures (5.11) and (5.12), respectively for the OECD$^+$ and EU$^+$ groups. Overall, the raw correlations are significantly reduced after the information encoded in the largest eigenvalue and its corresponding eigenvector is subtracted. In addition, we can see that at the time of financial crisis (exemplified here by the graph for 2007, which is the same for 2008 and 2009), the raw correlations between countries increase but their filtered counterparts exhibit reduced correlations. In other words, the increase in the raw correlations were accompanied by an increase in the fraction of the correlations associated with the market mode. Note that for the OECD$^+$ group, some significant correlations still appear after the filtering in some years of the sample period. They are actually mainly contributed by emerging markets like China or India, for which the informational signal associated with the collapse of the US housing market might have

been less relevant due to their limited exposure to toxic securities.

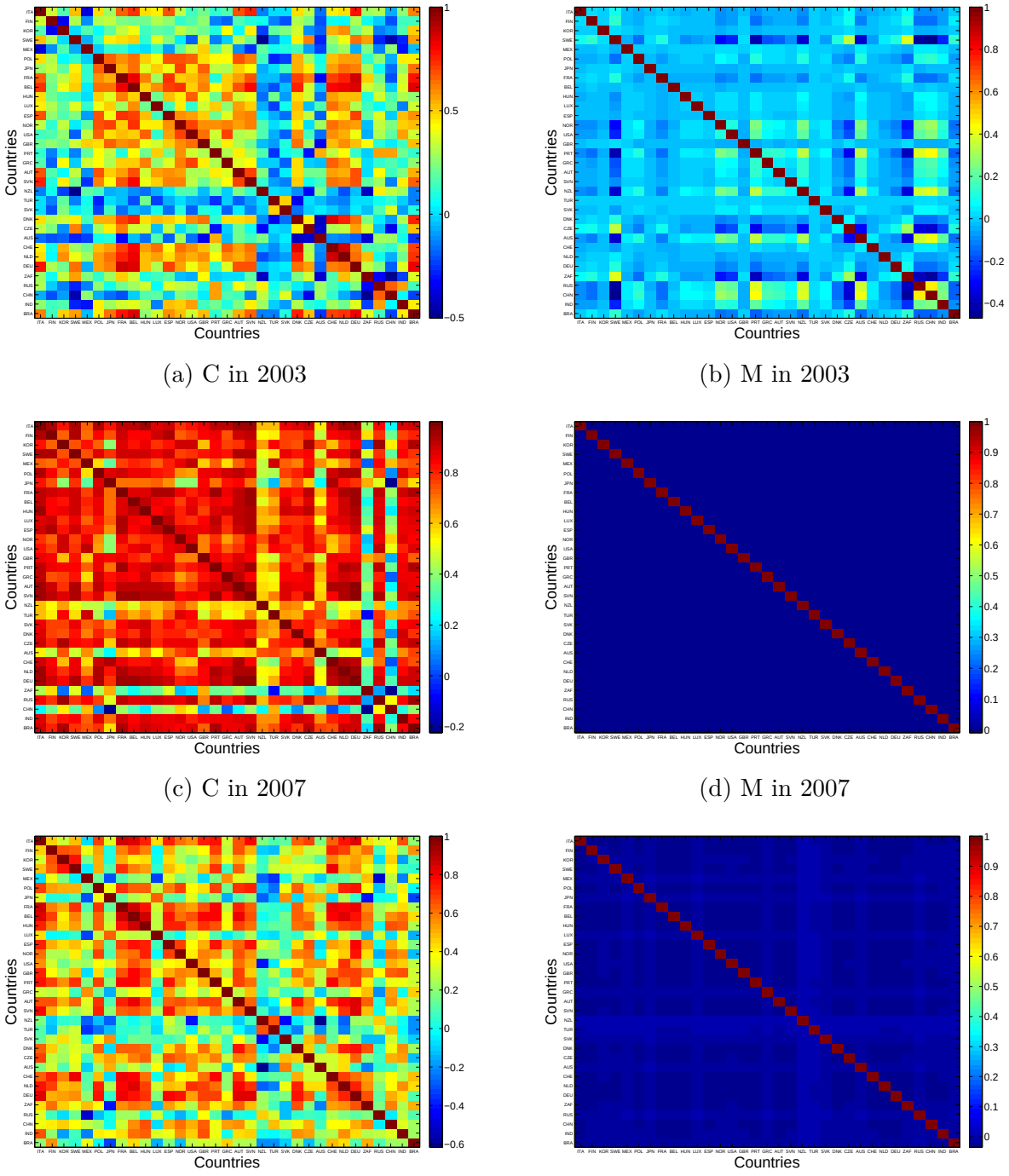

(a) C in 2003

(b) M in 2003

(c) C in 2007

(d) M in 2007

(e) C in 2011

(f) M in 2011

Figure 5.11: Correlations between countries, for BCI data in the OECD$^+$ group. The three left panels (a), (c), and (e) are the raw correlation matrices in 2003, 2007, and 2011. The three right panels (b), (d), and (f) are the correlation matrices filtered by the RMT method in 2003, 2007, and 2011.

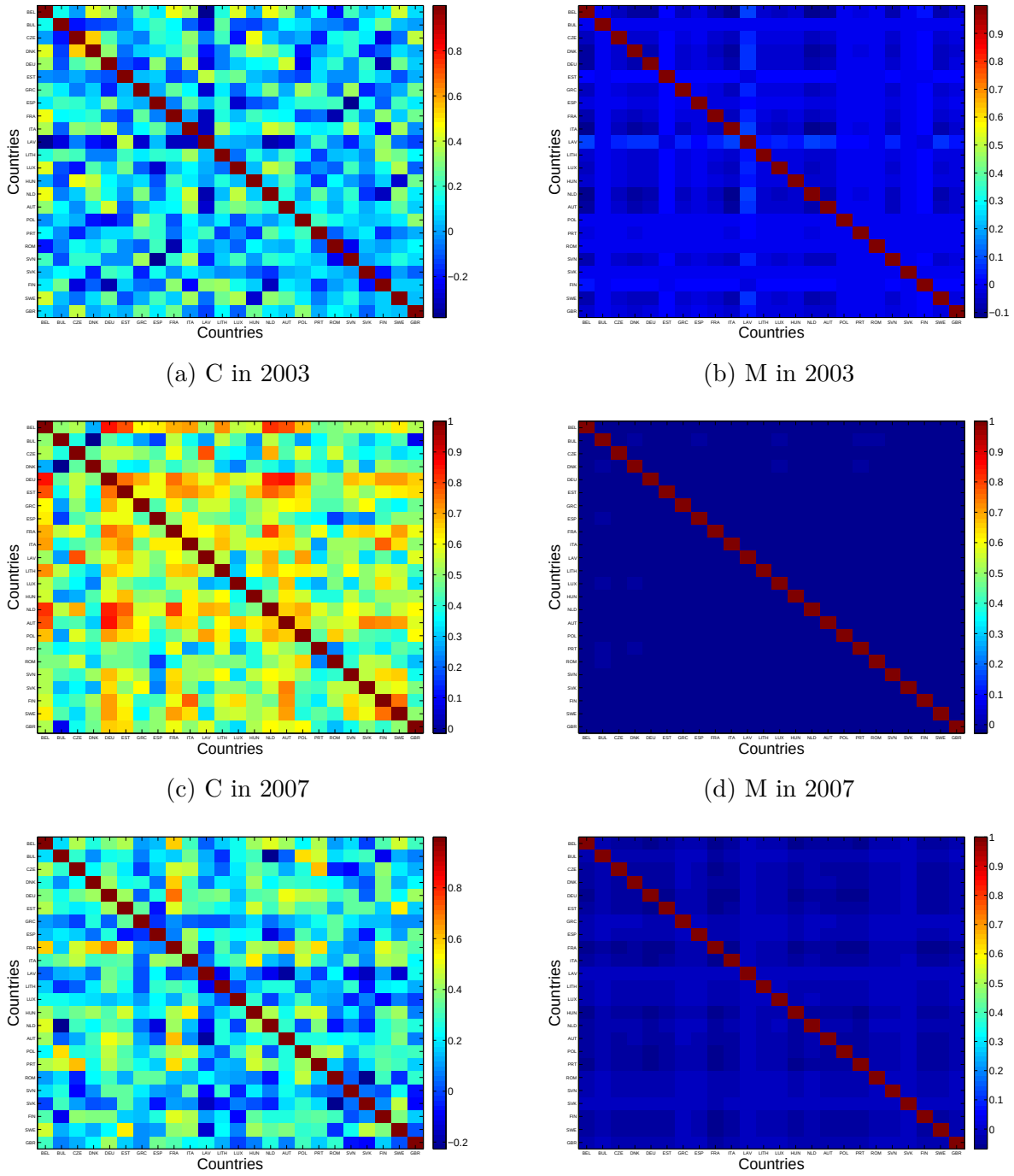

(a) C in 2003

(b) M in 2003

(c) C in 2007

(d) M in 2007

(e) C in 2011

(f) M in 2011

Figure 5.12: Correlations between countries, for ESI data in the EU$^+$ group. The three left panels (a), (c), and (e) are the raw correlation matrices in 2003, 2007, and 2011. The three right panels (b), (d), and (f) are the correlation matrices filtered by the RMT method in 2001, 2007, and 2011.

5.4 Conclusions

In this paper, we have analyzed the evolution of the empirical correlations between the macroeconomic sentiment indices in different countries. Overall, we observe different states in the correlation structure, associated with a varying importance of the common factor ("market mode"). The correlations between indices are significantly reduced after the effects of that common factor are subtracted.

It would seem that many of the information signals worldwide have a common component, since generally sentiment indices tend to comove. During normal times, however, the sentiment in various countries or groups of countries can "resist" the common factor or can even, on rare occasions, "swim against the tide". This is the case for some emerging markets like China, Turkey and other countries like Australia, New Zealand. However, in the presence of strong global information signals, we observe a strong synchronization of the sentiment dynamics all over the world. We consider the collapse of the US housing market (2007-2009) as an example of such global signals. In the case of the Eurozone debt crisis (2011-2013), the sentiment synchronization is high only within Europe, which can be interpreted as an indication that the Eurozone debt crisis is not perceived as a global information signal in countries outside of Europe. Information signals can also cause the sentiments to diverge, if the information has different implications for particular countries or groups of countries. We consider the interest rate convergence associated with the establishment of the Eurozone around the year 2000 to be an example of such an effect.

Overall, we believe that RMT and principal component analysis of the ensemble of worldwide or regional sentiment data can reveal important information on the correlations between business and consumer sentiment in different countries. The tools and results presented in this paper should provide relevant input for business cycle forecasts and the analysis of international co-movements of macroeconomic activity.

5.5 References

Akerlof G. A., Shiller R. J. 2009. *Animal spirits: How human psychology drives the economy, and why it matters for global capitalism.* Princeton University Press.

Arghyrou M. G., Gregoriou A. and Kontonikas A. 2009. Do real interest rates converge? Evidence from the European union. *Journal of International Financial Markets, Institutions and Money 19 (3), pp. 447- 460.*

Artis M., Chouliarakis G., Harischandra P. K. G. 2011. Business cycle synchronization since 1880. *The Manchester School 79 (2), pp. 173-207.*

Billio M., Getmansky M., Lo A. W., Pelizzon L. 2012. Econometric measures of systemic risk in the finance and insurance sectors. *Journal of Financial Economics 104 (3), pp. 535-559.*

Biroli G., Bouchaud J. -P., Potters M. 2007. On the top eigenvalue of heavy-tailed random matrices. *Europhysics Letters, 78 (1)*

Bouchaud J. -P., Potters M. 2009. Financial applications of random matrix theory: a short review. *Working Paper.* Available at: arXiv:0910.1205.

Bordo M. D., Helbling T. 2003. Have national business cycles become more synchronized?. *NBER Working Paper 10130.* Available at: http://www.nber.org/papers/w10130.

Bordo M. D., Helbling T. 2011. International business cycle synchronization in historical perspective. *The Manchester School 79 (2), pp. 208-238.*

Carriero A., Marcellino M. 2011. Sectoral survey-based confidence indicators for Europe. *Oxford Bulletin of Economics and Statistics 73 (2), pp. 175-206.*

EC. 2016. Economic sentiment index (indicator). Available at: http://ec.europa.eu/economy_finance/db_indicators/surveys/index_en.htm (Accessed on 29 January 2016).

Ferroni F., Klaus B. 2015. Euro area business cycles in turbulent times: Convergence or decoupling. *ECB Working Paper 1819.* Available at: https://www.ecb.europa.eu/pub/pdf/scpwps/ecbwp1819.en.pdf?8aacf9b049f3a7e6360b69d13e435844.

Hill B. M. 1975. A simple general approach to inference about the tail of a distribution. *The Annals of Statistics (3), pp.1163-1174.*

Howrey E. P. 2001. The predictive power of the index of consumer sentiment. *Brookings Papers on Economic Activity 2001 (1), pp. 175-207.*

Jiang X. F., Chen T. T., Zheng B. 2014. Structure of local interactions in complex financial dynamics. *Scientific Reports 4.*

Jolliffe I.T. 1986. *Principal component analysis.* Springer-Verlag, New York.

Keynes J. M. 1936. *The general theory of employment, interest and money.* New York: Harcourt, Brace & World.

Kim D. -H., Jeong H. 2005. Systematic analysis of group identification in stock markets. *Physical Review E 72 (4).*

Kose M. A., Otrok C., Prasad E. 2012. Global business cycles: Convergence or decoupling?. *International Economic Review 53 (2), pp. 511-538.*

Laloux L., Cizeau P., Bouchaud J. -P., Potters M. 1999. Noise dressing of financial correlation matrices. *Physical Review Letters 83 (7), pp.1467-1470.*

Laloux L., Cizeau P., Potters M., Bouchaud J. -P. 2000. Random matrix theory and financial correlations. *International Journal of Theoretical and Applied Finance 3 (3), pp. 391-397.*

MacMahon M., Garlaschelli D. 2015. Community detection for correlation matrices. *Physical Review X 5 (2).*

Milani F. 2011. Expectation shocks and learning as drivers of the business cycle. *The Economic Journal 121 (552), pp. 379-401.*

Milani F. 2014. Sentiment and the U.S. business cycle. *Working Paper.* Available at: http://www.economics.uci.edu/files/docs/workingpapers/2014-15/14-15-04-1.pdf.

Minsky H. 1977. The financial instability hypothesis: An interpretation of Keynes and an alternative to 'standard' theory. *Nebraska Journal of Economics and Business 16 (1), pp. 5-16.*

Meng H., Xie W. -J., Jiang Z. -Q., Podobnik B., Zhou W. -X., Stanley H. E. 2014. Systemic risk and spatiotemporal dynamics of the US housing market. *Scientific Reports 4.*

Münnix M. C., Shimada T., Schäfer R., Leyvraz F., Seligman T. H., Guhr T., Stanley H. E. 2012. Identifying states of a financial market. *Scientific Reports 2.*

Münnix M. C., Schäfer R., Grothe O. 2010. Estimating correlation and covariance matrices by weighting of market similarity. *Working Paper.* Available at: arXiv:1006.5847.

Nobi A., Lee J. W. 2016. State and group dynamics of world stock market by principal component analysis. *Physica A: Statistical Mechanics and its Applications 450, pp. 85-94.*

OECD. 2016. Business confidence index (indicator). Available at: https://data.oecd.org/leadind/business-confidence-index-bci.htm#indicator-chart (Accessed on 29 January 2016).

Ormerod P., Mounfield C. 2002. The convergence of European business cycles 1978-2000. *Physica A: Statistical Mechanics and its Applications 307 (3-4), pp. 494-504.*

Ormerod P. 2008. Random matrix theory and macro-economic time-series: An Illustration using the evolution of business cycle synchronisation, 1886–2006. *Economics: The Open-Access, Open-Assessment E-Journal 2, pp. 1-10.*

Plerou V., Gopikrishnan P., Rosenow B., Amaral L. A. N., Guhr T., Stanley H. E. 2002. Random matrix approach to cross correlations in financial data. *Physical Review E 65 (6).*

Pukthuanthong K., Roll R. 2009. Global market integration: An alternative measure and its application. *Journal of Financial Economics 94 (2), pp. 214-232.*

Santero T., Westerlund N. 1996. Confidence indicators and their relationship to changes in economic activity. *OECD Economics Department Working Papers, No. 170*, OECD Publishing. Aivailable at: http://dx.doi.org/10.1787/537052766455.

Taylor K., McNabb R. 2007. Business cycles and the role of confidence: Evidence for Europe. *Oxford Bulletin of Economics and Statistics 69 (2), pp. 185-208.*

Uechi L., Akutsu T., Stanley H. E., Marcus A. J., Kenett D. Y. 2015. Sector dominance ratio analysis of financial markets. *Physica A: Statistical Mechanics and its Applications 421, pp. 488–509.*

van Aarle B., Kappler M. 2012. Economic sentiment shocks and fluctuations in economic activity in the euro area and the USA. *Intereconomics 47 (1), pp. 44-51.*

Wang D., Podobnik B., Horvatic D., Stanley H. E. 2011. Quantifying and modeling long-range cross correlations in multiple time series with applications to world stock indices. *Physical Review E 83 (4).*

Zheng Z., Podobnik B., Feng L., Li B. 2012. Changes in cross-correlations as an indicator for systemic risk. *Scientific Reports 2.*

Appendix

In this section we will examine what happens to the upper bound of the largest eigenvalue if the random variables $X_{i,t}$ still have zero mean and unit variance but may have power law tails with exponent μ. In such a case large changes in the sentiment indices may cause spurious apparent correlations and substantial overestimation of the (theoretical) largest eigenvalue of the sample correlation matrix $C = \frac{1}{T}XX^T$ (e.g. see Biroli et al. (2007) and Bouchaud and Potters (2009)).

Denote S the largest element of $|\mathrm{X}_{i,t}|$ (for all $i = 1, 2, ...N$ and all t in the considered time window of length T). According to Biroli et al. (2007), whenever $S \leq (NT)^{1/4}$, the upper bound for the largest eigenvalue is $\lambda_{max} = (1+\sqrt{Q})^2$, and when $S > (NT)^{1/4}$, the largest eigenvalue becomes $\lambda_{max} = (1/Q + S/T^2)(1 + T/S^2)$. In addition, if $\mu > 4$, the largest element of $|\mathrm{X}_{i,t}|$ is order of $(NT)^{\mu}$, and it is smaller than $(NT)^{1/4}$. In this case, $\lambda_{max}^{RMT} = (1+\sqrt{Q})^2$ can be still used as the upper bound for the largest eigenvalue of C.

To check whether these conditions hold for our data sets, we first use the standard Hill estimator (e.g. Hill (1975)), to examine the behavior of the exponent μ in the tails of $|\mathrm{X}_{i,t}|$. After that, we compare S, the largest value of $\mathrm{X}_{i,t}$ (in absolute terms), with $(NT)^{1/4}$ to see whether we can still use $\lambda_{max}^{RMT} = (1+\sqrt{Q})^2$ as the upper bound of the eigenvalues of the null-model.

The Hill estimator for different lengths of the tail of $|\mathrm{X}_{i,t}|$ in terms of a percentage of the sample containing the largest observations in $|\mathrm{X}_{i,t}|$ (across all years and all countries in the respective groups) is shown in figure (5.13) for the ESI data and in figure (5.14) for the BCI data. We typically find that $|\mathrm{X}_{i,t}|$ have heavy tails with an exponent μ in the range from 2.7 to 7. In addition, when considering only the top 1% to 5% largest observations, μ is larger than 3.

Furthermore, in order to have a more comprehensive assessment on the behavior of the tail exponent, we decompose the entire observation period into separate time windows and then estimate μ for each window. As shown in figure (5.15), with the top 5% largest elements of $|\mathrm{X}_{i,t}|$, μ is larger than 4 for most of the windows. However, in the case of the ESI data (EU^+ group), for the time window associated with the time of the financial crisis (2007-2009), we observe that μ is in the range 3–4, implying the presence of large fluctuations in sentiment indices during that time.

While the existence of the fourth moment of the theoretical distribution of $|\mathrm{X}_{i,t}|$ seems not to be guaranteed for all sub-samples, the crucial inequality $S \leq (NT)^{1/4}$ holds for all considered time windows in both data sets (see Figure (5.16)). Taken together, these results

suggest that the relevant limit for the (theoretical) largest eigenvalue of C remains $\lambda_{max}^{RMT} = (1+\sqrt{Q})^2$.

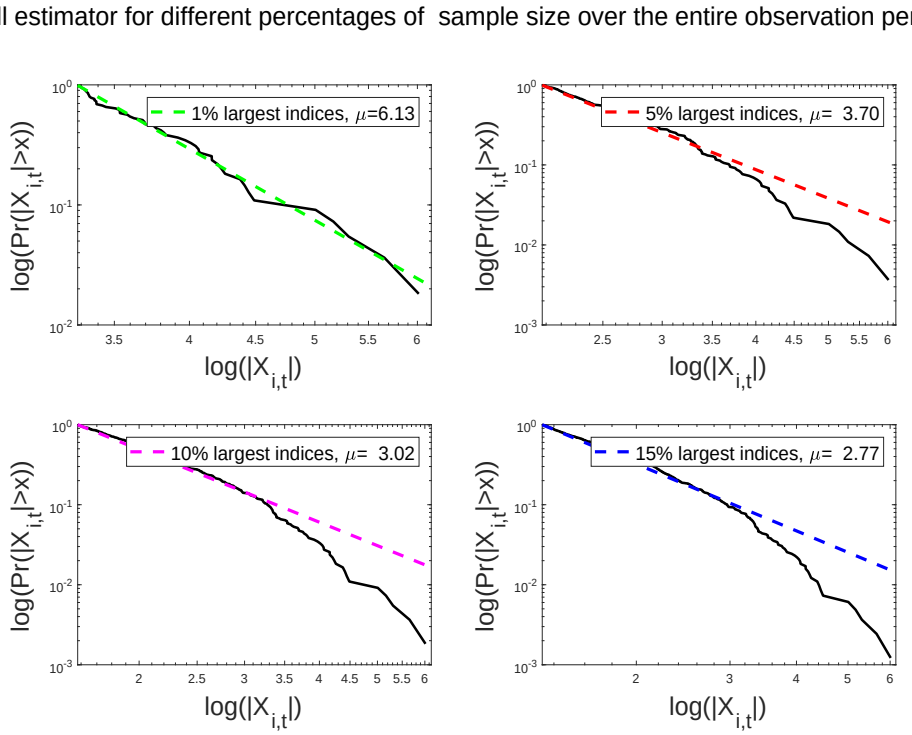

Figure 5.13: Hill estimates of the tail exponent of the distribution of $|X_{i,t}|$ based on different lengths of the tail over the entire observation period for the ESI data (EU^+ group). Panels (a), (b), (c), and (d) show the results for tails defined as 1%, 5%, 10%, and 15% of the largest observations in $|X_{i,t}|$, respectively. In each panel, we plot the empirical complementary cumulative distribution function (CCDF) of $|X_{i,t}|$ on a log-log scale. The solid line depicts the empirical CCDF, while the dashed line represents the power law $\Pr(|X_{i,t}| > x) \sim x^{-\mu}$ using the respective Hill estimate for μ.

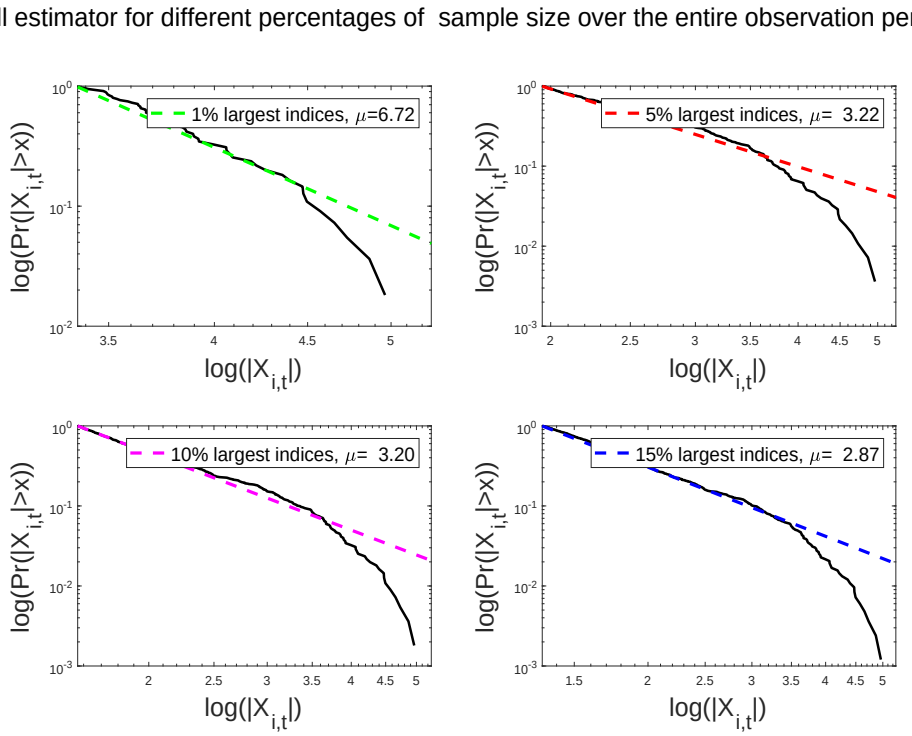

Figure 5.14: Hill estimates of the tail exponent of the distribution of $|X_{i,t}|$ based on different lengths of the tail over the entire observation period, for the BCI data (OECD$^+$ group). Panels (a), (b), (c), and (d) show the results for tails defined as 1%, 5%, 10%, and 15% of the largest observations in $|X_{i,t}|$, respectively. In each panel, we plot the empirical complementary cumulative distribution function (CCDF) of $|X_{i,t}|$ on a log-log scale. The solid line depicts the empirical CCDF, while the dashed line represents the power law $\Pr(|X_{i,t}| > x) \sim x^{-\mu}$ using the respective Hill estimate for μ.

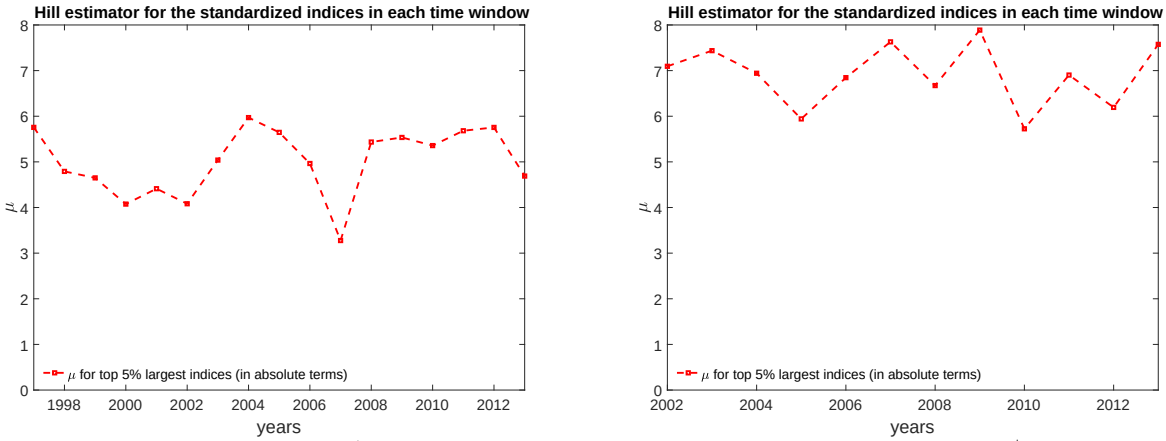

(a) for ESI data, EU$^+$ group

(b) for BCI data, OECD$^+$ group

Figure 5.15: The tail exponent μ of the distribution of $|X_{i,t}|$ in each time window, computed using the Hill estimator on the 5% largest observations in the respective window.

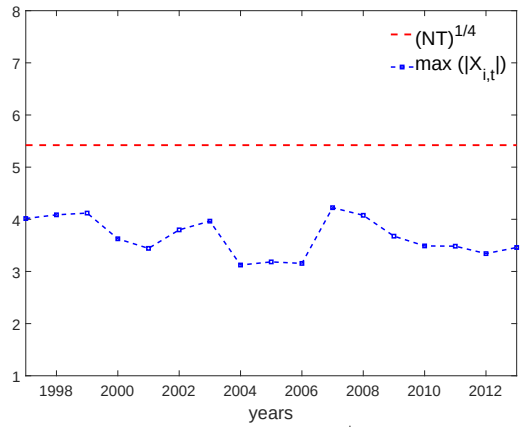

(a) for ESI data, EU^+ group

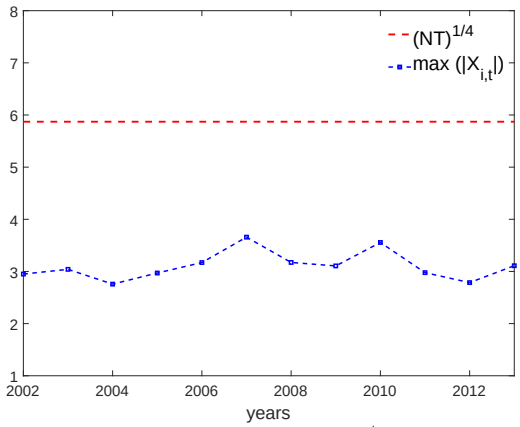

(b) for BCI data, $OECD^+$ group

Figure 5.16: The largest element of $|X_{i,t}|$ compared to $(NT)^{1/4}$ in each time window. We always observe that $\max(|X_{i,t}|) < (NT)^{1/4}$.

Chapter 6

Summary and Outlook

This thesis develops a macroeconomic framework for studying the interactions between the financial sector, the real sector and monetary policy in the context of an endogenous business cycle. It also explores different determinants of the long-run value of Tobin's average Q in the context of economic growth. Finally, this work also contributes to the existing literature on the empirical applications of network theory and random matrix theory to economic and financial complex systems.

The first essay (chapter 2) developed a particular approach to the relationship between the real and the financial sectors based on Tobin's average Q derived in the context of economic growth. We explored the interactions between the two sectors with monetary policy in the context of a model of endogenous business cycles rooted in the real sector. Using this model we examined the link between a particular observed behavior of the stock market and monetary policy over the business cycle and the effectiveness of the central bank's attempts to affect the opportunity cost of capital in the economy. This allowed us to provide potential explanations for the pro-cyclical stock market observed in particular during the last 25 years in the US.

Within this framework, we identified several factors that contribute to a pro-cyclical stock market. Firstly, the value of the firms in the real sector (Tobin's average Q) is affected by the profits generated in it. Therefore, a timid or ineffective monetary policy can allow for the stock market to be dominated by the fluctuations of the profits in the real sector. We modelled the potential ineffectiveness of monetary policy in terms of an endogenous risk premium. Finally, the adjustment speed of the financial markets to changes in the fundamentals of the model economy is also an important factor affecting the behavior of the stock market over the business cycle.

Using the above mentioned factors, we calibrate the model to fit key properties of the data from the last 25 years. In particular, the model can generate a pro-cyclical stock market in the presence of a counter-cyclical monetary policy.

The insights from this study can be used to assess the effectiveness of monetary policy. In the context of the model a strongly procyclical stock market can be interpreted as a signal that monetary policy is not able to significantly affect the borrowing conditions in the economy.

There are numerous possible extensions to the current study that come to mind. From a theoretical point of view the framework can be extended by explicitly modelling the capital structure in the economy (loans vs equity). This would allow for the analysis of Minsky's financial instability hypothesis in the context of this model.

From an empirical perspective, one potential area of future research is the rigorous estimation of the model. While the calibration exercise resulted in parameters that allowed for a very good fit to the cyclical component of the data, it would still be insightful to get some idea about the statistical significance of the individual parameters.

A more ambitious extension would be to take the raw data and try to conduct an estimation exercise in which the trend components implied by the model are filtered out for each series. In other words, to use the model as a filter instead of the HP filter imposed ex-ante on the raw series in our study. In theory, this might allow this endogenous business cycle framework to produce predictions about the macroeconomic variables involved.

In the second essay (chapter 3) a long-run equilibrium value of Tobin's Q was derived in the context of economic growth. At the heart of the derivation lies a no-arbitrage condition involving a comparison of the fundamental return on equity with the riskless base interest rate set by the central bank. We take into account that equity is not riskless by adjusting the base interest rate by a risk premium associated with equity risk. This approach involves the concept of a benchmark stock price inflation. It can be understood as the stock price inflation implied by the financing decisions of the firms and by the inflation in the real sector. The financing decision refers to the financing of desired investments in fixed capital and considers retained profits and the issuance equity and debt. The final solution for the long-run equilibrium value of Tobin's Q involves many variables of macroeconomic significance like the investment rate, the profit rate, inflation, corporate taxes, the base interest rate, an equity risk premium and the debt to asset and equity to asset ratios. A simplified version of

this framework was used in Chapter 2 when modelling the links between the financial and the real sectors.

Since Tobin's Q and the debt to asset and equity to asset ratios are not independent, we considered two specifications of the long-run fundamental value. In the first specification it depends on a fixed debt to asset ratio, while in the second a balanced portfolio argument was invoked which leads to a representation involving the desired fractions of equity and loans in the portfolios of rentiers.

We calibrated the model by using US macroeconomic data and investigated the sensitivity of the long-run equilibrium value of Tobin's Q under the two specifications to different values of the equity risk premium. Overall, we found that (ceteris paribus) variations in the risk premium within a reasonable range do not result in a very dramatic change in the long-run equilibrium value. A stronger impact was observed in the balanced portfolio framework. We also observed an asymmetry in the reactions of the equilibrium value. It increases by more as a result of a low premium, than it decreases for a high premium.

In the broader context of the first two essays, we find that under variations of the base interest rate, firm investments in fixed capital, inflation and profits, Tobin's Q can exhibit dramatic fluctuations over the business cycle. This is indicative of the aptitude of this modelling framework to reproduce macroeconomic stylized facts.

This framework for modelling real-financial interactions is very rich as it establishes relationships between a multitude of variables from the financial and real sectors of the economy. A potential extension would be the exploration of different causal relationships among the variables involved, because the equilibrium value itself does not give us any clues about which variables lead and which follow. Chapter 2 provides one possible set of such causal relationships in a simplified version of the framework in which debt is assumed to be the same as equity. Obviously, there are many other possibilities to explore.

From an empirical point of view various exercises can be conducted within this framework. For example, one could try to reconstruct the equilibrium value of Tobins's Q over time as implied by the model given some data on the macroeconomic variables involved. Then one could compare the reconstructed series with the observed values of Tobin's Q in the data. In this way it would be possible to gather some evidence in favour of the current framework or against it. Even though the equilibrium value is obviously an equilibrium concept, while the Tobin's Q observed in data might not be in equilibrium, overall, if the theory is any good,

the two series should not be too dissimilar. There are, however, many degrees of freedom involved in this exercise since many of the macroeconomic variables (like the debt to asset ratio or the different risk premia) do not have unambiguous counterparts in the macroeconomic data.

In the third essay (chapter 4), we provided a comprehensive analysis of the second as well as the third order structural correlations in all versions (binary vs weighted and undirected vs directed) of the Italian e-MID network. Our findings suggest that the observed structural correlations can vary across different versions of the network.

During our analysis of the evolution of the third order correlations among banks over time, we detected dramatic changes in the network structure surrounding the recent financial crisis in 2007. Moreover, by employing the various configuration models, we examined whether the information embedded in the observed degree sequence and/or the strength sequence can explain observed higher order structural correlations. The results show that, in the binary case, the degree sequence is informative in terms of explaining the main features of the structural correlations in the e-MID network.

In the weighted case, the randomized ensembles produced by the Enhanced Configuration Models, which constrains both the degree as well as the strength sequences, have a much greater predictive power than the randomized ensembles produced by the Weighted Configuration Models, which constrains only the strength sequences.

However, under scrutiny, both the binary as well as the weighted versions of the observed e-MID network do exhibit some non-random patterns that cannot completely be explained by the degree sequence(s) and/or strength sequence(s). One main feature not explained by the sequences of degrees and strengths of the network nodes themselves is the high level of clustering in the years preceding the crisis, i.e. the huge increase in various indirect exposures generated via more intensive interbank credit links.

Interestingly, the distance between the predictions of the Weighted Configuration Models and of the Enhanced Configuration Models for the averages of the measures for the third order correlations continuously increases from the adoption of the Euro up until the financial crisis in 2007 and then sharply decreases after that, revealing structural changes in the network associated with these two critical events. It also suggests that the importance of the degree sequence(s) and/or strength sequence(s) for the emergence of higher order correlation structures can vary over time.

This essay contributes to the existing literature on structural correlations in financial networks by assessing the role of various local constraints in all versions of the Italian e-MID network.

For future studies, it would be interesting to investigate whether some bank characteristics correlate with the extracted hidden variables. In addition, we suggest that the role of various constraints for the emergence of higher order structural correlations (or motifs) and for the meso-scale network structures such as the core-periphery and community structures should be studied further.

The fourth essay (chapter 5) analyzed the evolution of the empirical correlations between the macroeconomic sentiment indices in different countries. We observe that the dynamics of the sentiment indices across countries can be explained well by the evolution of a common component. However, during normal times, the sentiment in some countries can "resist" the common factor or can even, on rare occasions, "swim against the tide", meaning that we could detect a significant second factor driving the comovement of the indices. Nevertheless, in the presence of strong global information signals like the collapse of the US housing market (2007-2009), we observe a strong synchronization of the sentiment dynamics all over the world. In the case of the Eurozone debt crisis (2011-2013), the sentiment synchronization is high only within Europe, which can be interpreted as an indication that the Eurozone debt crisis is not perceived as a global information signal in countries outside of Europe. We believe that a similar analysis of the empirical co-movements between other macroeconomic indicators of different countries can be a fruitful direction for future research. Additionally, the methods employed in this study can be used to decompose the correlations between macroeconomic variables into components.

Affirmation

I hereby affirm that I have completed my doctoral thesis entitled, "Essays on Real-Financial Interactions and on the Application of Network and Random Matrix Theories to Economic Data" entirely on my own and unassisted, and that I have explicitly marked all of the quotes I have used from other authors as well as those passages in my work that are extremely close to the thoughts presented by other authors, and listed the sources in accordance with the regulations I have been given.

April 16, 2019 Boyan Yanovski